

# Synchronization in Periodically Driven and Coupled Stochastic Systems—A Discrete State Approach

## DISSERTATION

zur Erlangung des akademischen Grades  
doctor rerum naturalium  
(Dr. rer. nat.)  
im Fach Physik

eingereicht an der  
Mathematisch-Naturwissenschaftlichen Fakultät I  
der Humboldt-Universität zu Berlin

von  
Herrn Dipl. Phys. Tobias Prager  
geboren am 30.03.1974 in Tübingen

Präsident der Humboldt-Universität zu Berlin:  
Prof. Dr. Christoph Marksches

Dekan der Mathematisch-Naturwissenschaftlichen Fakultät I:  
Prof. Thomas Buckhout, PhD

Gutachter:

1. Prof. Dr. Lutz Schimansky-Geier
2. Prof. Dr. Igor Sokolov
3. Prof. Dr. Eckehard Schöll, PhD

eingereicht am: 11.01.2006  
Tag der mündlichen Prüfung: 23.03.2006

## Abstract

We investigate the behavior of stochastic bistable and excitable dynamics based on a discrete state modeling. In addition to the well known Markovian two state model for bistable dynamics we introduce a non Markovian three state model for excitable systems. Its relative simplicity compared to stochastic models of excitable dynamics with continuous phase space allows to obtain analytical results in different contexts.

First, we study the joint influence of periodic signals and noise, both based on a characterization in terms of spectral quantities and in terms of synchronization properties with the driving signal. We present expressions for the spectral power amplification and signal to noise ratio for renewal processes driven by weak periodic signals. Applying these results to the discrete model for excitable systems allows to estimate signal frequencies which are optimally amplified by the stochastic system. Stochastic synchronization of the system to the driving signal is investigated based on diffusion properties of the transition events between the discrete states. We derive general results for the mean frequency and effective diffusion coefficient which, beyond the application to the discrete models considered in this work, provide a new tool in the study of periodically driven renewal processes. Applied to the dichotomically driven Markovian two state model for bistable system exact analytical results are obtained. While this system only exhibits one to one synchronization the three state model for excitable system shows different  $m : n$  synchronization regimes. The very same discrete model for excitable systems can also be considered as a simple model for a molecular motor. We show that an appropriate periodic modulation of the concentration of the fuel molecules can lead to a very regular motion of the motor.

Finally the behavior of globally coupled excitable and bistable units is investigated based on the discrete state description. In contrast to the bistable systems, the excitable system exhibits synchronization and thus coherent oscillations. A non vanishing refractory period as well as an excitatory coupling are shown to be necessary conditions for synchronous firing to occur.

All investigations of the non Markovian three state model are compared with the prototypical continuous model for excitable dynamics, the FitzHugh-Nagumo system. They reveal a good agreement between both models, rendering the non Markovian discrete state model for excitable systems an appropriate simplification of continuous phase space dynamics commonly used in the modeling of excitable dynamics.

**Keywords:**

Excitable systems, Renewal processes, non Markovian discrete models,  
Synchronization

## Zusammenfassung

Wir untersuchen das Verhalten von stochastischen bistabilen und erregbaren Systemen auf der Basis einer Modellierung mit diskreten Zuständen. In Ergänzung zu dem bekannten Markovschen Zwei-Zustandsmodell zur Beschreibung bistabiler stochastischer Dynamik stellen wir ein nicht Markovsches Drei-Zustandsmodell für erregbare Systeme vor. Seine relative Einfachheit im Vergleich zu stochastischen Modellen erregbarer Dynamik mit kontinuierlichem Phasenraum ermöglicht es, analytische Ergebnisse in unterschiedlichen Zusammenhängen zu erzielen.

Zunächst analysieren wir den gemeinsamen Einfluß eines periodischen Treibens und Rauschens. Dieser wird entweder mit Hilfe spektraler Größen oder durch Synchronisationseigenschaften des Systems mit dem treibenden Signal charakterisiert. Wir leiten analytische Ausdrücke für die spektrale Leistungsverstärkung und das Signal-zu-Rauschen Verhältnis für schwach periodisch getriebene Renewal-Prozesse her. Angewandt auf das diskrete Modell für erregbare Dynamik, lassen sich damit Frequenzen abschätzen, die optimal verstärkt werden. Stochastische Synchronisation des Systems mit dem treibenden Signal wird auf der Basis der Diffusionseigenschaften der Übergangsereignisse zwischen den diskreten Zuständen untersucht. Wir leiten allgemeine Formeln her, um die mittlere Häufigkeit dieser Ereignisse sowie deren effektiven Diffusionskoeffizienten zu berechnen. Über die konkrete Anwendung auf die untersuchten diskreten Modelle hinaus stellen diese Ergebnisse ein neues Werkzeug für die Untersuchung periodischer Renewal-Prozesse dar. Die analytischen Ausdrücke für das dichotom getriebene Markovsche Zwei-Zustandsmodell zeigen nur 1 : 1 Synchronisation mit dem treibenden Signal. Im erregbaren Modell findet man dagegen verschiedene  $m : n$  Synchronisationsregime. Eben jenes System kann auch als ein einfaches Modell für molekulare Motoren verstanden werden. Wir zeigen, dass eine periodische Veränderung der Konzentration der Treibstoff-Moleküle zu einer sehr regulären Bewegung des Motors führt.

Schließlich betrachten wir noch das Verhalten global gekoppelter bistabiler und erregbarer Systeme, wiederum auf der Grundlage der diskreten Modelle. Im Gegensatz zu bistabilen Systemen können erregbare Systeme synchronisiert werden und zeigen kohärente Oszillationen. Wir demonstrieren, dass eine nicht verschwindende Refraktärperiode sowie eine anregende Kopplung notwendige Bedingungen für synchrones Verhalten ist.

Alle Untersuchungen des nicht Markovschen Drei-Zustandsmodells werden mit dem prototypischen Modell für erregbare Dynamik, dem FitzHugh-Nagumo System, verglichen. Wir finden eine gute Übereinstimmung zwischen beiden Modellen, so dass das diskrete Modell für erregbare Systeme eine geeignete Vereinfachung

kontinuierlicher Phasenraumsysteme, die man gemeinhin zur Modellierung stochastischer erregbarer Dynamik verwendet, darstellt.

**Schlagwörter:**

Anregbare Systeme, Renewal Prozesse, nicht Markovsche diskrete Modelle, Synchronisation



# Contents

<b>1</b>	<b>Introduction</b>	<b>1</b>
<b>2</b>	<b>Bistable and Excitable Systems – A Discrete State Approach</b>	<b>7</b>
2.1	Discrete Description and Renewal Dynamics for Continuous Stochastic Processes . . . . .	8
2.1.1	Bistable systems – Rate processes and master equations . . .	8
2.1.2	Excitable systems – Renewal processes and non Markovian master equations . . . . .	11
2.1.3	Renewal Processes . . . . .	18
2.2	Quantifying the behavior of a stochastic process . . . . .	21
2.2.1	The spectral power density . . . . .	22
2.2.2	Effective Diffusion . . . . .	26
2.3	Summary . . . . .	29
<b>3</b>	<b>Periodically Driven Systems-Spectral Based Quantification</b>	<b>31</b>
3.1	The structure of the spectral power density for periodic processes .	32
3.2	Spectral power amplification and signal to noise ratio . . . . .	33
3.3	SPA and SNR of periodically driven renewal processes . . . . .	35
3.3.1	A master equation approach . . . . .	36
3.3.2	An approach based on waiting time distributions . . . . .	48
3.4	Summary . . . . .	68
<b>4</b>	<b>Periodically Driven Systems-Stochastic Synchronization</b>	<b>69</b>
4.1	Properties of the number of events for periodically driven renewal processes . . . . .	71
4.2	A master equation approach . . . . .	74
4.2.1	Application to synchronization in a double well system . . .	81
4.2.2	Application to synchronization in excitable systems . . . . .	86
4.2.3	Application to molecular motors –Controlling random motion of Brownian steppers by periodic driving . . . . .	94
4.3	An approach based on waiting time distributions . . . . .	104

4.3.1	Comparison with known results for undriven renewal processes and periodically driven rate processes . . . . .	109
4.3.2	Numerical solution in Fourier space . . . . .	111
4.3.3	A simple toy model – comparison between theory and simulations . . . . .	111
4.3.4	Equivalence with the two state model for excitable systems	116
4.4	Summary . . . . .	118
<b>5</b>	<b>Coupled Systems</b>	<b>119</b>
5.1	The two state model for double well potential systems . . . . .	120
5.2	The three state model for excitable dynamics . . . . .	123
5.2.1	Conditions which do not allow for spontaneous global oscillations . . . . .	128
5.2.2	Application to excitable systems . . . . .	131
5.2.3	Delayed Coupling . . . . .	141
5.3	An approach based on waiting time distributions . . . . .	142
5.3.1	Equivalence with the three state model described by a master equation . . . . .	146
5.3.2	Application to the FHN system in the bistable regime . . . . .	147
5.4	Summary . . . . .	151
<b>6</b>	<b>Conclusions and Outlook</b>	<b>153</b>
<b>A</b>	<b>Detailed calculations for chapter 2</b>	<b>167</b>
A.1	Equivalence between the semi Markovian master equation and the three state model master equation . . . . .	167
A.2	Spectral power density of renewal Processes . . . . .	168
A.2.1	The spectral power density of renewal delta spike trains . . . . .	168
A.2.2	The spectral power density of renewal pulse sequence . . . . .	170
A.3	The Wiener-Khinchine theorem . . . . .	172
A.3.1	Stationary processes . . . . .	173
A.3.2	Periodic processes . . . . .	174
<b>B</b>	<b>Detailed calculations for chapter 3</b>	<b>177</b>
B.1	Sum of powers of a Markov operator . . . . .	177
B.2	The Fourier coefficients of the time periodic master operator . . . . .	178
B.3	The order in the driving signal amplitude . . . . .	179
B.3.1	The order in the signal amplitude of the Fourier coefficients of a general master operator . . . . .	180
B.3.2	The order in the signal amplitude of the Fourier coefficients of a time dependent waiting time distribution . . . . .	181



<b>C Detailed calculations for chapter 4</b>	<b>183</b>
C.1 Periodically modulated linear growth of the cumulants of a periodic point process . . . . .	183
C.2 Relation between the Kramers-Moyal coefficient and the growth of the cumulants . . . . .	185
C.3 Relation between moments and cumulants . . . . .	187
C.4 Expansion of the probability density governed by a Kramers-Moyal equation . . . . .	187
C.5 The phase velocity and effective diffusion for the excitable system in Fourier Space . . . . .	189
C.6 The defining equation for $\kappa^{[3]}(t)$ in Fourier space . . . . .	191
C.7 Time derivatives of integrals involving time dependent survival probabilities . . . . .	192
<b>D Detailed calculations for chapter 5</b>	<b>195</b>
D.1 Investigation of the criticality of the Hopf bifurcation in the globally coupled threestate model . . . . .	195
D.2 Some properties of Laplace transforms of waiting time distributions and survival probabilities . . . . .	199

# Chapter 1

## Introduction

Nous devons envisager l'état présent de l'univers comme l'effet de son état antérieur et comme la cause de celui qui va suivre. Une intelligence qui, pour un instant donné, connaîtrait toutes les forces dont la nature est animée et la situation respective des êtres qui la composent, si d'ailleurs elle était assez vaste pour soumettre ces données à l'analyse, embrasserait dans la même formule les mouvements des plus grands corps de l'univers et ceux du plus léger atome; rien ne serait incertain pour elle, et l'avenir, comme le passé, serait présent à ses yeux.

At the latest since the discovery of quantum mechanics this deterministic point of view formulated by Laplace [70] is obsolete. The outcomes of measurements are in general not deterministic and under the assumption of locality, which a physicist reluctantly abandons, we cannot assign this randomness to an insufficient knowledge of the present state, known under the keyword *local hidden variables* [4, 7, 28]. Instead, we have to abandon the principle of realism, stating that any measurable quantity has some value which is independent of the measurement.

Despite this principle probabilistic element due to the quantum mechanical nature of the world, there are three prerequisites mentioned in the citation of Laplace which are hardly fulfilled in the majority of physical or biological problems we face. The demand of knowing both the complete initial state and all the interactions between the constituents of the system and at the same time being able to process this information in order to predict the future evolution is in the majority of cases unsatisfiable. In addition to the impossibility of predicting the complete detailed evolution it is in many cases undesirable to deal with such a huge amount of information. Just think of a volume filled with a gas, where one is not interested in the precise velocities and positions of the gas molecules but rather in some macroscopic properties like pressure or temperature.

These restrictions led to the development of different concepts. The lack of knowledge of the precise microscopic state in systems consisting of a huge amount of identical particles is treated in thermodynamics and statistical physics. The theory of stochastic dynamics deals with the randomness in the description of a system, which might be caused by the influence of an incompletely specified environment or the description of the system in terms of mesoscopic variables, ignoring again the precise microscopic state. Finally, to deal with complex systems, whose constituents and interactions are not known in detail and by far too complex to be microscopically treated, phenomenological models are set up.

The present work touches the last two points just mentioned. But let us first take a little look at these topics from the historical point of view.

All processes occurring in real, non idealized systems, which are never perfectly isolated, are influenced by the environment. As the environment is too complex, consisting of a huge amount of degrees of freedom its state and thus the precise interaction with the system considered cannot be specified exactly. Due to the lack of this information, the influence of the environment is often modeled as a stochastic force. A paradigmatic example where this random impact of the environment can be observed is the erratic motion of a small particle submersed in a fluid. This *Brownian* motion, termed after the Scottish botanist Robert Brown (1773-1858) who discovered it when observing pollen swimming in water, attracted a lot of attention. His first conjecture that the motion is due to the pollen being alive was quickly rejected as also clearly non animated objects like dust showed this motion. A sound explanation of Brownian motion was not given until 1905, when Albert Einstein [27] investigated this phenomenon within a thermodynamical framework. Shortly thereafter, Langevin [69] considered the problem from a different point of view, explaining the fluctuations in the position of the particle by a zero average random force describing the random impact of the molecules in the liquid. Langevin's approach, leading to the same results Einstein has obtained, proved to be very useful to describe random fluctuations in various dynamical systems. A differential equation with a stochastic force term, which he set up to describe the Brownian particle's velocity, is therefore called *Langevin* equation.

Despite this external random impact, due to the interaction of the small system with the environment, randomness can also be present in the system itself for different reasons. On the one hand the considered system can be a mesoscopic or macroscopic object, whose coarse grained description in terms of a few macroscopic variables, may induce a stochastic element due to the lack of a precise specification of the microscopic state. On the other hand also the quantum character of the constituents generates randomness.

Nowadays the term *noise* is well established to name the random forces influencing a dynamical system. It stems from early investigations of random forces in

---

electrical circuits [58,93], where noise limited the sensitivity of amplifiers and thus constitutes the chief obstacle to further improvement of technical devices. In this field the aim was to understand the effects of noise in order to minimize its influence. However, despite this self-evident property to produce disorder in a system's behavior, it was later discovered that noise can sometimes also have an ordering influence in nonlinear dynamical systems. A paradigmatic example is the noise assisted amplification of weak signals, termed *stochastic resonance*. This effect was originally proposed to explain the periodicity of ice ages [9,10,91]. These ice ages recur periodically with a period of about 100000 years, which coincides with the period of the change in the earth's orbit's eccentricity due to the motion of the other planets. This induces a periodic modulation of the solar irradiation<sup>1</sup>, which however is much too weak to generate cold or warm periods by itself. Why the switching between warm and cold periods nevertheless happens regularly with this very same frequency can be explained using a simple bistable model of the earth: Either it is cold and there is a large coverage of the polar caps with ice, leading to a strong reflection of the incoming radiation from the sun, and thus it remains cold; or it is warm, there is less coverage of the polar caps with ice, more heat from the sun is absorbed and thus it remains warm. The switching between these two stable states cannot be caused by the very weak periodic modulation of the sun's radiation alone. However due to random fluctuations of earth's atmosphere, think of the weather or climate, volcanic eruptions etc., a switching becomes possible, occurring most likely from a warm period to an ice-age if the sun's radiation is a little bit less intensive and vice versa if it is more intensive.

In the example above we already touched the second concept mentioned in the beginning, namely to simplify the description of a complex system to such an extent that from the resulting model one can understand and explain the system's behavior. Generally when modeling something which happens in nature, like a solid body sliding down an inclined plane or a protein being cut into pieces in a cell by some protease, one has to map a part of the real world into a mathematical description. This is done by assigning mathematical objects to measurable quantities and describing their evolution by some equations. There are different levels of abstraction, ranging from very complex precise models which capture every detail of the system, to very simple restricted models which probably describe only a certain aspect of the system. At first glance one is tempted to judge the most complex models the best, as they cover more aspects of the system with higher accuracy. However the price paid is often too high. Consider for example a neuron in the brain. Such a neuron consist of a certain number, say  $10^{23}$ , different atoms whose dynamics to the present knowledge is governed by quantum mechanics and thus

---

<sup>1</sup>Actually the situation is a little bit more complex, as there are three superposed periodic modulations of the motion of earth involved, which all affect the solar irradiation.

described by a Schrödinger equation. A very accurate description of this neuron is thus obtained by prescribing an appropriate  $10^{23}$  particle Schrödinger equation to it. However, despite computational problems and the principal question to which extent it makes sense to describe macroscopically interacting objects by means of quantum mechanics, the understanding of the functioning of a neuron gained from such a description converges to zero. The aim therefore is to obtain simplified models amenable to interpretation and mathematical and computational treatment. Sticking to the neuron there is a whole zoo of different models starting from the detailed Hodgkin Huxley (HH) model [54]. This model is based on the physiological characterization of a neuron in terms of ion currents and the membrane potential which evolve according to the complex opening dynamics of some ion channels. Investigating the behavior of this model with the appropriate parameters taken from measurements of real neurons, there is one fast relaxing ion channel gating variable, which can be eliminated by a quasi steady state approximation. The two remaining gating variable can be lumped into one, finally ending up with a two variable model, the famous FitzHugh-Nagumo (FHN) model (see e.g. [45]). There already the physiological significance of the variables is vague and one would expect this model to be less predictive than the more complex Hodgkin-Huxley model. However many features of the behavior of real neurons are still captured within this model, which on the other hand has the advantage of being mathematically easier to handle. A further simplification is the leaky integrate and fire (LIF) neuron model [122]. It captures the fact, that (as seen in real neurons, the HH and FHN model) has some rest membrane potential which is changed due to incoming signals until it reaches a threshold. This leads to the generation of a spike, after which the neuron is insensible to signals during some refractory period. This model is quite simple and easy tractable and describes some general aspects of a neurons spike train, however nobody would expect it to reproduce for example the exact membrane potential in the course of time. Focusing on different aspects, though, like for example the behavior of coupled neurons, the LIF model probably reproduces as well as any other more complex model the collective behavior like global oscillations or waves.

There are two types of dynamics which we have already mentioned. The explanation of the periodic recurrence of ice ages was based on a *bistable* model, while a neuron exhibits a so called *excitable* dynamics. This was not coincidental but due to the fact that these types of dynamics are quite generic; they can be found throughout a variety of different fields. A bistable system, as already suggested by its name, has two stable states. Transitions between these states occur due to some external influence, a signal or external noise, or they may spontaneously occur due to fluctuations present in the system. Examples of bistable systems range from the above mentioned ice age – warm period model of earth [9, 10, 91] to electronic

---

circuits like a Schmitt-Trigger [31, 84] and chemical reactions like the detonation of explosives (although in this example the two states are not very symmetric) and so on thus probably covering the whole spectrum of nature.

In contrast to bistable systems, an excitable system has only a single stable state. Small perturbations of the system are damped. However, if the perturbation exceeds a certain threshold, the system responds with an excitation, i.e. a drastic change of its state, from which it finally relaxes back to its stable rest configuration. Apart from the already mentioned spiking dynamics of neurons, excitable behavior can be found in many different fields, including lasers, chemical reactions, climate dynamics and cardiovascular tissues to name but a few (see [73] and references therein). The above mentioned FHN model has gained importance beyond the description of neurons. It has been applied to model miscellaneous excitable systems and can be considered as the archetypal model of excitable behavior.

Because bistable and excitable dynamics are ubiquitous in nature, as is noise, their interrelation has attracted a lot of research. One paradigmatic example of a counterintuitive effect of noise is the amplification of weak signals at optimal noise levels, *stochastic resonance*, which we already mentioned as an explanation for the periodic recurrence of ice ages. After this first discovery, stochastic resonance has been found in a variety of systems on very different levels of complexity, ranging from physical (ring lasers [82]) and electronic (Schmitt trigger [31]) systems to chemical and complex biological systems (prey capture of the paddlefish [37, 39, 114]). Apart from bistable dynamics [10, 35], stochastic resonance can also be found in excitable [73] and monostable [123] system as well as in chaotic systems [2]. In stochastic excitable systems a different, intrinsic ordering effect of noise can be observed which is termed *coherence resonance* [43, 90, 100]. Due to the different dependencies on noise strength of the two time scales which govern on the one hand the excitation from the rest state and on the other hand the time the system stays in the excited state and thereafter needs to recover its rest state, there exists an optimal finite noise level at which these excitations happen most regularly. Beside these two paradigmatic effects there exist a variety of other constructive noise induced effects like noise induced phase transitions [12, 13], noise induced pattern formation [44] or the rectification of fluctuations leading to directed motion [6, 52].

Although being already simplified models, the above mentioned FHN system as well as the standard model for stochastic bistable dynamics, an overdamped particle in a double well potential subjected to noise, are both still challenging concerning mathematical and computational treatment. One possibility to further simplify such a model, consist in the reduction to a few discrete states. While for stochastic bistable systems a discrete state modeling is well known and widely used [83], it is less evident how to discretely model stochastic excitable systems, as a model for excitable dynamics with a few discrete states can no longer be Marko-

vian. In the introductory chapter 2 we recapitulate the mentioned Markovian two state model for bistable systems and propose a non Markovian discrete state model for excitable dynamics. In both models the transition times between the discrete states constitute a renewal process. The concept of renewal processes is outlined as well as different quantities to analyze these processes, like the spectral power density and the effective diffusion coefficient. In the next two chapters the influence of external periodic signals on bistable and excitable systems is investigated, based on the introduced discrete state models. While in chapter 3 the characterization is given in terms of spectral based quantities in chapter 4 stochastic synchronization is considered. We derive general concepts, to investigate periodically driven discrete state systems. These results are then applied to the discrete state models for bistable and excitable dynamics and compared with numerically obtained results from the archetypal model for excitable systems, the FHN system, and the bistable double well system respectively, showing good agreement. Finally in chapter 5 the behavior of globally coupled bistable and excitable systems is investigated. The reduced description in terms of discrete states allows for a partly analytical treatment. Again we find a good agreement between the behavior of the discrete systems and the respective continuous systems. Many of the calculations are presented in detail in a series of appendices.

## Chapter 2

# Bistable and Excitable Systems – A Discrete State Approach

Dynamical processes can be modeled on different scales of complexity. Going from very detailed models to more simplified models there are two opposed tendencies. On the one hand the more complex the model is the more precise it describes the underlying system. On the other hand, the simpler models, although being not able to reproduce all different possible aspects of the original process, may explain and illustrate some concrete features of the system, leading to an understanding, which otherwise remains hidden beneath the complexity of the model.

One possibility to simplify a continuous stochastic system is the reduction to a description in terms of a few discrete states. The system's behavior is then specified by the transition times between these discrete states. For example when investigating a neurons behavior, the important aspect are often only the times when a spike is emitted and not the complex evolution of the membrane potential [111]. In a double well potential system, depending on the questions asked, it may be sufficient to know in which of the two wells the system is located, neglecting the fluctuations in the wells as well as the actual dynamics when crossing from one well to the other. In these cases a reduction to a discrete description can be considered as an appropriate simplification. In this chapter we first review the two state description of bistable systems [83] and introduce a three state model for excitable dynamics. Both models are examples of so called renewal processes, for which the concepts of spectral power density and the effective diffusion coefficient are reviewed. These quantities will be used in the later chapters to measure some important aspects of the stochastic processes considered, like the regularity of the transitions between the discrete states or synchronization of the process to an external signal.



## 2.1 Discrete Description and Renewal Dynamics for Continuous Stochastic Processes

In this section we consider a discrete description for double well potential systems and excitable systems. While it is known that the coarse grained description of a stochastic double well potential system in terms of the two discrete states right and left well is still Markovian, leading to an ordinary master equation for the discrete probabilities, the description of excitable dynamics in terms of a few states is no longer Markovian. This implies that the discrete probabilities can not be described by an ordinary master equation, but one has to resort to semi Markovian master equations. We introduce a special type of master equation, which exploits some concrete features of the excitable dynamics and is well suited to generalize the model, making it possible to consider e.g. the influence of a time dependent external signal.

### 2.1.1 Bistable systems – Rate processes and master equations

Let us consider a particle in a symmetric double well potential driven by white noise Fig. 2.1. The dynamics of this system is described by a stochastic differential

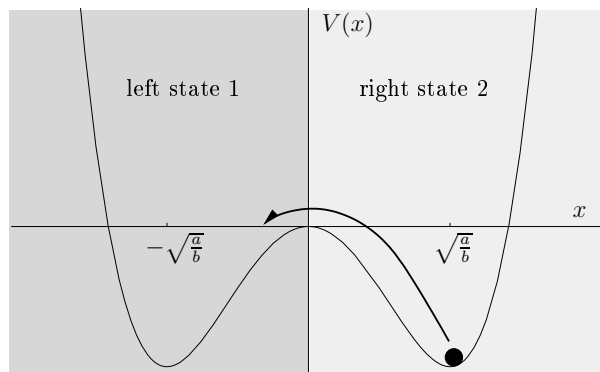


Figure 2.1: A bistable system as described by eq. (2.1). The reduced two state description is illustrated by the two differently colored half planes.

equation, called Langevin equation [69]

$$\dot{x} = -V'(x) + \sqrt{2D}\xi(t), \quad V(x) = -\frac{a}{2}x^2 + \frac{b}{4}x^4 \quad (2.1)$$

where  $\xi(t)$  is white noise with  $\langle \xi(t) \rangle = 0$  and  $\langle \xi(t)\xi(t + \tau) \rangle = \delta(\tau)$ . An equivalent description of the system can be given in terms of its conditioned probability

density  $P(x, t, x_0|t_0)$  to find the system at  $x$  at time  $t$  given that it was at position  $x_0$  at time  $t_0$ . This probability density is governed by the Fokker-Planck equation [34, 101]

$$\dot{P}(x, t|x_0, t_0) = \frac{\partial}{\partial x} [V'(x)P(x, t|x_0, t_0)] + D \frac{\partial^2}{\partial x^2} P(x, t|x_0, t_0).$$

with initial condition  $P(x, t_0|x_0, t_0) = \delta(x - x_0)$ . A comprehensive overview on Langevin and Fokker-Planck equations may be found in [1, 26, 63, 112, 124]

If we consider the output (position)  $x(t)$  in the course of time (see Fig. 2.2) we notice that the particle is jiggling most of the time in one of the two wells, only occasionally jumping from one well to the other.

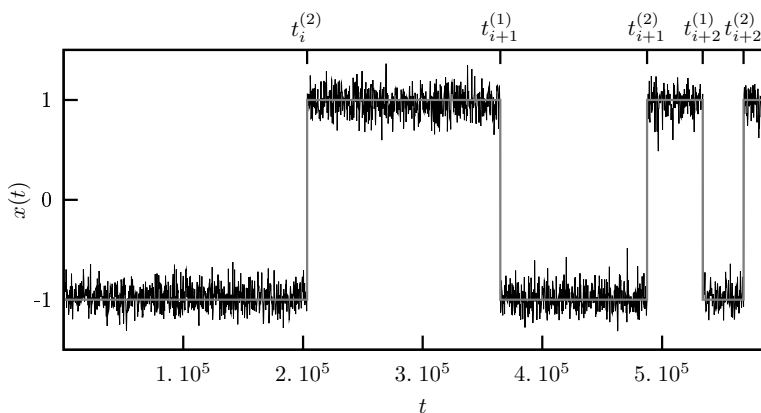


Figure 2.2: The output  $x(t)$  of a bistable system as described by eq. (2.1) with  $a = b = 1$  and  $D = 0.025$ . The reduced two state description is illustrated by the gray line.

In order to simplify the description on this system one neglects the fast relaxation dynamics in the potential wells and considers only the transitions from one well to the other which happen on a much slower time scale. It is known that under the assumption that the potential barrier  $\Delta U$  between the two wells is large compared to the noise strength  $D$ , implying that the relaxation in the wells is fast compared to the timescale of the jumps between the wells, the transitions can be considered as a rate process. Such a rate process has a probability per unit time to cross the barrier, which is independent on the time which has elapsed since the last crossing event. The resulting dynamics in the reduced discrete phase space which consists just of two discrete states namely *left* and *right* is still a Markovian one, i.e. the present state determines the future evolution to a maximal extent and knowledge about the past does not lead to additional knowledge about the future.

The transition rates  $\gamma_{1\rightarrow 2}$  from the left to the right well and  $\gamma_{2\rightarrow 1}$  from the right to the left well, which are both equal for the symmetric double well potential, are Kramers rates for the excitation over a potential barrier due to white noise. They can be calculated as [53, 67]

$$\gamma_{2\rightarrow 1} = \frac{\omega_0\omega_2}{2\pi} \exp\left(-\frac{V_0 - V_2}{D}\right) \quad (2.2)$$

$$\gamma_{1\rightarrow 2} = \frac{\omega_0\omega_1}{2\pi} \exp\left(-\frac{V_0 - V_1}{D}\right) \quad (2.3)$$

where  $\omega_0$ ,  $\omega_1$  and  $\omega_2$  are the frequencies (square roots of the modulus of the second derivatives of the potential) at the potential barrier and the left and right minimum respectively, while  $V_{0,1,2}$  are the corresponding values of the potential. The resulting waiting time distributions  $w^{(1)}(\tau)$  and  $w^{(2)}(\tau)$  in the left and right well are exponentially distributed (see Fig. 2.3),

$$w^{(1/2)}(\tau) = \gamma_{1/2\rightarrow 2/1} \exp(-\gamma_{1/2\rightarrow 2/1}\tau).$$

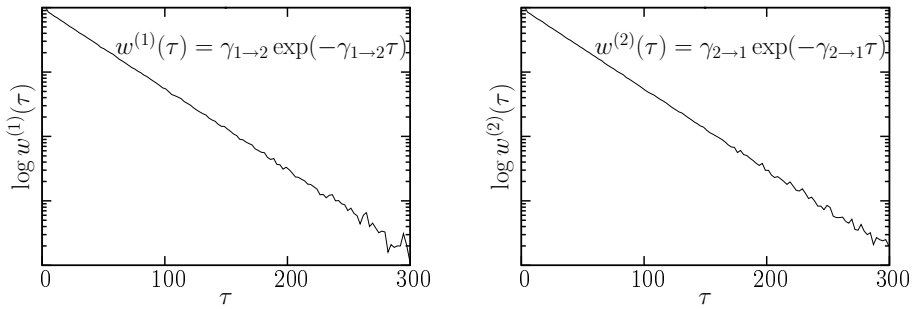


Figure 2.3: Waiting time distributions (non normalized) in the left and right well of the double well system taken from simulations of eq. (2.1) with  $D = 0.1$ .

The state of this discrete system is described by the two probabilities  $p^{(1)}(t)$  and  $p^{(2)}(t)$  to be in state 1 (left well) or state 2 (right well) at time  $t$ , respectively. Knowing the transition probability per unit time to cross the barrier from left to right or from right to left to be  $\gamma_{1\rightarrow 2}$  and  $\gamma_{2\rightarrow 1}$  respectively, we can express the probability current  $j^{(1)}(t)$  from state 1 to 2 and  $j^{(2)}(t)$  from state 2 to 1 in terms of the probabilities as

$$j^{(1)}(t) = \gamma_{1\rightarrow 2}p^{(1)}(t) \quad \text{and} \quad j^{(2)}(t) = \gamma_{2\rightarrow 1}p^{(2)}(t). \quad (2.4)$$

The change in time of the probability to be in a certain state is given by the difference of the probability current into this state and the probability current out

of this state, resulting in the well known Master equation

$$\dot{p}^{(1)}(t) = j^{(2)}(t) - j^{(1)}(t) = \gamma_{2 \rightarrow 1} p^{(2)}(t) - \gamma_{1 \rightarrow 2} p^{(1)}(t) \quad (2.5a)$$

$$\dot{p}^{(2)}(t) = j^{(1)}(t) - j^{(2)}(t) = \gamma_{1 \rightarrow 2} p^{(1)}(t) - \gamma_{2 \rightarrow 1} p^{(2)}(t). \quad (2.5b)$$

with the additional normalization condition  $p^{(1)}(t) + p^{(2)}(t) = 1$ . The possibility to obtain such an ordinary Master equation for the discrete description relied on the fact that the probability current (2.4) between the discrete states can be expressed in a simple manner in terms of the probabilities. This, in turn, is a consequence of the fact that the discrete description is still Markovian. Generally, if the noise induced transition between the different basins of attraction of a continuous stochastic system described by a Langevin equation, or a corresponding Fokker-Planck equation, happen on a much longer time scale than the relaxation within the basins one can assign an appropriate Markovian master equation to the discrete probabilities to be in one of the different basins of attraction<sup>1</sup>. In subsection 3.3.2 we investigate a bistable system, namely the bistable FitzHugh-Nagumo system, for which this assumption is no longer true, i.e. the transition times and relaxation times become comparable, and thus a Markovian discrete description can no longer be applied.

### 2.1.2 Excitable systems – Renewal processes and non Markovian master equations

In contrast to bistable systems an excitable system is monostable, i.e. its dynamics has one stable rest state. Small but sufficiently large perturbations, which may occur due to noise or an external signal, lead to a strong change in the system's state before it relaxes again to the rest state. Modeling excitable dynamics on a continuous plane phase space, the resulting system has to be at least a two dimensional non potential systems, which already points out some difficulties in the analytic treatment. However excitable dynamics can also be modeled as a dynamics on a circle [137] or as a one dimensional dynamics, with a superimposed threshold and reset condition, like the integrate-and-fire or leaky-integrate and-fire-model [122]. In this section we propose a different approach, modeling excitable dynamics as a discrete state system.

A prototypical system exhibiting excitable dynamics is the two dimensional FitzHugh-Nagumo system (FHN) which was independently proposed by FitzHugh [33] and Nagumo, Arimoto and Yoshizawa [87]. The FHN system is a simplified model of the famous four dimensional Hodgkin-Huxley model (HH) [54], which describes the dynamics of a neuron in terms of its membrane potential and ion

---

<sup>1</sup>The problem to obtain, for a more than one dimensional system, the transition rates between the different states is another story.

currents. However the FHN system has also obtained some relevance beyond the description of neurons [29, 80, 81]. The FitzHugh-Nagumo dynamics is governed by the Langevin equations

$$\dot{x} = x - x^3 - y + \sqrt{2D}\xi(t) \tag{2.6a}$$

$$\dot{y} = \epsilon(x + a_0 - a_1 y) \tag{2.6b}$$

where  $\xi(t)$  is white noise with  $\langle \xi(t) \rangle = 0$  and  $\langle \xi(t)\xi(t + \tau) \rangle = \delta(\tau)$ . In passing from the physiological HH model to the FHN model the physiological variables of the HH model are somehow mixed together. However the  $x$ -variable still represents the membrane potential of the neuron while the  $y$ -variable is a recovery variable with no direct physiological significance. The nullclines  $\dot{x} = 0$  and  $\dot{y} = 0$  together with a typical trajectory are shown in Fig. 2.4. Due to the small parameter  $\epsilon$  in eqs. (2.6)

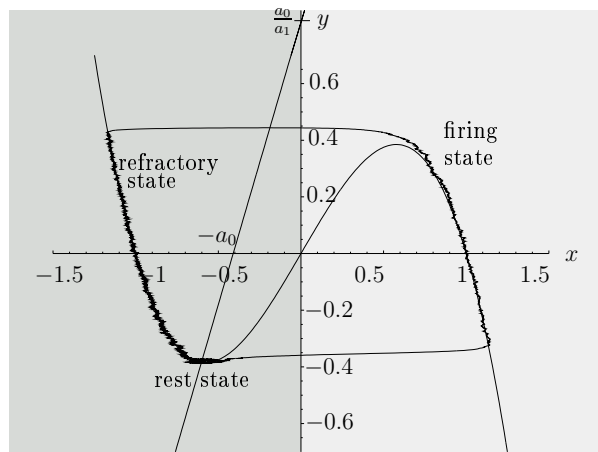


Figure 2.4: The FitzHugh-Nagumo system

the  $x$ -dynamics happen on a much faster time scale than the  $y$ -dynamics, leading in the limit  $\epsilon \rightarrow 0$  to a one dimensional dynamics on a topological circle. Let us look in more detail onto the behavior of the FHN system: From the stable fixed point at the intersection of both nullclines, which is also called *rest* state in the neuronal context, the system is excited by a sufficiently large perturbation, leading to a fast transition onto the right branch of the cubic  $x$ -nullcline. On the right branch the system assumes a high  $x$ -value, which at the neuronal level represents a high membrane potential, This state is called *firing* state. After having moved along the right branch the system returns back to the left branch. There the output ( $x$  variable) assumes again a low value like in the rest state, however the system cannot be directly re-excited, it first has to relax back to the rest state.

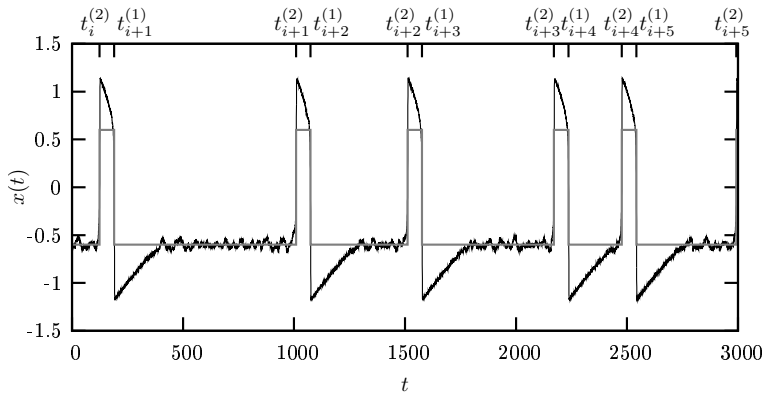


Figure 2.5: Output  $x(t)$  of the FHN system eqs. (2.6) with  $a_0 = 0.41$ ,  $a_1 = 0.5$ ,  $D = 0.0001$  and  $\epsilon = 0.01$ .

Therefore this state is called *refractory*. A typical output of the noisy FHN system showing the spiking behavior is presented in Fig. 2.5,

The strong timescale separation leads to a well defined distinction between rest and refractory state and firing state, because the transition from negative to positive  $x$ -values happens almost instantaneously, compared to the slower motion along the stable branches of the cubic nullcline. Therefore the exact position of the boundary which separates the discrete states in phase space does not matter when evaluating the waiting time distributions in these states. Using  $x = 0$  as the boundary those distributions have been evaluated numerically ( Fig. 2.6). In contrast to the double well system, where the transitions between the two

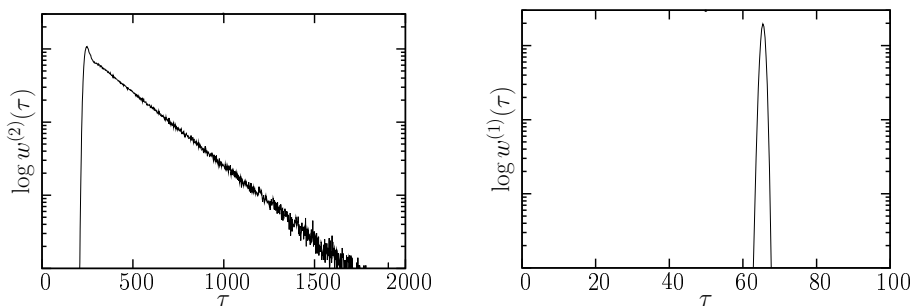


Figure 2.6: Waiting time distributions (non normalized) in the firing (sharp peak at about  $\tau = 65$ ) and rest and refractory state (right graph). The noise level is  $D = 0.0001$ . Other parameters (cf. eqs. (2.6)) are  $a_0 = 0.41$ ,  $a_1 = 0.5$ ,  $\epsilon = 0.01$ .

states were rate processes, implying an exponentially distributed waiting time,

the situation is more complex. The reduced description of the FHN system in terms of two (firing state and rest and refractory state) or three (firing state, refractory state and rest state) is no longer Markovian. Knowing the time when the system has entered the firing state, gives additional information on the future evolution, namely on the time when the firing state is left, then just knowing that the system is currently in the firing state. Specifying the state of the system by the two probabilities  $p^{(1)}(t)$  to be in the firing state at time  $t$  and  $p^{(2)}(t)$  to be in the refractory or rest state, a simple description in terms of an ordinary master equation is no longer possible, due to the fact that the probability current between the discrete states cannot be related to the probabilities in a simple way as it was possible in the Markovian case. Therefore we have to resort to the theory of so called *semi Markovian* or *time convoluted* master equations [47, 64]. These generalized master equations describe the evolution of a discrete state system with arbitrary waiting time distributions  $w^{(i)}(\tau)$  in the discrete states  $i$ . The term *semi Markovian* stems from the fact that although the description is not a Markovian one (the future evolution of the system does not only depend on the present state but also on the time of entering this state, i.e. on its past) however once the system has switched to a new state, the time it has waited in the former one no longer plays any role, i.e. it completely loses its memory. As semi Markovian master equations, although known for a long time, are not so familiar we briefly review their derivation following [47], however restricting ourselves to the case of two states.

Let us assume that the system has entered state 1 at time  $t_0 = 0$ . After having waited a time  $\tau^{(1)}$  in this state, which is drawn from a waiting time distribution  $w^{(1)}(\tau)$  the system switches into state 2. There again, it waits for a time  $\tau^{(2)}$  distributed according to  $w^{(2)}(\tau)$  before it returns to state 1 and so on. Denoting the probability current from state 1 to 2 at time  $t$  by  $j^{(1)}(t)$  and from state 2 to 1 by  $j^{(2)}(t)$  we obtain the relation

$$j^{(1)}(t) = \int_{t_0}^t dt' j^{(2)}(t') w^{(1)}(t - t') + \delta(t - t_0) \quad \text{and} \quad (2.7a)$$

$$j^{(2)}(t) = \int_{t_0}^t dt' j^{(1)}(t') w^{(2)}(t - t'). \quad (2.7b)$$

These relations express the fact that the probability current out of state  $i$  at time  $t$ ,  $j^{(i)}(t)$  is given by the probability current  $j^{(j)}(t')$  into this state at some time  $t'$  in the past, i.e. between  $t_0$  and  $t$ , times the probability  $w^{(i)}(t - t')$  that the systems waits the appropriate time  $t - t'$  in this state in order to leave it at time  $t$ . The additional term  $\delta(t - t_0)$  in the first equation accounts for the initial condition that

the system entered state 1 at time  $t_0$ . Introducing the survival probability

$$z^{(i)}(\tau) := 1 - \int_0^\tau d\tau' w^{(i)}(\tau') \quad (2.8)$$

to stay at least the time  $\tau$  in state  $i$  before leaving it, we can further relate the probabilities  $p^{(1)}(t)$  and  $p^{(2)}(t)$  to be in state 1 or 2 at time  $t$  to the probability currents by

$$p^{(1)}(t) = \int_{t_0}^t dt' j^{(2)}(t') z^{(1)}(t - t') \quad \text{and} \quad (2.9a)$$

$$p^{(2)}(t) = \int_{t_0}^t dt' j^{(1)}(t') z^{(2)}(t - t'). \quad (2.9b)$$

These equations arise from the fact that the probability  $p^{(i)}(t)$  to be in state  $i$  at time  $t$  is given by the probability current  $j^{(j)}(t')$  into this state at some time  $t'$  in the past between  $t$  and  $t_0$  times the probability  $z^{(i)}(t - t')$  to stay at least the time  $t - t'$  in this state, i.e. at least until time  $t$ . Having motivated eqs. (2.7) and (2.9) the missing steps to arrive at the semi Markovian master equation are straight forward. Laplace transforming eq.(2.7), (2.9) and (2.8), setting  $t_0 = 0$  for the sake of a simplicity one obtains

$$\hat{j}^{(i)}(u) = \hat{j}^{(j)}(u) \hat{w}^{(i)}(u) + \delta_{i,1}, \quad (i, j) = (1, 2) \text{ or } (2, 1) \quad (2.10)$$

$$\hat{p}^{(i)}(u) = \hat{j}^{(j)}(u) \hat{z}^{(i)}(u) \quad (2.11)$$

and

$$\hat{z}^{(i)}(u) = \frac{1 - \hat{w}^{(i)}(u)}{u}, \quad i = 1 \text{ or } 2, \quad (2.12)$$

Here

$$\hat{f}(u) := \int_0^\infty dt \exp(-ut) f(t)$$

denotes the Laplace transform of a function  $f(t)$ . Replacing  $\hat{j}^{(i)}(u)$  and  $\hat{j}^{(j)}(u)$  in eq. (2.10) with the help of eq. (2.11) one ends up with

$$u \hat{p}^{(i)}(u) - \delta_{i,1} = \frac{u \hat{w}^{(j)}(u)}{1 - \hat{w}^{(j)}(u)} \hat{p}^{(j)}(u) - \frac{u \hat{w}^{(i)}(u)}{1 - \hat{w}^{(i)}(u)} \hat{p}^{(i)}(u) \quad (2.13)$$

Eventually, taking into account the initial condition  $p^{(i)}(t_0) = \delta_{i,1}$  one obtains by backward Laplace transforming eq. (2.13) the final result

$$\frac{d}{dt} p^{(1)}(t) = \int_{t_0}^t d\tau \phi^{(2)}(t - \tau) p^{(2)}(\tau) - \int_{t_0}^t d\tau \phi^{(1)}(t - \tau) p^{(1)}(\tau) \quad (2.14a)$$

$$\frac{d}{dt} p^{(2)}(t) = \int_{t_0}^t d\tau \phi^{(1)}(t - \tau) p^{(1)}(\tau) - \int_{t_0}^t d\tau \phi^{(2)}(t - \tau) p^{(2)}(\tau) \quad (2.14b)$$



The memory kernels  $\phi^{(i)}(\tau)$  are related to the waiting time distributions  $w^{(i)}(\tau)$  in terms of their Laplace transforms as

$$\hat{\phi}^{(i)}(u) = \frac{u\hat{w}^{(i)}(u)}{1 - \hat{w}^{(i)}(u)}.$$

Eqs. (2.14) are valid under the assumption that state 1 (or 2) was entered at time  $t_0$ .

This general description, although being very elegant, has some drawbacks if one has to generalize the problem. For example including a time dependent external input implies waiting time distributions, which depend on the running time  $t$ . Thus the possibility to exploit the Laplace transform, which depends on the convolution structure of equations (2.7) and (2.9) is lost. To circumvent this problem we introduce a different master equation approach [88, 103], which relies on some special properties of an excitable system and thus of the observed waiting time distributions in such systems. This property is the stable fixed point, out of which the system is excited by noise, leading as in the double well system to a rate process for the excitation over some effective potential barrier. In the waiting time distributions Fig. 2.6 this rate process is recovered in the exponential decay for long waiting times. Thus the waiting time distribution in the left state can be decomposed into a convolution of a sharply peaked waiting time distribution, which accounts for the motion along the left stable branch of the cubic nullcline (refractory state) Fig. 2.4 and an exponentially decaying waiting time distribution which represents the excitation from the stable fixed point (rest state) over some effective potential barrier due to noise. The waiting time distribution in the firing state is again sharply peaked, accounting for the motion along the right stable branch of the cubic nullcline .

A discrete model for the FHN system in the different dynamical regimes, including excitable behavior, was already presented in [75]. In this work the precise waiting time distributions, under the assumption of a perfect time scale separation and linearization of the nullclines, were evaluated and used to construct a two state model. Our approach in contrast, is a phenomenological one, leading to a three state system, consisting of rest (1), firing (2) and refractory (3) state, where the transitions from firing to refractory and from refractory to rest state are governed by some sharply peaked waiting time distributions while the transition from rest to firing state is a rate process with some rate  $\gamma$ . The output of the three state system, which should be an analogue to the  $x$ -variable (membrane potential) in the FHN-system, assumes a high value in state 2 (firing) and a low value in state 1 and 3 (rest and refractory).

As already suggested it is the Markovian excitation step which allows for an elegant master equation for the evolution of the probabilities  $p^{(i)}(t)$ ,  $i = 1, 2, 3$  to

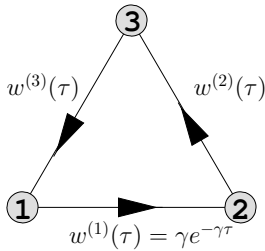


Figure 2.7: The three state model of excitable systems. The excitation from state 1 to 2 is a rate process with rate  $\gamma$  while the transitions from 2 to 3 and 3 to 1 are governed by the residence time distributions  $w^{(2)}(\tau)$  and  $w^{(3)}(\tau)$  respectively.

be in state  $i$  at time  $t$ . The crucial point is that knowing the probability  $p^{(1)}(t)$  to be in the rest state 1 we also know the probability current from state 1 to 2 which for a rate process is given by  $j^{(1)}(t) = \gamma p^{(1)}(t)$ . Having this probability current we can express the probability currents between the other states by an appropriate convolution with the respective waiting time distribution. For example the probability flux into state 1 is given by the integrated probability flux out of state 1 at some time  $t - \tau$  in the past weighted with the probability density  $w(\tau) = (w^{(2)} \circ w^{(3)})(\tau)$  to wait the time  $\tau$  in state 2 and 3 together, such that the system will come back to state 1 at time  $t$  and thus is contributing to the influx into state 1 at time  $t$ .

The resulting master equations, which describe the evolution of the probabilities if we started at time  $t_0$  in state 1 are

$$\begin{aligned} \frac{d}{dt}p^{(1)}(t) &= \int_{t_0}^t dt' \gamma p^{(1)}(t') (w^{(2)} \circ w^{(3)})(t - t') - \gamma p^{(1)}(t) \\ \frac{d}{dt}p^{(2)}(t) &= \gamma p^{(1)}(t) - \int_{t_0}^t dt' \gamma p^{(1)}(t') w^{(2)}(t - t') \\ \frac{d}{dt}p^{(3)}(t) &= \int_{t_0}^t dt' \gamma p^{(1)}(t') w^{(2)}(t - t') - \int_{t_0}^t dt' \gamma p^{(1)}(t') (w^{(2)} \circ w^{(3)})(t - t') \end{aligned} \quad (2.15a)$$

with initial conditions

$$p^{(i)}(t_0) = \delta_{i,1}. \quad (2.15b)$$

Note that due to the Markovian excitation step out of the rest state 1, it is sufficient to specify as an initial condition to *be* in state 1 at time  $t_0$  instead of demanding to *have entered* state 1 at time  $t_0$  as it was done for the general semi-Markovian master equation 2.14.

These special master equations can be shown (cf. appendix A.1) to be equivalent to an appropriate three state version of the general semi Markovian master eqs. (2.14) in the case of an exponentially distributed waiting time in state 1  $w^{(1)}(\tau) = \gamma e^{-\gamma\tau}$ , i.e.  $\phi^{(1)}(\tau) = \gamma\delta(\tau)$ . The advantage of our description comes

into play if, as will be done in the following chapters, we relax the restriction of stationarity but consider for example a periodic driving. In this case the waiting time distributions become time dependent and thus eqs. (2.14) are no longer valid. Even the derivation of some adapted versions of these equations is not possible, as the Laplace transform used in their derivation relies on the convolution between the waiting time distribution and the probability fluxes, a structure which in the case of time dependent waiting time distributions is lost. Our master equation approach however, directly generalizes to time dependent excitation rates  $\gamma \rightarrow \gamma(t)$  and even time dependent waiting time distributions  $w^{(2/3)}(\tau) \rightarrow w^{(2/3)}(\tau, t)$ . Later on it will turn out that to a good approximation it is only the excitation rate which is affected by an external driving or a coupling. The waiting time distributions in state 2 and 3 thus remain independent on the running time.

Finally we mention that the distinction between rest and refractory, does not result from a coarse graining of the phase space of the continuous FHN model. In contrast to the double well system, where the two discrete states were chosen to be the basins of attraction of the two stable stationary states, there is no well defined boundary in phase space which separates the rest and refractory state of the excitable dynamics, as archetypically modeled by the FHN system. Obviously we cannot assign the basin of attraction of the stationary fixed point, to be that part of the phase space which corresponds to the rest state, because this basin of attraction is actually the whole phase space. Although in the rest state the system will be somewhere in the neighborhood of the stable stationary point of the FHN system, it does neither make sense to assign some arbitrary neighborhood around the stable fixed point to the rest state. The distinction between rest and refractory state is solely made in terms of the observed dynamics, being composed of a sharply peaked time responsible for the motion along the right stable branch of the cubic nullcline and an exponentially distributed time representing the excitation dynamics.

### 2.1.3 Renewal Processes

We have considered two examples of a discrete state modeling of continuous systems in terms of a master equation description. Both discrete systems, also being quite different, shared the common property that the waiting times in the different states are independent of each other. As soon as the process has entered a certain state the future evolution does only depend on the time of entering this state. There are no correlations like “*If the process has spend a short time in the right well it will most probably spend a rather long time in the left well thereafter*” or “*If the interspike interval was long the next one will also be long*”. Such a point processes, where the time intervals between subsequent points (events) are independent on the history of the process are called *renewal processes* and have been extensively treated in the literature [22,23]. The term *renewal* stems from the fact

that these processes were first used to analyze statistics of failure times of some machinery components, which when a failure occurred were replaced by a new one. Having in mind the independence of subsequent waiting times, it is evident that the whole dynamics of such a renewal process is fully specified by the statistical properties of the waiting time between subsequent events. These statistics are specified by a waiting time distribution  $w(\tau)$  where  $dP = w(\tau)d\tau$  denotes the probability to observe a waiting time in the interval  $(\tau, \tau + d\tau)$ . In the simplest case this waiting time distribution  $w(\tau)$  between subsequent events is the same for all events. Let  $p_k(t)$  denote the probability to have had  $k$  events up to time  $t$  and  $j_k(t)$  the probability flux that event  $k + 1$  happens at time  $t$ . These quantities can be related to each other using the waiting time distribution. To this end we first have to specify an initial condition. An arbitrary however natural choice is to assume that event 1 happened at time  $t_0$ , which in terms of the probability currents translates to  $j_0(t) = \delta(t - t_0)$ . Then by the same considerations which lead to eqs. (2.9) and (2.7) we obtain

$$p_k(t) = \int_{t_0}^t dt' j_{k-1}(t') z(t - t'), \quad k \geq 1 \quad (2.16a)$$

$$j_k(t) = \int_{t_0}^t dt' j_{k-1}(t') w(t - t'), \quad k \geq 1. \quad (2.16b)$$

where the survival probability  $z(\tau)$  denotes the probability that the interval between two subsequent events will be at least  $\tau$ . In terms of the waiting time distribution this survival probability is given by

$$z(\tau) = 1 - \int_0^\tau d\tau' w(\tau').$$

Often one is confronted with the situation that the transition events are still renewal processes, however the distribution of the waiting times alternately varies. Consider for example an unsymmetric double well potential system or the excitable system, where the waiting time in the firing state obeys a different statistic than the waiting time in the rest and refractory state. Such an *alternating renewal processes* with  $n$  substates is described by  $n$  different waiting time distribution  $w^{(i)}(\tau)$ ,  $i = 1, \dots, n$  which govern consecutively the statistics of the time intervals between two subsequent events. We number the events by a tuple  $(k, i)$ , where  $k$  is augmented after a full sequence of events from 1 to  $n$  while  $i$  numbers the  $n$  different events (see Fig. 2.7). The events thus occur in the order  $\dots (k-1, n), (k, 1), \dots, (k, n), (k+1, 1), \dots$ . The interval between events  $(k, i)$  and  $(k, i+1)$  is governed by  $w^{(i)}(\tau)$  for  $i = 1, \dots, n-1$ , while the interval between events  $(k, n)$  and  $(k+1, 1)$  is determined by  $w^{(n)}(\tau)$ . Denoting by  $p_k^{(i)}(t)$  the probability

to have had event  $(k, i)$  up to time  $t$  and by  $j_k^{(i)}(t)$  the corresponding probability flux that event  $(k, i)$  happens at time  $t$ , we obtain

$$p_k^{(1)}(t) = \int_{t_0}^t dt' j_{k-1}^{(n)}(t') z(t-t'), \quad p_k^{(i)}(t) = \int_{t_0}^t dt' j_k^{(i-1)}(t') z(t-t') \quad (2.17a)$$

$$j_k^{(1)}(t) = \int_{t_0}^t dt' j_{k-1}^{(n)}(t') w(t-t'), \quad j_k^{(i)}(t) = \int_{t_0}^t dt' j_k^{(i-1)}(t') w(t-t'), \quad (2.17b)$$

with  $k \geq 1$  and  $i = 2, \dots, n$ . Again we imposed the initial condition that event  $(1, 1)$  happened at time  $t_0$ , i.e.  $j_0^{(n)}(t) = \delta(t-t_0)$ .

In contrast to the two examples of a bistable and an excitable system in the previous section this description in terms of the events  $(k, i)$  does not only take into account the actual state left or right, rest, firing, or refractory, as represented by  $i$ , but also considers the number of transitions from left to right or the number of spikes which have been emitted (compare Figs. 2.7 and 2.8). This additional

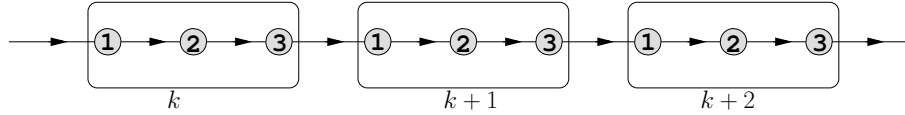


Figure 2.8: Diagrammatic view of the unwrapped discrete state model

information can be ignored by considering

$$p^{(i)}(t) := \sum_k p_k^{(i)}(t) \quad \text{and} \quad j^{(i)}(t) := \sum_k j_k^{(i)}(t)$$

From eqs. (2.17) one then easily obtains the corresponding  $n$  state version of eqs. (2.9) and (2.7),

$$p^{(1)}(t) = \int_{t_0}^t dt' j^{(n)}(t') z(t-t'), \quad p^{(i)}(t) = \int_{t_0}^t dt' j^{(i-1)}(t') z(t-t') \quad (2.18a)$$

and

$$j^{(1)}(t) = \int_{t_0}^t dt' j^{(n)}(t') w(t-t') + \delta(t-t_0) \quad (2.18b)$$

$$j^{(i)}(t) = \int_{t_0}^t dt' j^{(i-1)}(t') w(t-t'). \quad (2.18c)$$

The description of the renewal process in terms of the probabilities  $p_k^{(i)}(t)$  and the corresponding probability currents  $j_k^{(i)}(t)$ , i.e. by some general type of master

equation, is not the only possible way. As mentioned in the beginning of this section the defining quantity of a renewal process is the waiting time distribution  $w(\tau)$  or, in the case of an alternating  $n$  state renewal process  $w^{(1)}(\tau)$  to  $w^{(n)}(\tau)$ . They fully specify the statistics of the random sequence of event times  $\dots, t_k, t_{k+1}, \dots$  or, in the case of an alternating renewal process  $\dots, t_k^{(1)}, t_k^{(2)}, \dots, t_k^{(n)}, t_{k+1}^{(1)}, \dots$ . From these renewal point processes a corresponding stochastic process has to be constructed in order to consider for example spectral properties. Sticking to our examples, the double well system assumes some negative output  $x^{(1)}$  if it is in the left state, while it assumes some positive output  $x^{(2)}$  in the right state. Thus the corresponding stochastic process describing the output of the system is

$$\eta(t) = x^{(i)} \quad \text{if } t_k^{(i)} < t \leq t_k^{(i+1)} \quad (2.19)$$

which directly generalizes to alternating renewal processes with more than two substates. For an ordinary renewal process described by a single waiting time distribution  $w(\tau)$ , there are no substates in which the system's output may assume different values. One possibility to assign a stochastic process to such a renewal dynamics is to consider a sequence of delta spikes, located at the times  $t_i$  of the events

$$\chi(t) = \sum_k \delta(t - t_k). \quad (2.20)$$

This might be for example useful when considering spike trains of neurons. The actual output of the neuron can then be reconstructed from the delta spike train  $\chi(t)$  by a convolution with the stereotypical shape of a spike.

Having sometimes the waiting time distributions available, there are also situations, where we obtain more evidently a master equation for the probabilities of the renewal process. From these master equations the corresponding waiting time distributions do not immediately follow. Remember the three state model of an excitable dynamics eqs. (2.15) or the two state model for a double well system eqs. (2.5). Therefore, in the following chapters our analysis will follow two approaches, based on either some general master equation or the waiting time distributions as either description can be the manifest result of a discrete modeling of some continuous stochastic system.

## 2.2 Quantifying the behavior of a stochastic process

There are several possibilities to analyze and to extract information from a stochastic process  $x(t)$  by assigning quantities to it which have a clear, concrete interpretation. One important such quantity is the spectral power density  $S_x(\omega)$ , which,

in the context of renewal processes, will be introduced in subsection 2.2.1. If it is possible to somehow assign *events* to a stochastic process, the random number  $N_T$  of these events in a time interval of length  $T$  may serve to analyze the regularity of the process. We introduce the number of events, and in particular the mean frequency of events and the effective diffusion coefficient in subsection 2.2.2 and state the known results for renewal processes.

### 2.2.1 The spectral power density

The spectral power density  $S_x(\omega)$  of a stochastic process  $x(t)$  describes how the total power  $\langle x^2 \rangle$  of the stochastic process  $x(t)$  is distributed among the different frequencies. The sharper the spectral power density is concentrated around some frequency, the more regular, i.e. periodic, is the behavior of the stochastic process. In Fig. 2.9 we have plotted the spectral power density of the FHN system for three different noise levels. The most pronounced maximum of  $S_x(\omega)$  at some intermediate noise value, and thus a most regular behavior is termed *coherence resonance* [43, 74, 100].

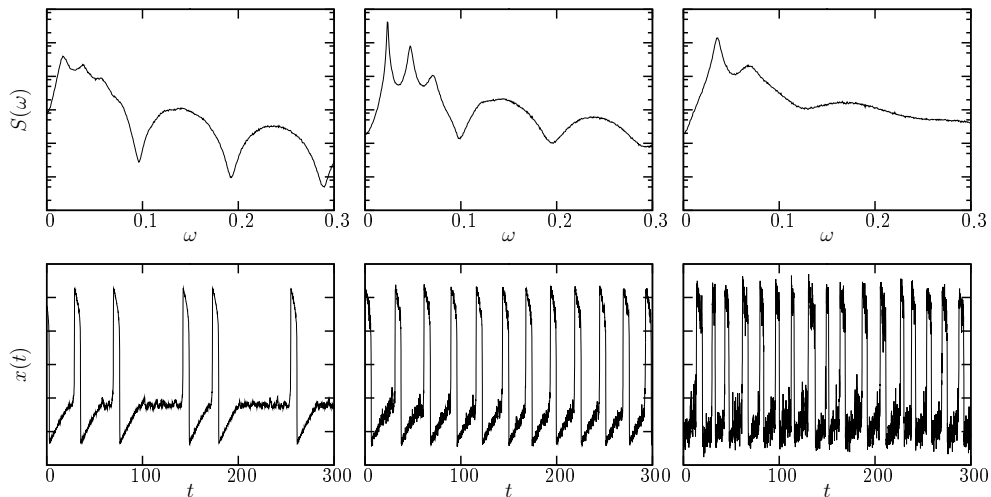


Figure 2.9: Spectrum of the FHN system (top) for different noise levels  $D = 0.0001$  (left),  $D = 0.003$  (middle) and  $D = 0.03$  (right) and a typical spike train (bottom). Other parameters (cf. eqs. (2.6)) are  $a_0 = 0.41$ ,  $a_1 = 0.5$ ,  $\epsilon = 0.01$ .

In our further calculations we use a definition of the spectral power density  $S_x(\omega)$ , which can for example be found in [63], modified by a factor of  $2\pi$  to be consistent with the most part of literature. Our starting point is the observation of

the stationary stochastic process  $x(t)$  on a finite time interval  $(0, T)$ ,  $x_T(t)$ , which can be represented in a Fourier series as

$$x_T(t) = \sum_{k=-\infty}^{\infty} c_{\omega_k, T} \exp(i\omega_k t), \quad \omega_k = \frac{2\pi k}{T} \quad (2.21a)$$

Its discrete Fourier coefficients are given by

$$c_{\omega_k, T} = \frac{1}{T} \int_0^T dt \exp(-i\omega_k t) x_T(t) \quad (2.21b)$$

The spectral power within a frequency interval  $(\omega_a, \omega_b)$  of the stochastic process  $x(t)$  is then given by the sum of all  $\langle |c_{\omega_n, T}|^2 \rangle$ , whose corresponding frequency  $\omega_n$  is in the interval  $(\omega_a, \omega_b)$ , in the limit  $T \rightarrow \infty$ , namely

$$\int_{\omega_a}^{\omega_b} d\omega S_x(\omega) = 2\pi \lim_{T \rightarrow \infty} \sum_{\omega_a < \omega_n < \omega_b} \langle |c_{\omega_n, T}|^2 \rangle. \quad (2.21c)$$

The spectral power density describes how the total power  $\langle x^2 \rangle$  of the stochastic process  $x(t)$  is distributed among the different frequencies. Namely from eq. (2.21a) Parseval's identity gives

$$\frac{1}{T} \int_0^T dt x^2(t) = \sum_{k=-\infty}^{\infty} |c_{\omega_k, T}|^2$$

and thus using the stationarity of the process  $x(t)$  the definition (2.21c) of the spectral power density leads to

$$\int_{-\infty}^{\infty} d\omega S_x(\omega) = 2\pi \langle x^2 \rangle$$

or, considering the spectral power density as a function of frequency  $f = \omega/(2\pi)$ ,

$$\int_{-\infty}^{\infty} df \tilde{S}_x(f) = \langle x^2 \rangle, \quad \tilde{S}(f) = S(2\pi f).$$

The spectral power density of the delta spike sequence eq. (2.20) as well as the spectral power density of the pulse sequence eq. (2.19) can be expressed explicitly in terms of the waiting time distributions  $w(\tau)$  or  $w^{(0)}(\tau)$  and  $w^{(1)}(\tau)$  respectively. These expressions were first derived in [124]. A different derivation of these results is given in appendix A.2. For the delta spike sequence eq. (2.20) one obtains

$$S_\chi(\omega) = \frac{2\pi}{\langle \tau \rangle^2} \delta(\omega) + \frac{1}{\langle \tau \rangle} \frac{1 - |\hat{w}(\omega)|^2}{|1 - \hat{w}(\omega)|^2} \quad (2.22)$$



where

$$\hat{w}(\omega) := \int_0^\infty d\tau e^{-i\omega\tau} w(\tau) \quad (2.23)$$

is the characteristic function of the waiting time density  $w(\tau)$  whereas

$$\langle \tau \rangle = \int_0^\infty d\tau \tau w(\tau)$$

denotes the mean waiting time. The corresponding result for the pulse sequence eq. (2.19) is

$$\begin{aligned} S_\eta(\omega) = & \frac{2\pi(a\langle\tau^{(0)}\rangle + b\langle\tau^{(1)}\rangle)^2}{(\langle\tau^{(0)}\rangle + \langle\tau^{(1)}\rangle)^2} \delta(\omega) \\ & + \frac{2(a-b)^2}{\omega^2(\langle\tau^{(0)}\rangle + \langle\tau^{(1)}\rangle)} \operatorname{Re} \frac{(1 - \hat{w}^{(0)}(\omega))(1 - \hat{w}^{(1)}(\omega))}{1 - \hat{w}^{(0)}(\omega)\hat{w}^{(1)}(\omega)} \end{aligned} \quad (2.24)$$

where again  $\hat{w}^{(0)}$  and  $\hat{w}^{(1)}$  are the characteristic functions of the respective waiting time density and  $\langle\tau^{(0)}\rangle$  and  $\langle\tau^{(1)}\rangle$  are the corresponding mean waiting times.

Finally we want to mention the relation between the spectral power density and the auto correlation function of the stochastic process (For a short derivation see appendix A.3). This relation, known as the Wiener-Khinchine theorem reads

$$S_x(\omega) = \int_{-\infty}^\infty d\tau \exp(-i\omega\tau) c_{x,x}(\tau) \quad (2.25)$$

where

$$c_{x,x}(\tau) = \langle x(t)x(t+\tau) \rangle$$

is the auto correlation function of the stochastic process  $x(t)$ . As  $x(t)$  is assumed to be stationary  $c_{\tilde{x},\tilde{x}}(\tau)$  is independent on  $t$ . Sometimes eq. (2.25) is taken as the definition of the spectral power density [124]. However if the process  $x(t)$  is not stationary but periodic in time this will lead to difficulties as the correlation function then depends explicitly on time  $t$ . In this case an additional time average over one period of the process is needed [60] (see section 3.1). Using the definition (2.21c) this additional averaging procedure is dispensable.

### The limits $\omega \rightarrow 0$ and $\omega \rightarrow \infty$ of the spectral power density

The spectral power density for the delta spike sequence eq. (2.22) and for the pulse sequence eq. (2.24) can be further evaluated in the limits  $\omega \rightarrow 0$  and  $\omega \rightarrow \infty$  (see

e.g. [72]). Expressing the characteristic function  $\hat{w}(\omega)$  eq. (2.23) of the waiting time density in terms of the moments of the waiting time,

$$\hat{w}(\omega) = \sum_{k=0}^{\infty} \frac{(-i\omega)^k}{k!} \langle \tau^k \rangle$$

one ends up with

$$\lim_{\omega \rightarrow 0} S_\chi(\omega) = \frac{\langle \tau^2 \rangle - \langle \tau \rangle^2}{\langle \tau \rangle^3} \quad (2.26)$$

and

$$\lim_{\omega \rightarrow 0} S_\eta(\omega) = (a - b)^2 \frac{\langle (\tau^{(0)} - \langle \tau^{(0)} \rangle)^2 \rangle \langle \tau^{(1)} \rangle^2 + \langle (\tau^{(1)} - \langle \tau^{(1)} \rangle)^2 \rangle \langle \tau^{(0)} \rangle^2}{(\langle \tau^{(0)} \rangle + \langle \tau^{(1)} \rangle)^3}$$

For  $\omega \rightarrow \infty$  the characteristic function of the waiting time density generally decreases to zero<sup>2</sup>. Thus from eqs. (2.22) and (2.24) one deduces

$$\lim_{\omega \rightarrow \infty} S_\chi(\omega) = \frac{1}{\langle \tau \rangle}, \quad \text{and} \quad \lim_{\omega \rightarrow \infty} S_\eta(\omega) = 0. \quad (2.27)$$

### The spectral power density—comparison between the threestate model and the FHN system

We finally want to compare the spectral power density of the FHN system (2.6) with the spectral power density of the threestate model for excitable systems (2.15). To this end we assume a fixed firing  $\tau^{(2)}$  and refractory time  $\tau^{(3)}$ , i.e.  $w^{(2)}(\tau) = \delta(\tau - \tau^{(2)})$  and  $w^{(3)}(\tau) = \delta(\tau - \tau^{(3)})$ . Assigning further the output 1 to the firing state and  $-1$  to the rest and refractory state, the spectral power density of the system can be evaluated according to eq. (2.24) (neglecting the term  $\propto \delta(\omega)$ ) as

$$S(\omega) = \frac{4}{(T + \frac{1}{\gamma})\omega^2} \frac{\sin^2 \frac{\omega\tau^{(2)}}{2}}{1 + 2\frac{\gamma^2}{\omega^2}(1 - \cos \omega T) + \frac{\gamma}{\omega} \sin \omega T}, \quad T = \tau^{(2)} + \tau^{(3)}. \quad (2.28)$$

The precise values of  $\tau^{(2)}$ ,  $\tau^{(3)}$  and  $\gamma$  are estimated from the waiting time distributions of the FHN Fig. 2.6 as

$$\tau^{(2)} = 65, \quad \tau^{(3)} = 220 \quad \text{and} \quad \gamma = 0.0046. \quad (2.29)$$

With these values we have compared the spectral power density of the threestate model (2.28) with the numerically obtained spectral power density of the output  $x(t)$  of the FHN system (2.6) with parameters as in Fig. 2.6. The result is presented in Fig. 2.10 showing a good quantitative agreement between the three state model spectral power density and the spectral power density of the archetypal excitable system, the FHN model.

---

<sup>2</sup>There exist pathological cases like a delta peaked waiting time density, i.e. a fixed non random waiting time for which this is not true

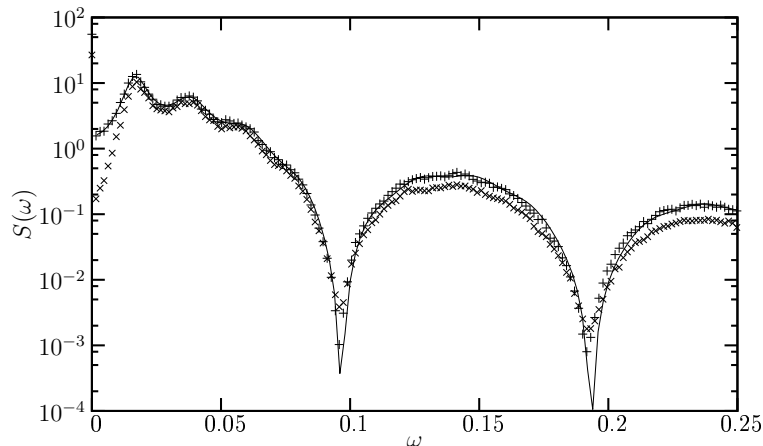


Figure 2.10: Spectral power density according to eq. (2.28) of a threestate system (solid line) with fixed waiting times  $\tau^{(2)} = 65$  and  $\tau^{(3)} = 220$  in state 2 and 3 respectively and an excitation rate  $\gamma_0 = 0.0046$  compared to the spectral power density of the output  $x(t)$  of the FitzHugh-Nagumo system eq. (2.6). ( $\times$  :  $x(t)$ ,  $+$ : dichotomically filtered output 1 if  $x(t) > 0$  and  $-1$  if  $x(t) \leq 0$ ) with  $a_0 = 0.41$ ,  $a_1 = 0.5$ ,  $\epsilon = 0.01$  and  $D = 0.0001$ .

## 2.2.2 Effective Diffusion

Assume that we can assign characteristic events to a stochastic process, like the crossing of the potential barrier in a double well system or the generation of a spike in an excitable system (see Figs. 2.2 and 2.5). If we already start from a discrete state system, the transitions between these states may naturally serve as characteristic events. Properties of the random sequence of such events  $\dots, t_{i-1}, t_i, t_{i+1}, \dots$  like the frequency of events or the regularity of their occurrence allow to characterize the underlying stochastic process. To visualize this effect we consider the spiking of the stochastic FHN model. In Fig. 2.11 we have plotted the number  $N_{0,t}$  of spikes in the time interval  $(0, t)$  as a function of the interval length  $t$  at three different noise levels. For each noise level we considered 20 different realizations of the process. The mean as well as the variance of  $N_{0,t}$  grow linearly with increasing  $t$  however the rate of growth is different. The smaller the variance grows the more regular is the process. Again we observe a most regular behavior at an intermediate noise level which is a fingerprint of *coherence resonance* [43, 74, 100] which was already represented in the spectral power density Fig. 2.9.

To put these observations on a firm ground, consider the random number of events  $N_{t_0,t}$  in a time interval  $(t_0, t]$ . The instantaneous mean frequency  $\nu_{t_0}(t)$  of

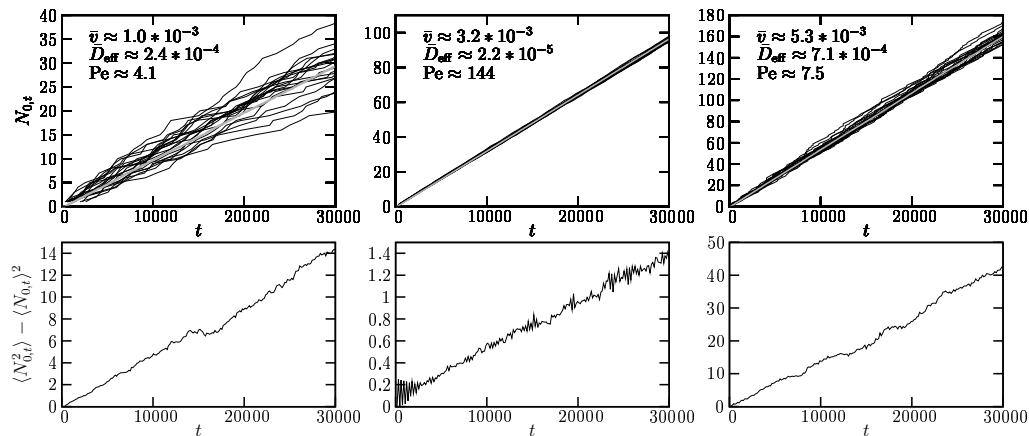


Figure 2.11: Top: 20 realizations of the number of spikes  $N_{0,t}$  (black lines) as well as the mean number of spikes  $\langle N_{0,t} \rangle$  (gray line) for the FHN system for different noise levels  $D = 0.0001$  (left),  $D = 0.001$  (middle) and  $D = 0.01$  (right) and the corresponding mean velocity  $\bar{v}$  and effective diffusion constant  $\bar{D}_{\text{eff}}$  as well as the Péclet number.

Bottom: The variance  $\langle N_{0,t}^2 \rangle - \langle N_{0,t} \rangle^2$  of the number of spikes (taken from 200 realization).

Other parameters (cf. eqs. (2.6)) are  $a_0 = 0.41$ ,  $a_1 = 0.5$ ,  $\epsilon = 0.01$ .

events is defined as the increase of the mean number of events in time,

$$v_{t_0}(t) = \frac{d}{dt} \langle N_{t_0,t} \rangle$$

while the instantaneous effective diffusion constant quantifies the increase of the variance of the number of events in time,

$$D_{\text{eff},t_0}(t) = \frac{d}{dt} \frac{\langle N_{t_0,t}^2 \rangle - \langle N_{t_0,t} \rangle^2}{2}.$$

Often the long time averaged quantities

$$\bar{v} = \lim_{t \rightarrow \infty} \frac{\langle N_{t_0,t} \rangle}{t} \quad \text{and} \quad \bar{D}_{\text{eff}} = \lim_{t \rightarrow \infty} \frac{\langle N_{t_0,t}^2 \rangle - \langle N_{t_0,t} \rangle^2}{2t}$$

provide the information of interest. For the stationary processes considered here the instantaneous mean frequency and the instantaneous effective diffusion coefficient do neither explicitly depend on  $t_0$  nor on  $t$  but only on the length  $t - t_0$  of the considered interval. They therefore agree with the long time averaged quantities

$\bar{v}$  and  $\bar{D}_{\text{eff}}$ . However if we relax the assumption of stationarity and consider for example periodic renewal processes as will be done in chapter 4 the instantaneous mean frequency  $v_{t_0}(t)$  and instantaneous effective diffusion coefficient  $D_{\text{eff},t_0}(t)$  are no longer constant. Then the corresponding long time averaged quantities  $\bar{v}$  and  $\bar{D}_{\text{eff}}$  are the appropriate mean to capture the system's behavior by a few numbers.

The effective diffusion constant quantifies how fast the number of events of different realizations of the process diverge on average. A process running at twice the speed has a twice the mean frequency and effective diffusion constant. To have a measure of the regularity of the process which is independent on its absolute speed one considers the Péclet number

$$\text{Pe} = \frac{\bar{v}}{\bar{D}_{\text{eff}}} = \lim_{T \rightarrow \infty} \frac{2\langle N_{t_0,t} \rangle}{\langle N_{t_0,t}^2 \rangle - \langle N_{t_0,t} \rangle^2}.$$

This number no longer depends on the absolute speed of the process and thus is better suited to measure the regularity of the process than the effective diffusion constant. The higher the Péclet number the more regular is the process. The Péclet number can be interpreted as the mean number of events which happen until the variance of the number of events is one. Namely assume that the variance is one. This happens after a time  $T_0$  defined by  $T_0 \bar{D}_{\text{eff}} = 1$ . Then it immediately follows from the definition that  $\text{Pe} = T_0 v$  which is the average number of events which happened within the time interval  $T_0$ . Thus Pe gives the average number of events after which the variance of the event number has grown to one on average.

For a renewal process with a waiting time  $w(\tau)$  between subsequent events these quantities can be calculated [22]. Denoting the moments of the waiting time by

$$\langle \tau^n \rangle = \int_0^\infty d\tau \tau^n w(\tau)$$

one obtains

$$\bar{v} = \frac{1}{\langle \tau \rangle} \quad \text{and} \quad \bar{D}_{\text{eff}} = \frac{\langle \tau^2 \rangle - \langle \tau \rangle^2}{2\langle \tau \rangle^3}. \quad (2.30)$$

and therefore

$$\text{Pe} = \frac{2\langle \tau \rangle^2}{\langle \tau^2 \rangle - \langle \tau \rangle^2}.$$

Interestingly the mean frequency  $v$  agrees with the high frequency limit (2.27) of the spectral density of the corresponding delta spike train  $\chi(t)$ ,

$$\bar{v} = \lim_{\omega \rightarrow \infty} S_\chi(\omega)$$

while the effective diffusion coefficient (2.30) agrees up to a factor of 2 with the low frequency limit (2.26) of the spectral density of a delta spike train [72]

$$\bar{D}_{\text{eff}} = \frac{1}{2} \lim_{\omega \rightarrow 0} S_{\chi}(\omega)$$

The Péclet number can thus be expressed as

$$\text{Pe} = \frac{2 \lim_{\omega \rightarrow 0} S_{\chi}(\omega)}{\lim_{\omega \rightarrow \infty} S_{\chi}(\omega)}$$

At the end of section 4.1 we will show that this equivalence is preserved if we consider periodic instead of stationary delta sequences. Additionally, this equivalence is not a consequence of the renewal property of the underlying process but holds for general periodic or stationary point processes and the corresponding delta sequences which will be shown in section 4.1.

## 2.3 Summary

We have introduced two examples of a discrete state description of continuous stochastic systems, the well known two state Markovian approximation of the dynamics of an overdamped particle in a double well potential [83] and a three state non Markovian model for excitable dynamics [88, 103]. While the first one is described by an ordinary master equation the second one is described by a generalized master equation. We introduced a special type of master equation, which relied on the fact that the discrete three state model of excitable dynamics exhibits a Markovian step which describes the excitation from the rest state. In contrast to the known semi Markovian master equation for general renewal processes, our description is amenable to further generalizations, like for example the influence of a time dependent external signal. The introduced three state model for excitable dynamics will play a central role in the following chapters.

In both models the transition times between the states constitute a renewal process, which is fully characterized by the waiting time distributions in the discrete states. We introduced the spectral power density as well as the effective diffusion coefficient and the Péclet number as measures to quantify certain aspects of the corresponding stochastic process, especially its regularity, and reviewed the known results for these quantities for stationary renewal processes. In the following chapters the situation will be extended to periodically driven systems, leading to periodic renewal processes and finally globally coupled models are considered. Depending on the specific situation either a description in terms of a generalized master equation or in terms of the waiting time distributions will be advantageous. Therefore we will pursue both approaches in the rest of the present work.



# Chapter 3

## Periodically Driven Systems-Spectral Based Quantification

Periodic signals naturally occur in a variety of different systems, ranging from light and sound to less evident examples like the periodic modulation of the earth's orbit's eccentricity. Nowadays equally important are technically generated periodic signals, like radio waves. This ubiquity of periodic signals encouraged a lot of research on the behavior of periodically driven systems. In cooperation with noise, periodic driving generates some counter intuitive effects, subsumed under the notion of *stochastic resonance*. This phenomenon, describing a most periodic response to the periodic signal at some finite non vanishing noise level has been observed in many different systems ranging from ring lasers [82] to the prey capture of animals [37, 114] (for a comprehensive overview see [1] and references therein). In an ensemble of coupled systems this effect may be further enhanced [62, 119], subsumed under the notion of *array enhanced stochastic resonance*.

In the next two chapters we investigate the behavior of periodically driven bistable and excitable stochastic systems. The analysis is based on the discrete modeling introduced in chapter 2. While in the present chapter we consider spectral properties of the periodically driven stochastic system leading to the well known characterization of stochastic resonance in terms of *spectral power amplification* and *signal to noise ratio* (for an overview see [41]), in chapter 4 synchronization properties of the system to the periodic signal are investigated [36, 40, 96, 127]. In both chapters the main focus is on the development of methods to calculate some characteristic quantities of the system's response to the periodic signal. These methods are then applied to the discrete state models of bistable and excitable system. The analytic results obtained for the discrete systems reproduce well the observed behavior of the underlying continuous stochastic dynamics.



### 3.1 The structure of the spectral power density for periodic processes

Consider a periodic stochastic process  $x(t)$  with periodicity  $\mathcal{T} = 2\pi/\Omega$ . A periodic stochastic process is a stochastic process whose statistical properties, like mean value, correlation functions, one time probability distribution etc. are invariant with respect to a discrete time shift of integer multiples of the period  $\mathcal{T}$ . A single realization of the process certainly is not periodic.

The mean value of a periodic process, being a periodic function of  $t$ , can be expanded into a Fourier series

$$\langle x(t) \rangle = \sum_{k=-\infty}^{\infty} \hat{x}_k \exp(ik\Omega t), \quad \hat{x}_k = \hat{x}_{-k}^*. \quad (3.1)$$

Its auto correlation function no longer depends solely on the time difference as is the case for stationary processes, i.e. processes which are invariant under arbitrary time shifts. It also depends on the actual time. Subtracting the product of the time dependent mean values from the autocorrelation function the resulting function

$$c_{\tilde{x},\tilde{x}}(t,t') \quad : \quad = \langle x(t)x(t') \rangle - \langle x(t) \rangle \langle x(t') \rangle = \langle (x(t) - \langle x(t) \rangle)(x(t') - \langle x(t') \rangle) \rangle \quad (3.2)$$

is assumed to exponentially decay to zero for increasing time difference  $t - t'$  due to the stochastic nature of the process. This means, that although the correlation function does not vanish or decay to a constant value for long time distances, this is only due to the periodicity, which modulates the expectation value. To investigate the structure of the spectral power density for such a periodic stochastic process we consider the coefficients

$$\langle |c_{\omega,T}|^2 \rangle = \frac{1}{T^2} \int_0^T dt \int_0^T dt' e^{-i\omega(t-t')} \langle x(t)x(t') \rangle. \quad (3.3)$$

as used in the definition of the power spectral density eq. (2.21c). Substituting eq. (3.2) therein we obtain

$$\langle |c_{\omega,T}|^2 \rangle = \left| \frac{1}{T} \int_0^T dt e^{-i\omega t} \langle x(t) \rangle \right|^2 + \frac{1}{T^2} \int_0^T dt \int_0^T dt' e^{-i\omega(t-t')} c_{\tilde{x},\tilde{x}}(t,t').$$

As  $c_{\tilde{x},\tilde{x}}(t,t') \rightarrow 0$  for  $|t - t'| \rightarrow \infty$  the second summand will tend to zero as  $\frac{1}{T}$  as  $T$  goes to  $\infty$ . Inserting  $\langle x(t) \rangle$  from eq. (3.1) into the first summand one easily verifies that for  $\omega \neq n\Omega$ ,  $n \in \mathbb{Z}$ , this term vanishes in the limit  $T \rightarrow \infty$  as  $\frac{1}{T^2}$ . However if  $\omega = n\Omega$  it does not vanish but is given by  $|\hat{x}_n|^2$ . These non vanishing

coefficients lead to the appearance of delta spikes in the power spectral density while the coefficients vanishing as  $\frac{1}{T}$  constitute the continuous part of the spectral power density (cf. the existence of a delta peak at  $\omega = 0$  for stationary processes with non vanishing mean, appendix A.2). Thus the spectral power density adopts the form

$$S_x(\omega) = S_{\text{bg}}(\omega) + 2\pi \sum_{n=-\infty}^{\infty} s_n \delta(\omega - n\Omega), \quad s_n = |\hat{x}_n|^2. \quad (3.4)$$

The continuous part

$$S_{\text{bg}}(\omega) = \lim_{T \rightarrow \infty} \frac{1}{T} \int_0^T dt \int_0^T dt' e^{-i\omega(t-t')} c_{\bar{x},\bar{x}}(t,t'). \quad (3.5)$$

is called background spectral power density in the following. Note that the delta peak at  $\omega = 0$  is not contained in  $S_{\text{bg}}(\omega)$  but represented by  $s_0$  although it persists in the case of stationary processes.

In contrast to stationary processes, the Wiener-Khinchine theorem in its original form (2.25) is no longer valid for periodic processes as already the correlation function no longer depends only on the time difference but also on the running time. However replacing the auto correlation function with the corresponding period averaged auto correlation function

$$\bar{c}_{x,x}(\tau) := \frac{1}{T} \int_0^T dt c_{x,x}(t, \tau) \quad (3.6)$$

the Wiener-Khinchine theorem for periodic processes

$$S_x(\omega) = \int_{-\infty}^{\infty} d\tau e^{-i\omega\tau} \bar{c}_{x,x}(\tau) \quad (3.7)$$

holds [60] (for a short derivation see appendix A.3.2).

In our analysis of the spectral properties of periodic renewal processes in the following sections our starting point will always be the definition (2.21c) of the spectral power density, and not the generalized Wiener-Khinchine theorem eq. (3.7). We thus avoid the need of an additional period average.

## 3.2 Spectral power amplification and signal to noise ratio

In the previous section we have seen that the periodicity of the stochastic process leads to delta peaks appearing at integer multiples of the driving frequency in the

spectral power density. They reflect the fact, that the correlation function of the process no longer vanishes (or becomes constant if the process has a non vanishing mean) for increasing time differences but remains oscillating with finite amplitude for arbitrary time differences. If the periodicity of the process is induced by a periodic driving one probably wants to quantify its influence. Consider a periodic signal

$$s(t) = A_{\text{in}} \exp(i\Omega t) + c.c. \quad (3.8)$$

which somehow affects the system's dynamics rendering the process periodic with the period  $\mathcal{T} = \frac{2\pi}{\Omega}$  of the signal. The larger the power  $s_1$  of the process at the frequency  $\Omega$  of the signal compared to the power  $|A_{\text{in}}|^2$  of the signal itself the better (in some sense) the signal is amplified by the process. Therefore the relation between signal power and the spectral power of the process at the signal frequency is called spectral power amplification (SPA),

$$\text{SPA} = \frac{s_1}{|A_{\text{in}}|^2}. \quad (3.9)$$

As the power  $s_1$  corresponds to the squared oscillation amplitude  $|\hat{x}_1|^2$  of the mean value of the process (see eqs. (3.1) and (3.4)) the spectral power amplification can also be interpreted as the relation between the signal amplitude and the amplitude of the mean value of the process at the signal frequency  $\Omega$ . If the SPA is greater than 1 the input signal  $s(t)$  is amplified in the sense, that the amplitude of the oscillations of the systems mean value is larger than the amplitude of the signal.

However the result of some measurement is in general not the mean value of the process but a single realization restricted to some time interval  $(0, T)$ . As the system is stochastic, the oscillations of the mean value can be hidden beneath the fluctuations in such a single observation of the process. To quantify this effect one introduces the signal to noise ratio (SNR) as the relation between the oscillation power and the background spectral power at the corresponding frequency,

$$\text{SNR} = \frac{2\pi s_1}{S_{\text{bg}}(\Omega)} \quad (3.10)$$

Sometimes one also uses a variant of the SNR, which is scaled by the input power of the signal. However as we only consider the SNR in linear response for some fixed small signal amplitude and not its dependence on the signal amplitude itself, the unscaled SNR as defined in eq. (3.10) is sufficient for our purposes. Generally the SNR and in particular its scaled variant provides a more adequate mean to quantify the quality, in the sense of signal extraction from a noisy background, of the response to a periodic signal than the SPA if only a limited observation time is available. We mention that there exist other measures to quantify the

response of a stochastic system to a signal, based on cross correlations between signal and system [20,21], on the structure of the resulting waiting (residence) time distributions [18,141], on the relative entropies and other information theoretical quantities. In contrast to the SNR and SPA they can also be applied to quantify the response to non periodic signals, leading to the effect of aperiodic stochastic resonance [21]. Considering only periodic signals, though, we restrict our analysis to the SPA and SNR.

### 3.3 SPA and SNR of periodically driven renewal processes

In this section we develop concepts to evaluate the spectral power amplification and the signal to noise ratio for renewal processes driven by a weak periodic signal. These periodic processes are a generalization of the stationary renewal processes introduced in chapter 2, which occurred as a discrete state approximation to excitable or bistable dynamics. Thus we expect periodic renewal processes to be the right object to be studied when modeling periodically driven bistable or excitable dynamics as discrete state systems.

As mentioned in chapter 2 a renewal process can be either specified by a master equation, i.e. a linear equation governing the probabilities to be in a certain discrete state, or by directly specifying the statistics of the waiting time between subsequent events. In the case of periodic renewal processes these waiting times however are no longer governed by a time independent waiting time distribution  $w(\tau)$  or, for the alternating renewal process, alternatingly by  $w^{(i)}(\tau)$ . Instead the periodicity is reflected by the fact, that the waiting time distributions now depend on the time  $t$  of the previous event in a periodic way,

$$w(\tau) \longrightarrow w(\tau, t) = w(\tau, t + \mathcal{T})$$

or

$$w^{(i)}(\tau) \longrightarrow w^{(i)}(\tau, t) = w^{(i)}(\tau, t + \mathcal{T})$$

respectively, where  $\mathcal{T} = 2\pi/\Omega$  is the period of the driving. These periodically time dependent waiting time distributions govern the probability

$$dP = w(\tau, t_i)d\tau$$

that event  $i + 1$  happens in the time interval  $(t_i + \tau, t_i + \tau + d\tau]$  if event  $i$  has been happened at time  $t_i$ . Normalization holds at arbitrary time  $t$

$$\int_0^\infty d\tau w(\tau, t) = 1.$$

The resulting periodic process still has the renewal property in the sense that as soon as we know the actual time of an event ( or equivalently the respective signal phase) the time up to the next event is statistically fully determined, i.e. independent on the history of the process. Especially it is independent of the previous waiting time. However due to the periodic driving the correlation function between subsequent intervals is not zero. To render this statement more precisely, let  $\tau_{i-1} = t_i - t_{i-1}$  denote the interval between event  $i - 1$  and event  $i$  and  $\tau_i = t_{i+1} - t_i$  the interval between event  $i$  and event  $i + 1$ . Then

$$\langle \tau_i \tau_{i+1} \rangle - \langle \tau_i \rangle \langle \tau_{i+1} \rangle \neq 0$$

in general, i.e. subsequent intervals are correlated. However subsequent intervals, conditioned on the time  $t_i$  or equivalently on the phase  $\phi_i = \Omega t_i \bmod 2\pi$  of the event  $i$  in between are independent,

$$\langle \tau_i \tau_{i+1} | \phi_i \rangle - \langle \tau_i | \phi_i \rangle \langle \tau_{i+1} | \phi_i \rangle = 0.$$

In a master equation description the periodicity is reflected by the fact that the master operator  $\mathcal{M}$  becomes periodically time dependent with the period of the periodic driving, which we notationally represent by a subscript  $t$ ,  $\mathcal{M} \longrightarrow \mathcal{M}_t = \mathcal{M}_{t+\mathcal{T}}$ .

Depending on the situation either approach might be favorable. Sometimes it is straight forward to set up a master equation for the system considered, while in other cases, the periodically time dependent waiting time distribution might be given. Therefore, we investigate the spectral properties of periodic renewal processes in the framework of both approaches. In contrast to the case of stationary renewal processes a closed evaluation of the full spectral power density is in general no longer possible for a periodic renewal process, notwithstanding the closed evaluation of the full spectral power density in a dichotomically periodically driven Markovian two state renewal process [15]. The weights of the delta peaks at integer multiples of the driving frequency however, can still be evaluated, leading for weak signals in linear order in the signal amplitude to closed expressions for the SPA and SNR in terms of easily evaluable properties of the master operator or the time dependent waiting time distributions respectively.

### 3.3.1 A master equation approach

Consider a discrete  $n$  state system described by the probabilities  $p^{(i)}(t)$  to be in state  $i$  at time  $t$ . We assume that this system is influenced by a periodic signal with period  $\mathcal{T} = 2\pi/\Omega$ . The evolution of these probabilities is supposed to be governed by some generalized master equation

$$\mathcal{M}_t^{(i)}[p^{(1)}, \dots, p^{(n)}](t) = 0, \quad i = 1, \dots, n \quad (3.11)$$

where  $\mathcal{M}_t$  is the linear master operator, supplemented with the normalization condition

$$\sum_{j=1}^n p^{(j)}(t) = 1. \quad (3.12)$$

Due to this normalization condition we can neglect one of the  $n$  parts of the master equation (3.11) which we choose to be the first one,  $i = 1$ . The periodic driving is reflected by the periodicity of the master operator

$$\mathcal{M}_{t+\mathcal{T}} = \mathcal{M}_t. \quad (3.13)$$

To illustrate this setting we consider two examples. A Markovian two state system with periodic driving is governed by [83]

$$\frac{d}{dt}p^{(1)}(t) = -\gamma_{1\rightarrow 2}(t)p^{(1)}(t) + \gamma_{2\rightarrow 1}(t)p^{(2)}(t) \quad (3.14)$$

$$\frac{d}{dt}p^{(2)}(t) = \gamma_{1\rightarrow 2}(t)p^{(1)}(t) - \gamma_{2\rightarrow 1}(t)p^{(2)}(t). \quad (3.15)$$

With the normalization condition (3.12) one of these two equation becomes obsolete, which we choose to be the first one. Then the corresponding master operator is given by

$$\mathcal{M}_t^{(2)}[p^{(1)}, p^{(2)}](t') = \frac{d}{dt'}p^{(2)}(t') + \gamma_{2\rightarrow 1}(t)p^{(2)}(t') - \gamma_{1\rightarrow 2}(t)p^{(1)}(t')$$

which due to the periodicity of the rates  $\gamma_{i\rightarrow j}(t) = \gamma_{i\rightarrow j}(t + \mathcal{T})$  obviously fulfills (3.13). Another example is the periodically driven three state model for excitable systems which is obtained from the three state model for excitable dynamics introduced in subsection 2.1.2 by considering a periodically modulated excitation rate. Its is governed by<sup>1</sup>

$$p^{(2)}(t) = \int_0^\infty d\tau \gamma(s(t-\tau))p^{(1)}(t-\tau)z^{(2)}(\tau) \quad (3.16a)$$

$$p^{(3)}(t) = \int_0^\infty d\tau \gamma(s(t-\tau))p^{(1)}(t-\tau) \int_0^\tau d\tau' w^{(2)}(\tau')z^{(3)}(\tau-\tau'). \quad (3.16b)$$

supplemented with the normalization condition

$$1 = p^{(1)}(t) + p^{(2)}(t) - p^{(3)}(t) \quad (3.16c)$$

---

<sup>1</sup> the motivation and derivation of these equations is postponed to subsection 3.3.1 where this system will be analyzed in greater detail

In this case

$$\begin{aligned}\mathcal{M}_t^{(2)}[p^{(1)}, p^{(2)}, p^{(3)}](t') &= p^{(1)}(t') - \int_0^\infty d\tau \gamma(s(t-\tau)) p^{(1)}(t'-\tau) z^{(2)}(\tau) \\ \mathcal{M}_t^{(3)}[p^{(1)}, p^{(2)}, p^{(3)}](t') &= p^{(2)}(t') - \int_0^\infty d\tau \gamma(s(t-\tau)) p^{(1)}(t'-\tau) \\ &\quad \int_0^\tau d\tau' w^{(2)}(\tau') z^{(3)}(\tau-\tau').\end{aligned}\quad (3.17)$$

Again the periodicity condition (3.13) is met.

Assigning the output  $x^{(i)}$  to state  $i$  the mean output of the system is given by

$$\langle x(t) \rangle = \sum_{i=1}^n x^{(i)} p^{(i)}(t). \quad (3.18)$$

Thus given the asymptotic periodic solution of the master eqs. (3.11) we can evaluate the weights of the delta peaks in the spectral power density at integer multiples of the driving frequency according to eq. (3.1) and (3.4). The periodic solutions of the  $p^{(i)}(t)$  can be expressed in a Fourier series

$$p^{(i)}(t) = \sum_{k=-\infty}^{\infty} \hat{p}_k^{(i)} \exp(ik\Omega t), \quad \Omega = \frac{2\pi}{\mathcal{T}}. \quad (3.19)$$

Due to the linearity of the master operator its action in Fourier space is also linear. Thus eqs. (3.11) can be expressed in Fourier space as

$$\sum_{j=1}^n \sum_{l=-\infty}^{\infty} \hat{\mathcal{M}}_{k,l}^{(i,j)} \hat{p}_l^{(j)} = 0, \quad i = 2, \dots, n \quad (3.20a)$$

with the normalization condition (3.12)

$$\sum_{j=1}^n \hat{p}_k^{(j)} = \delta_{k,0} \quad (3.20b)$$

The coefficients  $\hat{\mathcal{M}}_{k,l}^{(i,j)}$  can be obtained as (see appendix B.2)

$$\hat{\mathcal{M}}_{k,l}^{(i,j)} = \frac{1}{\mathcal{T}} \int_0^{\mathcal{T}} dt \mathcal{M}_t^{(i)}[\dots, 0, \exp(il\Omega \cdot), 0, \dots](t) \exp(-ik\Omega t). \quad (3.21)$$

If we assume, that the periodicity of the master operator is due to the influence of an external periodic signal with amplitude  $A_{\text{in}}$  (not necessarily harmonic) the

only coefficients  $\hat{\mathcal{M}}_{k,l}^{(i,j)}$  which do not vanish with vanishing input signal, i.e. for  $A_{\text{in}} \rightarrow 0$  are  $\hat{\mathcal{M}}_{k,k}^{(i,j)}$ . Thus eqs. (3.20) reduces in  $O(1)$  to

$$\sum_{j=1}^n \hat{\mathcal{M}}_{0,0}^{(i,j)} \hat{p}_0^{(j)} = 0, \quad i = 2, \dots, n \quad \text{and} \quad \sum_{j=1}^n \hat{p}_0^{(j)} = 1. \quad (3.22)$$

All other  $p_k^{(j)}$  are 0 in  $O(1)$  due to the normalization condition (3.20b). In order  $O(A_{\text{in}})$  eqs. (3.20) are given by

$$\sum_{j=1}^n \hat{\mathcal{M}}_{k,0}^{(i,j)} \hat{p}_0^{(j)} + \hat{\mathcal{M}}_{k,k}^{(i,j)} \hat{p}_k^{(j)} = 0, \quad i = 2, \dots, n \quad \text{and} \quad \sum_{j=1}^n \hat{p}_k^{(j)} = 0. \quad (3.23)$$

Although these equations can be in principle solved for arbitrary  $n$  we only present the general solution for  $n = 2$  and  $n = 3$ . For  $n = 2$  we obtain

$$\hat{p}_0^{(1)} = \frac{-\hat{\mathcal{M}}_{0,0}^{(2,2)}}{\hat{\mathcal{M}}_{0,0}^{(2,1)} - \hat{\mathcal{M}}_{0,0}^{(2,2)}} \quad \text{and} \quad \hat{p}_0^{(2)} = \frac{\hat{\mathcal{M}}_{0,0}^{(2,1)}}{\hat{\mathcal{M}}_{0,0}^{(2,1)} - \hat{\mathcal{M}}_{0,0}^{(2,2)}} \quad (3.24)$$

and

$$\hat{p}_k^{(1)} = -\hat{p}_k^{(2)} = \frac{\hat{\mathcal{M}}_{0,0}^{(2,2)} \hat{\mathcal{M}}_{k,0}^{(2,1)} - \hat{\mathcal{M}}_{0,0}^{(2,1)} \hat{\mathcal{M}}_{k,0}^{(2,2)}}{(\hat{\mathcal{M}}_{0,0}^{(2,1)} - \hat{\mathcal{M}}_{0,0}^{(2,2)})(\hat{\mathcal{M}}_{k,k}^{(2,1)} - \hat{\mathcal{M}}_{k,k}^{(2,2)})} \quad (3.25)$$

For  $n = 3$  the results for  $\hat{p}_0^{(i)}$  are (we use a sum convention, i.e. indices appearing twice are summed over from 1 to 3).

$$\hat{p}_0^{(i)} = \frac{2\epsilon_{ijh} \hat{\mathcal{M}}_{0,0}^{(2,j)} \hat{\mathcal{M}}_{0,0}^{(3,h)}}{\epsilon_{ljh} \hat{\mathcal{M}}_{0,0}^{(2,l)} (\hat{\mathcal{M}}_{0,0}^{(3,j)} - \hat{\mathcal{M}}_{0,0}^{(3,h)})} \quad (3.26)$$

while  $\hat{p}_k^{(i)}$  reads in  $O(A_{\text{in}})$

$$\hat{p}_k^{(i)} = \frac{-\epsilon_{ijh} \epsilon_{mno} \hat{\mathcal{M}}_{0,0}^{(2,n)} \hat{\mathcal{M}}_{0,0}^{(3,o)} \left[ \hat{\mathcal{M}}_{k,0}^{(3,m)} (\hat{\mathcal{M}}_{k,k}^{(2,j)} - \hat{\mathcal{M}}_{k,k}^{(2,h)}) + \hat{\mathcal{M}}_{k,0}^{(2,m)} (\hat{\mathcal{M}}_{k,k}^{(3,j)} - \hat{\mathcal{M}}_{k,k}^{(3,h)}) \right]}{\epsilon_{jhl} \epsilon_{mno} \hat{\mathcal{M}}_{k,k}^{(2,j)} (\hat{\mathcal{M}}_{k,k}^{(3,h)} - \hat{\mathcal{M}}_{k,k}^{(3,l)}) \hat{\mathcal{M}}_{0,0}^{(2,m)} (\hat{\mathcal{M}}_{0,0}^{(3,n)} - \hat{\mathcal{M}}_{0,0}^{(3,o)})} \quad (3.27)$$

Here  $\epsilon_{ijk}$  is the totally antisymmetric tensor which is 1 if  $(i, j, k)$  is an even permutation of  $(1, 2, 3)$ ,  $-1$  if it is an odd permutation and 0 otherwise. Eventually, according to eqs. (3.4), (3.9), (3.18) and (3.27) the SPA can be evaluated as

$$\text{SPA} = \frac{|\sum_{j=1}^n x^{(j)} \hat{p}_1^{(j)}|^2}{|A_{\text{in}}|^2}. \quad (3.28)$$



Finally, if we assume that the periodicity of  $\mathcal{M}_t^{(i)}$  is caused by a harmonic periodic signal  $s(t) = A_{\text{in}} \exp(i\Omega t) + c.c.$  and that further the master operator  $\mathcal{M}_t^{(i)}$  depends smoothly on  $s(t)$  one can show (see Appendix B.3.1) that

$$\hat{\mathcal{M}}_{k,l}^{(i,j)} = O(|A_{\text{in}}|^{k-l}). \quad (3.29)$$

Then from eq. (3.20a) one deduces that  $p_k^{(i)}$  is of order  $O(A_{\text{in}}^{|k|})$ . This implies, that only the delta peak at the driving frequency  $\Omega$  is of order  $O(A_{\text{in}})$ , while the delta peaks at higher harmonics  $k\Omega$  vanish in  $O(A_{\text{in}})$ .

### Application to the FHN model

Let us come back to the discrete state modeling of the excitable dynamics of a FHN system, introduced in subsection 2.1.2. The external periodic driving  $s(t) = s_{x/y}(t) = A_{\text{in}} \exp(i\Omega t) + c.c.$  is assumed to act additively on either the slow recovery variable  $y$  or the fast voltage variable  $x$ ,

$$\dot{x} = x - x^3 - y + s_x(t) + \sqrt{2D}\xi(t) \quad (3.30a)$$

$$\dot{y} = \epsilon(x + a_0 - a_1 y - s_y(t)) \quad (3.30b)$$

A sketch of this system is given in Fig. 3.1. If the system is already close to

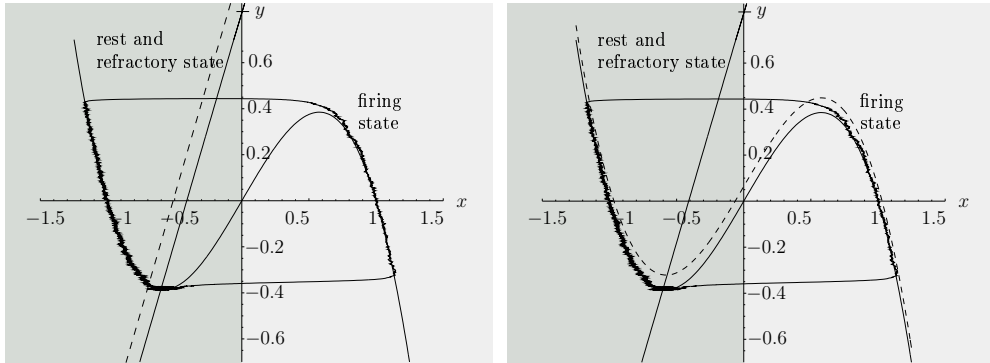


Figure 3.1: An excitable FHN system subjected to an external driving  $s_y(t)$  acting on the slow recovery variable  $y$  (left) or  $s_x(t)$  acting on the voltage variable  $x$  (right) as described by eq. (3.30). The signal applied to  $y$  moves the  $y$ -nullcline upwards and downwards, thus moving the stable fixed point towards the excitation barrier and back again. The signal applied to  $x$  moves the  $x$ -nullcline upwards and downwards, thus having a similar effect on the the excitation barrier.

the excitation threshold and we add a small signal one might assume that the

excitation rate is quite strongly affected while the relaxation dynamics along the stable branches of the  $x$  nullcline is less affected. This behavior is recovered in the waiting time distribution plots for three different constant values of the external signal Fig. 3.2.

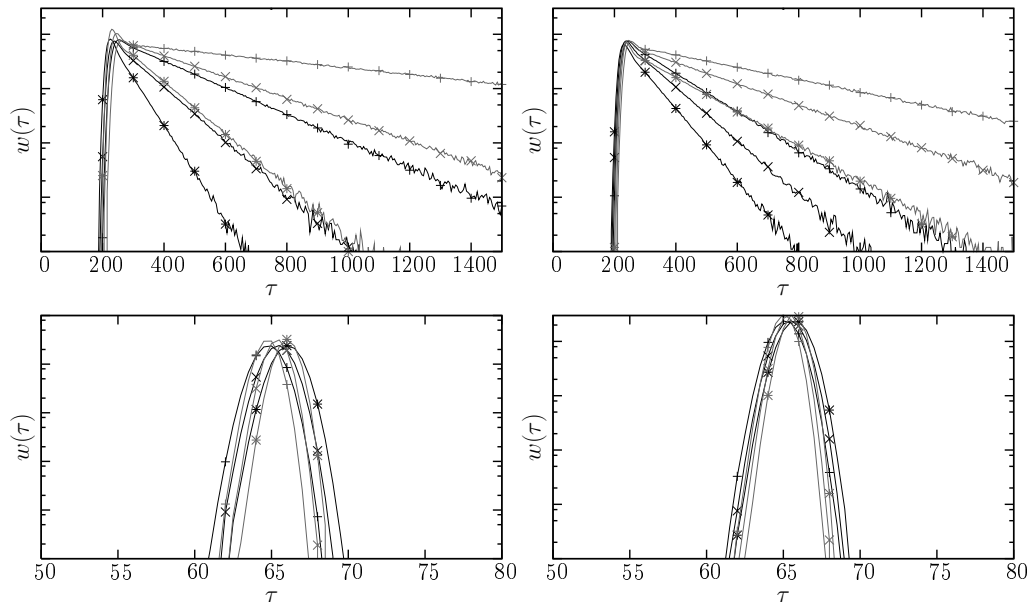


Figure 3.2: Logarithmic plot of the waiting time distributions in rest and refractory state (top) and the firing state (bottom) of the FHN system eq. (3.30) for different constant values of the external signal  $s_y(t)$  (left) or  $s_x(t)$  (right) and two different noise levels.  $s_{x/y}(t) = 0.01$  (\*),  $s_{x/y}(t) = 0.0$  (×) and  $s_{x/y}(t) = -0.01$  (+). Other parameters  $a_0 = 0.41$ ,  $a_1 = 0.5$ ,  $D = 0.0001$  (gray) or  $D = 0.0002$  (black) and  $\epsilon = 0.01$ .

We notice that to a good approximation the waiting time distribution in the firing state is not affected by the external signal. As this waiting time density is sharply peaked for low noise levels, we finally approximate it with a fixed waiting time  $T_f$ , i.e. a delta peaked waiting time density  $w^{(2)}(\tau) = \delta(\tau - T_f)$  to get some concrete analytical results. The same considerations are true for the refractory state, represented by the well defined step in the joint waiting time distribution in rest and refractory state,  $w^{(3)}(\tau) = \delta(\tau - T_r)$ . The signal however strongly affects the excitation rate, as represented by the different slopes of the waiting time density in the rest and refractory state for different constant values of the signal  $s(t) \equiv s_{x/y}(t)$ . If we assume that the external signal varies on a much slower timescale than the relaxation timescale at the stable fixed point, the excitation process will still be a rate process as in the case of a constant signal however now with a

signal and therefore time dependent rate  $\gamma(s(t))$ . This adiabatic assumption was also required in the two state Markovian description of the double well potential system. We can now easily modify the master equation description for the undriven FHN system eqs. (2.15) by including the signal dependent rate, leading to

$$\frac{d}{dt}p^{(1)}(t) = \int_{t_0}^t dt' \gamma(s(t')) p^{(1)}(t') (w^{(2)} \circ w^{(3)})(t-t') - \gamma(s(t)) p^{(1)}(t) \quad (3.31a)$$

$$\frac{d}{dt}p^{(2)}(t) = \gamma(s(t)) p^{(1)}(t) - \int_{t_0}^t dt' \gamma(s(t')) p^{(1)}(t') w^{(2)}(t-t') \quad (3.31b)$$

$$\frac{d}{dt}p^{(3)}(t) = \int_{t_0}^t dt' \gamma(s(t')) p^{(1)}(t') \left[ w^{(2)}(t-t') - (w^{(2)} \circ w^{(3)})(t-t') \right] \quad (3.31c)$$

with the initial condition  $p^{(1)}(t_0) = 1$  and  $p^{(2/3)}(t_0) = 0$ . Depending on the discrete state of the system the output  $x(t)$  assumes either a high value  $x_1$  (firing state) or a low value  $x_0$  (rest and refractory state). The stochastic process we are interested in is thus given by

$$x(t) = \begin{cases} x_0 & \text{if the system is in state 1 or 3} \\ x_1 & \text{if the system is in state 2 (firing)} \end{cases} \quad (3.32)$$

In order to calculate the asymptotic periodic output

$$\langle x(t) \rangle = x_0(p^{(1)}(t) + p^{(3)}(t)) + x_1 p^{(2)}(t) = x_0 + (x_1 - x_0) p^{(2)}(t) \quad (3.33)$$

we have to calculate the asymptotic periodic solutions of eqs. (3.31). The asymptotic solution is obtained by shifting the initial time  $t_0$  to  $-\infty$ . However in this limit the initial condition is not well defined and without initial condition eqs. (3.31) have no unique solution in the limit  $t_0 \rightarrow \infty$  even if supplemented with the normalization condition  $p^{(1)}(t) + p^{(2)}(t) + p^{(3)}(t) = 1$ . Namely, if  $[p^{(1)}(t), p^{(2)}(t), p^{(3)}(t)]$  is a normalized periodic solution so is  $[cp^{(1)}(t), cp^{(2)}(t), cp^{(3)}(t) - c + 1]$ .

Thus, before performing the limit  $t_0 \rightarrow -\infty$  it is advantageous to pass to an integral version of eqs. (3.31). This integral master equation is obtained by formally integrating eqs. (3.31) with respect to  $t$  from  $t_0$  to  $t$ , taking into account the initial condition. The resulting equations

$$p^{(1)}(t) = 1 - p^{(2)}(t) - p^{(3)}(t) \quad (3.34a)$$

$$p^{(2)}(t) = \int_{t_0}^t dt' \gamma(s(t')) p^{(1)}(t') z^{(2)}(t-t') \quad (3.34b)$$

$$p^{(3)}(t) = \int_{t_0}^t dt' \gamma(s(t')) p^{(1)}(t') \int_{t'}^t d\tau w^{(2)}(\tau-t') z^{(3)}(t-\tau) \quad (3.34c)$$

automatically satisfy the initial condition  $p^{(1)}(t_0) = 1$  and  $p^{(2/3)}(t_0) = 0$ . Therein

$$z^{(2/3)}(\tau) = 1 - \int_0^\tau d\tau' w^{(2/3)}(\tau')$$

denotes the survival probability in state 2 or 3 respectively, i.e. the probability to stay at least the time  $\tau$  in the respective state. These equations can now be considered in the limit  $t_0 \rightarrow -\infty$ ,

$$p^{(1)}(t) = 1 - p^{(2)}(t) - p^{(3)}(t) \quad (3.35a)$$

$$p^{(2)}(t) = \int_0^\infty d\tau \gamma(s(t-\tau)) p^{(1)}(t-\tau) z^{(2)}(\tau) \quad (3.35b)$$

$$p^{(3)}(t) = \int_0^\infty d\tau \gamma(s(t-\tau)) p^{(1)}(t-\tau) \int_0^\tau d\tau' w^{(2)}(\tau') z^{(3)}(\tau - \tau'). \quad (3.35c)$$

In contrast to eqs. (3.31) they have in general a unique periodic solution which we express in a Fourier series as

$$p^{(i)}(t) = \sum_{k=-\infty}^{\infty} \hat{p}_k^{(i)} \exp(ik\Omega t)$$

The master operator which corresponds to the master equation (3.35) was already presented in eq. (3.17). Expanding the periodic excitation rate  $\gamma$  into a Fourier series

$$\gamma(s(t)) = \sum_{k=-\infty}^{\infty} \hat{\gamma}_k \exp(ik\Omega t) \quad (3.36)$$

we eventually obtain its Fourier coefficients  $\hat{\mathcal{M}}_{k,l}^{(i,j)}$  according to eq. (3.21) as

$$\hat{\mathcal{M}}_{k,l}^{(2,1)} = -\gamma_{k-l} \hat{z}_k^{(2)}, \quad \hat{\mathcal{M}}_{k,l}^{(2,2)} = \delta_{k,l}, \quad (3.37)$$

$$\hat{\mathcal{M}}_{k,l}^{(3,1)} = -\gamma_{k-l} \hat{w}_k^{(2)} \hat{z}_k^{(3)}, \quad \hat{\mathcal{M}}_{k,l}^{(3,3)} = \delta_{k,l} \quad (3.38)$$

$$\hat{\mathcal{M}}_{k,l}^{(i,j)} = 0, \quad (i,j) \neq (2,1), (3,1), (2,2), (3,3) \quad (3.39)$$

Therein the Fourier coefficients

$$\hat{z}_k^{(i)} = \int_0^\infty d\tau z^{(i)}(\tau) \exp(-ik\Omega\tau) \quad \text{and} \quad \hat{w}_k^{(i)} = \int_0^\infty d\tau w^{(i)}(\tau) \exp(-ik\Omega\tau).$$

are related by

$$\hat{z}_k^{(i)} = \frac{1 - \hat{w}_k^{(i)}}{ik\Omega}$$

For the sake of notation we introduce the waiting time distribution in state 1 of the undriven system

$$w^{(1)}(\tau) = \gamma_0 \exp(-\gamma_0 \tau), \quad \hat{w}_k^{(1)} = \frac{\gamma_0}{\gamma_0 + ik\Omega}. \quad (3.40)$$

Applying the general result (3.26) and (3.27) we obtain in linear order in the input amplitude  $A_{\text{in}}$  for  $p_0^{(i)}$

$$\hat{p}_0^{(i)} = \frac{\langle \tau^{(i)} \rangle}{T}, \quad T = \langle \tau^{(1)} \rangle + \langle \tau^{(2)} \rangle + \langle \tau^{(3)} \rangle, \quad \langle \tau^{(1)} \rangle = \frac{1}{\gamma_0} \quad (3.41)$$

where we used the fact that the mean waiting time  $\langle \tau^{(i)} \rangle$  in state  $i$  can be expressed in terms of the survival probability as

$$\langle \tau^{(i)} \rangle = \int_0^\infty d\tau z^{(i)}(\tau) = \hat{z}_0^{(i)} \quad (3.42)$$

The coefficients  $p_{\pm 1}^{(i)}$  are obtained from eq. (3.27) as

$$\hat{p}_1^{(1)} = \hat{p}_{-1}^{(1)*} = \frac{i\hat{\gamma}_1}{T\gamma_0\Omega} \frac{(1 - \hat{w}_1^{(1)})(1 - \hat{w}_1^{(2)}\hat{w}_1^{(3)})}{1 - \hat{w}_1^{(1)}\hat{w}_1^{(2)}\hat{w}_1^{(3)}} \quad (3.43a)$$

$$\hat{p}_1^{(2)} = \hat{p}_{-1}^{(2)*} = -\frac{i\hat{\gamma}_1}{T\gamma_0\Omega} \frac{(1 - \hat{w}_1^{(1)})(1 - \hat{w}_1^{(2)})}{1 - \hat{w}_1^{(1)}\hat{w}_1^{(2)}\hat{w}_1^{(3)}} \quad (3.43b)$$

$$\hat{p}_1^{(3)} = \hat{p}_{-1}^{(3)*} = -\frac{i\hat{\gamma}_1}{T\gamma_0\Omega} \frac{(1 - \hat{w}_1^{(1)})\hat{w}_1^{(2)}(1 - \hat{w}_1^{(3)})}{1 - \hat{w}_1^{(1)}\hat{w}_1^{(2)}\hat{w}_1^{(3)}} \quad (3.43c)$$

Eventually the SPA evaluated according to eq. (3.28) is given by [104]

$$\text{SPA} = \frac{(x_1 - x_0)^2}{|A_{\text{in}}|^2} \left| \frac{\hat{\gamma}_1}{T\gamma_0\Omega} \right|^2 \left| \frac{(1 - \hat{w}_1^{(1)})(1 - \hat{w}_1^{(2)})}{1 - \hat{w}_1^{(1)}\hat{w}_1^{(2)}\hat{w}_1^{(3)}} \right|^2 \quad (3.44)$$

Up to now we did not specify the signal dependence of the excitation rate. Having in mind the excitable FHN dynamics we want to model, we assume that the periodic driving modulates the effective excitation barrier the system has to surmount by noise in order to be excited. The resulting Kramers type rate, is then given by

$$\gamma(s(t)) = r_0 \exp\left(-\frac{\Delta U(s(t))}{D}\right) = \gamma_0(1 + \alpha s(t)) + O(A_{\text{in}}^2)$$

where  $D$  is the strength of the noise. Introducing the excitation rate without signal

$$\gamma_0 = r_0 \exp\left(-\frac{\Delta U(0)}{D}\right)$$

the total excitation rate can be written in first order in the signal amplitude as

$$\gamma(s(t)) = \gamma_0(1 + \alpha s(t)) + O(A_{\text{in}}^2).$$

Therein

$$\alpha = \frac{1}{\gamma(0)} \frac{d}{ds} \gamma(s) \Big|_{s=0} = -\frac{1}{D} \frac{d}{ds} \Delta U(s) \Big|_{s=0}$$

denotes the sensibility of the system with respect to the external signal. Thus the Fourier coefficients of the periodic excitation rate are

$$\hat{\gamma}_1 = \hat{\gamma}_{-1}^* = \gamma_0 \alpha A_{\text{in}} + O(A_{\text{in}}^2).$$

With this excitation rate (3.44) eventually reads

$$\text{SPA} = \frac{(x_1 - x_0)^2 \alpha^2}{T^2 \Omega^2} \left| \frac{(1 - \hat{w}_1^{(1)})(1 - \hat{w}_1^{(2)})}{1 - \hat{w}_1^{(1)} \hat{w}_1^{(2)} \hat{w}_1^{(3)}} \right|^2 \quad (3.45)$$

We have already noted that for small noise levels the waiting time densities in firing and refractory state are sharply peaked, thus allowing for an approximation by fixed waiting times  $T_f$  and  $T_r$ . Accordingly

$$w^{(2)}(\tau) = \delta(\tau - T_f) \quad \text{and} \quad w^{(3)}(\tau) = \delta(\tau - T_r).$$

Then the SPA (3.45) can be further evaluated to

$$\text{SPA} = \frac{4(x_1 - x_0)^2 \alpha^2}{\left(\frac{1}{\gamma_0} + T_f + T_r\right)^2 \Omega^2} \frac{\sin^2 \frac{\Omega T_f}{2}}{1 + 2 \frac{\gamma_0^2}{\Omega^2} (1 - \cos(\Omega(T_f + T_r))) + 2 \frac{\gamma_0}{\Omega} \sin(\Omega(T_f + T_r))} \quad (3.46)$$

There are altogether four parameters which describe the system's response to the external periodic signal, namely the firing and refractory time  $T_f$  and  $T_r$  respectively and the excitation rate without driving  $\gamma_0$  as well as the sensibility  $\alpha$ , which describes the change in the excitation rate  $\gamma$  if one changes the signal  $s(t)$ . These parameters have to be somehow extracted from the FHN system considered. We estimate them from the numerically obtained waiting time densities Fig. 3.2 for  $D = 0.0001$  as

$$T_f = 65.5, \quad T_r = 220, \quad \gamma_0 = 0.0046 \quad \text{and} \quad \alpha \approx 100$$

for the signal in the inhibitor  $y$

$$T_f = 65.5, \quad T_r = 220, \quad \gamma_0 = 0.0046 \quad \text{and} \quad \alpha \approx 50$$

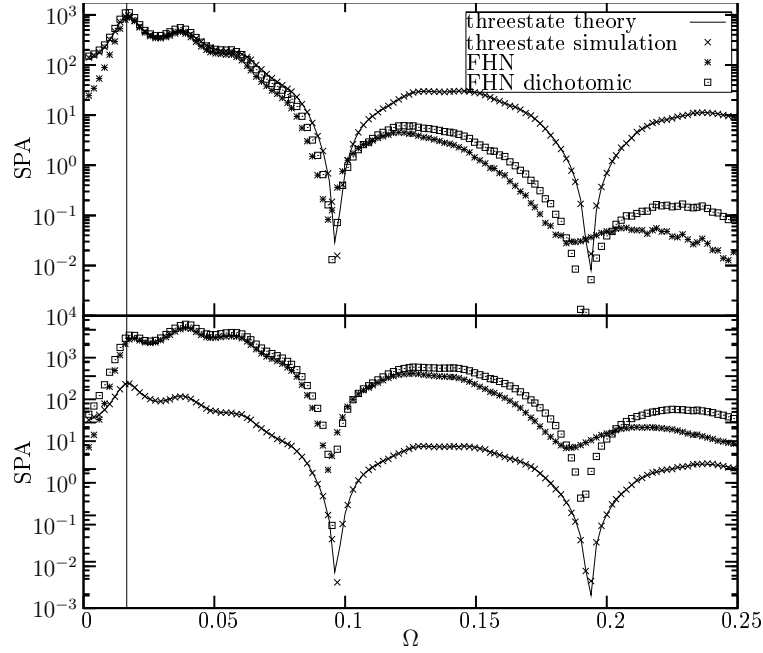


Figure 3.3: SPA of the threestate model (theory and simulation) compared to the SPA of the output  $x(t)$  of the FHN system and a dichotomically filtered output. Top: Signal entering into the  $y$  dynamics. Bottom: Signal entering into the  $x$  dynamics. Other parameters  $a_0 = 0.41$ ,  $a_1 = 0.5$ ,  $D = 0.0001$  and  $\epsilon = 0.01$ . The vertical line shows the frequency where the theory predicts the maximum SPA.

for the signal in the activator  $x$ . With these values and the output  $x_0 = -1$  and  $x_1 = 1$  we have compared the analytical expression eq. (3.46) with the numerically evaluated SPA of the output  $x(t)$  of the FHN system in Fig. 3.3. In addition, we further considered the SPA of a binarily filtered output of the FHN system

$$\tilde{x}(t) = \begin{cases} -1 & \text{if } x(t) < 0 \\ 1 & \text{if } x(t) \geq 0 \end{cases} \quad (3.47)$$

in order to avoid the influence of the form factor of the spikes, which actually are not rectangular pulses as supposed in the discrete state model (see Fig. 2.5). The numerical simulations of the FHN and threestate model were done with a signal amplitude  $A_{\text{in}} = 0.002$ .

First we notice that although there are strong quantitative derivations, the structure of the SPA as a function of the driving frequency is nevertheless well reproduced. Due to the analytic result eq. (3.46) it can be easily interpreted. Namely the deep minima stem from the approximately fixed firing time  $T_f$  and are located at frequencies  $\Omega = 2\pi n/T_f$ . They represent the fact that in a sequence

of rectangular pulses with width  $T_f$  located at arbitrary positions, there is no frequency proportional to  $2\pi n/T_f$  in the Fourier transformed.

The small minima and maxima in between these deep minima are contributions of the denominator in eq. (3.46). For  $\gamma_0 \ll \Omega$  we may neglect the term  $\frac{\gamma_0^2}{\Omega^2}$ . In this limit the maxima are therefore located at frequencies for which  $\sin(\Omega(T_f + T_r)) = -1$ , i.e.

$$\Omega_{\max} = \frac{2n\pi - \frac{\pi}{2}}{T_f + T_r}, \quad n \in \mathbb{N}$$

For  $\gamma_0 \gg \Omega$  the term  $\frac{\gamma_0^2}{\Omega^2}$  dominates the term  $\frac{\gamma_0}{\Omega}$ . Thus the maxima are located at frequencies where  $\cos(\Omega(T_f + T_r)) = 1$ , i.e.

$$\Omega_{\max} = \frac{2n\pi}{T_f + T_r}, \quad n \in \mathbb{N}$$

Let us assume that  $\gamma_0 \ll \Omega$ . Then the first maximum is located at  $\Omega = 3/2\pi/(T_f + T_r) \approx 0.0165$ , which is indeed greater than  $\gamma_0 \approx 0.0046$ . The maximum value of the SPA is as predicted observed at  $\Omega \approx 0.0165$  (see Fig. 3.3). Thus the theoretical treatment allows to predict the frequencies which are optimally amplified by the excitable system by just measuring the firing and refractory time as well as the excitation rate of the undriven system. For the signal acting additively on the  $y$  dynamics there is a strong damping for higher frequencies in the FHN system compared to the three state model. This might be due to the fact, that for these frequencies the adiabatic assumption, that the signal is sufficiently slowly varying, such that the excitation process can be considered as rate process with a time dependent rate is no longer valid. The real shape of a spike leads to a form factor which suppresses the low frequencies, compared to the form factor of a rectangular pulse, as can be seen by comparing the results for the FHN output  $x(t)$  and the corresponding rectangular pulse train  $\tilde{x}(t)$  eq. (3.47).

The sensibility parameter  $\alpha$  has been estimated from waiting time distributions for different *constant* values of the driving amplitude. With this  $\alpha$  the SPA is well estimated for the dynamics entering into the  $y$  variable. However the SPA is strongly underestimated for the signal entering into the  $x$  dynamics. This means that the periodic signal has a much stronger effect onto the excitation rate as has a constant signal. If this derivation would occur at certain driving frequencies only, it probably could be understood as a resonance of the signal with the eigenfrequency of the FHN at the fixed point. However the derivation is nearly uniform with a factor of about 100 in a large range of driving frequencies. This implies that a periodic signal entering into the  $x$  dynamics of a FHN system, which in case of a neuron is the natural place to include signals, is much more amplified than one would expect from the change of the excitation rate for constant or adiabatically slowly varying signals.



### 3.3.2 An approach based on waiting time distributions

In this section our starting point is a time dependent waiting time distribution, which specifies the periodic renewal process. This time dependent waiting time distribution can be given as a starting point or, if the discrete periodic renewal process is the result of a discrete model of some continuous system has to be somehow extracted from this continuous model, e.g. by calculating the first passage times between.

In order to apply the concept of spectral power density to the periodic renewal process, which is a point process, we have to map it onto a stochastic process, i.e. we have to assign some value to the process for each time  $t$ . This is done in exactly the same way as for a stationary renewal process presented in section 2.1.3 (see eqs. (2.19) and (2.20)). For the ordinary periodic renewal process, described by a single time dependent waiting time distribution we consider the sequence of delta spikes at the times of the events, while for an alternating  $n$  state periodic renewal process, where the intervals between subsequent events are alternatingly governed by  $w^{(1)}(\tau, t), \dots, w^{(n)}(\tau, t), w^{(1)}(\tau, t), \dots$ , the corresponding stochastic process assumes different constant values  $x^{(1)}$  to  $x^{(n)}$ . For the sake of notational simplicity we restrict ourselves to alternating two state processes. However a generalization is straight forward.

#### Periodic renewal delta spike sequences

Let us first consider the renewal delta spike sequence (2.20)

$$\chi(t) = \sum_i \delta(t - t_i) \quad (3.48)$$

where the intervals  $\tau = t_{i+1} - t_i$  between subsequent events are governed by the time dependent waiting time distribution  $w(\tau, t_i)$ , i.e. the probability  $dP$  to have the event  $i + 1$  in the time interval time  $(t_i + \tau, t_i + \tau + d\tau)$  is

$$dP = w(\tau, t_i)d\tau.$$

To analyze the spectral power density eq. (2.21c) we insert the stochastic process eq. (3.48) into eq. (2.21b) resulting in

$$\langle |c_{n\Omega, T}|^2 \rangle = \frac{1}{T^2} \langle \sum_{k,j}^{0 < t_k, t_j < T} \exp(in\Omega(t_k - t_j)) \rangle \quad (3.49)$$

There are two random components for which the ensemble mean has to be taken, namely the number  $N_T$  of events in the interval  $(0, T)$  and the actual spiking

times  $t_i$ . Therefore it is not immediately possible to interchange the mean and the summation. However in the limit  $T \rightarrow \infty$  which we are concerned with, the mean and variance of  $N_T$  grow linearly with  $T$  superposed with a periodic modulation (see appendix C.1) and therefore the variance of  $N_T/T$  will tend to zero while  $N_T/T$  tends to a fixed (non random) value  $\langle \tau \rangle$  which is the mean interval between subsequent events. In this limit  $T \rightarrow \infty$ , which is assumed in the following

$$\langle |c_{n\Omega, T}|^2 \rangle = \frac{1}{T^2} \sum_{k,j=1}^{\langle N_T \rangle} \langle \exp(in\Omega(t_k - t_j)) \rangle$$

where  $\langle N_T \rangle = T/\langle \tau \rangle$  is the mean number of events in the interval  $(0, T)$ . In this expression the actual spiking times  $t_i$  are no longer important but only the corresponding phases of the periodic signal  $\phi_i = \Omega t_i \bmod 2\pi$  [102], leading to

$$\langle |c_{n\Omega, T}|^2 \rangle = \frac{1}{T^2} \sum_{k,j=1}^{\langle N_T \rangle} \langle \exp(in(\phi_k - \phi_j)) \rangle \quad (3.50)$$

The following calculation will benefit from the fact that the stochastic process  $\{\phi_i\}_i$  is a stationary Markov process in contrast to the non stationary process  $\{t_i\}_i$ .

Splitting the double sum in eq. (3.50) into a diagonal part and a upper and lower diagonal part we arrive at

$$\langle |c_{n\Omega, T}|^2 \rangle = \frac{1}{T^2} \sum_{k=1}^{\langle N_T \rangle} \sum_{j=1}^k \langle \exp(in(\phi_j - \phi_0)) \rangle + c.c. \quad (3.51)$$

where we used the fact that in the limit  $T \rightarrow \infty$  the diagonal part  $N_T/T^2$  is zero and that the process is stationary. To proceed further we introduce the phase evolution operator

$$(\mathcal{L}f)(\phi) := \int_0^{2\pi} d\psi P(\phi|\psi) f(\psi) \quad (3.52)$$

whose integral kernel  $P(\phi|\psi)$  is the conditioned probability to have a signal phase  $\phi$  at the time of an event if the previous event had a signal phase  $\psi$ . This operator acting on the space  $L_1([0, 2\pi])$  is a so called Markov operator [71], having the properties

$$\mathcal{L}f \geq 0 \quad \text{if } f \geq 0 \quad \text{and} \quad \|\mathcal{L}f\| = \|f\|.$$

Introducing the two point probability  $P_j(\phi; \psi)$  that the phase of event  $i$  is  $\psi$  and the phase of event  $j+i$  is  $\phi$  as

$$P_j(\phi; \psi) := \int_0^{2\pi} d\alpha_1 \dots \int_0^{2\pi} d\alpha_{j-1} P(\phi|\alpha_{j-1}) \dots P(\alpha_1|\psi) P^{\text{st}}(\psi)$$

where  $P^{\text{st}}(\phi)$  is the stationary phase distribution, we can express the expectation value  $\langle \exp(in(\phi_j - \phi_0)) \rangle$  in eq. (3.51) in terms of this evolution operator as

$$\begin{aligned} \langle e^{in(\phi_j - \phi_0)} \rangle &:= \int_0^{2\pi} d\phi \int_0^{2\pi} d\psi \exp(in(\phi - \psi)) P_j(\phi; \psi) \\ &= \langle f_n, \mathcal{L}^j(f_n P^{\text{st}}) \rangle_{\mathbb{C}} \end{aligned} \quad (3.53)$$

where  $f_n(\phi) := \exp(-in\phi)$  and we have introduced the inner product  $\langle f, g \rangle_{\mathbb{C}} = \int_0^{2\pi} d\phi f^*(\phi) g(\phi)$ .

We assume in the following that the original periodic renewal process is sufficiently well behaved such that the phase process  $\{\phi_i\}$  has a unique stationary density. Then (cf. appendix B.1) in the limit  $T \rightarrow \infty$

$$\frac{1}{T^2} \sum_{k=1}^{\langle N_T \rangle} \sum_{j=1}^k \mathcal{L}^j f = \frac{\langle 1, f \rangle_{\mathbb{C}}}{2\langle \tau \rangle^2} P^{\text{st}} \quad (3.54)$$

Expressing now the ensemble means in eq. (3.51) by powers of  $\mathcal{L}$  as shown in eq. (3.53) using eq. (3.54), the weights

$$2\pi s_n = \lim_{\epsilon \rightarrow 0} \int_{n\Omega - \epsilon}^{n\Omega + \epsilon} d\omega S(\omega) = 2\pi \lim_{T \rightarrow \infty} \langle |c_{n\Omega, T}|^2 \rangle \quad (3.55)$$

of the delta peaks in the spectral power density eq. (3.4) are finally expressed by the stationary phase distribution  $P^{\text{st}}(\phi)$  and the mean inter spike interval  $\langle \tau \rangle$  as

$$s_n = 2 \frac{|\langle f_n, P^{\text{st}} \rangle_{\mathbb{C}}|^2}{2\langle \tau \rangle^2} = \frac{1}{\langle \tau \rangle^2} \left| \int_0^{2\pi} d\phi \exp(in\phi) P^{\text{st}}(\phi) \right|^2 \quad (3.56)$$

This equation, which can also be found in [117] relates the weights of the delta peaks at integer multiples of the driving frequency in the power spectrum of the delta sequence (3.48) to the stationary phase distribution of the point process and is valid for any periodically driven renewal process having a unique stationary phase distribution. An equivalent formula expressing these weights in terms of the time dependent mean spiking rate has been derived in [61] by different means, considering the averaged correlation function.

In the following we relate the stationary phase distribution to the time dependent waiting time distribution  $w(\tau, t)$  of the periodic renewal process. The stationary phase distribution  $P^{\text{st}}$  is invariant under the action of the phase evolution operator eq. (3.52), i.e.

$$P^{\text{st}}(\phi) = \int_0^{2\pi} d\psi P(\phi|\psi) P^{\text{st}}(\psi). \quad (3.57)$$

The integral kernel  $P(\phi|\psi)$  expresses the probability that an event has a signal phase  $\phi$  if the signal phase of the previous event was  $\psi$ . It can be expressed in terms of the time dependent waiting time distribution  $w(\tau, t)$  which defines the periodical renewal process as

$$P(\phi|\psi) = \frac{1}{\Omega} \sum_{n=n_0}^{\infty} w\left(\frac{\phi - \psi + 2\pi n}{\Omega}, \frac{\psi}{\Omega}\right) \quad (3.58)$$

where  $n_0 = 0$  if  $\phi > \psi$  and  $n_0 = 1$  otherwise.

Expressing  $P(\phi|\psi)$  in a Fourier series as

$$P(\phi|\psi) = \frac{1}{2\pi} \sum_{j,k=-\infty}^{\infty} \hat{P}_{j,k} \exp(ij\phi) \exp(ik\psi) \quad (3.59)$$

with the Fourier coefficients

$$\hat{P}_{j,k} = \frac{1}{2\pi} \int_0^{2\pi} d\phi \int_0^{2\pi} d\psi \exp(-ij\phi) \exp(-ik\psi) P(\phi, \psi)$$

eq. (3.58) can be written more elegantly as

$$\hat{P}_{j,k} = \hat{w}_{j,j+k} \quad (3.60)$$

where  $\hat{w}_{k,l}$  is related to the time dependent waiting time distribution  $w(\tau, t)$  by

$$\hat{w}_{k,l} = \int_0^{\infty} d\tau e^{-ik\Omega\tau} \hat{w}_l(\tau) = \frac{\Omega}{2\pi} \int_0^{\frac{2\pi}{\Omega}} dt \int_0^{\infty} d\tau e^{-ik\Omega\tau} e^{-il\Omega t} w(\tau, t). \quad (3.61)$$

The Fourier coefficients

$$\hat{P}_k^{\text{st}} = \frac{1}{2\pi} \int_0^{2\pi} P^{\text{st}}(\phi) \exp(-ik\phi)$$

of the stationary phase distribution  $P^{\text{st}}(\phi)$  are then defined (cf. eq. (3.57), (3.60)) by

$$\hat{P}_k^{\text{st}} = \sum_{j=-\infty}^{\infty} \hat{P}_{k,j} \hat{P}_{-j}^{\text{st}} = \sum_{j=-\infty}^{\infty} \hat{w}_{k,k+j} \hat{P}_{-j}^{\text{st}}, \quad \hat{P}_0^{\text{st}} = 1 \quad (3.62)$$

Having the Fourier coefficients  $\hat{P}_k^{\text{st}}$  of the stationary phase distribution, the weights  $s_n$  can be easily evaluated from eq. (3.56) as

$$s_n = 4\pi^2 \frac{|\hat{P}_n^{\text{st}}|^2}{\langle \tau \rangle^2} \quad (3.63)$$

The infinite set of linear equations (3.62) for the stationary phase distributions cannot in general be solved analytically. Therefore some approximations are needed one of which is the weak driving approximation. Namely if the periodic driving is sufficiently weak, i.e. if its amplitude  $A_\epsilon$  is small we may neglect terms of order  $A_{\text{in}}^k$ ,  $k \geq 2$  in eq. (3.62).

This allows to solve eq. (3.62) for  $\hat{P}_k^{\text{st}}$  in first order in  $A_{\text{in}}$ , leading to

$$\begin{aligned}\hat{P}_0^{\text{st}} &= \frac{1}{2\pi} + O(A_{\text{in}}^2) \\ \hat{P}_k^{\text{st}} &= (\hat{P}_{-k}^{\text{st}})^* = \frac{1}{2\pi} \frac{\hat{P}_{-k,0}}{1 - \hat{P}_{k,-k}} + O(A_{\text{in}}^2).\end{aligned}$$

The stationary phase distribution is therefore given by

$$\hat{P}^{\text{st}}(\phi) = \frac{1}{2\pi} \left[ 1 + 2\text{Re} \sum_{k=1}^{\infty} \left[ \frac{\hat{P}_{-k,0}}{1 - \hat{P}_{k,-k}} \exp(ik\phi) \right] \right] + O(A_{\text{in}}^2).$$

To calculate the mean inter event interval  $\langle \tau \rangle$  of the driven process we have to average the mean inter event intervals for a given signal phase with respect to the stationary phase distribution,

$$\begin{aligned}\langle \tau \rangle &= \int_0^{2\pi} d\phi P^{\text{st}}(\phi) \int_0^\infty d\tau \tau w(\tau, \frac{\phi}{\Omega}) = 2\pi \sum_{k=-\infty}^{\infty} \hat{P}_k^{\text{st}} \int_0^\infty d\tau \tau \hat{w}_{-k}(\tau) \\ &= \int_0^\infty d\tau \tau \hat{w}_0(\tau) + O(A_{\text{in}}^2) = \langle \tau \rangle_0 + O(A_{\text{in}}^2).\end{aligned}\tag{3.64}$$

where

$$\langle \tau \rangle_0 := \frac{1}{T} \int_0^T dt \int_0^\infty d\tau \tau w(\tau, t)$$

is the period averaged mean waiting time. Taken together eq. (3.63) reads

$$s_{\pm 1} = \frac{1}{\langle \tau \rangle_0^2} \frac{|\hat{P}_{1,0}|^2}{|1 - \hat{P}_{1,-1}|^2} + O(A_{\text{in}}^4) = \frac{1}{\langle \tau \rangle_0^2} \frac{|\hat{w}_{1,1}|^2}{|1 - \hat{w}_{1,0}|^2} + O(A_{\text{in}}^4)\tag{3.65}$$

From this expression the spectral power amplification can be directly calculated according to eq. (3.9) as

$$\text{SPA} = \frac{1}{|A_{\text{in}}|^2 \langle \tau \rangle_0^2} \frac{|\hat{w}_{1,1}|^2}{|1 - \hat{w}_{1,0}|^2} + O(A_{\text{in}}^2).$$

The SPA does not depend on  $A_{\text{in}}$  in lowest order as  $s_1$  does not have any contribution proportional to  $|A_{\text{in}}|^3$ .

To calculate the SNR, we have to know the background spectral density  $S_{\text{bg}}(\Omega)$  (cf. eq. (3.4)) for the driven process, which we cannot calculate analytically. However in order  $O(A_{\text{in}}^2)$  it agrees with the spectral power density of the corresponding undriven process obtained by setting  $A_{\text{in}} = 0$ , i.e.

$$S_{\text{bg}}(\Omega) = S_{\text{un}}(\Omega) + O(A_{\text{in}}^2)$$

One can easily convince oneself that there are no terms proportional to  $A_{\text{in}}$  in  $S_{\text{bg}}(\Omega)$  as it must be invariant under  $A_{\text{in}} \rightarrow -A_{\text{in}}$ , which is just a phase shift of the external signal. The spectral power density of the undriven and thus stationary process is known to be [124] (see eq. (2.22))

$$S_{\text{un}}(\omega) = \frac{2\pi}{\langle \tau \rangle_{\text{un}}^2} \delta(\omega) + \frac{1}{\langle \tau \rangle_{\text{un}}} \frac{1 - |\hat{w}_{\text{un}}(\omega)|^2}{|1 - \hat{w}_{\text{un}}(\omega)|^2}$$

Here  $\hat{w}_{\text{un}}(\omega) := \int_0^\infty d\tau \exp(-i\omega\tau) w_{\text{un}}(\tau)$  denotes the characteristic function of the waiting time distribution  $w_{\text{un}}(\tau)$  of the undriven process, while  $\langle \tau \rangle_{\text{un}} = \int_0^\infty d\tau \tau \hat{w}_{\text{un}}(\tau)$  is the mean waiting time. Now the waiting time distribution  $w_{\text{un}}(\tau)$  of the undriven system is given in order  $O(A_{\text{in}}^2)$  by the period averaged waiting time distribution of the driven system, which in turn is given by the zeroth Fourier coefficient  $\hat{w}_0(\tau)$  of the time dependent waiting time distribution, i.e.

$$w_{\text{un}}(\tau) = \hat{w}_0(\tau) + O(A_{\text{in}}^2)$$

Therefore we eventually obtain

$$\langle \tau \rangle_{\text{un}} = \langle \tau \rangle_0 + O(A_{\text{in}}^2),$$

and

$$\hat{w}_{\text{un}}(\omega) = \frac{2\pi}{\Omega} \int_0^{\frac{\Omega}{2\pi}} dt \int_0^\infty d\tau \exp(-i\omega\tau) w(\tau, t) + O(A_{\text{in}}^2).$$

Setting  $\omega = \Omega$  one therefore gets (see eq. (3.61))

$$\hat{w}_{\text{un}}(\Omega) = \hat{w}_{1,0} + O(A_{\text{in}}^2)$$

Eventually this leads to

$$S_{\text{bg}}(\Omega) = \frac{1}{\langle \tau \rangle_0} \frac{1 - |\hat{w}_{1,0}|^2}{|1 - \hat{w}_{1,0}|^2} + O(A_{\text{in}}^2)$$

Thus the SNR of the driven system is according to eq. (3.10)

$$\text{SNR} = \frac{2\pi}{\langle \tau \rangle_0} \frac{|\hat{w}_{1,1}|^2}{1 - |\hat{w}_{1,0}|^2} + O(A_{\text{in}}^4)$$

Finally we want to mention that if the periodicity of the waiting time distributions is due to a weak harmonic driving with frequency  $\Omega$ ,  $s(t) = A_{\text{in}} \exp(i\Omega t) + c.c.$ , and if additionally the waiting time distribution  $w(\tau, t)$  depends smoothly on this driving, then (cf. appendix B.3), the Fourier coefficients  $\hat{w}_l(\tau)$  and  $\hat{w}_{k,l}$  as defined by eq. (3.61) are of order  $O(A_{\text{in}}^{|l|})$ . Then according to eq. (3.60) the Fourier coefficients  $\hat{P}_{k,j}$  are of order  $O(A_{\text{in}}^{|k+j|})$  and all Fourier coefficients  $\hat{P}_k^{\text{st}}$  with  $k \geq 2$  vanish in order  $O(A_{\text{in}})$ . This implies that the weights of the delta peaks at higher harmonics  $k\Omega$ ,  $|k| \geq 2$  vanish in  $O(A_{\text{in}})$ .

### Periodic two state renewal processes

In this subsection we calculate the SPA and SNR of the alternating renewal process as defined by eq. (2.19),

$$\eta(t) = \begin{cases} x^{(0)} & \text{if } t_i^{(0)} < t \leq t_i^{(1)} \\ x^{(1)} & \text{if } t_i^{(1)} < t \leq t_{i+1}^{(0)} \end{cases} \quad (3.66)$$

where the intervals  $\tau^{(0)} = t_i^{(1)} - t_i^{(0)}$  are distributed according to  $w^{(0)}(\tau^{(0)}, t_i^{(0)})$  while the intervals  $\tau^{(1)} = t_{i+1}^{(0)} - t_i^{(1)}$  according to  $w^{(1)}(\tau^{(1)}, t_i^{(1)})$ . The derivation is to a large extent analogously to the derivation of the SPA and SNR of a delta pulse sequence shown in the previous subsection 3.3.2 and is thus presented less detailed.

For the sake of a simple notion we set  $x^{(0)} = 0$  and  $x^{(1)} = 1$ . For different choices of  $x^{(0)}$  and  $x^{(1)}$  the resulting expressions for the spectral quantities have only to be rescaled by  $(x^{(0)} - x^{(1)})^2$ . Inserting this process into the definition of the  $\langle |c_{n\Omega, T}|^2 \rangle$  (3.49) and following the same procedure as in the previous section the corresponding eq. (3.51) is given by

$$\langle |c_{n\Omega, T}|^2 \rangle = \frac{1}{n^2 \Omega^2 T^2} \sum_{k=1}^{\langle N_T \rangle} \sum_{j=1}^k \left[ \langle (e^{in\phi_j^{(1)}} - e^{in\phi_j^{(0)}})(e^{-in\phi_0^{(1)}} - e^{-in\phi_0^{(0)}}) \rangle + c.c. \right] \quad (3.67)$$

where  $\langle N_T \rangle = T/(\langle \tau^{(0)} \rangle + \langle \tau^{(1)} \rangle)$  is the mean number of pulses in the interval  $(0, T)$ ,  $\langle \tau^{(0)} \rangle$  and  $\langle \tau^{(1)} \rangle$  are the mean waiting times in the two different states and  $\phi_i^{(s)}$  are the signal phases at the corresponding times  $t_i^{(s)}$ . Next we introduce two phase evolution operators

$$\begin{aligned} (\mathcal{L}_{(1 \rightarrow 0)} f)(\phi) &:= \int_0^{2\pi} d\psi P_{(1 \rightarrow 0)}(\phi|\psi) f(\psi) \\ (\mathcal{L}_{(0 \rightarrow 1)} f)(\phi) &:= \int_0^{2\pi} d\psi P_{(0 \rightarrow 1)}(\phi|\psi) f(\psi) \end{aligned}$$

where  $P_{(1 \rightarrow 0)}(\phi|\psi)$  is the conditioned probability to find a phase  $\phi$  for an event (0) if the phase at the previous event (1) was  $\psi$  and  $P_{(0 \rightarrow 1)}(\phi|\psi)$  is the conditioned probability to find a phase  $\phi$  at an event(1) if the phase of the previous event (0) was  $\psi$ . From these operators we can construct the operators

$$\mathcal{L}_{(1)} := \mathcal{L}_{(0 \rightarrow 1)}\mathcal{L}_{(1 \rightarrow 0)} \quad \text{and} \quad \mathcal{L}_{(0)} := \mathcal{L}_{(1 \rightarrow 0)}\mathcal{L}_{(0 \rightarrow 1)}$$

which describe the phase evolution from one event (1) to the following event (1) and from one event (0) to the following event (0), respectively. In contrast to the operators  $\mathcal{L}_{(1 \rightarrow 0)}$  and  $\mathcal{L}_{(0 \rightarrow 1)}$ , these operators have a stationary density  $P_{(0)}^{\text{st}}$  and  $P_{(1)}^{\text{st}}$  respectively, which are the stationary phase distribution for the events (1) or (0) respectively and are assumed to be unique. We now express the mean in eq. (3.67) in terms of these operators and the stationary phase distributions as in the previous section,

$$\begin{aligned} \langle (e^{in\phi_j^{(1)}} - e^{in\phi_j^{(0)}})(e^{-in\phi_0^{(1)}} - e^{-in\phi_0^{(0)}}) \rangle = \\ \langle f_n, L_{(1)}^j(f_n P_{(1)}) \rangle_{\mathbb{C}} - \langle f_n, L_{(1 \rightarrow 0)} L_{(1)}^{j-1}(f_n P_{(1)}) \rangle_{\mathbb{C}} \\ - \langle f_n, L_{(0 \rightarrow 1)} L_{(0)}^j(f_n P_{(0)}) \rangle_{\mathbb{C}} + \langle f_n, L_{(0)}^j(f_n P_{(0)}) \rangle_{\mathbb{C}} \end{aligned}$$

According to appendix B.1 eq. (B.3) in the limit  $T \rightarrow \infty$  to

$$\frac{1}{T^2} \sum_{k=1}^{\langle N_T \rangle} \sum_{j=1}^k \mathcal{L}_{(0/1)}^j f = \frac{\langle 1, f \rangle_{\mathbb{C}}}{2(\langle \tau^{(0)} \rangle + \langle \tau^{(1)} \rangle)^2} P_{(0/1)}^{\text{st}} \quad (3.68)$$

and therefore eventually

$$\begin{aligned} s_n &= 2 \frac{|\langle f_n, P_{(1)}^{\text{st}} - P_{(0)}^{\text{st}} \rangle_{\mathbb{C}}|^2}{2n^2 \Omega^2 (\langle \tau^{(0)} \rangle + \langle \tau^{(1)} \rangle)^2} \\ &= \frac{\left| \int_0^{2\pi} d\phi \exp(in\phi) P_{(1)}^{\text{st}}(\phi) - \int_0^{2\pi} d\phi \exp(in\phi) P_{(0)}^{\text{st}}(\phi) \right|^2}{n^2 \Omega^2 (\langle \tau^{(0)} \rangle + \langle \tau^{(1)} \rangle)^2}. \end{aligned} \quad (3.69)$$

As in the previous section we express the Fourier coefficients  $\hat{P}_{j,k}^{(r \rightarrow s)}$  of the integral kernels  $P_{(r \rightarrow s)}(\phi, \psi)$ , defined by

$$P_{(r \rightarrow s)}(\phi, \psi) = \frac{1}{2\pi} \sum_{j,k=-\infty}^{\infty} \hat{P}_{j,k}^{(r \rightarrow s)} \exp(ij\phi) \exp(ik\psi),$$

by the Fourier coefficients of the time dependent waiting time distributions  $w^{(1)}(\tau, t)$  and  $w^{(0)}(\tau, t)$  (cf. eqs. (3.58) and (3.60)) as

$$\hat{P}_{j,k}^{(r \rightarrow s)} = \hat{w}_{j,j+k}^{(r)}$$



The stationary phase distributions  $P_{(0)}^{\text{st}}$  and  $P_{(1)}^{\text{st}}$  are defined by

$$P_{(r)}^{\text{st}}(\phi) = \int_0^{2\pi} d\theta \int_0^{2\pi} d\psi P_{(s \rightarrow r)}(\phi, \theta) P_{(r \rightarrow s)}(\theta, \psi) P_{(r)}(\psi)$$

The Fourier components  $\hat{P}_k^{(0)}$  and  $\hat{P}_k^{(1)}$  of the stationary phase distributions  $P_{(0)}(\phi)$  and  $P_{(1)}(\phi)$  are accordingly defined by

$$\hat{P}_k^{(r)\text{st}} = \sum_{i,j=-\infty}^{\infty} \hat{P}_{k,i}^{(s \rightarrow r)} \hat{P}_{-i,j}^{(r \rightarrow s)} \hat{P}_{-j}^{(r)\text{st}}, \quad \hat{P}_0^{(r)\text{st}} = 1. \quad (3.70)$$

Having these Fourier coefficients, the weights  $s_n$  can be easily evaluated from eq. (3.69) as

$$s_n = \frac{4\pi^2}{n^2 \Omega^2 (\langle \tau^{(0)} \rangle_0 + \langle \tau^{(1)} \rangle_0)^2} |\hat{P}_n^{(0)\text{st}} - \hat{P}_n^{(1)\text{st}}|^2. \quad (3.71)$$

Again, this result is valid for arbitrary not necessarily small driving signals. As in the previous subsection, we solve eq. (3.70) in linear order in the amplitude  $A_{\text{in}}$  of the periodic driving, leading to

$$\begin{aligned} \hat{P}_0^{(r)\text{st}} &= \frac{1}{2\pi}, \quad r = 0, 1 \\ \hat{P}_k^{(r)\text{st}} = (\hat{P}_{-k}^{(r)\text{st}})^* &= \frac{\hat{P}_{k,0}^{(s \rightarrow r)} + \hat{P}_{k,-k}^{(s \rightarrow r)} \hat{P}_{k,0}^{(r \rightarrow s)}}{2\pi(1 - \hat{P}_{k,-k}^{(s \rightarrow r)} \hat{P}_{k,-k}^{(r \rightarrow s)}), \quad (r, s) = (0, 1), (1, 0). \end{aligned}$$

These results together with the appropriate time dependent waiting time density for a double well system reproduce the stationary phase distribution calculated in [18].

Now we can evaluate  $s_{\pm 1}$  from eq. (3.71) in order  $O(A_{\text{in}}^2)$ , taking again into account (cf. eq. (3.64)) that the mean waiting time in a state of the driven system  $\langle \tau^{(r)} \rangle$  agrees up to order  $O(A_{\text{in}}^2)$  with the respective mean waiting time  $\langle \tau^{(r)} \rangle_0$  of the undriven system. The resulting expressions are

$$s_{\pm 1} = \frac{1}{\Omega^2 (\langle \tau^{(0)} \rangle_0 + \langle \tau^{(1)} \rangle_0)^2} \left| \frac{\hat{w}_{1,1}^{(1)}(1 - \hat{w}_{1,0}^{(0)}) - \hat{w}_{1,1}^{(0)}(1 - \hat{w}_{1,0}^{(1)})}{1 - \hat{w}_{1,0}^{(1)} \hat{w}_{1,0}^{(0)}} \right|^2 \quad (3.72)$$

which agrees with the result found in [49, 50] by means of an approach based on asymptotic periodic solutions of driven renewal equations. From eq. (3.72) we can calculate the SPA and SNR as in the previous section. If we consider now the general situation with values  $x^{(0)}$  and  $x^{(1)}$  in state 0 and 1 respectively, the

spectral power density is scaled by  $(x^{(0)} - x^{(1)})^2$ , leading to the same factor in the SPA while the SNR remains invariant. Thus

$$\text{SPA} = \frac{(x^{(0)} - x^{(1)})^2}{|A_{\text{in}}|^2 \Omega^2 (\langle \tau^{(0)} \rangle_0 + \langle \tau^{(1)} \rangle_0)^2} \left| \frac{\hat{w}_{1,1}^{(1)}(1 - \hat{w}_{1,0}^{(0)}) - \hat{w}_{1,1}^{(0)}(1 - \hat{w}_{1,0}^{(1)})}{1 - \hat{w}_{1,0}^{(0)} \hat{w}_{1,0}^{(1)}} \right|^2 + O(A_{\text{in}}^2) \quad (3.73)$$

To calculate the SNR according to eq. (3.10) we need again the background spectral density, which in lowest order in the input amplitude can be taken as the spectral power density of the undriven process eq. (2.24), leading to

$$\text{SNR} = \frac{\pi}{\langle \tau^{(0)} \rangle_0 + \langle \tau^{(1)} \rangle_0} \frac{|\hat{w}_{1,1}^{(1)}(1 - \hat{w}_{1,0}^{(0)}) - \hat{w}_{1,1}^{(0)}(1 - \hat{w}_{1,0}^{(1)})|^2}{\text{Re} [(1 - \hat{w}_{1,0}^{(0)})(1 - \hat{w}_{1,0}^{(1)})(1 - \hat{w}_{-1,0}^{(0)} \hat{w}_{-1,0}^{(1)})]} + O(A_{\text{in}}^4) \quad (3.74)$$

### Application of the driven renewal process approach to the FHN system in the bistable and excitable regime

In this section we apply the results of periodic renewal processes from the previous section to the spike train of a periodically driven FitzHugh-Nagumo system

$$\begin{aligned} \dot{x} &= x - x^3 - y + \sqrt{2D}\xi(t) \\ \dot{y} &= \epsilon(x + a_0 - s_a(t) - (a_1 + s_p(t))y) \end{aligned} \quad (3.75)$$

In contrast to the application of the non Markovian master equation approach to the FHN system in subsection 3.3.1 we consider only signals in the slow inhibitor dynamics ( $y$  variable). However we go beyond the excitable regime. Namely, depending on the choice of parameters the FHN system is either bistable, oscillatory or excitable. Here we are interested in the excitable and bistable regime. All numerical investigations which follow are done with the parameter values

$$a_0 = 0.1, \quad a_1 = 1.25, \quad \text{and} \quad \epsilon = 0.001 \quad (3.76)$$

for the excitable regime and

$$a_0 = 0, \quad a_1 = 1.51, \quad \text{and} \quad \epsilon = 0.001 \quad (3.77)$$

for the bistable regime. The external periodic driving is chosen to act additively ( $s_a(t)$ ) or parametrically ( $s_p(t)$ ) on the  $y$  dynamics which corresponds to a shifting of the  $y$ -nullcline (see Fig. 3.4) upwards and downwards or a rotation of the  $y$ -nullcline around the point  $(a_0, 0)$  respectively. In the following all signals are sub

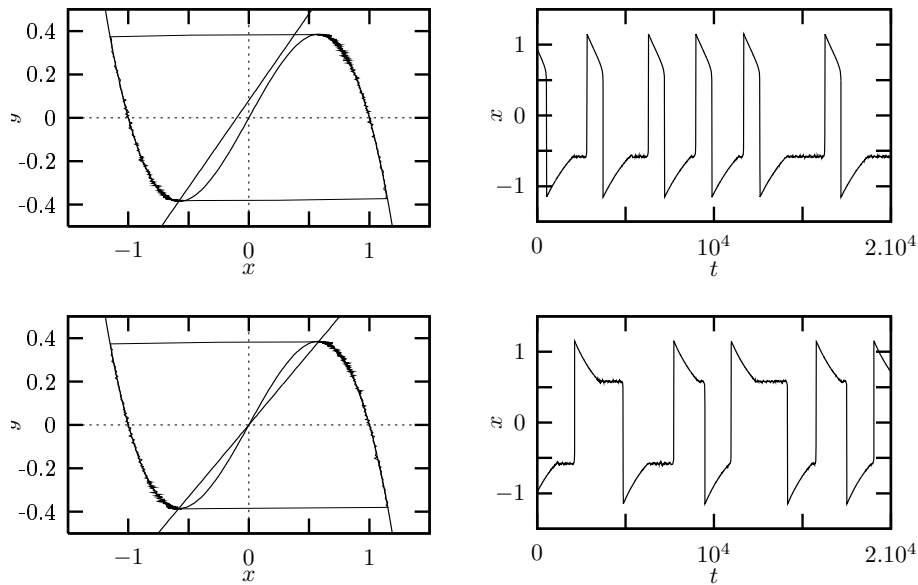


Figure 3.4: Left: Nullclines  $\dot{x} = 0$  and  $\dot{y} = 0$  of the FHN system without noise and signal, and a typical trajectory of the noisy undriven system in the excitable regime with parameters from eq. (3.76) (top) and bistable regime (bottom, parameters from eq. (3.77)). Right: Corresponding spiketrain  $x(t)$  for a noise level  $D = 1.0 \cdot 10^{-6}$ .

threshold signals, i.e. the fixed point structure and the stability properties of the fixed points do not change due to the driving.

A typical trajectory as well as the nullclines of the undriven system and a typical output spike train for the excitable and bistable situation are shown in Fig. 3.4. Due to a strong timescale separation  $\epsilon = 0.001$  the system very quickly moves between the right and left stable branch of the  $x$  nullcline. We thus approximate it with a two state description, where the two states correspond to the left and right stable branch of the cubic nullcline, neglecting the fast motion between the branches. The output of the system, i.e. the  $x$  coordinate remains approximately constant on these branches, namely 1 or -1. This approximation is shown for the bistable case in Fig. (3.5).

As already noticed previously, the dynamics of the FHN system has two ingredients. First, an excitation process from the stable fixed point(s) and second the motion along the stable branches of the nullclines. The excitation process is strongly influenced by the driving or a change in noise strength. while the motion along the stable branches of the cubic nullcline does not depend on the noise level and driving for small driving amplitudes and a small noise level .

This behavior has been recovered in the waiting time distributions on the left

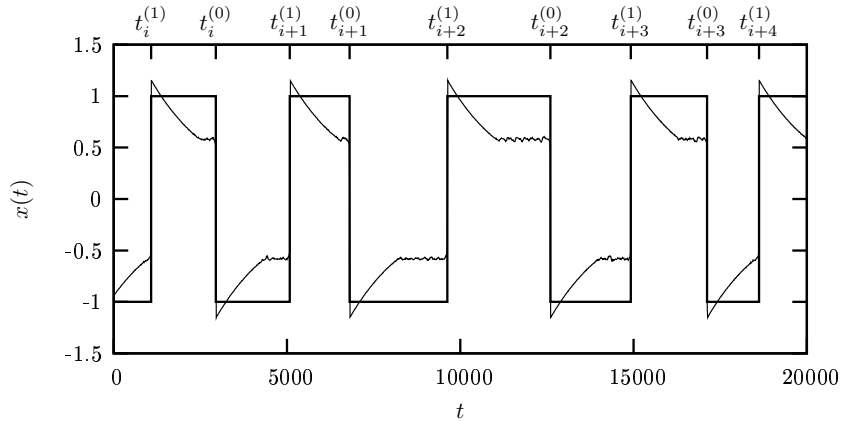


Figure 3.5: Typical spiketrain  $x(t)$  of the FHN system eqs. (3.75) in the bistable regime with noise strength  $D = 1.0 \cdot 10^{-6}$  and the corresponding two state approximation.

and right branch Fig. 3.6. Numerically evaluated for different small constant values of the signal and different low noise levels they show no waiting times shorter than a certain threshold  $T$ , which approximately does not depend on noise level and signal strength (Fig. 3.6). This threshold  $T$  is the time needed to travel along the stable branch. The following excitation step from the stable fixed point onto the excitation loop is to a good approximation a rate process, represented by the an exponentially distributed waiting time. In the logarithmic plot of the waiting time distributions Fig. 3.6 this is represented by linear decrease beyond the threshold. The rate of this excitation process strongly depends on both the signal and noise level. Within an adiabatic approximation, assuming that the time scale of the external signal is much slower than the relaxation time scale around the stable fixed point, the excitation step for time varying signals becomes a rate process with a signal and therefore time dependent rate  $\gamma(t)$ . In the case of the excitable regime with one stable fixed point on the left branch of the cubic nullcline we thus obtain the waiting time distributions distribution

$$w^{(0)}(\tau, t) = \Theta(\tau - T^{(0)})\gamma^{(0)}(t + \tau) \exp\left(-\int_{t+T^{(0)}}^{t+\tau} d\tau' \gamma^{(0)}(\tau')\right) \quad (3.78a)$$

$$w^{(1)}(\tau, t) = \delta(\tau - T^{(1)}) \quad (3.78b)$$

while in the bistable situation with two stable fixed points the waiting time distributions are given by

$$w^{(i)}(\tau, t) = \Theta(\tau - T^{(i)})\gamma^{(i)}(t + \tau) \exp\left(-\int_{t+T}^{t+\tau} d\tau' \gamma^{(i)}(\tau')\right), \quad i = 0, 1. \quad (3.79)$$

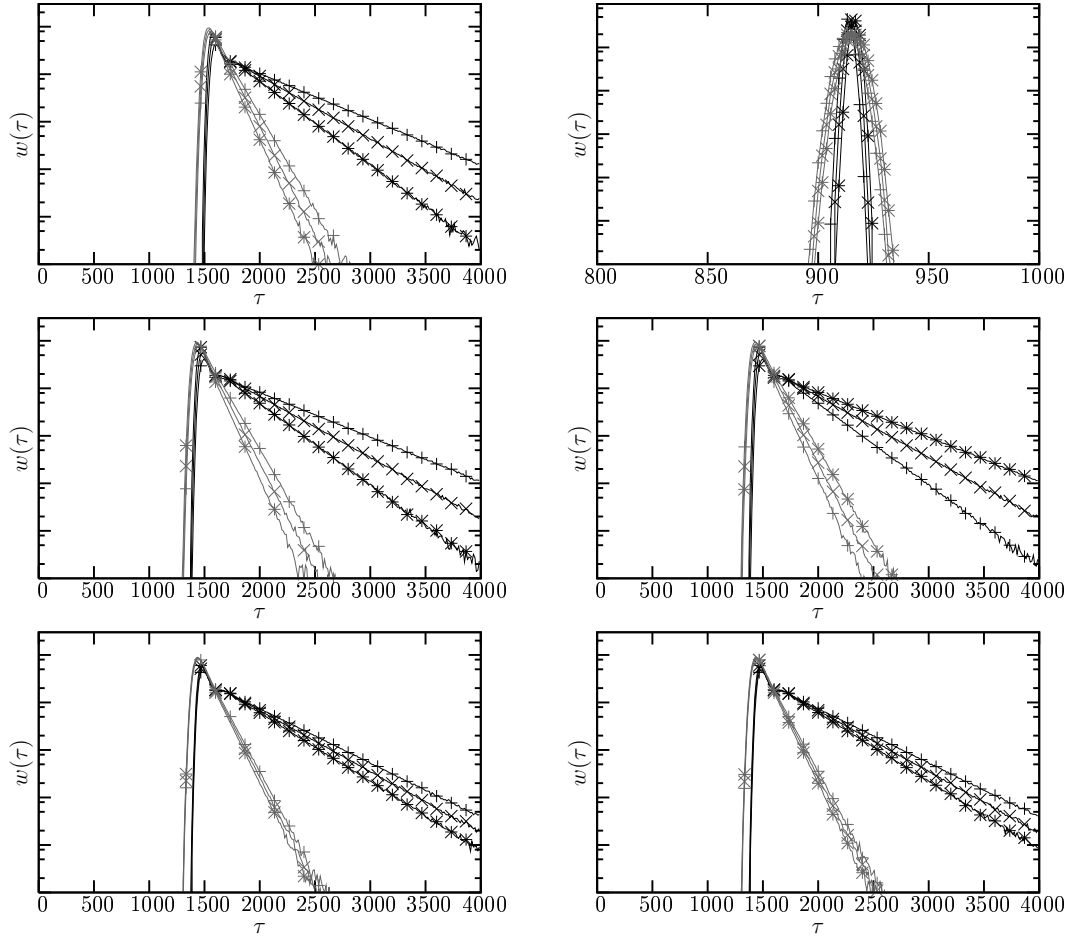


Figure 3.6: Non normalized waiting time distributions plotted in logarithmic scale in the left (left) and right state (right) for the excitable regime with additive driving (top) and bistable regime with additive (middle) and parametric driving (bottom) Noise levels  $D = 1. * 10^{-5}$  (gray) and  $D = 2. * 10^{-6}$  (black) and three different constant input signals  $s_{a/p}(t) = -10^{-3}$  (+) ,  $s_{a/p}(t) = 0.0$  (×) and  $s_{a/p}(t) = 10^{-3}$  (\*). Other parameters as given in eqs. (3.76) and (3.77)

Considering a weak periodic signal  $s(t) = A_{\text{in}} \exp(i\Omega t) + c.c.$ , the time dependent excitation rate  $\gamma(t)$  within an adiabatic approximation is given by

$$\gamma^{(i)}(t) = \gamma_0^{(i)}(1 + \alpha^{(i)}s(t)) + O(A_{\text{in}}^2). \quad (3.80)$$

where the rate without driving  $\gamma_0^{(i)}$  as well as the sensibility  $\alpha^{(i)}$  depend on noise strength  $D$ . With this excitation rate and the waiting time distributions eq. (3.78) the SPA and SNR can be evaluated from eqs. (3.73) and (3.74). The SPA for

excitable system is given by (setting  $\gamma_0 \equiv \gamma_0^{(0)}$  and  $\alpha \equiv \alpha^{(0)}$ )

$$\text{SPA} = \frac{(x^{(0)} - x^{(1)})^2 \alpha^2}{\left(\frac{1}{\gamma_0} + T^{(0)} + T^{(1)}\right)^2 \Omega^2} \frac{\sin^2 \frac{\Omega T^{(1)}}{2}}{(1 + 2\frac{\gamma_0^2}{\Omega^2}(1 - \cos \Omega(T^{(0)} + T^{(1)})) + 2\frac{\gamma_0}{\Omega} \sin \Omega(T^{(0)} + T^{(1)}))} \quad (3.81a)$$

while the SNR reads

$$\text{SNR} = \frac{2\pi\alpha^2 A_{\text{in}}^2}{\frac{1}{\gamma_0} + T^{(0)} + T^{(1)}} \quad (3.81b)$$

Eq. (3.81a) agrees with the result eq. (3.46) from subsection 3.3.1.

For the bistable regime general expressions can be derived for the SPA and SNR, however we restrict ourselves to the symmetric situation  $T^{(0)} = T^{(1)} \equiv T$ ,  $\gamma_0^{(0)} = \gamma_0^{(1)} \equiv \gamma_0$  to keep the number of parameters and the resulting formulas manageable. For an additive driving  $\alpha^{(1)} = -\alpha^{(0)} \equiv \alpha$  the resulting expressions for the SPA and SNR are given by

$$\text{SPA} = \frac{(x^{(0)} - x^{(1)})^2 \alpha^2}{\Omega^2 \left(\frac{1}{\gamma_0} + T\right)^2 (1 + 2\frac{\gamma_0^2}{\Omega^2}(1 + \cos \Omega T) - 2\frac{\gamma_0}{\Omega} \sin \Omega T)} \quad (3.82a)$$

$$\text{SNR} = \frac{2\pi\alpha^2 A_{\text{in}}^2}{\frac{1}{\gamma_0} + T} \quad (3.82b)$$

In the limit  $T \rightarrow 0$  which corresponds to the two state approximation of a double well potential system, one recovers from eqs. (3.82a) and (3.82b) the well known expressions [41]<sup>2</sup>

$$\text{SPA}_0 = \frac{(x^{(0)} - x^{(1)})^2 \alpha^2 \gamma_0^2}{\Omega^2 + 4\gamma_0^2} \quad \text{and} \quad \text{SNR}_0 = 2\pi\alpha^2 A_{\text{in}}^2 \gamma_0$$

We can now express the SPA of the two state model for the bistable FHN system in terms of the SPA<sub>0</sub> of the double well potential system and an amplification factor  $a$  as

$$\text{SPA} = \text{SPA}_0 a\left(\frac{\gamma_0}{\Omega}, \frac{T\Omega}{2\pi}\right)$$

---

<sup>2</sup>The factor of 2 in SNR<sub>0</sub> compared to the expression in [41] has two reasons, namely the SNR as defined in [41] is twice the SNR as used in this work and the definition of our signal as  $s(t) = A_{\text{in}} \exp(i\Omega t) + c.c.$  leads to a doubled amplitude as compared to  $s(t) = A_{\text{in}} \cos \Omega t$  and thus to a factor of 4 in  $|A_{\text{in}}|^2$ . As this factor cancels in the SPA our expression for SPA<sub>0</sub> has an additional factor  $\frac{1}{2}$  compared to [41]

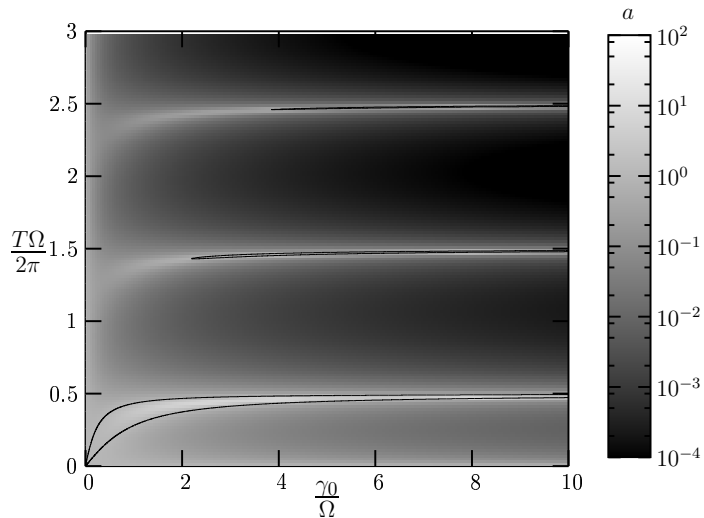


Figure 3.7: Amplification factor  $a$  as a function of  $\frac{\gamma_0}{\Omega}$  and  $\frac{T\Omega}{2\pi}$ . The contour line separates regions where  $a > 1$  from regions where  $a < 1$ .

where the amplification factor  $a$  is given by

$$a(c_1, c_2) = \frac{1 + 4c_1^2}{(1 + 2\pi c_1 c_2)^2 (1 + 2c_1^2 (1 + \cos 2\pi c_2) - 2c_1 \sin 2\pi c_2)}$$

Fig. 3.7 shows a plot of this amplification factor. First we notice that there are regions where  $a > 1$ , i.e. the additional fixed waiting time  $T$  improves the SPA compared to a double well potential system's SPA without fixed waiting time. The amplification factor for the optimal waiting time  $T$  increases like  $\gamma_0^2/\Omega^2$  for  $\gamma_0 \gg \Omega$ . For these large excitation rates the optimal fixed waiting times  $T$  for a given driving frequency  $\Omega$  are approximately located at  $T = \frac{(2n+1)\pi}{\Omega}$ ,  $n = 0, 1, \dots$

If we consider the symmetric bistable regime with a parametric driving the situation changes completely. In this case  $\alpha^{(0)} = \alpha^{(1)}$  and the SNR as well as the SPA vanish. This is not an effect of the approximations we made but an effect of symmetry which also holds beyond the two state approximation and beyond linear response as can be understood as follows: Due to the type of the driving there is no preferred state (left branch of the cubic nullcline or right branch of the cubic nullcline) for a given signal phase. In the continuous description the state  $(x, y)$  is as probable as the state  $(-x, -y)$  for a given signal phase. The coefficients  $c_{\omega, T}$  as defined in eq. (2.21b) therefore vanish in the limit  $T \rightarrow \infty$  for arbitrary  $\omega$ . Then also  $\langle |c_{\omega, T}|^2 \rangle$  vanish and accordingly there are no delta peaks in the spectral power density. However, although the SPA and SNR is exactly zero the system

nevertheless can be strongly influenced by the periodic input. It may even show nearly periodic behavior (Fig. 3.8). This leads to the need of different non spectral based measures to quantify the response to a periodic signal as the spectral based measures SNR and SPA clearly fail in this case.

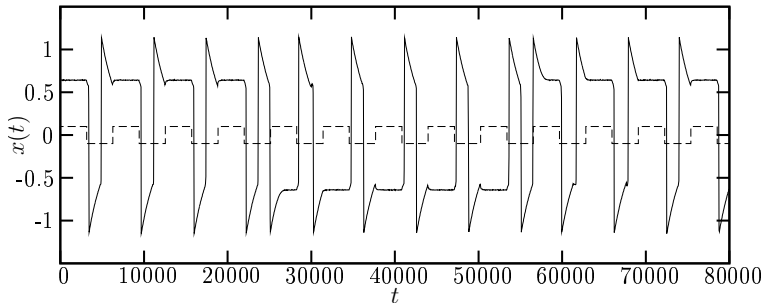


Figure 3.8: A typical output trajectory (solid line) and corresponding input signal (dashed line) for the FHN system in the symmetric bistable regime (parameters given in eq. (3.77)) with parametric driving and a driving frequency  $\Omega = 0.001$  and driving amplitude  $A_{\text{in}} = 0.1$ .

Finally we compare our theoretical results with simulations of the FHN system with additive driving  $s_a(t) = 0.001 \exp(i\Omega t) + c.c.$ . To this end we have to adapt the parameters of the two state model to the continuous FHN model. From the numerical evaluations of the FHN system's waiting time distributions Fig. (3.6) we estimate for  $D = 2.0 \cdot 10^{-6}$  for the bistable situation

$$T^{(0)} = T^{(1)} \approx 1430, \gamma_0^{(0)} = \gamma_0^{(1)} \approx 0.003, \alpha^{(0)} = -\alpha^{(1)} \approx 290 \quad (3.83)$$

and for the excitable system

$$T^{(0)} \approx 1550, T^{(1)} \approx 915, \gamma_0^{(0)} \approx 0.003, \alpha^{(0)} \approx 300 \quad (3.84)$$

while for  $D = 1.0 \cdot 10^{-5}$  the bistable regime has

$$T^{(0)} = T^{(1)} \approx 1430, \gamma_0^{(0)} = \gamma_0^{(1)} \approx 0.01, \alpha^{(0)} = -\alpha^{(1)} \approx 127 \quad (3.85)$$

and the excitable regime

$$T^{(0)} \approx 1550, T^{(1)} \approx 915, \gamma_0^{(0)} \approx 0.01, \alpha^{(0)} \approx 123 \quad (3.86)$$

With these parameters we have compared the expressions (3.81) and (3.82) with the SPA and SNR of the FHN system (Fig. 3.9 and 3.10) as obtained by numerical simulations and found a very good agreement. The deviation for low frequencies is due to the fact that the form factor of the real pulses suppresses the



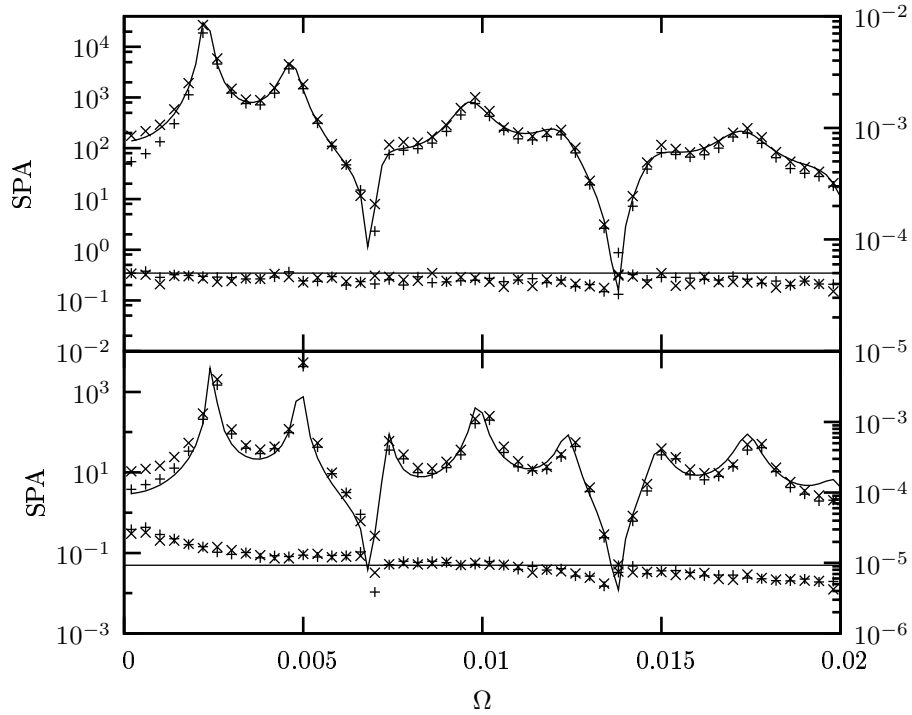


Figure 3.9: SPA (upper curves) and SNR (lower curves) of the two state theory (solid lines) compared to simulations of a FHN system (symbols) in the excitable regime for two different noise levels  $D = 2 \cdot 10^{-6}$  (top) and  $D = 1 \cdot 10^{-5}$  (bottom). The  $\times$ -symbols correspond to a digitally filtered spiketrain of the FHN system, where we assigned the value 1 to the system's output on the right branch of the cubic nullcline and -1 on the left branch (see Fig. 3.5). The  $+$ -symbols correspond to the unfiltered spiketrain  $x(t)$  of the FHN system. Parameters for the two state theory are given in eqs. (3.84) (top) and (3.86) (bottom). Parameters for the FHN system according to eq. (3.76).

low frequency range compared to the form factor of an rectangular pulse. As the form factor cancels for the SNR, there is no significant deviation for low frequencies from the expected constant value.

Up to now we did not consider the dependence of the system parameters on noise. We only made the assumption that the noise level influences the SPA and SNR via the excitation rates  $\gamma_0^{(0)}$  and  $\gamma_0^{(1)}$  and the amplification parameters  $\alpha^{(0)}$  and  $\alpha^{(1)}$ . This assumption has proven to be a good approximation for low noise levels. To consider the SPA and SNR as a function of noise strength we additionally assume an Arrhenius type excitation rate  $\gamma(t) \equiv \gamma^{(0)}(t)$  with an effective potential

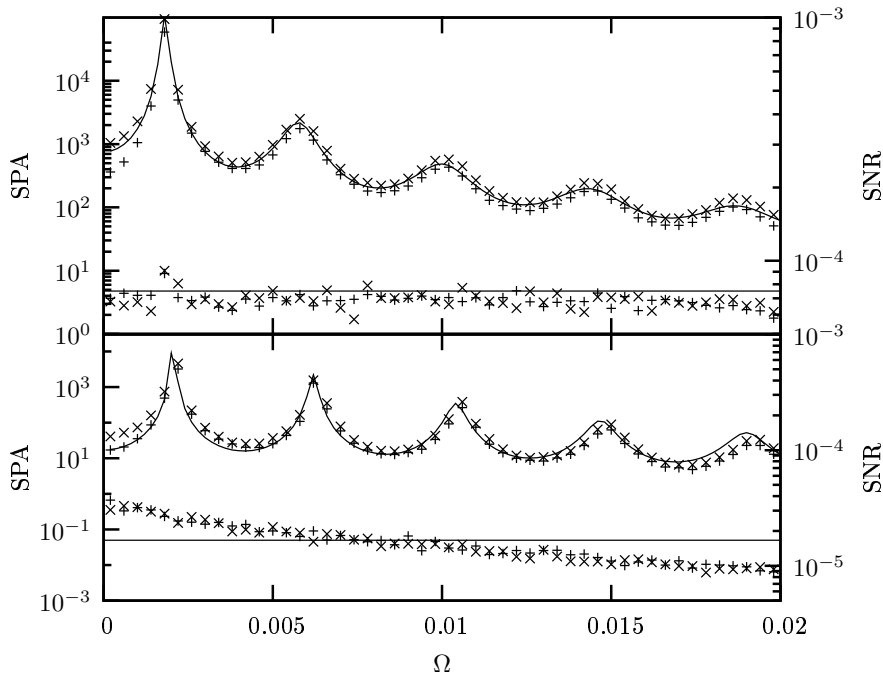


Figure 3.10: SPA (upper curves) and SNR (lower curves) of the two state theory (solid lines) compared to simulations of a FHN system (symbols) in the bistable regime for two different noise levels  $D = 2 \cdot 10^{-6}$  (top) and  $D = 1 \cdot 10^{-5}$  (bottom). The meaning of the symbols is explained in the caption of Fig. 3.9. Parameters for the two state theory are given in eqs. (3.83) (top) and (3.85) (bottom). Parameters for the FHN system according to eq. (3.77).

barrier  $\Delta U$  which is modulated by the external small signal, i.e.

$$\gamma(t) = r_0 \exp\left(-\frac{\Delta U - \beta s(t)}{D}\right) = \gamma_0 \left(1 + \frac{\beta s(t)}{D}\right). \quad (3.87)$$

With this excitation rate we can fit the parameters  $r_0$ ,  $\Delta U$  and  $\beta$  to our system (see Fig. 3.11). Within this approximation we have plotted the SPA (3.81a) as a function of noise strength and driving frequency Fig.3.12. As already observed the SPA shows a complex structure, with multiple minima and maxima as a function of driving frequency. However, also as a function of noise strength the SPA shows a maximum. There is an optimal noise level at which periodic signals are maximally amplified by the stochastic excitable system, which is the famous effect of stochastic resonance in excitable systems. [41, 73, 75, 77, 137]. This optimal noise level only weakly depends on the driving frequency. The existence of an optimal noise level is a joint effect of an decreasing sensibility  $\alpha$  and at the same time an

increasing mean excitation rate  $\gamma_0$  with increasing noise. This is different from the coherence resonance effect of excitable systems, which is due to a different dependence of the excitation time and the firing and refractory time on the noise level. [100]. Here we did not consider any dependence of the firing and refractory time on noise at all.

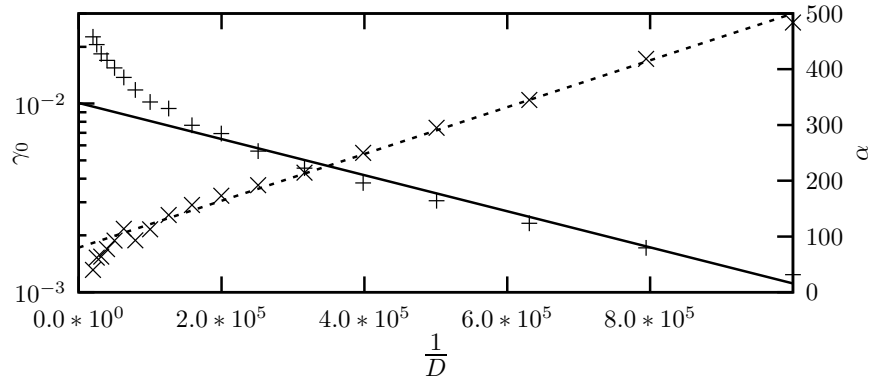


Figure 3.11: Excitation rate  $\gamma_0$  of the FitzHugh-Nagumo model in the excitable regime without external signal (+) and parameter  $\alpha$  (x) from eq. (3.80) as a function of noise strength. The lines corresponds to an Arrhenius type dependence  $\gamma_0 = r_0 \exp(-\frac{\Delta U}{D})$  with  $r_0 = 0.0082$  and  $\Delta U = 2.2 \cdot 10^{-6}$  (solid line) and  $\alpha = -0.00042/D$ , i.e  $\beta = 0.00042$  (dotted line) in eq. (3.87).

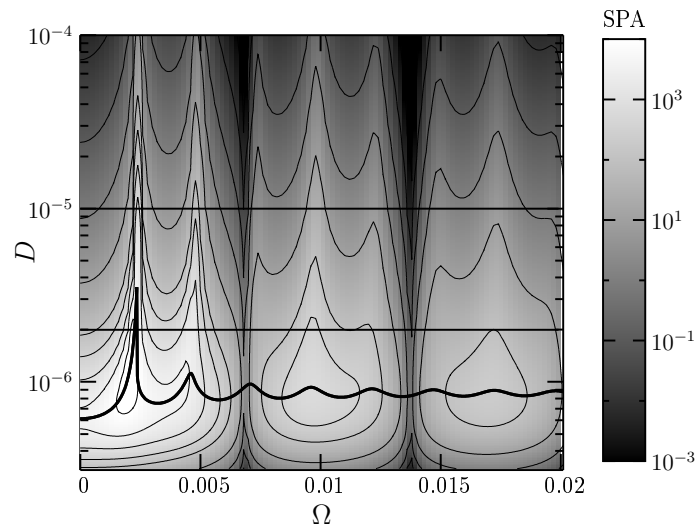


Figure 3.12: SPA according to eq. (3.81a) with  $T^{(0)} = 1550$  and  $T^{(1)} = 900$  and  $\gamma(t)$  according to eq. (3.87) with  $r_0 = 0.0082$  and  $\Delta U = 2.2 \cdot 10^{-6}$  and  $\beta = 0.00042$ . The thick solid line indicates the optimal noise level, at which the SPA is maximal. The horizontal sections at  $D = 2 \cdot 10^{-6}$  and  $D = 1 \cdot 10^{-5}$  correspond to the plots in Fig. 3.9.

## 3.4 Summary

The response of periodically driven stochastic systems to the driving signal can be measured by means of the spectral based quantities SPA and SNR. We derived results for the SNR and SPA of periodic renewal processes, both based on a master equation description and based on the time dependent waiting time distributions between subsequent events. These periodic renewal processes occur as a generalization of the stationary renewal processes, introduced in chapter 2, if the underlying system, e.g. the double well potential system or the FHN system, is influenced by a periodic signal. We then applied the general results to the discrete state model of the FHN system. Fitting a few parameters, the firing and refractory time as well as the stationary excitation rate, the theoretical result for the SNR and SPA obtained within the periodic renewal process approach quite well reproduce and explain the observed behavior of the underlying continuous FHN dynamics. A simple example, namely the parametrically driven symmetric bistable FHN system, revealed the limits of spectral based measures of the response to the driving signal. In this example both the SPA and the SNR are exactly zero, although the system shows a very pronounced response to the periodic signal. In the next chapter we investigate the concept of synchronization between the process and the signal, which overcomes this shortcoming.

## Chapter 4

# Periodically Driven Systems-Stochastic Synchronization

Synchronization of deterministic nonlinear oscillatory systems to a periodic driving is a widely observed phenomenon. Depending on the amplitude of the driving and the mismatch between the driving frequency and the systems' frequency, synchronization regions with different rational relations between these frequencies can be observed. In these synchronization regions, known as Arnold tongues when plotted as a function of signal amplitude and frequency, the system performs a resonant motion on a torus in the joint phase space.

Considering stochastic systems these concepts have to be revised [14, 36, 40]. Due to the influence of noise, a perfect synchronization between the system's dynamics and the signal is no longer possible but there is always a finite probability of so called phase slips, namely an additional or missing cycle of the system. The rarer these phase slips are the better the system is synchronized.

Departing from the picture of stochastic oscillatory systems, let us consider an arbitrary system whose behavior is characterized by some recurrent events, like for example the generation of a spike in an excitable system, or the transition between the two wells in a double well system [36]. As pointed out in subsection 2.2.2 for undriven systems, the Péclet number which is the ratio between mean frequency and the effective diffusion constant of the number of events, characterizes the regularity of the occurrence of these events, and thus of the system's dynamics which generates the events.

Imagine now that the system is influenced by a periodic signal. If this influence is very strong, such that the events are triggered by the periodic signal in an approximately deterministic way one observes an integer ratio between system frequency and signal frequency. At the same time the effective diffusion of the number of events is approximately zero, as the events inherit the deterministic behavior of the signal. Thus the Péclet number is very high. A high Péclet

number and a rational relation between system and signal frequency are thus indicating that the system and signal are stochastically synchronized with phase slips occurring only very rarely. On the other hand, if the influence of the external signal is weak, the occurrence of the events happens in a stochastic way governed by the stochastic dynamics of the system considered. In this case the system frequency is not locked to the signal frequency and due to the stochastic nature of the system, the effective diffusion constant is different from zero. leading to a larger Péclet number. Thus the mean frequency, effective diffusion constant and Péclet number may serve as a measure of synchronization to the periodic signal. However one has to be careful. A high Péclet number alone is not a foolproof sign of stochastic synchronization, as it can just be due to a very regular motion of the system itself. Even an integer relation between mean system frequency and signal frequency can exist by chance. However observing plateaus in the relation between system and signal frequency when varying the driving frequency, which are accompanied with a strong decrease of the effective diffusion coefficient and thus with a strong increase of the Péclet number is an undecceptive sign of synchronization. To demonstrate this behavior we have numerically evaluated the above mentioned quantities for the periodically driven FHN system in Fig. 4.1. The plateaus in the frequency ratio accompanied by a low effective diffusion coefficient indicate synchronization regions. Although merely visible, even in the regions of nearly perfect synchronization the actual excitation times and thus the systems dynamics is still random (see Fig. 4.1, right plot).

The following three sections are devoted to the calculation of the mean frequency, effective diffusion coefficient and Péclet number in periodically driven discrete state models. While in the next section we investigate general properties of the number of events of a periodic renewal process, in sections 4.2 and 4.3 we present two methods to actually calculate the mean frequency and effective diffusion coefficient of the event number.

In section 4.2 we considers discrete state models, whose stochastic dynamics is assumed to be governed by some generalized master equation. This approach will be used to investigate stochastic synchronization in a Markovian two state model for double well potential systems (subsection 4.2.1) and a non Markovian model for excitable dynamics (subsection 4.2.2). Finally we apply it to investigate the control of molecular motors by periodically varying fuel concentrations in subsection 4.2.3.

The second approach is more general. We present a method to calculate the mean frequency and effective diffusion coefficient of the number of events of periodically driven renewal processes, defined by a periodically time dependent waiting time distribution  $w(\tau, t)$ . Finally in subsection 4.3.4 we show equivalence between the two approaches for the two state non Markovian model of excitable dynamics.

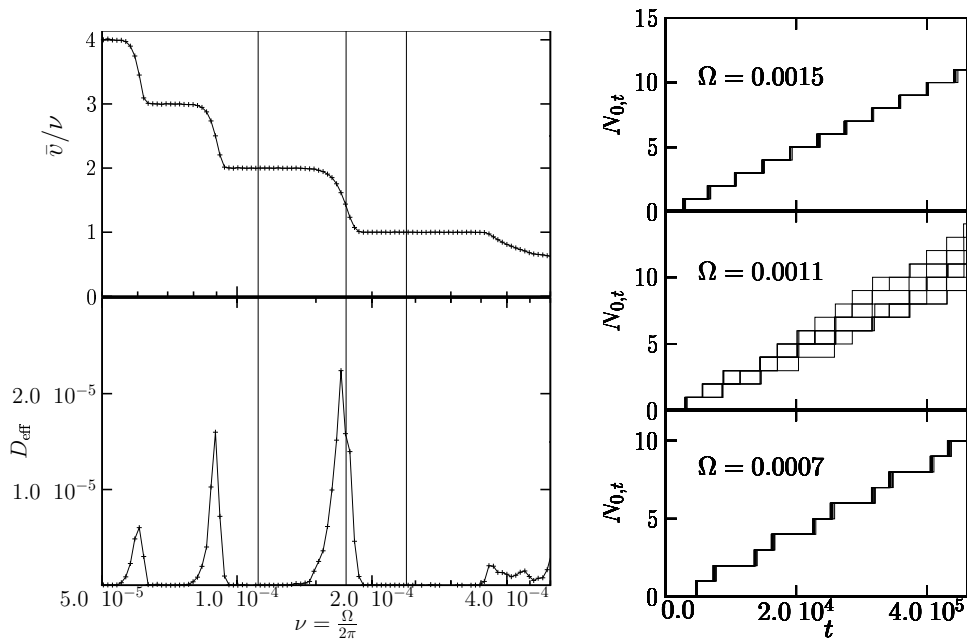


Figure 4.1: Synchronization in the FHN system. The left figure shows the relation between mean frequency  $\bar{v}$  of the system and driving frequency  $\nu = \frac{\Omega}{2\pi}$  and the effective diffusion coefficient  $\bar{D}_{\text{eff}}$  as a function of the driving frequency  $\nu = \frac{\Omega}{2\pi}$ . For three different driving frequencies, corresponding to 1 : 1 (bottom), 2 : 1, (top) and no synchronization, we have plotted 20 realizations of the corresponding number of spikes  $N_{0,t}$  of the FHN system (right figure). Parameters of the FHN system eqs. (3.30):  $a_0 = 0.405$ ,  $a_1 = 0.5$ ,  $\epsilon = 0.001$ ,  $D = 1.0 \times 10^{-5}$ , and a dichotomic driving  $s(t) = \pm 0.015$ .

## 4.1 Properties of the number of events for periodically driven renewal processes

Consider a periodic renewal process. As motivated above, stochastic synchronization to the periodic driving can be characterized as an integer or rational relation between driving frequency and the frequency of the events  $\bar{v}$  and at the same time, a decrease in the effective diffusion coefficient  $\bar{D}_{\text{eff}}$ , i.e. a more regular (periodic) behavior. In terms of the number  $N_{t_0,t}$  of events in the interval  $(t_0, t]$  the instantaneous mean frequency and instantaneous effective diffusion coefficient are defined as

$$v_{t_0}(t) = \frac{d}{dt} \langle N_{t_0,t} \rangle \quad \text{and} \quad D_{\text{eff},t_0}(t) = \frac{d}{dt} \frac{\langle N_{t_0,t}^2 \rangle - \langle N_{t_0,t} \rangle^2}{2}. \quad (4.1)$$



Asymptotically, i.e. for  $t_0 \rightarrow -\infty$  the instantaneous mean frequency and the instantaneous effective diffusion coefficient eqs. (4.1) become periodic functions of time (for a proof see appendix C.1) and we may express their long time averaged values

$$\bar{v} = \lim_{t \rightarrow \infty} \frac{\langle N_{t_0,t} \rangle}{t} \quad \text{and} \quad \bar{D}_{\text{eff}} = \lim_{t \rightarrow \infty} \frac{\langle N_{t_0,t}^2 \rangle - \langle N_{t_0,t} \rangle^2}{2t} \quad (4.2)$$

as averages over one period of the asymptotically periodic instantaneous values  $v(t) = \lim_{t_0 \rightarrow -\infty} v_{t_0}(t)$  and  $D_{\text{eff}}(t) = \lim_{t_0 \rightarrow -\infty} D_{\text{eff},t_0}(t)$ , i.e.

$$\bar{v} = \frac{1}{T} \int_0^T dt v(t) \quad \text{and} \quad \bar{D}_{\text{eff}} = \frac{1}{T} \int_0^T dt D_{\text{eff}}(t). \quad (4.3)$$

Also the higher cumulants grow periodically (see again appendix C.1). Denoting by

$$\kappa^{[i]}(t) := \lim_{t_0 \rightarrow -\infty} \frac{d}{dt} K_{t,t_0}^{[i]} \quad (4.4)$$

the asymptotic periodic growth of the  $i$ th cumulant  $K_{t,t_0}^{[i]}$  of the number of events  $N_{t_0,t}$  in the interval  $(t_0, t]$ , one immediately obtains  $v(t) = \kappa^{[1]}(t)$  and  $D_{\text{eff}}(t) = \kappa^{[2]}(t)/2$ .

Up to now we have defined the mean frequency and the effective diffusion coefficient for the number of events. However in many cases the quantity of interest is not directly the number  $N$  of events but some quantity proportional to it. This can be for example a phase  $\phi := 2\pi N$  of the system, which increases by  $2\pi$  for each event. This phase will be considered in the context of stochastic synchronization with the external signal in subsections 4.2.1 and 4.2.2<sup>1</sup>. Or it can be the position  $x = \ell N$  along a track, if an event corresponds to a step of length  $\ell$  on the track, as is the case when investigating a model for molecular motors in subsection 4.2.3. Denoting the proportionality constant by  $\mathfrak{L}$ , the drift and diffusion properties of the resulting quantity are obtained by

$$\bar{v}_{\mathfrak{L}} = \mathfrak{L}\bar{v} \quad \text{and} \quad \bar{D}_{\text{eff},\mathfrak{L}} = \mathfrak{L}^2 \bar{D}_{\text{eff}}. \quad (4.5)$$

Therefrom the Péclet number

$$\text{Pe} = \frac{\mathfrak{L}\bar{v}_{\mathfrak{L}}}{\bar{D}_{\text{eff},\mathfrak{L}}} \quad (4.6)$$

---

<sup>1</sup>To consider a phase which increases by  $2\pi$  for each event, and compare it to the angular velocity of the signal, instead of directly comparing the frequency of events with the frequency of the driving signal, has historical reasons, as the concept of synchronization stems from oscillatory system where the notion of a phase is inherently given.

can be calculated, which no longer depends on  $\mathfrak{L}$ . As explained in chapter 2 subsection 2.2.2 it can be interpreted as the averaged number of steps performed until the system is randomized over one step length.

Finally we want to mention that also in the case of periodic renewal processes the equivalence between the low frequency limit of the spectral power density  $S_\chi(\omega)$  of the corresponding delta peak processes

$$\chi(t) = \sum_i \delta(t - t_i) \quad (4.7)$$

and twice the effective diffusion coefficient of the point process  $\{t_i\}_i$  is preserved. (For the stationary case cf. eqs. (2.26) and (2.30)). Likewise, the relation between mean frequency and the high frequency limit of  $S_\chi(\omega)$  carries over to periodic processes. (cf. eqs. (2.27) and (2.30)). Although we do not exploit this fact in the calculation of the effective diffusion coefficient in this chapter it is nevertheless worth to be shown. Namely consider a sequence of events at times  $t_i$  as. If  $N_{t_0,t}$  denotes the number of events in the time interval  $(t_0, t]$ , the corresponding stochastic process consisting of delta peaks at the event times is given by

$$\chi(t) = \frac{d}{dt} N_{t_0,t}, \quad t \geq t_0 \quad \text{and vice versa} \quad N_{t_0,t} = \int_{t_0}^t dt' \chi(t').$$

For this process the asymptotic effective diffusion coefficient is given by

$$\begin{aligned} \bar{D}_{\text{eff}} &:= \lim_{T \rightarrow \infty} \frac{\langle N_{t_0,T}^2 \rangle - \langle N_{t_0,T} \rangle^2}{2T} \\ &= \lim_{T \rightarrow \infty} \frac{1}{2T} \left[ \langle \int_0^T dt \chi(t) \int_0^T dt' \chi(t') \rangle - \langle \int_0^T dt \chi(t) \rangle \langle \int_0^T dt' \chi(t') \rangle \right] \\ &= \lim_{T \rightarrow \infty} \lim_{\omega \rightarrow 0} \frac{1}{2T} \int_0^T dt \int_0^T dt' e^{-i\omega(t-t')} c_{\tilde{\chi}, \tilde{\chi}}(t, t') \end{aligned}$$

In the second step we have changed the lower integral boundary from  $t_0$  to 0 which is possible as the finite difference tends to zero as  $T \rightarrow \infty$  due to the prefactor  $1/T$ . Upon exchanging the two limits  $T \rightarrow \infty$  and  $\omega \rightarrow 0$ , which is possible as the background spectral density of  $\chi(t)$  as defined by (3.5) is continuous at  $\omega = 0$ , we eventually obtain

$$\bar{D}_{\text{eff}} = \frac{S_{\text{bg}}(0)}{2} = \frac{1}{2} \lim_{\omega \rightarrow 0} S(\omega). \quad (4.8)$$

For the mean frequency  $\nu$  one obtains

$$\begin{aligned} \lim_{\omega \rightarrow \infty} S_\chi(\omega) &= \lim_{\omega \rightarrow \infty} \lim_{T \rightarrow \infty} T \langle |c_\omega, T|^2 \rangle = \lim_{\omega \rightarrow \infty} \lim_{T \rightarrow \infty} \frac{1}{T} \sum_{k,l=0}^{\langle N_T \rangle} \exp(i\omega(t_k - t_l)) \quad (4.9) \\ &= \lim_{T \rightarrow \infty} \frac{\langle N_T \rangle}{T} = \bar{\nu} \quad (4.10) \end{aligned}$$

where in the one before the last step we used the fact that in the limit  $\omega \rightarrow \infty$  the sum over the  $\exp(i\omega(t_k - t_l))$  with  $k \neq l$  vanishes and only the summands with  $k = l$  which are 1 remain. We did not use any consequence of the periodic point process being a renewal process. Relations (4.8) and (4.9) thus hold for arbitrary periodic or stationary point processes.

## 4.2 A master equation approach

Consider a periodically driven stochastic  $n$  state system described by the probabilities  $\mathbf{p}(t) = [p^{(1)}(t), \dots, p^{(n)}(t)]$  to be in state  $1, 2, \dots, n$  respectively at time  $t$  Fig. 4.2. We consider the transition into state 1 as an event and ask for the drift and diffusion properties of the number of these events (cf. subsection 2.2.2). [105].

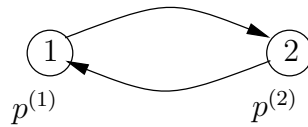


Figure 4.2: A two state system

We further assume that the underlying process is a periodic renewal process and that the evolution of the probabilities in time can be expressed in terms of some generalized master equation, which relates the temporal change of the probabilities  $p^{(i)}(t)$  to be in state  $i$  at time  $t$  to the probabilities themselves by some linear master operator  $\mathcal{M}_t$ ,

$$\frac{d}{dt}p^{(i)}(t) = \mathcal{M}_t^{(i)}[\mathbf{p}](t), \quad i = 1, \dots, n \quad (4.11)$$

with  $\mathbf{p} = [p^{(1)}(t), \dots, p^{(n)}(t)]$ . These equations have to be supplemented with the normalization condition.

$$\sum_{i=1}^n p^{(i)}(t) = 1. \quad (4.12)$$

The periodicity of the problem is reflected by the periodicity of the master operator, i.e.

$$\mathcal{M}_{t+\mathcal{T}} = \mathcal{M}_t. \quad (4.13)$$

where  $\mathcal{T}$  denotes the period of the driving. As we are interested in the number of events which happened up to some time  $t$  we have to unwrap the system. That is,

we additionally have to take the number  $k$  of events, i.e. of transitions from state  $n$  to state 1, into account. Denoting by  $p_k^{(i)}(t)$  the probability to be in state  $i$  at time  $t$  and to have had  $k$  events, its dynamics is given by

$$\frac{d}{dt}p_k^{(i)}(t) = \mathcal{M}_t^{(i),+}[\mathbf{p}_{k-1}](t) + \mathcal{M}_t^{(i),0}[\mathbf{p}_k](t), \quad i = 1, \dots, n \quad (4.14)$$

with  $\mathbf{p}_k(t) = [p_k^{(1)}(t), \dots, p_k^{(n)}(t)]$ . The operator  $\mathcal{M}_t^{(i),+}[\mathbf{p}_{k-1}](t)$  accounts for the probability influx into state  $k$  and thus for the probability efflux out of state  $k-1$  while  $\mathcal{M}_t^{(i),0}[\mathbf{p}_k](t)$  is responsible for the evolution within the state  $k$ , i.e. between the different substates  $i$  and for the efflux out of state  $k$ . The original master operator is thus split into the sum of the two master operators, which result from unwrapping the system,

$$\mathcal{M}_t^{(i)}[\mathbf{p}](t) = \mathcal{M}_t^{(i),+}[\mathbf{p}](t) + \mathcal{M}_t^{(i),0}[\mathbf{p}](t) \quad (4.15)$$

Due to the renewal property of the process the states  $k-2$  and  $k$  are not directly linked, i.e. there is no part of the unwrapped master equation which directly relates the probabilities  $\mathbf{p}_{k-2}(t)$  and  $\mathbf{p}_k(t)$ . Denoting by  $p_k(t)$  the total probability to have had  $k$  events at time  $t$ , the normalization condition eq. (4.12) reads

$$\sum_{i=1}^n p_k^{(i)}(t) = p_k(t). \quad (4.16)$$

Let us shortly present our two discrete models within this setting, starting with the Markovian two state model for a double well potential system. Its probabilities to be in state 1 or 2 are governed by

$$\frac{d}{dt}p^{(1)}(t) = -\gamma_{1 \rightarrow 2}(t)p^{(1)}(t) + \gamma_{2 \rightarrow 1}(t)p^{(2)}(t) \quad (4.17a)$$

$$\frac{d}{dt}p^{(2)}(t) = \gamma_{1 \rightarrow 2}(t)p^{(1)}(t) - \gamma_{2 \rightarrow 1}(t)p^{(2)}(t). \quad (4.17b)$$

If we additionally take into account the number  $k$  of events, i.e. transitions from 2 to 1 this leads to the unwrapped master equation

$$\frac{d}{dt}p_k^{(1)}(t) = -\gamma_{1 \rightarrow 2}(t)p_k^{(1)}(t) + \gamma_{2 \rightarrow 1}(t)p_{k-1}^{(2)}(t) \quad (4.18a)$$

$$\frac{d}{dt}p_k^{(2)}(t) = \gamma_{1 \rightarrow 2}(t)p_k^{(1)}(t) - \gamma_{2 \rightarrow 1}(t)p_k^{(2)}(t). \quad (4.18b)$$

Thus the splitting of the master operator into  $\mathcal{M}_t^{(i),+}$  and  $\mathcal{M}_t^{(i),0}$  in eq. (4.14) results in

$$\begin{aligned} \mathcal{M}_t^{(1),0}[\mathbf{p}_k](t') &= -\gamma_{1 \rightarrow 2}(t)p_k^{(1)}(t'), & \mathcal{M}_t^{(1),+}[\mathbf{p}_{k-1}](t') &= \gamma_{2 \rightarrow 1}(t)p_{k-1}^{(2)}(t') \\ \mathcal{M}_t^{(2),0}[\mathbf{p}_k](t') &= \gamma_{1 \rightarrow 2}(t)p_k^{(1)}(t') - \gamma_{2 \rightarrow 1}(t)p_k^{(2)}(t'), & \mathcal{M}_t^{(2),+}[\mathbf{p}_{k-1}](t') &= 0 \end{aligned}$$

The next example, the non Markovian three state model for excitable systems as introduced in section 2.1.2 may, in the context of synchronization, be reduced to only two states, by lumping the firing and refractory state together to one state 1 while the rest state 2 remains on its own. This reduction is possible because here we are not concerned with the output of the excitable system, which obviously is different in firing and refractory state. The evolution of the probabilities in this model is correspondingly given by (compare eqs. (2.15) and their derivation)

$$\frac{d}{dt}p^{(1)}(t) = \gamma(s(t))p^{(2)}(t) - \int_0^\infty d\tau\gamma(s(t-\tau))p^{(2)}(t-\tau)w(\tau) \quad (4.19a)$$

$$\frac{d}{dt}p^{(2)}(t) = -\gamma(s(t))p^{(2)}(t) + \int_0^\infty d\tau\gamma(s(t-\tau))p^{(2)}(t-\tau)w(\tau) \quad (4.19b)$$

where  $w(\tau)$  is the waiting time density in firing and refractory state together while  $\gamma(s(t))$  is the signal dependent excitation rate of the rest state. Again taking into account the number of events  $k$  we obtain

$$\frac{d}{dt}p_k^{(1)}(t) = \gamma(s(t))p_{k-1}^{(2)}(t) - \int_0^\infty d\tau\gamma(s(t-\tau))p_{k-1}^{(2)}(t-\tau)w(\tau) \quad (4.20a)$$

$$\frac{d}{dt}p_k^{(2)}(t) = -\gamma(s(t))p_k^{(2)}(t) + \int_0^\infty d\tau\gamma(s(t-\tau))p_{k-1}^{(2)}(t-\tau)w(\tau) \quad (4.20b)$$

In this case the master operator is given by

$$\begin{aligned} \mathcal{M}_t^{(1),0}[\mathbf{p}_k](t') &= 0 \\ \mathcal{M}_t^{(1),+}[\mathbf{p}_{k-1}](t') &= \gamma(s(t))p_{k-1}^{(2)}(t') - \int_0^\infty d\tau\gamma(s(t-\tau))p_{k-1}^{(2)}(t'-\tau)w(\tau) \\ \mathcal{M}_t^{(2),0}[\mathbf{p}_k](t') &= -\gamma(s(t))p_k^{(2)}(t') \\ \mathcal{M}_t^{(2),+}[\mathbf{p}_{k-1}](t') &= \int_0^\infty d\tau\gamma(s(t-\tau))p_{k-1}^{(2)}(t'-\tau)w(\tau) \end{aligned}$$

However as already explained in connection with spectral based measures of the periodically driven threestate model in subsection 3.3.1 this differential form does not lead to a unique solution even together with the normalization condition (4.16). We have to additionally impose that

$$p_k^{(1)}(t) = \int_0^\infty d\tau\gamma(s(t-\tau))p_{k-1}^{(2)}(t-\tau)z(\tau) \quad (4.22)$$

stating that the probability that the system is in state  $(k, 1)$  at time  $t$  is the probability flux out of state  $(k-1, 2)$  at time  $t-\tau$  in the past,  $\gamma(s(t-\tau))p_{k-1}^{(2)}(t-\tau)$ , times the probability that state 1 is not already left again,  $z(\tau)$ , integrated over the

past. Note that the time derivative of the above equation is equal to eq. (4.20a). Taking the normalization condition (4.16) into account eq. (4.22) leads to

$$\int_0^\infty d\tau \gamma(s(t-\tau)) p_{k-1}^{(2)}(t-\tau) z(\tau) + p_k^{(2)}(t) = p_k(t). \quad (4.23)$$

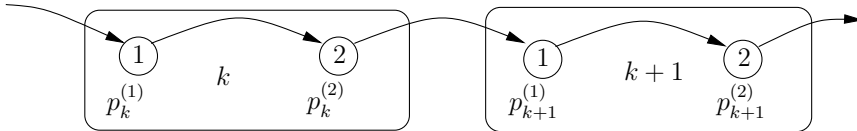


Figure 4.3: The two state system is unwrapped in order to take into account the number of events.

Our aim is to evaluate the asymptotic mean frequency  $\bar{v}$  as well as the effective diffusion coefficient  $\bar{D}_{\text{eff}}$ . Their definition (4.2) is based on the mean number of events as well as its variance, which can in principle be calculated in terms of the probabilities  $\mathbf{p}_k$  as

$$\langle N_{t_0,t} \rangle = \sum_{k=-\infty}^{\infty} k \sum_{i=1}^n p_k^{(i)}(t) \quad \text{and} \quad \langle N_{t_0,t}^2 \rangle = \sum_{k=-\infty}^{\infty} k^2 \sum_{i=1}^n p_k^{(i)}(t). \quad (4.24)$$

However to obtain the probabilities  $\mathbf{p}_k(t)$  one has to solve the general time dependent unwrapped master equation (4.14) with some appropriate initial condition, which in general is not feasible. Therefore we propose a different approach. According to section 4.1 the instantaneous mean phase velocity and instantaneous effective phase diffusion coefficient as defined in eqs. (4.1) asymptotically become periodic functions of  $t$ . In this asymptotic regime the mean frequency  $\bar{v}$  and effective diffusion coefficient  $\bar{D}_{\text{eff}}$  can be expressed as the period average of the periodic instantaneous mean frequency and diffusion coefficient (see eq. (4.3)). In the following we derive equations for the periodic asymptotic instantaneous mean frequency and effective diffusion coefficient, i.e. we reduce the problem to the calculation of a periodic solutions of some equations. This task is in general easier to perform (analytically or numerically) than solving the whole unwrapped master equation (4.14) with some initial condition to calculate the mean and variance of the number of events eq. (4.24) and then finally passing to the asymptotic limit in order to obtain  $\bar{v}$  and  $\bar{D}_{\text{eff}}$  according to eqs. (4.2).

How can we relate the instantaneous mean frequency  $v(t)$  and instantaneous effective diffusion coefficient  $D_{\text{eff}}(t)$  in a simple way to the microscopic dynamics (4.14)? To this end we introduce a continuous probability density  $\mathcal{P}(x,t)$  as an envelope of the discrete probability distribution of the number of events  $k$  as given

by  $p_k(t) := \sum_{i=1}^n p_k^{(i)}$  (for an application of such an envelope approach to undriven systems see also [38, 130]), namely

$$\int_{k-\frac{1}{2}}^{k+\frac{1}{2}} dx \mathcal{P}(x, t) = p_k(t). \quad (4.25)$$

Of cause this relation does not uniquely determine  $\mathcal{P}(x, t)$ . What kind of evolution equation does the continuous probability distribution  $\mathcal{P}(x, t)$  has to obey in order that this embedding remains true in the course of time? We will not consider this question in general, but focus only on the asymptotic case, in which the probabilities tend more and more to a uniform distribution. In this limit we assume that if eq. (4.25) was once true and if the cumulants and therefore also the moments of both the continuous probability density and the discrete probabilities grow with the same rate then eq. (4.25) remains true in the course of time. The cumulants of the discrete process are known to grow periodically in the considered asymptotic limit (see appendix C.1), with a rate denoted by  $\kappa^{[i]}(t)$ , where the first two coefficients  $v(t) = \kappa^{[1]}(t)$  and  $D_{\text{eff}}(t) = \kappa^{[2]}(t)/2$  are in the focus of our interest. To have this very same growth of the cumulants for the continuous probability density we assign the Kramers Moyal equation

$$\begin{aligned} \frac{\partial}{\partial t} \mathcal{P}(x, t) &= \sum_{n=1}^{\infty} \frac{(-1)^n}{n!} \kappa^{[n]}(t) \frac{\partial^n}{\partial x^n} \mathcal{P}(x, t) \\ &= -v(t) \frac{\partial}{\partial x} \mathcal{P}(x, t) + D_{\text{eff}}(t) \frac{\partial^2}{\partial x^2} \mathcal{P}(x, t) + O(3). \end{aligned} \quad (4.26)$$

to the evolution of the continuous probability density  $\mathcal{P}(x, t)$  (see appendix C.2). In this equation  $O(3)$  denotes derivatives of order  $\geq 3$  with respect to  $x$ . The microscopical dynamics however is not given in terms of the  $p_k(t)$  but we also have to include the substates  $i$  in our considerations. To this end we have to relate the  $p_k^{(i)}(t)$  to the continuous probability density  $\mathcal{P}(x, t)$ . We assume that these probabilities can be expanded as

$$p_k^{(i)}(t) = \sum_{m=0}^{\infty} q_m^{(i)}(t) \frac{\partial^m}{\partial x^m} \mathcal{P}(x, t) \Big|_{x=k}, \quad i = 1, \dots, n \quad (4.27)$$

with some  $\mathcal{T}$ -periodic coefficients  $q_m^{(i)}(t)$ . Expanding the integrand around  $k$  in eq. (4.25) we obtain

$$p_k(t) = \mathcal{P}(k, t) + \frac{1}{24} \frac{\partial^2}{\partial x^2} \mathcal{P}(x, t) \Big|_{x=k} + O(4) \quad (4.28)$$

which according to eq. (4.27) implies

$$\sum_{i=1}^n q_0^{(i)} = 1, \quad \sum_{i=1}^n q_1^{(i)} = 0 \quad \text{and} \quad \sum_{i=1}^n q_2^{(i)} = \frac{1}{24}. \quad (4.29)$$

Having related the  $p_k^{(i)}(t)$  to the continuous envelope  $\mathcal{P}(x, t)$  by eq. (4.27) we next have to analyze different structures which may occur in the generalized master equation (4.14). The first one is the time derivative  $\frac{d}{dt}p_k^{(i)}(t)$ . Inserting the ansatz (4.27) into this expression and using the Kramers-Moyal equation (4.26) to process the resulting time derivatives we end up with

$$\begin{aligned} \frac{d}{dt}p_k^{(i)}(t) &= \left[ \frac{d}{dt}q_0^{(i)}(t) \right] \mathcal{P}(x, t) \Big|_{x=k} + \left[ \frac{d}{dt}q_1^{(i)}(t) - v(t)q_0^{(i)}(t) \right] \frac{\partial}{\partial x} \mathcal{P}(x, t) \Big|_{x=k} \\ &+ \left[ \frac{d}{dt}q_2^{(i)}(t) - v(t)q_1^{(i)}(t) + D_{\text{eff}}(t)q_0^{(i)}(t) \right] \frac{\partial^2}{\partial x^2} \mathcal{P}(x, t) \Big|_{x=k} + O(3). \end{aligned} \quad (4.30)$$

We further need the probabilities  $p_k^{(i)}(t - \tau)$  in the past because a general master equation may be non local in time. Additionally we need the probabilities  $p_{k-1}^{(i)}(t - \tau)$  for the previous event  $k - 1$ . By expanding  $\mathcal{P}(x - \Delta x, t - \tau)$  around  $(x, t)$  in a Taylor series and transforming the time derivatives to derivatives with respect to  $x$  with the help of eq. (4.26) (cf. appendix C.4 ) we obtain

$$\begin{aligned} p_{k-\Delta}^{(i)}(t - \tau) &= \quad (4.31) \\ &q_0^{(i)}(t - \tau) \mathcal{P}(x, t) \Big|_{x=k} + [q_1^{(i)}(t - \tau) + q_0^{(i)}(t - \tau)c_t^{[1]}(\tau, \Delta)] \frac{\partial}{\partial x} \mathcal{P}(x, t) \Big|_{x=k} \\ &+ [q_2^{(i)}(t - \tau) + q_1^{(i)}(t - \tau)c_t^{[1]}(\tau, \Delta) + q_0^{(i)}(t - \tau)c_t^{[2]}(\tau, \Delta)] \frac{\partial^2}{\partial x^2} \mathcal{P}(x, t) \Big|_{x=k} \\ &+ O(3) \end{aligned}$$

Therein the functions  $c_t^{[1]}(\tau, \Delta)$  and  $c_t^{[2]}(\tau, \Delta)$  are given by (see appendix C.4

$$\begin{aligned} c_t^{[1]}(\tau, \Delta) &= \int_0^\tau d\tau' v(t - \tau') - \Delta \\ c_t^{[2]}(\tau, \Delta) &= \frac{\Delta^2}{2} - \int_0^\tau d\tau' D_{\text{eff}}(t - \tau') \\ &+ \int_0^\tau d\tau' v(t - \tau') \left[ \int_0^{\tau'} d\tau'' v(t - \tau'') - \Delta \right]. \end{aligned}$$

Inserting expressions (4.30) and (4.31) into the master equation (4.14) and sorting the coefficients of  $\mathcal{P}(k, t)$ ,  $\frac{\partial}{\partial x} \mathcal{P}(x, t) \Big|_{x=k}$  and  $\frac{\partial^2}{\partial x^2} \mathcal{P}(x, t) \Big|_{x=k}$  eventually leads to the



following equations

$$\frac{d}{dt}q_0^{(i)}(t) = \mathcal{M}_t^{(i)}[\mathbf{q}_0](t) \quad (4.32a)$$

$$\frac{d}{dt}q_1^{(i)}(t) = \mathcal{M}_t^{(i)}[\mathbf{q}_1 + \tilde{c}_{t,0}^{[1]}\mathbf{q}_0](t) - \mathcal{M}_t^{(i),+}[\mathbf{q}_0](t) + v(t)q_0^{(i)}(t) \quad (4.32b)$$

$$\begin{aligned} \frac{d}{dt}q_2^{(i)}(t) &= \mathcal{M}_t^{(i)}[\mathbf{q}_2 + \tilde{c}_{t,0}^{[1]}\mathbf{q}_1 + \tilde{c}_{t,0}^{[2]}\mathbf{q}_0](t) - \mathcal{M}_t^{(i),+}[\mathbf{q}_1 + \tilde{c}_{t,\frac{1}{2}}^{[1]}\mathbf{q}_0](t) \\ &\quad + v(t)q_1^{(i)}(t) - D_{\text{eff}}(t)q_0^{(i)}(t). \end{aligned} \quad (4.32c)$$

to determine the periodic coefficients  $\mathbf{q}_m := [q_m^{(1)}, \dots, q_m^{(n)}]$ . For the sake of a simple notation we introduced the abbreviations  $\tilde{c}_{t,\Delta}^{[1]}(t - \tau) := c_t^{[1]}(\tau, \Delta)$ .

$\mathbf{q}_0$  in eq. (4.32a) shows the same dynamics as  $\mathbf{p}$  in the two state system without taking into account the number of events, (4.11), which one would also expect as this term corresponds to an equipartition of the event number  $\mathcal{P}(k, t) = \text{const}$  in the expansion (4.27). The higher order terms  $\mathbf{q}_n$  are corrections which emerge due to the fact that we are considering a non equipartition of the events  $k$  resulting in drift and diffusion. By summing up all components  $i$  of eqs. (4.32b) and (4.32c), using the normalization condition (4.29) and the fact that  $\sum_{i=1}^n \mathcal{M}_t^{(i)} = 0$  we arrive at

$$v(t) = \sum_{i=1}^n \mathcal{M}_t^{(i),+}[\mathbf{q}_0](t) \quad (4.33)$$

$$\begin{aligned} D_{\text{eff}}(t) &= - \sum_{i=1}^n \mathcal{M}_t^{(i),+}[\mathbf{q}_1 + \tilde{c}_{t,\frac{1}{2}}^{[1]}\mathbf{q}_0](t) \\ &= \frac{v(t)}{2} - \sum_{i=1}^n \mathcal{M}_t^{(i),+}[\mathbf{q}_1 + \tilde{c}_{t,0}^{[1]}\mathbf{q}_0](t) \end{aligned} \quad (4.34)$$

Having solved eq. (4.32a) for  $\mathbf{q}_0$  we can evaluate  $v(t)$  according to eq. (4.33), this result can then be inserted into eq. (4.32b) which in turn is solved for  $\mathbf{q}_1$  from which we finally obtain  $D_{\text{eff}}(t)$  according to eq. (4.34). The mean frequency  $\bar{v}$  and the effective diffusion coefficient  $\bar{D}_{\text{eff}}$  can then be determined as a period average of the periodic solutions  $v(t)$  and  $D_{\text{eff}}(t)$ . The calculation is thus reduced to the solution of a periodic problem, which in general is simpler than solving the whole non stationary problem (4.14) with some initial conditions and then considering the asymptotic limit.

In the following subsections we investigate stochastic synchronization in the double well potential systems and excitable systems. To this end we apply the general results (4.33) and (4.34) to the Markovian two state model for the double well potential system eqs (4.17) and the non Markovian two state model eqs. (4.19)

for excitable systems. Finally we use the results to analyze the improvement of regularity in the motion of a periodically driven molecular motor.

### 4.2.1 Application to synchronization in a double well system

Consider the Markovian two state system with periodically modulated rates  $\gamma_{1\rightarrow 2}(t)$  and  $\gamma_{2\rightarrow 1}(t)$ . This model was introduced in [83] as an approximation to describe the behavior of a noisy overdamped particle in a double well potential driven by white noise (see section 2.1.1). We are interested in quantifying the stochastic synchronization of this system to the external periodic signal. To this end we introduce a phase  $\phi$  of the system which increases by  $2\pi$  within a full cycle, namely within one transition from left to right and back to left again. As the long time averaged diffusion behavior does not depend on the precise choice of this phase we assume a discrete phase  $\phi$  which increase by  $2\pi$  at each transition from right (state 2) to left (state 1). Thus  $\phi = 2\pi N$  where  $N$  denotes the number of transitions. The instantaneous mean phase velocity  $\omega(t)$  and effective phase diffusion coefficient  $\mathcal{D}_{\text{eff}}(t)$  can then be obtained according to section 4.1, eq. (4.5), by an appropriate scaling by  $2\pi$  and  $4\pi^2$  respectively of the mean frequency  $v(t)$  and effective diffusion coefficient  $D_{\text{eff}}(t)$  of the number of events.

The unwrapped master operator of this Markovian two state model has already been presented in eqs. (4.18). Due to the Markovian nature of this system, which renders the action of the master operator local in time eqs. (4.32) greatly simplify. As  $c_{i,t}(t) = 0$  the arguments of the master operators involving these terms vanish. Eqs. (4.33) and (4.34) then reduce to

$$\omega(t) = 2\pi\gamma_{2\rightarrow 1}(t)q_0^{(2)}(t) \quad (4.35a)$$

$$\mathcal{D}_{\text{eff}}(t) = 2\pi^2\gamma_{2\rightarrow 1}(t)q_0^{(2)}(t) - 4\pi^2\gamma_{2\rightarrow 1}(t)q_1^{(2)}(t). \quad (4.35b)$$

while eqs. (4.32a) and (4.32b) for  $q_0^{(2)}(t)$  and  $q_1^{(2)}(t)$  are given by

$$\dot{q}_0^{(2)}(t) = -\dot{q}_0^{(1)}(t) = \gamma_{1\rightarrow 2}(t)q_0^{(1)}(t) - \gamma_{2\rightarrow 1}(t)q_0^{(2)}(t) \quad (4.36a)$$

$$\dot{q}_1^{(2)}(t) = \gamma_{1\rightarrow 2}(t)q_1^{(1)}(t) - \gamma_{2\rightarrow 1}(t)q_1^{(2)}(t) + \frac{\omega(t)}{2\pi}q_0^{(2)}(t) \quad (4.36b)$$

$$\dot{q}_1^{(1)}(t) = -\gamma_{1\rightarrow 2}(t)q_1^{(1)}(t) + \gamma_{2\rightarrow 1}(t)q_1^{(2)}(t) + \frac{\omega(t)}{2\pi}q_0^{(1)}(t) \quad (4.36c)$$

Eqs. (4.36) can be readily solved by the method of variation of constants, using the normalization (4.29)  $q_0^{(1)}(t) = 1 - q_0^{(2)}(t)$  and  $q_1^{(1)}(t) = -q_1^{(2)}(t)$ . The asymptotic

periodic solutions eventually read

$$q_0^{(2)}(t) = \frac{\int_0^{\mathcal{T}} d\tau \gamma_{1 \rightarrow 2}(t - \tau) \exp(-s(\tau, t))}{1 - \exp(-s(\mathcal{T}, t))} \quad (4.37)$$

$$q_1^{(2)}(t) = \frac{\int_0^{\mathcal{T}} d\tau \omega(t - \tau) q_0^{(2)}(t - \tau) \exp(-s(\tau, t))}{2\pi(1 - \exp(-s(\mathcal{T}, t)))} \quad (4.38)$$

where  $s(\tau, t) := \int_{t-\tau}^t d\tau' (\gamma_{1 \rightarrow 2}(\tau') + \gamma_{2 \rightarrow 1}(\tau'))$ . Note that  $s(\mathcal{T}, t)$  no longer depends on  $t$  due to the periodicity of the rates.

For a dichotomic symmetric driving with period  $\mathcal{T} = 2\pi/\Omega$ ,

$$\gamma_{1 \rightarrow 2}(t) = \begin{cases} r_1 & \text{if } t \in [n\mathcal{T}, (n + \frac{1}{2})\mathcal{T}) \\ r_2 & \text{if } t \in [(n + \frac{1}{2})\mathcal{T}, (n + 1)\mathcal{T}) \end{cases}$$

and vice versa for  $\gamma_{2 \rightarrow 1}(t)$  eqs. (4.37) and (4.38) can be readily evaluated leading after some cumbersome algebra to the mean phase velocity and effective phase diffusion constant

$$\bar{\omega} = \omega_{\text{st}} + \alpha\Omega \tanh R \quad (4.39)$$

and

$$\bar{\mathcal{D}}_{\text{eff}} = \pi\omega_{\text{st}} \left[ \frac{1}{2} + \alpha \left( \frac{1}{2} + \cosh^{-2} R \right) \right] + \pi\alpha\Omega \tanh R \left[ -1 + \alpha \left( \frac{1}{2} \cosh^{-2} R + 1 \right) \right] \quad (4.40)$$

where we have introduced the mean phase velocity without driving  $\omega_{\text{st}} := 2\pi / (\frac{1}{r_1} + \frac{1}{r_2})$ , a quantifier for the driving strength  $\alpha = \frac{(r_1 - r_2)^2}{(r_1 + r_2)^2}$  and some ratio between inner time scale and driving frequency  $R = \frac{\pi(r_1 + r_2)}{2\Omega}$ . These results agree with the results found independently in [16] using a different approach. Having calculated the effective diffusion coefficient and the mean phase velocity we can evaluate the Péclet number

$$\text{Pe} := \frac{2\pi\bar{\omega}}{\bar{\mathcal{D}}_{\text{eff}}}. \quad (4.41)$$

Let us first consider some limiting cases. Without signal, i.e.  $\alpha = 0$  and thus  $r_1 = r_2$ , eq. (4.40) reduces to  $\bar{\mathcal{D}}_{\text{eff}} = \pi\omega_{\text{st}}$ , which agrees with known result for undriven renewal processes eq. (2.30), [22],

$$\bar{\mathcal{D}}_{\text{eff}} = (2\pi)^2 \frac{\langle \tau^2 \rangle - \langle \tau \rangle^2}{2\langle \tau \rangle^3}$$

where

$$\langle \tau \rangle = \frac{2}{r_1} \quad \text{and} \quad \langle \tau^2 \rangle = \frac{6}{r_1^2}$$

are the mean and the second moment of the time needed for one transition  $1 \rightarrow 2 \rightarrow 1$ .

Next we consider the small and large noise limits of the phase velocity  $\bar{\omega}$  and phase diffusion constant  $\bar{D}_{\text{eff}}$  for the case of Arrhenius rates  $r_{1/2} = r_0 \exp(-\frac{\Delta U \pm A}{D})$ . In this case  $\alpha = \tanh^2(\frac{A}{D})$ . If for a fixed driving frequency the noise level is sufficiently small such that  $R \ll 1$  eqs. (4.39) and (4.40) reduce to

$$\begin{aligned} \bar{\omega} &\approx \omega_{\text{st}} + \alpha\Omega R = \frac{\pi}{2}(r_1 + r_2) \approx \frac{\pi}{2}r_2 \\ \bar{D}_{\text{eff}} &\approx \pi\omega_{\text{st}}\left(\frac{1}{2} + \frac{3}{2}\alpha\right) + \pi\alpha\Omega R(-1 + \frac{3}{2}\alpha) = \frac{\pi^2}{4}(r_1 + r_2) \approx \frac{\pi^2}{4}r_2 \end{aligned}$$

where in the last step we used the fact that  $r_2$  dominates  $r_1$  for small noise levels. Therefore, at the level of phase velocity and phase diffusion, the process behaves like a process without driving whose rates are both equal to  $\frac{r_2}{2}$ . On the other hand if the noise level is large and the driving frequency is small compared to  $r_0$  such that  $R \gg 1$  we get

$$\begin{aligned} \bar{\omega} &\approx \omega_{\text{st}} + \alpha\Omega = 2\pi\frac{r_1r_2}{r_1 + r_2} + \Omega\frac{(r_1 - r_2)^2}{(r_1 + r_2)^2} \\ \bar{D}_{\text{eff}} &\approx \frac{\pi}{2}\omega_{\text{st}}(1 + \alpha) + \pi\alpha\Omega(-1 + \alpha) = 2\pi^2\frac{r_1r_2(r_1^2 + r_2^2)}{(r_1 + r_2)^3} - 4\pi\Omega\frac{(r_1 - r_2)^2}{(r_1 + r_2)^4} \end{aligned}$$

The first terms in these expressions correspond to a process without driving with one rate equal to  $r_1$  and the other equal to  $r_2$ , while the second terms are corrections which vanish for vanishing driving frequency. Between these regions we have a competing behavior. If for a fixed driving amplitude  $A$ , the noise strength  $D$  is sufficiently small, such that  $\alpha \approx 1$  and  $\omega_{\text{st}} \approx 0$ , and simultaneously, for a fixed driving frequency  $\Omega$ ,  $D$  is sufficiently large such that  $R \gg 1$ , i.e.  $\tanh R \approx 1$  we have

$$\bar{\omega} \approx \Omega \quad \text{and} \quad \bar{D}_{\text{eff}} \approx 0$$

i.e. frequency and phase locking occur.

In Fig.4.4 the theoretical results (4.39), (4.40) and (4.41) are compared to simulations of the driven two state system, where we have again chosen an Arrhenius type dependence of the rate on the noise strength.

$$r_{1/2} = r_0 \exp\left(-\frac{\Delta U \pm A}{D}\right)$$

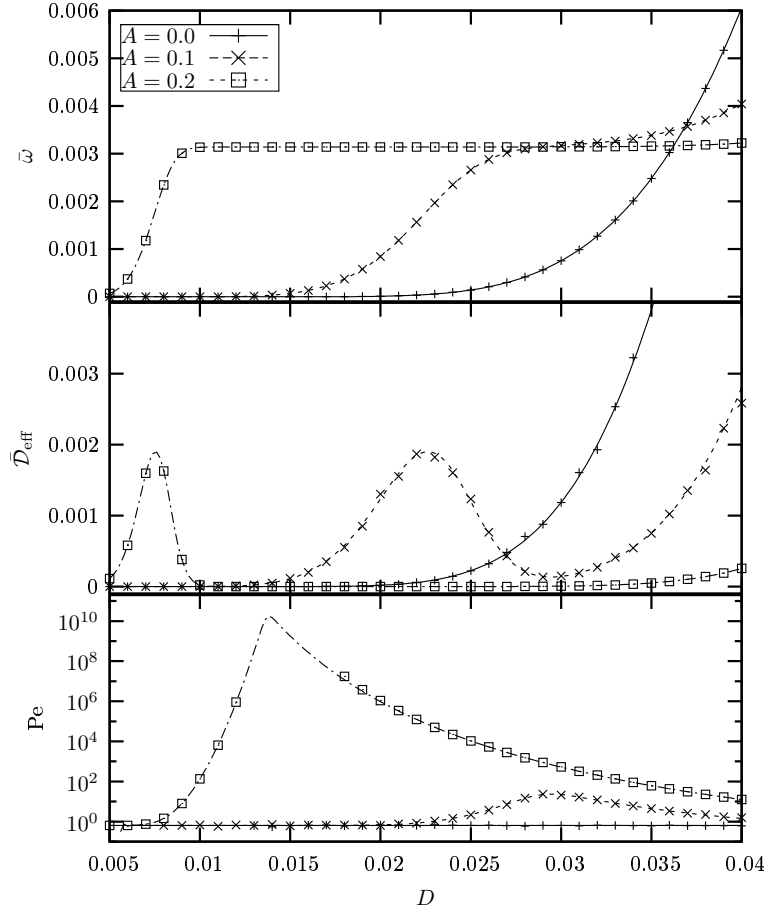


Figure 4.4: Mean phase velocity  $\bar{\omega}$  (top), effective phase diffusion constant  $\bar{D}_{\text{eff}}$  (middle) and Péclet number  $Pe$  (bottom) of the Markovian model for different values of the driving amplitude. Symbols are simulation data of the two state system, lines according to eqs. (4.39), (4.40) and (4.41), respectively. Other parameters:  $r_0 = 1$  and  $\Delta U = 0.25$ ,  $\Omega = 0.001\pi$ . The missing simulation points for the Péclet number at the maximum are due to the limited simulation time, which leads to an effective diffusion coefficient equal to 0 and thus to a diverging Péclet number.

To compute these results we have modified an algorithm presented in [46] taking into account that the transition rates are piecewise constant in time due to the dichotomic driving. Let us assume we start at time  $t$  in state 1 and the input defines the rate to have the value  $r_1$ . Then we draw a random number  $\tau$  according to the corresponding waiting time distribution  $w_{r_1}(\tau) = r_1 \exp(-r_1\tau)$ . If  $t + \tau$  is smaller than the time  $t_s$  of the next switching of the input we set the running time to  $t + \tau$  and perform the transition to the second state of the system. This

state 2 will be left with rate  $r_2$  and we proceed accordingly. Contrary if during the interval  $[t, t + \tau]$  a switching of the input occurs we set the running time equal to the switching time  $t_s$  but remain in state 1. After switching of the input the rate for leaving state 1 is now  $r_2$  and we proceed by drawing a new waiting time according to the new density  $w_{r_2}(\tau) = r_2 \exp(-r_2\tau)$ .

The Péclet number shows a maximum as a function of noise strength, indicating stochastic resonance. For a strong driving, it varies over several orders of magnitude with varying noise strength  $D$ . The sharp peak at the optimal noise level is not a cusp but the Péclet number remains a smooth function of the noise level. This stands in contrast to the non-smooth cusp-like behavior of the mean locking episodes as a function of noise strength claimed in [96].

Interestingly the Péclet number shows also a non monotonic behavior as a function of driving frequency for a fixed noise level, i.e. using this number as a measure of the quality of the response to the external signal we discover a “bona fide” resonance (Fig. 4.5). Such a bona fide resonance has been also reported for

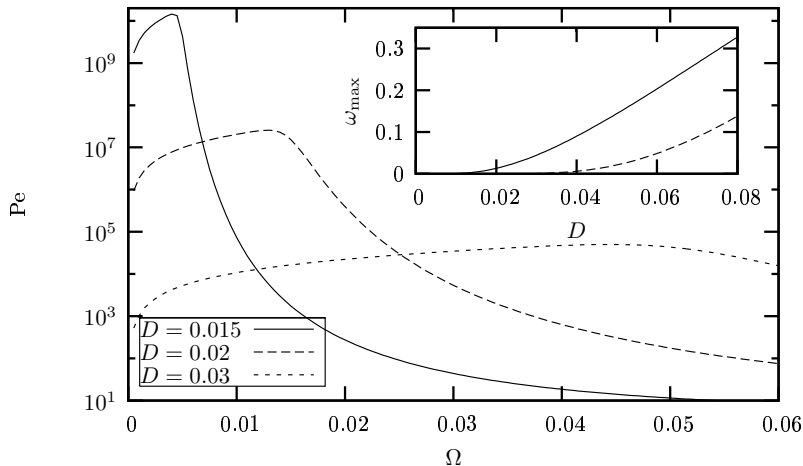


Figure 4.5: Péclet number  $Pe$  of the Markovian model as a function of driving frequency  $\Omega$  for different noise values showing a “bona fide” resonance.  $A = 0.2$ , other parameters as in Fig. 4.4. The inset shows the driving frequency (solid line) at which the Péclet number attains its maximum and the intrinsic frequency  $\omega_{st}$  without driving ( $A = 0$ ) (dashed line) as a function of noise strength.

other measures like the fraction of the transitions with a waiting time around  $\mathcal{T}/2$ , namely in the interval  $(\mathcal{T}/2 - \alpha\mathcal{T}, \mathcal{T}/2 + \alpha\mathcal{T})$ , [42] ( $\mathcal{T}/2$  and not  $\mathcal{T}$  because the waiting time there accounts for a single transition from left to right or from right to left respectively). However it was doubted [18] that this is actually a fingerprint of a bona fide resonance as even in the absence of a driving, setting the driving amplitude to 0 this quantity may show a maximum with respect to the driving

frequency. This results from the fact that this measure is explicitly based on the driving frequency  $\Omega = 2\pi/\mathcal{T}$ , a drawback which the Péclet number obviously does not have.

Finally, we want to compare the two state theory with a double well potential system

$$\dot{x} = -\frac{\partial}{\partial x}V(x, t) + s(t) + \sqrt{2D}\xi(t), \quad V(x, t) = -\frac{a}{2}x^2 + \frac{b}{4}x^4 \quad (4.42)$$

influenced by a dichotomic periodic signal

$$s(t) = \begin{cases} A & \text{if } t \in [n\mathcal{T}, (n + \frac{1}{2})\mathcal{T}) \\ -A & \text{if } t \in [(n + \frac{1}{2})\mathcal{T}, (n + 1)\mathcal{T}) \end{cases}$$

The transition rates between the two states are [67]

$$\gamma_{\pm} = \frac{\omega_{\pm}\omega_0}{2\pi} \exp\left(-\frac{V_0 - V_{\pm}}{D}\right) \quad (4.43)$$

Therein  $\omega_{\pm}$  are the square roots of the of the modulus of the second derivatives of the potential in the left and right minimum respectively and  $\omega_0$  is the second derivatives of the potential in the maximum.  $V_{\pm}$  and  $V_0$  are the values of the potential in the minima and in the maximum respectively. This formula is valid if the potential difference  $V_0 - V_{\pm}$  is much larger than the noise strength  $D$ . In Fig. 4.6 the mean phase velocity, effective phase diffusion constant and Péclet number, numerically evaluated for the double well system eq. (4.42) are compared to the analytical results (4.39), (4.40) and (4.41) with the respective rates  $r_1$  and  $r_2$  taken from eq. (4.43). Generally we find a good agreement. The deviation between theory and simulations in the effective diffusion constant and Péclet number, in the regions where they take their minimum and maximum value respectively is due to a limited simulation time. The derivation for high values of the noise strength  $D$  is due to limitations in the Kramers rate approximation for high noise levels compared to the potential barrier between the wells.

## 4.2.2 Application to synchronization in excitable systems

In this section we consider the phase velocity and effective phase diffusion of the non Markovian two state model for excitable systems. This model is the same as the three state model considered in subsection 3.3.1 in the context of spectral based measures of the response to a periodic signal, except that the firing and refractory state are now lumped together into one discrete state, representing the motion along the excitation loop. This simplification is possible as the different output in firing and refractory state loses its significance when considering the

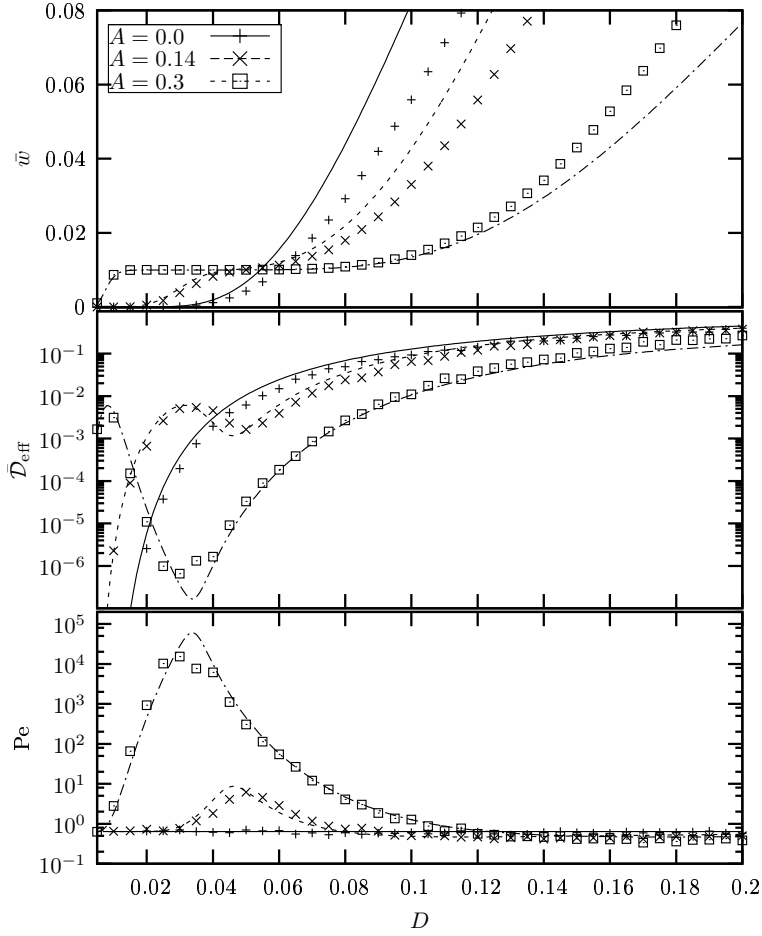


Figure 4.6: Mean phase velocity  $\bar{\omega}$  (top), effective phase diffusion constant  $\bar{D}_{\text{eff}}$  (middle) and Péclet number  $\text{Pe}$  (bottom) of the Markovian model (lines) for different values of the driving amplitude compared to simulation data of a double well potential system eq. (4.42) with  $a = b = 1$  for a driving frequency  $\Omega = 0.01$  (symbols).

synchronization behavior to an external signal. Denoting the rest state by 2 and the motion along the excitation loop by 1, its probabilities evolve according to eqs. (4.20). Then, according to eqs. (4.33) and (4.34), the time dependent phase velocity  $\omega(t)$  and effective phase diffusion constant  $\mathcal{D}_{\text{eff}}(t)$  are given by

$$\omega(t) = 2\pi\gamma(t)q_0^{(2)}(t) \quad (4.44a)$$

$$\mathcal{D}_{\text{eff}}(t) = 2\pi^2\gamma(t)q_0^{(2)}(t) - 4\pi^2\gamma(t)q_1^{(2)}(t). \quad (4.44b)$$

These are the same expressions as in the Markovian case eqs. (4.35) as the operator  $\sum_i \mathcal{M}_t^{(i),+} = \mathcal{M}_t^{(1),+} + \mathcal{M}_t^{(2),+}$ , which describes the probability flux from state  $k$



into state  $k + 1$  is the same in both cases. This stems from the fact that in both cases the step which increases the number of events is a rate process. However the equations governing the  $\mathbf{q}^{(i)}$  are different. They are obtained from eq. (4.23) as

$$\int_0^\infty d\tau z(\tau) \gamma(t - \tau) q_0^{(2)}(t - \tau) + q_0^{(2)}(t) = 1 \quad (4.45a)$$

$$\int_0^\infty d\tau z(\tau) \gamma(t - \tau) q_1^{(2)}(t - \tau) + \int_0^\infty d\tau z(\tau) \gamma(t - \tau) q_0^{(2)}(t - \tau) \left( \frac{1}{2\pi} \int_0^\tau d\tau' \omega(t - \tau') - 1 \right) + q_1^{(2)}(t) = 0. \quad (4.45b)$$

The periodic solutions of eqs. (4.45) can be numerically obtained in Fourier space (see appendix C.5) using a linear solver like LAPACK.

In the following we assume a fixed waiting time  $T$  on the excitation loop, i.e.  $w(\tau) = \delta(T - \tau)$  and  $z(\tau) = \theta(T - \tau)$ . Such an assumption is justified in the low noise limit of the FitzHugh-Nagumo model (cf. Fig. 2.6 and 3.2). To investigate the role of noise in this low noise regime on the synchronization in excitable system we choose an Arrhenius type excitation rate for the transition from the rest state 2 onto the excitation loop 1. We further assume that the external driving acts as a modulation of the potential barrier. Again we consider a dichotomic periodic driving, i.e. the excitation rate  $\gamma(t)$  periodically switches between the two values  $r_1 = r_0 \exp(-(\Delta U - A)/D)$  and  $r_2 = r_0 \exp(-(\Delta U + A)/D)$ .

The resulting phase velocity, effective phase diffusion and Péclet number as a function of noise strength  $D$  are shown in Fig. 4.7. To obtain these results we solved eqs. (4.44a), (4.44b) and (4.45) for the periodic solution, by truncating the infinite dimensional system in Fourier space (see C.5) to 100 coefficients and then solving it numerically using LAPACK. As in the case of bistable systems we observe frequency and phase locking, however there exist preferred driving frequencies for which high synchronization is achieved and other frequencies which show no synchronization at all.

The Péclet number shows a local maximum at a finite noise strength. Contrary to the bistable situation however, the phase diffusion constant decreases again and the Péclet number therefore increases for large noise levels. This behavior is originated in the fixed time  $T$  on the excitation loop. Taking into account the high rate and therefore small waiting time and variance of the excitation step for high noise levels this leads to a low variance of the spiking, which implies a low diffusion of the phase. We mention that this low phase diffusion does not imply synchronization since the frequencies are not locked. Also we note that in real excitable systems the behavior differs. For higher noise levels the variance of the time spent on the excitation loop will increase in these systems which yields an increasing phase diffusion with growing noise.

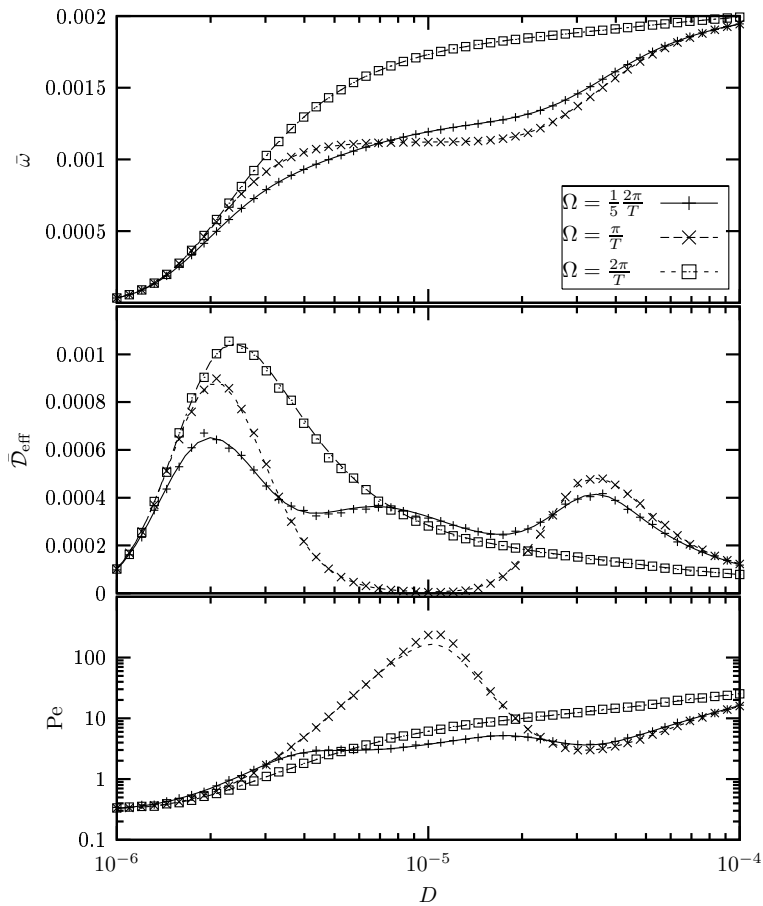


Figure 4.7: Mean phase velocity  $\bar{\omega}$  (top), effective phase diffusion coefficient  $\bar{D}_{\text{eff}}$  (middle) and Péclet number  $Pe$  (bottom) of the non Markovian model as a function of noise strength  $D$  for different values of the driving frequency  $\Omega$ . Symbols are simulation data of the two state system, lines according to numerical evaluation of the theory. Other parameters:  $T = 2800$ ,  $r_0 = 0.0044$ ,  $\Delta U = 5.6 \cdot 10^{-5}$  and  $A = 5.0 \cdot 10^{-5}$ .

As seen in Fig. 4.7 the synchronization behavior strongly depends on the driving frequency. To further analyze this effect we have plotted in Fig. 4.8 the mean phase velocity, phase diffusion coefficient and the Péclet number as function of the driving frequency. They show a complex sequence of different locking regions between the driving and the system's response, represented by shaded regions. Such a complex sequence of different locking regions have also been observed in the Hodgkin-Huxley model in [98] and the FHN model [78]. In these locking regions the effective phase diffusion is small Fig. 4.9. We mention that the maximal frequency of the excitable system is  $\bar{\omega}_{\text{max}} = 2\pi/T$  where  $T$  is the

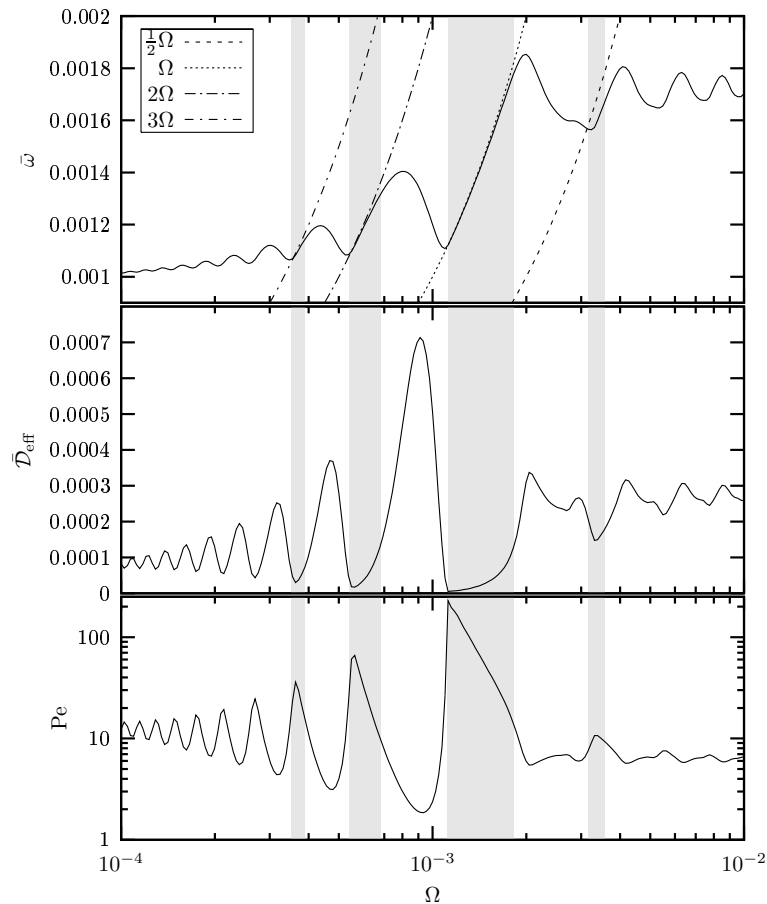


Figure 4.8: Mean phase velocity  $\bar{\omega}$  (top), effective phase diffusion constant  $\bar{D}_{\text{eff}}$  (middle) and Péclet number  $Pe$  (bottom) of the non Markovian model as a function of driving frequency  $\Omega$  for  $D = 0.00001$ . The selected shaded regions are a guide for the eye to show that regions of frequency synchronization are accompanied with a small effective phase diffusion and therefore with a high Péclet number. Other parameters:  $T = 2800$ ,  $r_0 = 0.0044$ ,  $\Delta U = 5.6 \cdot 10^{-5}$  and  $A = 5.0 \cdot 10^{-5}$ .

time on the excitation loop. There can not be 1 : 1 synchronization for  $\Omega > \bar{\omega}_{max}$ .

Let us for a moment assume the extremal case where one excitation rate  $r_1$  is infinity and the other  $r_2$  is zero. Then the system remains in the rest state as long as the input causes the vanishing excitation rate. After the input changes the system immediately starts with the excitation loop where it stays the time  $T$ . For a 1 : 1 locking this time  $T$  must be larger than half the period but smaller the full period  $2\pi/\Omega$  of the driving. Otherwise, if the duration of the excitation loop would be smaller than half the period the system returns to the rest state where it immediately starts a new excitation. In consequence 1 :  $n$  locking where the

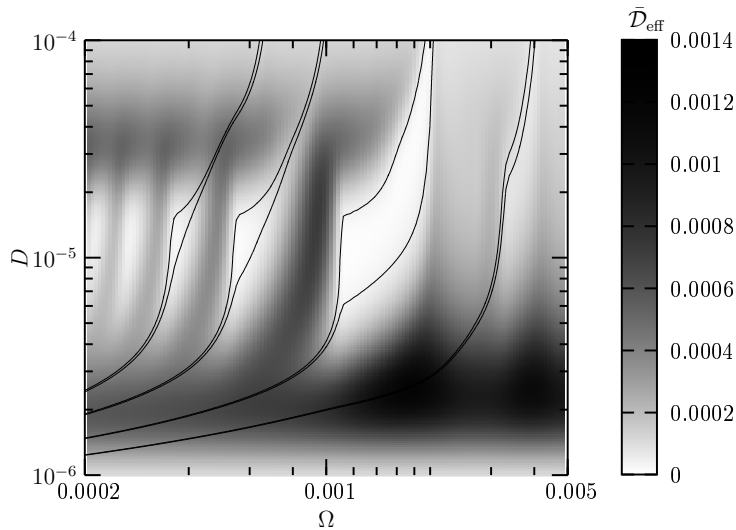


Figure 4.9: Effective phase diffusion constant  $\bar{D}_{\text{eff}}$  of the non Markovian model, as a function of driving frequency  $\Omega$  and noise level  $D$ . The black lines show regions of frequency locking  $(1 - \epsilon)\Omega < n\bar{\omega} < (1 + \epsilon)\Omega$ ,  $\epsilon = 0.01$  with (from left to right)  $n = 3, 2, 1, \frac{1}{2}$ . These regions of frequency locking coincide with low phase diffusion. Other parameters as in Figs. 4.7 and 4.8.

output frequency is  $n$  times higher than the input frequency occurs if the period of the driving is between  $(n - 1/2)T$  and  $nT$ .

The opposite case where a fast input locks a slow output occur if multiple periods of the input fit into the excitation time. During the excitation the system does not respond to the changes of the input. If the input has the phase with long waiting time after the system has completed the excitation loop, it has to wait until the input changes to the phase with the small waiting time, leading to a  $n : 1$  synchronization where  $n$  is the number of signal periods which fit into the excitation time  $T$ .

However if the system finds the high excitation rate after excursion it immediately starts a new excitation loop and repeats these until it will find the phase with long waiting times. This yields a  $n : m$  frequency locking with  $n > m$ . Note that there are no  $n : m$  locking modes with  $n < m$  except the  $1 : m$  modes described above.

Realistic noise dependent time scales will weaken the extreme behavior of the situation considered above. There are two competing effects namely increasing the noise increases  $r_1$  as well as  $r_2$  while decreasing the noise increases the ratio between

$r_1$  and  $r_2$  and therefore the effect of the driving. Hence, we find synchronization in a finite window of noise intensities where the two activation times enclose the time  $T$  on the excitation loop,

$$\frac{1}{r_1} \ll T \ll \frac{1}{r_2}. \quad (4.46)$$

We point out that this latter time plays the essential role within the synchronization process, i.e. this time scale and the period of the external drive have to be tuned appropriately to get phase synchronization. Noise as well as the amplitude of driving define the two excitation rates and have to be chosen such that eq. (4.46) is optimally fulfilled, i.e. that the input acts as much as possible as a on-off switch on the excitation process. A deviation from this extremal behavior leads to a narrowing of the driving frequency windows amenable to frequency locking and a shift of these windows to lower frequencies.

Inequality (4.46) allows for an estimation of noise levels, for which one can expect synchronization. If, in particular, we specify this inequality by  $1/r_1 < T/4$  and  $1/r_2 > 4T$ , the parameters used in Fig. 4.9 lead to a noise range from  $D \approx 5 * 10^{-6}$  to  $D \approx 3 * 10^{-5}$  which coincides with the range of noise levels for which phase synchronization is actually observed.

Finally we compare the theory to a dynamical system with excitable dynamics, namely the FHN model [33, 87]

$$\dot{x} = x - x^3 - y + \sqrt{2D}\xi(t) \quad (4.47a)$$

$$\dot{y} = \epsilon(x + a_0 - a_1 y - s(t)) \quad (4.47b)$$

This system is driven by a dichotomic periodic signal  $s(t)$  with values  $\pm A$  where  $A = 0.015$ . Setting  $a_0 = 0.405$  and  $a_1 = 0.5$  the system is in the excitable regime for both values of the signal, i.e. the signal is a sub-threshold signal. We further consider a strong time scale separation  $\epsilon = 0.001$  as well as a small noise level  $D = 10^{-5}$ . The phase of the system is defined to increase by  $2\pi$  each time a spike is generated. From simulations of the inter spike interval distribution (see Fig. 4.10) for constant signal  $\pm A$  we find the corresponding parameters of the two state model to be  $T \approx 2620$ ,  $r_1 \approx 0.0087$  and  $r_2 \approx 8.3 \cdot 10^{-8}$ .

The results for the phase velocity  $\bar{\omega}$  and effective phase diffusion constant  $\bar{D}_{\text{eff}}$  for the FHN system (numerical simulation of eqs. (4.47)) and the theory (4.44a) and (4.44b) are shown in Fig. 4.11. They show a good qualitative agreement over a large range of driving frequencies. The deviation for larger driving frequencies is due to the fact that, in contrast to the assumptions of our two state model, the time  $T$  spent on the excitation loop depends if only weakly on the driving.

Last but not least the very same expressions as for the excitable system can also be used to describe the synchronization in a parametrically driven bistable

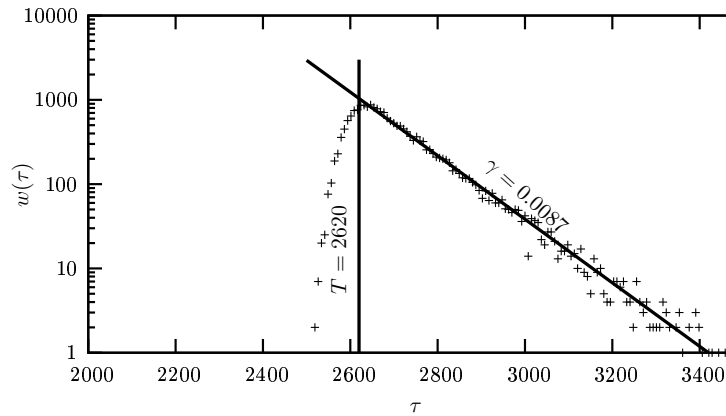


Figure 4.10: Inter spike interval distribution of the FHN system (4.47) with constant signal  $s(t) = 0.015$  for a low noise level  $D = 10^{-5}$  and strong time scale separation  $\epsilon = 0.001$ . Other parameters see text.

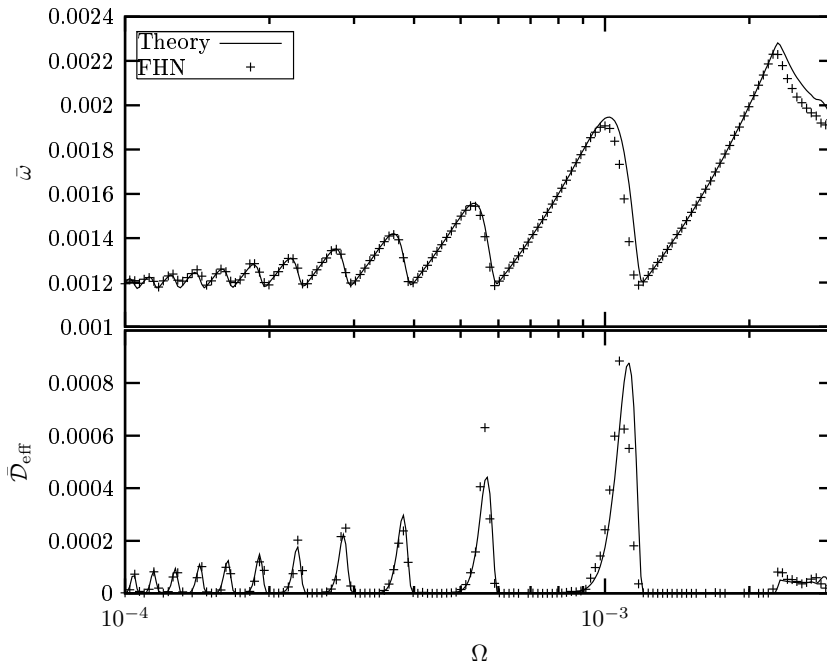


Figure 4.11: Comparison between theory and FHN system eqs. (4.47) for mean phase velocity  $\bar{w}$  (top) and effective phase diffusion constant  $\bar{D}_{\text{eff}}$  (bottom) as a function of driving frequency. Parameters see text.

symmetric FHN system as introduced in subsection 3.3.2. To this end we consider the dynamics on the right stable branch and the left stable branch of the bistable system as one full cycle of the excitable system, being composed of a fixed time and

a periodically modulated rate excitation. Then one cycle of the bistable system corresponds to two cycles of the excitable system, which changes the mean velocity and effective diffusion coefficient by a factor of  $1/2$  and  $1/4$  respectively. The additively driven bistable FHN system however cannot be described in this way, as the influence of the driving on either the left or the right excitation step is opposite.

### 4.2.3 Application to molecular motors –Controlling random motion of Brownian steppers by periodic driving

For many physicists the term “molecular motor” is associated with a Brownian ratchet. The latter is a simple model consisting of a particle in a spatially asymmetric potential, subjected to friction and noise. Directed motion becomes possible if one departs from thermal equilibrium, e.g by periodically modulating the potential or by considering a periodically modulated temperature. (for an overview see [110]). An abundant literature is devoted to the questions of rectified current (particle’s velocity) [120], thermodynamic efficiency [121], current reversals and many other intriguing properties of such systems both in underdamped and in overdamped regimes, under adiabatic or non-adiabatic modulation conditions (see [1, 99, 110] for reviews, and references therein). In the context of molecular motors Brownian ratchets have been discussed in [79].

However, the majority of real molecular motors powering our cells and their organelles are not rectifying fluctuations. They are more similar to deterministically working car motors, whose functioning implies a sequence of well-defined processes, which, in an analogy with a heat engines, are called strokes (see e.g. [32, 76, 92, 94]), which are triggered and powered by the consumption of some fuel molecules, normally ATP. These motors hardly show the reversal of their motion, are highly efficient and best suited for performing their well-defined simple task.

There is, however, a considerable difference between the way of the functioning of molecular motors [5] and macroscopic ones: Due to their microscopic size, the importance of inertia and masses (being proportional to  $L^3$  with  $L$  being the size of the system) , is negligible compared to the importance of friction, which, in the Stokes’ case, is proportional to  $L$ . Another difference is that the motor is so tiny that the influence of the thermal motion of the molecules of the surrounding medium can not be neglected. Thus, although the strokes themselves are well-defined, we cannot neglect the effects of randomness, introduced by the impacts of these molecules. These might be constructively used by the motors whose working cycle might include thermally activated or diffusive steps. M. Bier coined a description of such a motor (a simplified model of a two-headed kinesin walking along a biopolymer microtubule) as a Brownian stepper [11].

The paradigmatic model of a Brownian stepper might be used as a prototype of tiny engines on the nano-scale. Thus the question on the possibility to control the motion of a stepper can be posed. Such control cannot be easily realized by changing the properties of the molecule itself, though. It will be much easier to modulate the properties of the surrounding medium by changing, for example, the concentrations of some molecules (fuel molecules or special transmitters), just as adopted in biological prototypes.

This is exactly the mechanism of control we consider in some detail [107], using the theory developed in section 4.2. We investigate the influence of a periodic modulation of the fuel molecule concentration on the transport properties of the stepper. The transport properties of interest are the mean velocity  $\bar{v}$  and the effective diffusion coefficient  $\bar{D}_{\text{eff}}$  of the molecular motor. The first one determines the effectiveness of transport, and the second one, describing the spread of the actual positions in different realizations around the mean, gives us a measure of how precise this molecular step motor works. The characteristic measure of this precision is the dimensionless Péclet number,  $\text{Pe} = \ell v / D_{\text{eff}}$  where  $\ell$  is the length of one step [38]. Although we use the same notation,  $v$  and  $D_{\text{eff}}$  differ by a factor of  $\ell$  and  $\ell^2$  respectively from the mean frequency and effective diffusion coefficient as defined previously, as they now characterize the position  $x = \ell N$  instead of the number of steps  $N$  itself.

## The model

We consider a Brownian stepper which moves along a track in discrete forward steps (see Fig. 4.12) of length  $\ell$ . Each step is induced by the consumption of a fuel molecule. This initiation of a step happens according to a rate process with a rate  $\gamma$ , which is proportional to the concentration of the fuel molecules. After a step is triggered, the motor molecule performs some conformational changes before returning back to its initial configuration, however having advanced one step on the track. This sequence of conformational changes takes some random time  $\tau_{\text{stroke}}$  to perform which is distributed according to  $w_{\text{stroke}}(\tau)$ . We control the motor by periodically modulating the fuel concentration [107]. This leads to a periodically varying step initiation rate  $\gamma(t)$  while the stroke time distribution  $w_{\text{stroke}}(\tau)$  is assumed to remain unaffected by the fuel concentration. This Brownian stepper mimics the behavior of a kinesin on a microtubule, which is known to advance in discrete steps [92] by consuming one ATP per step [55]. The dependence of the mean velocity of kinesin on the ATP concentration was measured in [133] for different external forces. It shows for low ATP concentrations a linear increase of the logarithm of the mean velocity as a function of the logarithm of the ATP concentration with a force dependent offset. For high ATP concentrations the mean velocity finally saturates at some force dependent maximal velocity. This



velocity dependence is reproduced by our model without driving. Assuming a rate  $\gamma = c[\text{ATP}]$  the mean velocity of the Brownian stepper is given by

$$v = \frac{\ell}{\langle \tau_{\text{stroke}} \rangle + \frac{1}{c[\text{ATP}]}}$$

which in the limit of low and high ATP-concentration reduces to

$$\log v \approx \log \ell + \log c + \log[\text{ATP}] \quad \text{as} \quad [\text{ATP}] \rightarrow 0$$

and

$$\log v \approx \log \ell + \log \frac{1}{\langle \tau_{\text{stroke}} \rangle} \quad \text{as} \quad [\text{ATP}] \rightarrow \infty$$

respectively. Assuming the constant  $c$  as well as the mean stroke time  $\langle \tau_{\text{stroke}} \rangle$  to be dependent on the external force, we qualitatively recover in our model the results measured in [133]. The parameter we use to control the motor in our model, however, is not the force but the concentration of the fuel molecules and thus the trigger rate  $\gamma = c[\text{ATP}]$ . More precisely we consider periodically modulated fuel

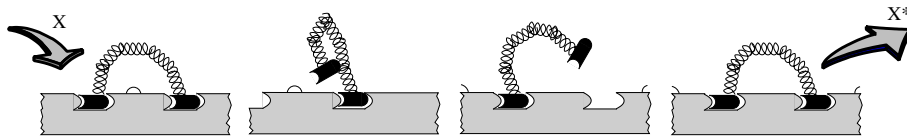


Figure 4.12: One step of the Brownian stepper. The step is induced by the binding of a fuel molecule  $X$  according to a rate process with a rate  $\gamma(t)$  which is proportional to the concentration  $[X](t)$  of the fuel molecules. Afterwards the motor molecule undergoes conformational changes, thereby releasing the used fuel  $X^*$  and advancing by one step Length  $\ell$ . These conformational changes take some time  $\tau_{\text{stroke}}$  which is distributed according to  $w_{\text{stroke}}(\tau)$ .

concentrations. One step of the motor thus is composed of a periodically modulated rate process and a somehow distributed waiting time. This is exactly the discrete model we considered in the previous subsection 4.2.2 to describe a periodically driven excitable dynamics. Thus we can profit from the mathematical investigations we have performed there. However this application is different in spirit from the previous applications as we are not primarily interested in synchronization phenomena but rather in the control of the regularity of the motion of the Brownian stepper, although a highly regular behavior is inherently connected to the synchronization with the external periodic driving. This regularity is characterized by the very same quantities we used to characterize synchronization,

namely the mean velocity  $\bar{v}$  and the effective diffusion constant  $\bar{D}_{\text{eff}}$  and resulting therefrom the Péclet number  $\text{Pe}$ . Taking into account the length  $\ell$  of a step the instantaneous mean velocity and effective diffusion coefficients are governed by (cf. eqs. (4.44))

$$v(t) = \ell\gamma(t)q_2^{(0)}(t) \quad (4.48a)$$

$$D_{\text{eff}}(t) = \frac{\ell^2}{2}\gamma(t)q_2^{(0)}(t) - \ell^2\gamma(t)q_2^{(1)}(t), \quad (4.48b)$$

with  $q_2^{(0)}$  and  $q_2^{(1)}$  obeying the very same equations (4.45),

$$q_2^{(0)}(t) + \int_0^\infty d\tau z_{\text{stroke}}(\tau)\gamma(t-\tau)q_2^{(0)}(t-\tau) = 1 \quad (4.49a)$$

$$q_2^{(1)}(t) + \int_0^\infty d\tau z_{\text{stroke}}(\tau)\gamma(t-\tau)q_2^{(1)}(t-\tau) \quad (4.49b)$$

$$+ \int_0^\infty d\tau z_{\text{stroke}}(\tau)\gamma(t-\tau)q_2^{(0)}(t-\tau)\left(\frac{1}{\ell}\int_0^\tau d\tau'v(t-\tau') - 1\right) = 0.$$

Averaging  $v(t)$  and  $D_{\text{eff}}(t)$  over one period gives the mean velocity  $\bar{v}$  and effective diffusion coefficient  $\bar{D}_{\text{eff}}$  from which we obtain the Péclet number  $\text{Pe} = \frac{\ell\bar{v}}{\bar{D}_{\text{eff}}}$  to characterize the regularity of the stepper. Experimentalists often consider instead the so called randomness  $r$  which is the inverse of the Péclet number.

To begin with let us shortly discuss the behavior of the undriven model. Without driving the initiation of a step happens with a time independent rate  $\gamma = \text{const.}$  The stepping times then constitute a stationary renewal process, because two steps are independent of each other. These times between two subsequent steps are distributed according to

$$w_{\text{tot}}(\tau) = (w_{\text{init}} \circ w_{\text{stroke}})(\tau) = \int_0^\tau d\tau' w_{\text{init}}(\tau')w_{\text{stroke}}(\tau - \tau').$$

Therein  $w_{\text{init}}(\tau) = \gamma \exp(-\gamma\tau)$  is the distribution of initiation times. Introducing the mean and the variance of the step time

$$\langle\tau\rangle = \int_0^\infty d\tau\tau w_{\text{tot}}(\tau) \quad \text{and} \quad \langle\tau^2\rangle = \int_0^\infty d\tau\tau^2 w_{\text{tot}}(\tau)$$

the mean velocity and effective diffusion coefficient can be expressed as (see section 2.2.2, [22])

$$\bar{v} = \frac{\ell}{\langle\tau\rangle} \quad \text{and} \quad \bar{D}_{\text{eff}} = \frac{\ell^2}{2} \frac{\langle\tau^2\rangle - \langle\tau\rangle^2}{\langle\tau\rangle^3}.$$

This leads to the Péclet number

$$\text{Pe} = 2 \frac{\langle \tau \rangle^2}{\langle \tau^2 \rangle - \langle \tau \rangle^2}. \quad (4.50)$$

In our further calculations we take the stroke time to be distributed according to a  $\Gamma$ -distribution.

$$w_{\text{stroke}}(\tau) \equiv w_{n,T}(\tau) = \frac{1}{\Gamma(n)} \left( \frac{\tau n}{T} \right)^n \frac{\exp(-\frac{\tau n}{T})}{\tau}. \quad (4.51)$$

In Fig. 4.13 this waiting time distribution is illustrated for different values of

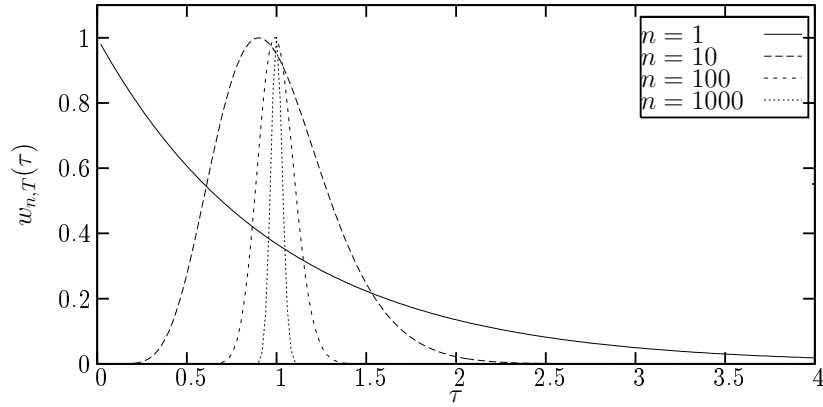


Figure 4.13: The gamma distribution eq. (4.51) with mean  $T = 1$  and two different values of  $n$ . The plots are non normalized, but scaled such that the maximum value is 1.

$n$ , ranging from an exponential distribution for  $n = 1$  pertinent to a single rate process, to a delta distribution for  $n \rightarrow \infty$  corresponding to a fixed non random stroke time. In particular, the mean stroke time is

$$\langle \tau_{\text{stroke}} \rangle := \int_0^\infty d\tau \tau w_{n,T}(\tau) = T$$

while its variance reads

$$\langle \tau_{\text{stroke}}^2 \rangle - \langle \tau_{\text{stroke}} \rangle^2 := \int_0^\infty d\tau \tau^2 w_{n,T}(\tau) - \langle \tau_{\text{stroke}} \rangle^2 = \frac{T^2}{n}.$$

Both can be varied independently by appropriately choosing  $T$  and  $n$ . With this stroke time distribution the Péclet number eq. (4.50) of the undriven Brownian stepper reads (see also [11])

$$\text{Pe} = 2 \frac{(\frac{1}{\gamma} + T)^2}{\frac{1}{\gamma^2} + \frac{T^2}{n}}. \quad (4.52)$$

In the following we will fix the value of  $T = 5$  and use in examples  $n = 100$  and  $n = 1000$ . Then in the undriven case  $Pe$  from eq. (4.52) ranges between 2 and 200 for  $n = 100$ , respectively 2000 for  $n = 1000$  if  $\gamma$  increase from zero to infinity. Later on, for the driven case we will find values which exceed these values by one order of magnitude.

To present specific results we consider two types of periodic driving, namely a dichotomic activation rate

$$\gamma_d(t) = \begin{cases} r_1 & \text{if } t \in [n\mathcal{T}, (n + \frac{1}{2})\mathcal{T}) \\ r_2 & \text{if } t \in [(n + \frac{1}{2})\mathcal{T}, (n + 1)\mathcal{T}) \end{cases} \quad (4.53)$$

where  $\mathcal{T}$  is the period of the modulation and a harmonic driving

$$\gamma_h(t) = \frac{r_1 + r_2}{2} + \frac{r_1 - r_2}{2} \cos \Omega t. \quad (4.54)$$

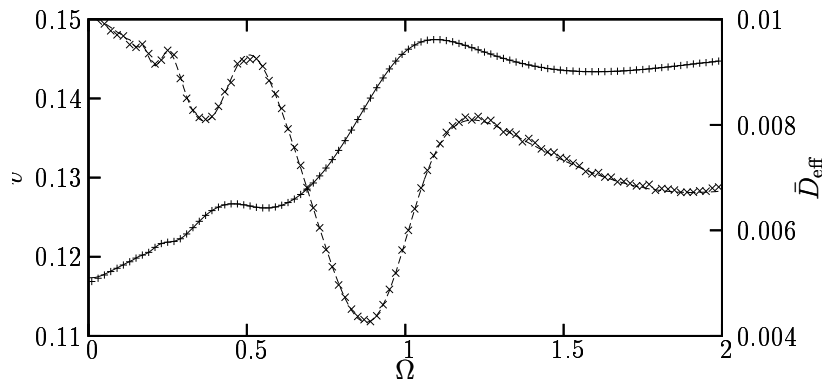


Figure 4.14: Mean velocity  $\bar{v}$  (solid line and +) and effective diffusion coefficient  $\bar{D}_{\text{eff}}$  (dashed line and  $\times$ ) of the dichotomically driven model with  $r_1 = 0.1$ ,  $r_2 = 1.0$ ,  $T = 5.0$  and  $n = 20$ . The step length  $\ell$  is chosen to be 1. Symbols are simulations of the driven renewal process, while the lines correspond to the theory eqs. (4.48a) and (4.48b).

First of all, let us consider a situation where the periodic driving (4.53) or (4.54) induces a change in the attachment rates  $\gamma$  by one order of magnitude. i.e.  $r_2/r_1 = 10$ . Fig. 4.14 shows results for  $\bar{v}$  and  $\bar{D}_{\text{eff}}$  evaluated according to the theory eqs. (4.48) numerically and compares them with mean velocities  $\bar{v}$  and diffusion coefficients  $\bar{D}_{\text{eff}}$  obtained from simulations of an ensemble of 100000 Brownian steppers. Both curves agree within simulation precision. Deviations occur due to finite simulation times. The effective diffusion coefficient exhibits a sharp minimum near  $\Omega \approx 1$ . This minimum corresponds to a 1 : 1 synchronization

with the periodic driving. The steppers follow the periodic driving with high precision.

A second synchronization window appears for smaller frequencies, i.e. for longer periods. During half of the period when the excitation rate  $\gamma(t)$  is large the stepper succeeds to perform two steps. Again the diffusion coefficient becomes smaller compared to regions without synchronization.

Fig. 4.14 also allows the discussion of the limits of fast driving  $\Omega \rightarrow \infty$  and slow driving  $\Omega \rightarrow 0$ . In the case of fast driving the mean velocity and effective diffusion coefficient of the stepper coincide with the value of the undriven case if  $\gamma(t)$  is replaced by the arithmetic mean of the rate, i.e.  $\gamma(t) \rightarrow (r_1 + r_2)/2$ . Otherwise, if the switching frequency is vanishingly small one can average between the two mean velocities and effective diffusion coefficients of the undriven situations. Therefore the mean velocity becomes  $v = (v_1 + v_2)/2$ , where  $v_1$  is its stationary value with rate  $r_1$ , respectively  $v_2$  and  $r_2$ . The limiting values of the effective diffusion coefficient can be obtained in the same way.

In order to amplify the regularity we increase the difference of the two fuel attachment rates and decrease the variance of the stroke time. We now put the ratio  $r_2/r_1 = 100$ . Fig. 4.15 shows again the dependence of the mean velocity, effective diffusion coefficient and Péclet number on the driving frequency in case of dichotomic driving (4.53) for these rates.

We observe different regions with high Péclet numbers and thus a very regular motion of the motor. These regions show a rational relation between driving frequency and step frequency which is proportional to the velocity. The frequency locking is accompanied by a low effective diffusion. Between these regions the effective diffusion coefficient strongly increases, showing a less coherent motion of the motor.

The behavior of the harmonically driven motor (4.54) is qualitatively the same as the behavior of the dichotomically (4.53) motor. Again we obtain very high Péclet numbers with locked velocity and low diffusion if the motion of the stepper is synchronized with the periodic drive. However, as seen in Fig. 4.16 the harmonical driving allows a more precise tuning of the driven motor, since the stepper exhibits also a 3 : 2 synchronization regime, i.e. 3 steps of the motor lie within 2 periods of the driving. Such behavior was not observed for the dichotomically driven system.

In the high frequency limit both driving types lead to the same behavior, however for low frequencies the velocity in the harmonically driven system (averaged over an ensemble with random drive  $\cos(\varphi_0)$ ) is higher, while the effective diffusion coefficient is much lower, leading to an increased Péclet number compared to the dichotomically driven system.

Next let us compare the periodically driven system in presence and in absence of synchronization with the corresponding undriven system (see Figs. 4.17). To

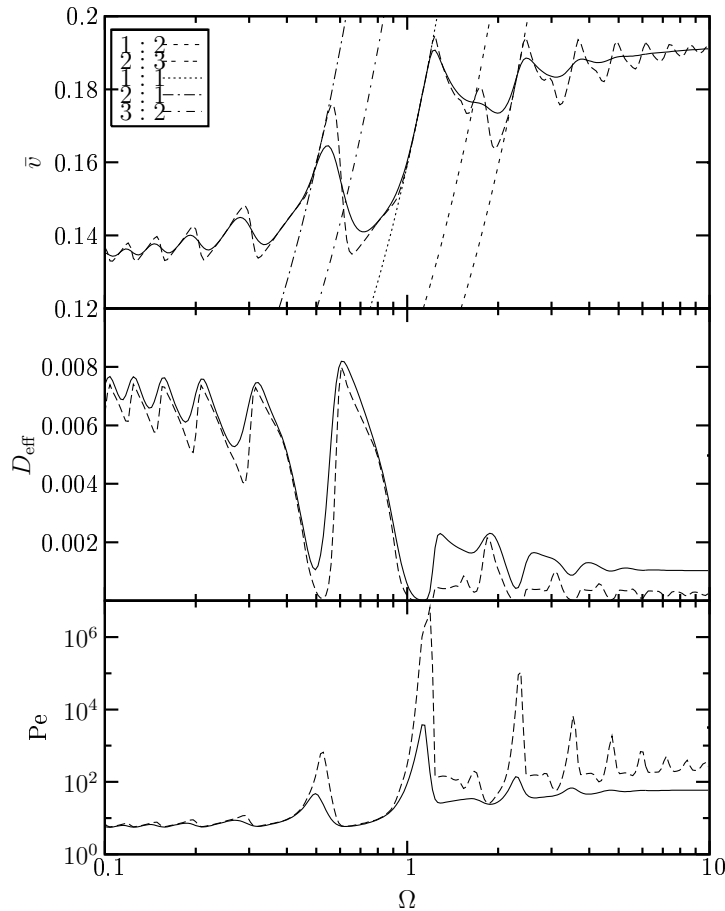


Figure 4.15: Mean velocity (top), effective diffusion coefficient (middle) and Péclet number (bottom) as a function of driving frequency of the dichotomically driven system. Two situations with different dispersion of the stroke times are shown. Parameters:  $r_1 = 0.1$ ,  $r_2 = 10.0$ ,  $T = 5.0$ ,  $n = 100$  (solid line)  $r_1 = 0.1$ ,  $r_2 = 10.0$ ,  $T = 5.0$ ,  $n = 1000$  (dashed line). The corresponding two values for the undriven system with initiation rate  $\gamma = \frac{r_1+r_2}{2}$  are  $\bar{v} = 0.192(0.192)$ ,  $\bar{D}_{\text{eff}} = 0.001(0.00023)$  and  $\text{Pe} = 93(416)$  (values in parentheses:  $n = 1000$ ). The additional curves in the top figure indicate perfect synchronization between the motion of the stepper and the periodic drive, the corresponding ratios are shown in the key.

this end we have chosen the excitation rate of the undriven system between the maximum rate  $r_2$  and the minimum rate  $r_1$  of the driven system, such that the motion is most regular, i.e. the Péclet number is maximal. This optimal value  $r_{\text{opt}}$  is depicted in both figures (dashed lines). The Péclet numbers for the driven system and the undriven system are shown as a function of the variance of the stroke time

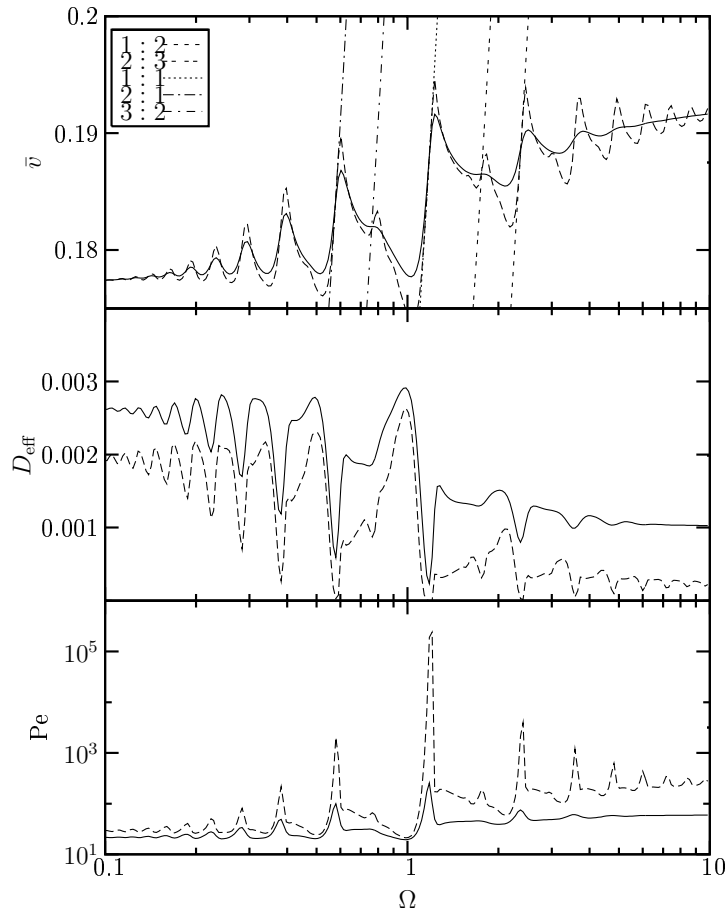


Figure 4.16: Mean velocity (top), effective diffusion coefficient (middle) and Péclet number (bottom) as a function of driving frequency for the harmonically driven system. Two situations with different dispersion of the stroke times. Parameters:  $r_1 = 0.1$ ,  $r_2 = 10.0$ ,  $T = 5.0$ ,  $n = 100$  (solid line)  $r_1 = 0.1$ ,  $r_2 = 10.0$ ,  $T = 5.0$ ,  $n = 1000$  (dashed line). The additional curves in the top figure indicate perfect synchronization between the motion of the stepper and the periodic drive, the corresponding ratios are shown in the key.

for two different driving frequencies, one lying within the 1 : 1 synchronization regime and the other in a region without synchronization. We see that in case of synchronization the coherence of motion can be significantly increased. Out of synchrony the periodic drive reduces the level of the regularity of the motion. For smaller values of the stroke time variance the optimal rate is the maximal rate  $r_{opt} = r_2$ . In the undriven case a quick attachment of fuel molecules and small variances of stroke times result in a nearly periodic motion. If this situation is perturbed periodically by changing to a smaller rate  $r_1 \ll r_{opt}$  much disorder

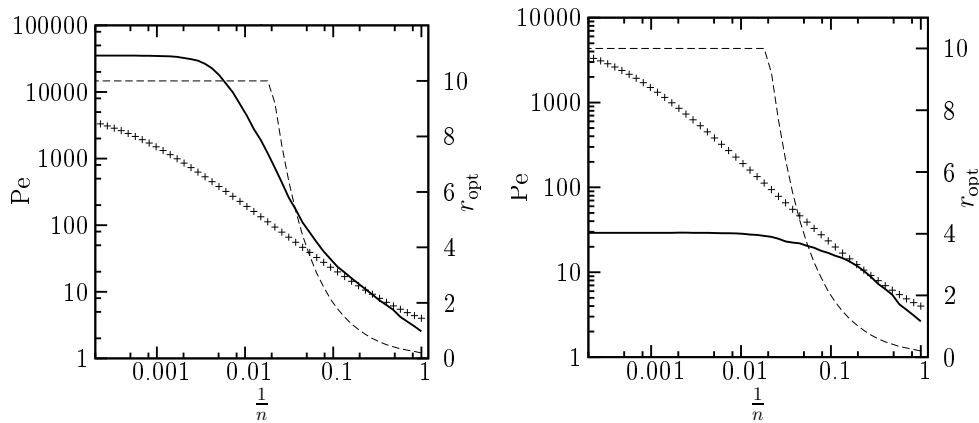


Figure 4.17: Comparison between the Péclet numbers of the dichotomically driven (solid line) and the undriven system (+) as a function of the relative variance of the stroke time  $\frac{\text{var}\tau_{\text{stroke}}}{\langle\tau_{\text{stroke}}\rangle^2} = \frac{1}{n}$ . Left: 1 : 1 synchronization regime. Parameters:  $r_1 = 0.1$ ,  $r_2 = 10.0$ ,  $T = 5.0$ ,  $\omega = 1.1$ . Right: Out of synchronization. Parameters:  $r_1 = 0.1$ ,  $r_2 = 10.0$ ,  $T = 5.0$ ,  $\omega = 0.8$ . The rate for the undriven system is chosen between  $r_1$  and  $r_2$  such that the Péclet number is maximized. This optimal rate  $r_{\text{opt}}$  is indicated by the dashed line.

is added to the motion, since during staying in the state with small rate the dispersion is  $\propto 1/r_1$ . This leads to the significant decrease of the Péclet number out of synchrony.

The periodic drive might be an instrument for probing the characteristic times of the configurational change. In case of a significant periodic variation of fuel attachment rate  $\gamma(t)$  the synchronization between the motor and the periodic driving, as indicated by a high Péclet number, is observed for driving frequencies which are equal or slightly less than integer multiples of  $2\pi$  times the mean stroke time  $T$  of the motor. Thus by tuning the driving frequency and measuring the Péclet number one can deduce the mean stroke time  $T$ . This is presented in Fig. 4.18 where the bright regions indicate high Péclet numbers as function of the frequency of the periodic drive  $\Omega$  and the mean stroke time  $T$ . One sees immediately the several regions of  $n : m$  synchronization which might be used to determine the mean stroke time. Both types of driving, i.e. dichotomic (left) and harmonical (right) exhibit qualitatively the same behavior. Again the harmonic drive allows a finer tuning of the stepper.

Recapitulating, the periodic driving, be it dichotomic or harmonic, may regularize the motion of the molecular motor. Maximal Péclet numbers were found if the motor synchronizes to the periodic drive. Several regions of  $n : m$  synchronizations with locked velocity and small effective diffusion were found. Oppositely,



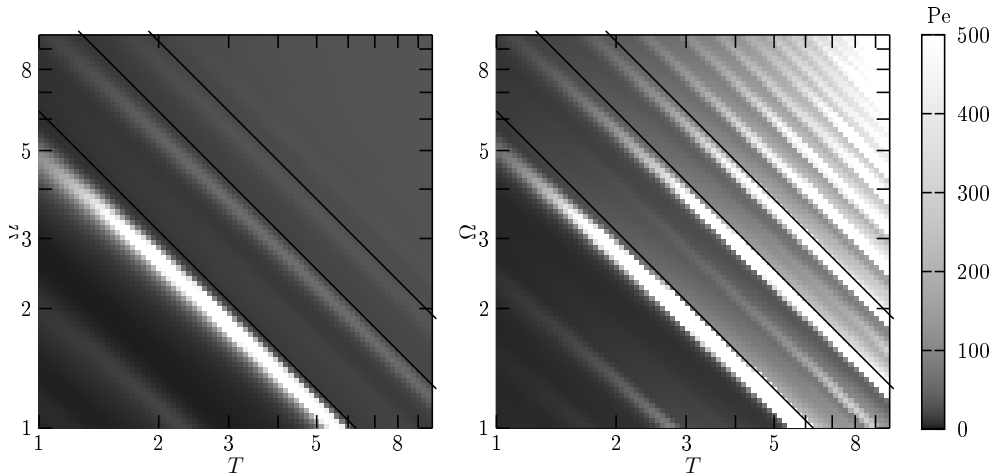


Figure 4.18: Péclet number as a function of driving frequency  $\Omega$  and mean stroke time  $T$  for the dichotomically (left) harmonically driven (right) model with  $r_1 = 0.1$ ,  $r_2 = 10$  and  $n = 100$ . The solid line correspond to  $\Omega = 2\pi/T$ ,  $\Omega = 4\pi/T$  and  $\Omega = 6\pi/T$ . The synchronization regions as indicated by highest Péclet number may thus be used to determine the mean stroke time  $T$ .

out of synchrony the stepper performs more disordered motion compared with the stationary undriven case where the attachment rate is optimized to yield maximal Péclet numbers. We have further shown that periodic driving can be used to figure out parameters of the Brownian stepper like the mean stroke time. We believe that more complex models than the Brownian stepper can be synchronized to high Péclet numbers as well. Therefore the proposed periodic driving of molecular motors might be a new technique for improvement and regularization of the random motion.

### 4.3 An approach based on waiting time distributions

In the previous section we have developed a method to calculate the drift and diffusion properties of the number of transitions between the discrete states in a periodically driven discrete state system, described by a master equation. However often one does not have a master equation at hand but the time dependent waiting time distribution  $w(\tau, t)$ , which governs the interval between subsequent events. It is this time dependent waiting time distribution, on which the calculation of the mean frequency and effective diffusion coefficient is based in the following [106].

Let us consider the probabilities  $p_k(t)$  to have had  $k$  events up to time  $t$ .

Furthermore let  $j_k(t)$  be the probability flux from state  $k$  to state  $k + 1$ , i.e. the probability per time that the  $k + 1^{\text{st}}$  event happens at time  $t$ . This probability obeys the continuity equation

$$\frac{d}{dt}p_k(t) = j_{k-1}(t) - j_k(t). \quad (4.55)$$

If we further assume as initial condition that event 1 happened at time  $t_0$ , i.e.

$$j_0(t) = \delta(t - t_0), \quad (4.56)$$

the relation between the probability fluxes of the renewal process is given by

$$j_k(t) = \int_{t_0}^t dt' j_{k-1}(t') w(t - t', t'), \quad k \geq 1. \quad (4.57a)$$

Using this relation one readily obtains from the continuity equation (4.55)

$$p_k(t) = \int_{t_0}^t dt' j_{k-1}(t') z(t - t', t'), \quad k \geq 1 \quad (4.57b)$$

where  $z(\tau, t) = 1 - \int_0^\tau d\tau' w(\tau', t)$  is the survival probability to wait longer than  $\tau$  until the next event, if the last event happened at  $t$ . Eqs. (4.57) generalize eqs. (2.16) to time dependent waiting time distributions. In the case of a Markovian renewal process with time dependent rate  $\gamma(t)$  the probability flux  $j_k$  is related to the probability  $p_k$  by  $j_k(t) = \gamma(t)p_k(t)$ . Thus in this case the dynamics can be completely expressed in terms of the probabilities  $p_k$ . In the general case however we need a formulation in terms of  $p_k$  and  $j_k$  as expressed in eqs. (4.57). Based on these probabilities we can define the moments of the number of events as

$$M_{t_0,t}^{[l]} := \sum_{k=0}^{\infty} k^l p_k(t). \quad (4.58)$$

These moments define the corresponding cumulants  $K_{t_0,t}^{[l]}$  from which finally the growth coefficients of the cumulants

$$\kappa_{t_0,t}^{[l]} := \frac{d}{dt} K_{t_0,t}^{[l]} \quad (4.59)$$

are obtained, which in the limit  $t_0 \rightarrow -\infty$  become periodic functions  $\kappa^{[l]}(t)$  of  $t$  (see appendix C.1). The first coefficient  $\kappa^{[1]}(t)$  is the instantaneous mean frequency  $\nu(t)$  while  $\kappa^{[2]}(t)$  is twice the instantaneous effective diffusion coefficient  $D_{\text{eff}}(t)$ . In principle they can be calculated from the solutions of eqs. (4.57) according to eqs. (4.58) and (4.59). However, in practice this is not feasible, as one has to

calculate an infinite sum over the  $p_k(t)$  where each  $p_k$ , according to eqs. (4.57b) and (4.57a), is a  $k$ -fold integral involving the waiting time distributions  $w(\tau, t)$  and the corresponding survival probabilities  $z(\tau, t)$ .

To find a simpler relation between the periodic coefficients  $\kappa^{[n]}(t)$  and the time dependent waiting time  $w(\tau, t)$ , which governs the microscopic dynamics, we again construct a continuous embedding in the asymptotic limit  $t_0 \rightarrow -\infty$ . The ideas are the very same as in section 4.2, where we considered alternating periodic renewal processes described by a generalized master equation, except that in the present case we additionally have to relate the discrete probability flux  $j_k(t)$  to the probability flux of the continuous embedding.

Consider an envelope  $\mathcal{P}(x, t)$  of the discrete probabilities  $p_k(t)$  as a probability distribution on a continuous state space. Thus, respecting the normalization, we adopt again the relation (cf. Fig. 4.19)

$$p_k(t) = \int_{k-\frac{1}{2}}^{k+\frac{1}{2}} dx \mathcal{P}(x, t). \quad (4.60)$$

As in section 4.2 we assume that asymptotically, i.e. when the  $p_k(t)$  and  $\mathcal{P}(x, t)$

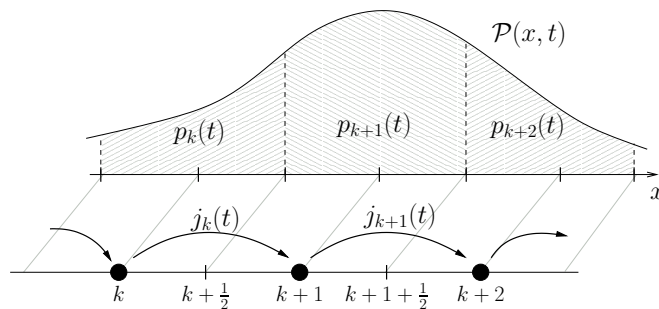


Figure 4.19: Schematic view of the discrete event dynamics  $p_k(t)$  and the continuous description in terms of  $x$ .

approach more and more a uniform distribution, this equation remains valid in the course of time if the cumulants in both, the discrete and continuous setting grow in the same way. Again this is assured by assigning a Kramers Moyal equation to the evolution of the continuous probability density,

$$\frac{\partial}{\partial t} \mathcal{P}(x, t) = \sum_{n=1}^{\infty} \frac{(-1)^n}{n!} \kappa^{[n]}(t) \frac{\partial^n}{\partial x^n} \mathcal{P}(x, t) \quad (4.61)$$

whose Kramers Moyal coefficients coincide with the periodic cumulant growth coefficients  $\kappa^{[n]}(t)$  of the discrete description. (cf. appendix C.2, [124]).

Having related the discrete and continuous probability we can likewise relate the probability current  $j_k(t)$  of the discrete system to the probability current  $\mathcal{J}(x, t)$  of the continuous envelope description. According to the relation between the discrete and continuous probability eq. (4.60), the discrete probability current  $j_k(t)$  from  $k$  to  $k + 1$  is equal to the continuous probability current  $\mathcal{J}(x, t)$  at  $x = k + \frac{1}{2}$  (see Fig. 4.19),

$$j_k(t) = \mathcal{J}\left(k + \frac{1}{2}, t\right). \quad (4.62)$$

The continuous probability current  $\mathcal{J}(x, t)$  is related to the probability distribution  $\mathcal{P}(x, t)$  by the continuity equation

$$\frac{\partial}{\partial t} \mathcal{P}(x, t) = -\frac{\partial}{\partial x} \mathcal{J}(x, t). \quad (4.63)$$

and therefore according to eq. (4.61)

$$\mathcal{J}(x, t) = -\sum_{n=1}^{\infty} \frac{(-1)^n}{n!} \kappa^{[n]}(t) \frac{\partial^{n-1}}{\partial x^{n-1}} \mathcal{P}(x, t). \quad (4.64)$$

Thus from eq. (4.62) we deduce

$$j_k(t) = -\sum_{n=1}^{\infty} \frac{(-1)^n}{n!} \kappa^{[n]}(t) \frac{\partial^{n-1}}{\partial x^{n-1}} \mathcal{P}(x, t) \Big|_{x=k+\frac{1}{2}} \quad (4.65)$$

Additionally we want to mention that the more general embedding of the discrete process

$$p_k(t) = \int_{k-1+l}^{k+l} dx \mathcal{P}(x, t) \quad \text{and} \quad j_k(t) = \mathcal{J}(k+l, t), \quad l \text{ arbitrary}, \quad (4.66)$$

would lead to the same results on  $\kappa^{[i]}(t)$  as the embedding chosen in eqs. (4.60) and (4.62), which corresponds to choosing  $l = \frac{1}{2}$  in eq. (4.66).

Having fixed the relation between the probabilities and probability fluxes of the discrete renewal process and the continuous embedding, it is now possible to relate the coefficients  $\kappa^{[n]}(t)$  appearing in the continuous description (4.61) to the waiting time distribution  $w(\tau, t)$  of the renewal process, involved in the microscopic dynamics (4.57a) and (4.57b). As we are considering the asymptotic behavior we have to pass to the asymptotic limit in eqs. (4.57a) and (4.57b) by shifting the initial time  $t_0 \rightarrow -\infty$ . This results in

$$p_k(t) = \int_0^{\infty} d\tau j_{k-1}(t-\tau) z(\tau, t-\tau). \quad (4.67)$$

and

$$j_k(t) = \int_0^\infty d\tau j_{k-1}(t-\tau)w(\tau, t-\tau). \quad (4.68)$$

Inserting eqs. (4.60) and (4.65) into the above eq. (4.67) we end up with

$$\begin{aligned} \int_{-\frac{1}{2}}^{\frac{1}{2}} d\Delta x \mathcal{P}(x - \Delta x, t) &= - \int_0^\infty d\tau z(\tau, t - \tau) \\ &\sum_{n=1}^{\infty} \frac{(-1)^n}{n!} \kappa^{[n]}(t - \tau) \frac{\partial^{n-1}}{\partial x^{n-1}} \mathcal{P}(x - \frac{1}{2}, t - \tau) \end{aligned} \quad (4.69)$$

with  $x = k$ . The probability  $\mathcal{P}(x - \Delta x, t - \tau)$  can be expressed in terms of the probability  $\mathcal{P}(x, t)$  and its derivatives  $\frac{\partial^m}{\partial x^m} \mathcal{P}(x, t)$  by performing a Taylor expansion of  $\mathcal{P}(x - \Delta x, t - \tau)$  around  $x, t$  and converting the time derivatives to derivatives with respect to the state  $x$  using the Kramers-Moyal equation (4.61). This results in (cf. appendix C.4)

$$\begin{aligned} \mathcal{P}(x - \Delta x, t - \tau) &= \\ &\mathcal{P}(x, t) + c_i^{[1]}(\tau, \Delta x) \frac{\partial}{\partial x} \mathcal{P}(x, t) + c_i^{[2]}(\tau, \Delta x) \frac{\partial^2}{\partial x^2} \mathcal{P}(x, t) + O(3) \end{aligned} \quad (4.70)$$

with

$$c_i^{[1]}(\tau, \Delta x) = \int_0^\tau d\tau' \kappa^{[1]}(t - \tau') - \Delta x.$$

and

$$\begin{aligned} c_i^{[2]}(\tau, \Delta x) &= \frac{\Delta x^2}{2} - \Delta x \int_0^\tau d\tau' \kappa^{[1]}(t - \tau') \\ &- \frac{1}{2} \int_0^\tau d\tau' \kappa^{[2]}(t - \tau') + \int_0^\tau d\tau' \kappa^{[1]}(t - \tau') \int_0^{\tau'} d\tau'' \kappa^{[1]}(t - \tau'') \end{aligned}$$

In eq. (4.70),  $O(3)$  denotes terms proportional to  $\frac{\partial^m}{\partial x^m} \mathcal{P}(x, t)$  with  $m \geq 3$ .

Equating the coefficients of  $\mathcal{P}(x, t)$  and  $\frac{\partial}{\partial x} \mathcal{P}(x, t)$  on both sides of eq. (4.69), we end up with

$$\int_0^\infty d\tau \kappa^{[1]}(t - \tau) z(\tau, t - \tau) = 1 \quad (4.71a)$$

$$\begin{aligned} \frac{1}{2} \int_0^\infty d\tau \kappa^{[2]}(t - \tau) z(\tau, t - \tau) &= \\ &\int_0^\infty d\tau \kappa^{[1]}(t - \tau) \left[ \int_0^\tau d\tau' \kappa^{[1]}(t - \tau') - \frac{1}{2} \right] z(\tau, t - \tau). \end{aligned} \quad (4.71b)$$

Eq. (4.71b) can be further simplified using eq. (4.71a), which leads to

$$\int_0^\infty d\tau \kappa^{[2]}(t-\tau) z(\tau, t-\tau) = 2 \int_0^\infty d\tau \kappa^{[1]}(t-\tau) \int_0^\tau d\tau' \kappa^{[1]}(t-\tau') z(\tau, t-\tau) - 1. \quad (4.71c)$$

These two expressions relate the asymptotic drift and diffusion properties of a periodically driven renewal process as expressed by  $\kappa^{[1]}(t)$  and  $\kappa^{[2]}(t)$  to its microscopic properties defined by the time dependent survival property  $z(\tau, t)$ .

Equations which govern the higher cumulant growth coefficients  $\kappa^{[n]}(t)$ ,  $n \geq 3$ , can also be derived using this method by evaluating the coefficients of higher order derivatives of  $\mathcal{P}(x, t)$ . The coefficients of  $\frac{\partial^2}{\partial x^2} \mathcal{P}(x, t)$  lead to an equation for  $\kappa^{[3]}(t)$ ,

$$\begin{aligned} \int_0^\infty d\tau \kappa^{[3]}(t-\tau) z(\tau, t-\tau) &= \int_0^\infty d\tau z(\tau, t-\tau) \quad (4.71d) \\ &\left[ 3\kappa^{[2]}(t-\tau) \int_0^\tau d\tau' \kappa^{[1]}(t-\tau') + 3\kappa^{[1]}(t-\tau) \int_0^\tau d\tau' \kappa^{[2]}(t-\tau') \right. \\ &\left. - 6\kappa^{[1]}(t-\tau) \int_0^\tau d\tau' \kappa^{[1]}(t-\tau') \int_0^{\tau'} d\tau'' \kappa^{[1]}(t-\tau'') \right] + 1 \end{aligned}$$

Finally one may ask, why it is justified to prescribe a continuous Markovian envelope dynamics to an inherently non Markovian discrete process. The obvious idea, that the non Markovian nature of the discrete process is rendered Markovian by being mapped onto an extended continuous state space is misleading. The point is, that the continuous Markovian process  $x(t)$  as described by eq. (4.61) is not an envelope dynamics of the full discrete non Markovian process, but it only covers the asymptotic behavior of the non Markovian process.

### 4.3.1 Comparison with known results for undriven renewal processes and periodically driven rate processes

Let us evaluate expressions (4.71) for an undriven renewal process, i.e.  $z(\tau, t) \equiv z(\tau)$ . Then it follows that  $\kappa^{[1]}(t) = \bar{\kappa}^{[1]}$  is constant and eq. (4.71a) leads to

$$\bar{\kappa}^{[1]} = \frac{1}{\langle T \rangle}$$

with

$$\langle T^n \rangle := \int_0^\infty d\tau \tau^n w(\tau).$$

To derive this result we have used the fact that

$$\int_0^\infty d\tau \tau^n z(\tau) = \int_0^\infty d\tau \frac{\tau^{n+1}}{n+1} w(\tau) = \frac{1}{n+1} \langle T^{n+1} \rangle$$

which holds if  $z(\tau)$  decreases sufficiently fast for  $\tau \rightarrow \infty$ . Accordingly eq. (4.71c) gives

$$\kappa^{[2]}(t) = \bar{\kappa}^{[2]} = \frac{\langle T^2 \rangle - \langle T \rangle^2}{\langle T \rangle^3}$$

which agrees with the known results for stationary renewal processes [22], eq. (2.30). Finally eq. (4.71d) leads to

$$\kappa^{[3]}(t) = \bar{\kappa}^{[3]} = \frac{\langle T \rangle^4 - 3\langle T^2 \rangle \langle T \rangle^2 + 3\langle T^2 \rangle^2 - \langle T \rangle \langle T^3 \rangle}{\langle T \rangle^5}.$$

Next we consider a periodically driven rate process, i.e.

$$w(\tau, t) = \gamma(t + \tau) \exp \left( - \int_t^{t+\tau} d\tau' \gamma(\tau') \right)$$

and

$$z(\tau, t) = \exp \left( - \int_t^{t+\tau} d\tau' \gamma(\tau') \right).$$

Then it can be easily shown that eq. (4.71a) is solved by

$$\kappa^{[1]}(t) = \gamma(t).$$

The first term on the right hand side of eq. (4.71c) can then be simplified using integration by parts to give 1. Therefore  $\kappa^{[2]}(t)$  is governed by

$$\int_0^\infty d\tau \kappa^{[2]}(t - \tau) z(\tau, t - \tau) = 1$$

which is again solved by

$$\kappa^{[2]}(t) = \gamma(t)$$

Using the same reasoning, eq. (4.71d) leads to

$$\kappa^{[3]}(t) = \gamma(t).$$

For more complicated processes with general time dependent waiting time distributions eqs. (4.71a) and (4.71c) can only be solved numerically for the periodic solution.

### 4.3.2 Numerical solution in Fourier space

As eqs. (4.71a) and (4.71c) cannot be solved analytically for arbitrary waiting time distributions  $w(\tau, t - \tau)$  and corresponding survival probabilities  $z(\tau, t - \tau)$  one has to resort to numerical methods. To this end we perform a Fourier expansion of the periodic function  $\kappa^{[1]}(t)$  and  $\kappa^{[2]}(t)$ ,

$$\kappa^{[i]}(t) = \sum_{k=-\infty}^{\infty} \hat{\kappa}_k^{[i]} \exp(ik\Omega t), \quad \hat{\kappa}_k^{[i]} = \frac{1}{\mathcal{T}} \int_0^{\mathcal{T}} dt \kappa^{[i]}(t) \exp(-ik\Omega t), \quad (4.72)$$

where  $\Omega = 2\pi/\mathcal{T}$  is the frequency of the external driving. We further expand the survival probability  $z(\tau, t)$  with respect to the second periodic argument as

$$z(\tau, t) = \sum_{k=-\infty}^{\infty} \hat{z}_k(\tau) \exp(ik\Omega t) \quad \hat{z}_k(\tau) = \frac{1}{\mathcal{T}} \int_0^{\mathcal{T}} dt z(\tau, t) \exp(-ik\Omega t)$$

Abbreviating

$$\hat{z}_{k,l} = \int_0^{\infty} d\tau \hat{z}_k(\tau) \exp(-il\Omega\tau), \quad \hat{h}_{k,l} = \int_0^{\infty} d\tau \tau \hat{z}_k(\tau) \exp(-il\Omega\tau) \quad (4.73)$$

eq. (4.71a) can be written as

$$\sum_{k=-\infty}^{\infty} \hat{\kappa}_k^{[1]} \hat{z}_{m-k,m} = \delta_{m,0}, \quad m = -\infty, \dots, \infty \quad (4.74)$$

while eq. (4.71c) reads

$$\begin{aligned} \sum_{k=-\infty}^{\infty} \hat{\kappa}_k^{[2]} \hat{z}_{m-k,m} = & \quad (4.75) \\ 2 \sum_{k=-\infty}^{\infty} \left[ \sum_{l=-\infty, l \neq 0}^{\infty} \frac{\hat{\kappa}_l^{[1]} \hat{\kappa}_k^{[1]}}{il\Omega} (\hat{z}_{m-k-l, m-l} - \hat{z}_{m-k-l, m}) + \hat{\kappa}_0^{[1]} \hat{\kappa}_k^{[1]} \hat{h}_{m-k, m} \right] - \delta_{m,0}. \end{aligned}$$

These infinite dimensional inhomogeneous linear equations can then be numerically solved, after being truncated to a finite dimensional system. The corresponding results for  $\kappa^{[3]}(t)$  are presented in appendix C.6

### 4.3.3 A simple toy model – comparison between theory and simulations

Consider the periodic renewal process, where the time between subsequent events is composed of a fixed waiting time, which depends on the signal phase of the previous



event and a rate process with constant rate  $\gamma$ . The waiting time distribution is then given by

$$w(\tau, t) = \theta(\tau - T(t))\gamma e^{-\gamma(\tau - T(t))}. \quad (4.76)$$

Suppose further that the fixed waiting time is either  $T_0$  or  $T_1$  depending on whether the signal phase of the previous event was within  $[0, \pi)$  or  $[\pi, 2\pi)$ , i.e

$$T(t) = \begin{cases} T_0 & \text{if } \Omega t \bmod 2\pi \in [0, \pi) \\ T_1 & \text{if } \Omega t \bmod 2\pi \in [\pi, 2\pi) \end{cases} \quad (4.77)$$

A sketch of this system is shown in Fig. 4.20 while the corresponding waiting time distribution is plotted in Fig. 4.21.

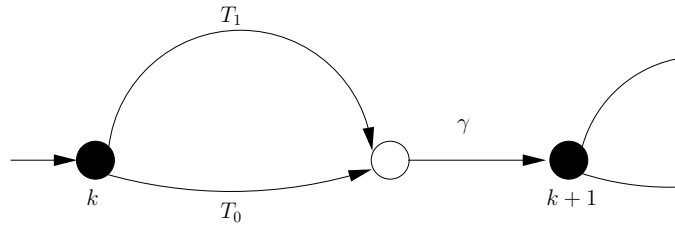


Figure 4.20: Depending on whether the periodic signal is in the first or second half period the system either waits the fixed time  $T_0$  or  $T_1$ . In both cases the system waits an additional exponentially with rate  $\gamma$  distributed time.

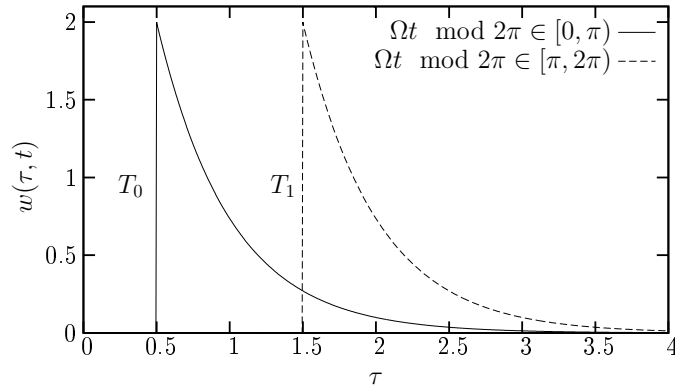


Figure 4.21: Waiting time distribution of the toy model eqs. (4.76) and (4.77) with  $T_0 = 0.5$ ,  $T_1 = 1.5$  and  $\gamma = 2$ . Depending on the signal phase of the event, the system waits either a long (dashed line) or a short time (solid line) plus an exponentially distributed time until the next event.

The corresponding Fourier coefficients  $\hat{z}_{k,l}$  and  $\hat{h}_{k,l}$  as defined in eqs. (4.73) can be analytically evaluated for this waiting time distribution, however the final

results, being too long and at the same time yielding not much information, will not be presented here. Having evaluated these Fourier coefficients, we numerically calculated the mean frequency and the effective diffusion coefficient according to eqs. (4.74) and (4.75) as well as the third cumulant growth coefficient  $\kappa^{[3]}$  eq. (C.21) using LAPACK to solve the linear equations. The results are compared to simulations of the renewal process in Figs. 4.22 and 4.23, showing perfect agreement.

Although this model shows minima of the effective diffusion coefficient as a function of the driving frequency Fig. 4.22, these minima do not correspond to frequency synchronization as the system frequency and the signal frequency do not have an integer relation. This stands in contrast to the similar model with a fixed waiting time and a dichotomically periodically modulated rate, used to describe periodically driven excitable systems in subsection 4.2.2. In this model we found several different  $n : m$  synchronization regions.

Also the full periodically time dependent coefficients  $\kappa^{[1]}(t)$  and  $\kappa^{[2]}(t)$  as determined by our theory (4.71a) and (4.71c) agree with results taken from simulations of the underlying renewal process Fig. 4.23. Interestingly the effective diffusion coefficient becomes negative for some values of the signal phase. However this evidently does not imply that the periodic driving can be used to concentrate an ensemble of these systems as the period averaged effective diffusion coefficient  $\bar{\kappa}^{[2]}$  is always positive. However  $\bar{\kappa}^{[3]}$  can be negative.

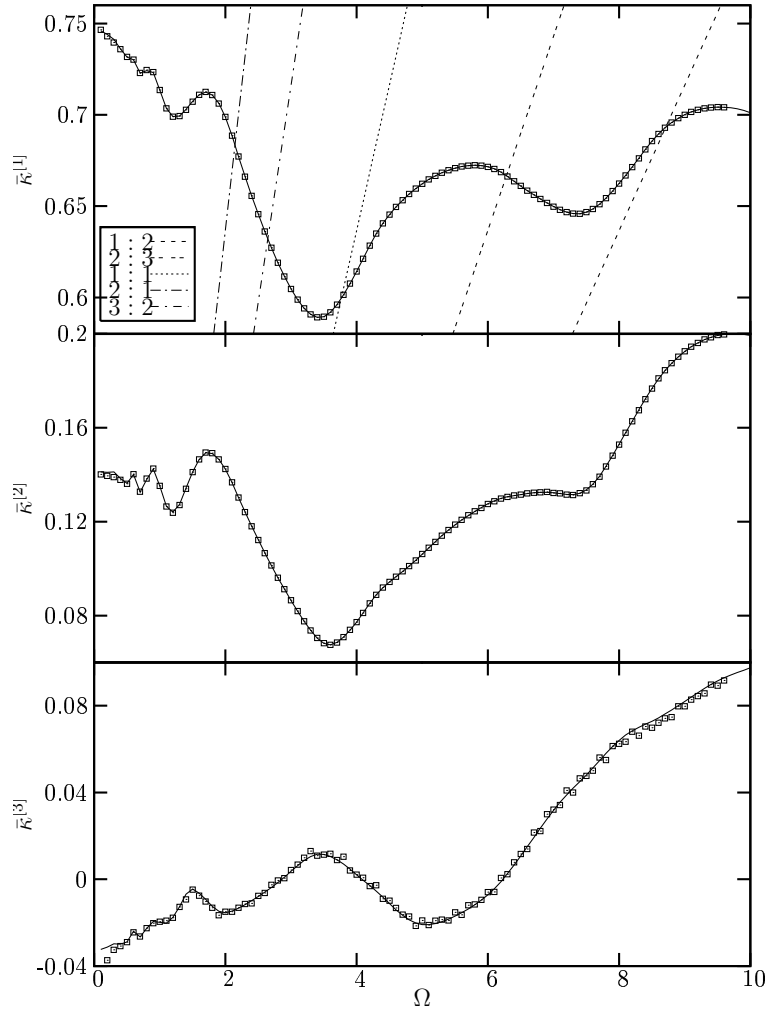


Figure 4.22: Comparison of the period averaged mean frequency  $\bar{\kappa}^{[1]} = \frac{1}{T} \int_0^T dt \kappa^{[1]}(t)$ , the period averaged effective diffusion coefficients  $\bar{\kappa}^{[2]} = \frac{1}{T} \int_0^T dt \kappa^{[2]}(t)$  and the third cumulant growth coefficient  $\bar{\kappa}^{[3]} = \frac{1}{T} \int_0^T dt \kappa^{[3]}(t)$  ( $T = 2\pi/\Omega$  denotes the period of the signal) for the toy model eq. (4.76) with  $T_0 = 0.5$ ,  $T_1 = 1.5$  and  $\gamma = 2$ . The solid lines are results of the theory eqs. (4.71), numerically evaluated according to eqs. (4.74), (4.75) and (C.21) truncated to 40 coefficients, while the symbols are obtained from direct simulations of the driven renewal process. The straight lines in the upper plot indicate  $n : m$  relations between system frequency and signal frequency, i.e. frequency locking. Clearly the system does not show this behavior.

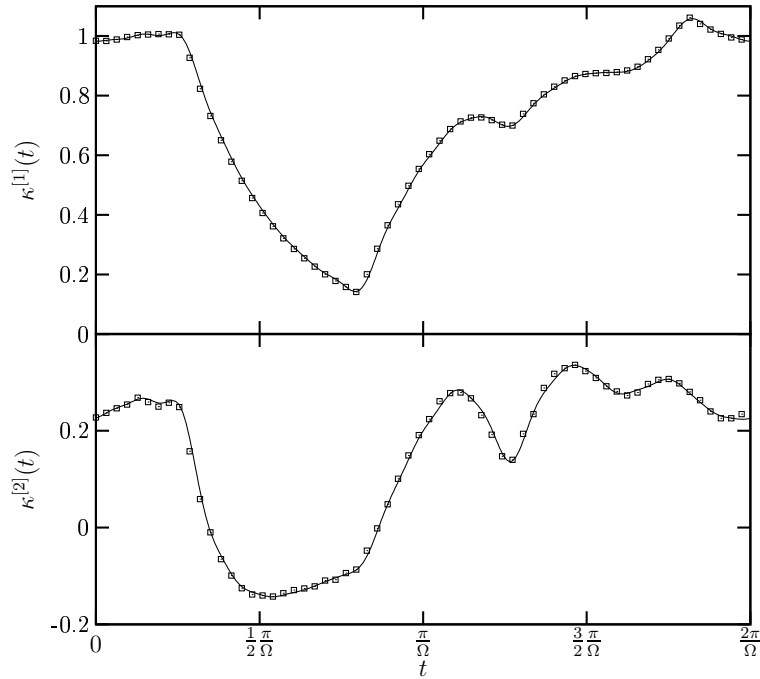


Figure 4.23: Comparison of the mean frequency  $\kappa^{[1]}(t)$  and the effective diffusion coefficients  $\kappa^{[2]}(t)$  for the toy model eq. (4.76) with  $T_0 = 0.5$ ,  $T_1 = 1.5$  and  $\gamma = 2$  and  $\Omega = 1.7$ . The solid lines are results of the theory eqs. (4.71a) and (4.71c), numerically evaluated according to eqs. (4.74) and (4.75) truncated to 20 coefficients, while the symbols are obtained from direct simulations of the driven renewal process.

### 4.3.4 Equivalence with the two state model for excitable systems

One may wonder whether the two different approaches, based on a time dependent waiting time distribution as presented in this section or on some general master equation as presented in section 4.2 lead to the same results. In this subsection we show this agreement for the two state non Markovian model of excitable systems, thus confirming that both approaches are consistent with each other.

The waiting time between two events in this model is given by the sum of the time spent on the excitation loop and the excitation time. The time on the excitation loop is distributed according  $w^{(1)}(\tau)$  while the excitation time, being due to a rate process with time dependent rate  $\gamma(t)$ , is distributed according to

$$w^{(2)}(\tau, t) = \gamma(t + \tau) \exp\left(-\int_t^{t+\tau} d\tau' \gamma(\tau')\right). \quad (4.78)$$

The total time dependent waiting time distribution between two subsequent events, i.e. between two subsequent excitations is then given by the generalized convolution

$$\begin{aligned} w(\tau, t) &= \int_0^\tau d\tau' w^{(1)}(\tau') w^{(2)}(\tau - \tau', t + \tau') \\ &= \int_0^\tau d\tau' w^{(1)}(\tau') \gamma(t + \tau) \exp\left(-\int_{t+\tau'}^{t+\tau} d\tau'' \gamma(\tau'')\right). \end{aligned} \quad (4.79)$$

while the corresponding survival probability reads

$$z(\tau, t) = \int_0^\tau d\tau' w^{(1)}(\tau') \exp\left(-\int_{t+\tau'}^{t+\tau} d\tau'' \gamma(\tau'')\right) + z^{(1)}(\tau) \quad (4.80)$$

where  $z^{(1)}(\tau) = 1 - \int_0^\tau d\tau' w^{(1)}(\tau')$  is the probability to spent a time longer than  $\tau$  on the excitation loop. From these equations we eventually obtain the relation

$$\gamma(t) z(\tau, t - \tau) = w(\tau, t - \tau) + z^{(1)}(\tau). \quad (4.81)$$

In the two state model the mean phase velocity  $\omega(t)$  is governed by eq. (4.44a) while the effective phase diffusion coefficient obeys eq. (4.44b). The auxiliary variables  $q_2^{(0)}$  and  $q_2^{(1)}$  as defined by eqs. (4.45) can be eliminated, leading to

$$\gamma(t) \int_0^\infty d\tau \omega(t - \tau) z^{(1)}(\tau) + \omega(t) = 2\pi\gamma(t) \quad (4.82)$$

and

$$\begin{aligned} \gamma(t) \int_0^\infty d\tau D_{\text{eff}}(t - \tau) z^{(1)}(\tau) + D_{\text{eff}}(t) = \\ -2\pi^2\gamma(t) + 2\pi\omega(t) + \gamma(t) \int_0^\infty d\tau \omega(t - \tau) \int_0^\tau d\tau' \omega(t - \tau') z^{(1)}(\tau). \end{aligned} \quad (4.83)$$

In the following we show that these equations for  $\omega(t)$  and  $D_{\text{eff}}(t)$  are equivalent to our general eqs. (4.71a) and (4.71c) which taking into account the factor  $2\pi$  for  $\omega(t)$  and  $4\pi^2$  for  $D_{\text{eff}}(t)$  read

$$\int_0^\infty d\tau \omega(t-\tau) z(\tau, t-\tau) = 2\pi \quad (4.84)$$

and

$$\begin{aligned} \int_0^\infty d\tau D_{\text{eff}}(t-\tau) z(\tau, t-\tau) = \\ \int_0^\infty d\tau \omega(t-\tau) \int_0^\tau d\tau' \omega(t-\tau+\tau') z(\tau, t-\tau) - 2\pi^2 \end{aligned} \quad (4.85)$$

Multiplying eqs. (4.84) and (4.85) by  $\gamma(t)$  and replacing the time dependent survival probability  $z(\tau, t-\tau)$  according to eq.(4.81) we obtain

$$\gamma(t) \int_0^\infty d\tau \omega(t-\tau) z^{(1)}(\tau) + \int_0^\infty d\tau \omega(t-\tau) w(\tau, t-\tau) = 2\pi\gamma(t) \quad (4.86)$$

and

$$\begin{aligned} \gamma(t) \int_0^\infty d\tau [D_{\text{eff}}(t-\tau) - \omega(t-\tau) \int_0^\tau d\tau' \omega(t-\tau-\tau')] z^{(1)}(\tau) + \\ \int_0^\infty d\tau [D_{\text{eff}}(t-\tau) - \omega(t-\tau) \int_0^\tau d\tau' \omega(t-\tau-\tau')] w(\tau, t-\tau) = -2\pi^2\gamma(t) \end{aligned} \quad (4.87)$$

The second term on the left hand side in both equations can be further simplified. To this end we differentiate eqs. (4.84) and (4.85) with respect to  $t$  (see appendix C.7), using eq. (4.84) to simplify the time derivative of eq. (4.85) which results in

$$\omega(t) = \int_0^\infty d\tau \omega(t-\tau) w(\tau, t-\tau) \quad (4.88)$$

and

$$\begin{aligned} D_{\text{eff}}(t) = \\ \int_0^\infty d\tau [D_{\text{eff}}(t-\tau) - \omega(t-\tau) \int_0^\tau d\tau' \omega(t-\tau-\tau')] w(\tau, t-\tau) + 2\pi\omega(t). \end{aligned} \quad (4.89)$$

Note that the above equations can be equivalently derived from eq. (4.68) by performing the same procedure we have applied to eq. (4.67) in order to obtain eqs. (4.71a) and (4.71c).

Inserting finally eqs. (4.88) and (4.89) into eqs. (4.86) and (4.87), eventually leads to the two state model eqs. (4.82) and (4.83).

Thus we have shown that solutions of  $D_{\text{eff}}(t)$  and  $\omega(t)$  of the general driven renewal process based theory presented in section 4.3 are also solutions of the two state model for excitable systems investigated in subsection 4.2.2 based on a generalized master equation. As these solutions, being defined by an inhomogeneous linear equation, are in general unique we have shown the equivalence between the two approaches.

## 4.4 Summary

Based on discrete state renewal processes we have investigated the synchronization of bistable and excitable stochastic systems to a periodic signal. To this end we have derived general concepts to calculate the mean frequency and effective diffusion coefficient of the number of events of a periodic renewal process. These quantities were shown to agree with the high and low frequency limit of the spectral power density of a corresponding delta spike process, as is known for stationary processes [72]. However this relation was not exploited in the calculation of the mean frequency and effective diffusion coefficient, as the calculation of the spectral power density of periodically driven renewal processes is not evident. Instead we presented a different approach, based on a continuous embedding of the discrete probabilities of the number of events. Applied to the well known Markovian discrete model for an overdamped particle in a bistable potential we derived analytical results for the mean frequency, effective diffusion coefficient and Péclet number for a dichotomic periodic driving. The Péclet number as a measure of stochastic synchronization shows not only a maximum as a function of noise strength, namely *stochastic resonance* but also as a function of driving frequency, i.e. a *bona fide* resonance. Applied to the non Markovian discrete model for excitable system we found a complex synchronization behavior with several different frequency locking regions. The observed phenomena in the excitable FHN system are exactly reproduced by the discrete model. The very same model can also be interpreted as a molecular motor model in a periodically varying ATP concentration. Within this context we showed that the periodic modulation can lead to a very regular motion of the motor.

# Chapter 5

## Coupled Systems

The collective behavior of ensembles of coupled dynamical units and in particular collective oscillations play an important role in many different fields of science, ranging from the dramatic consequences of synchronously firing neurons as the reason of Parkinson disease [129, 131] or, on the other hand a lack of synchronization as a possible reason of autism [135], to chemical [65, 68, 85] and physical systems and even economical and sociological systems [86, 89]. Starting from the pioneering work of Winfree [138], who proposed a model of globally coupled phase oscillators to describe the onset of spontaneous oscillations in a variety of large populations of biological objects such as flashing fireflies or cardiac pacemaker, a lot of research has been devoted to refine and analyze this model [3, 68, 118, 126]. Kuramoto [68] put this model on a firmer foundation by showing that arbitrary nearly identical globally coupled limit cycle oscillators can be described by a phase oscillator model, similar to the above mentioned Winfree model. This *Kuramoto* model has been applied to many different systems, ranging from globally coupled arrays of semiconductor lasers [66] or Josephson junctions [136] to neutrino flavor oscillations [95] and even delays in the coupling have been investigated [17]. Including a non constant force term into the dynamics of the single phases the resulting *active rotator* model introduced in [118] has become one of the most investigated systems in the study of globally coupled system. This system no longer only describes oscillatory system but also excitable dynamics are covered. In these excitable systems the influence of noise, being able to trigger excitations, is no longer negligible. Within this model the influence of noise on the dynamics of coupled excitable systems was studied [19, 97, 140] and even the joint effects of noise and coupling with respect to the response to a weak periodic stimulation have been investigated [128]. The essential behavior of more realistic models like FitzHugh-Nagumo [140] or Hodgkin Huxley systems [134] are well reproduced, however the relative simplicity of the active rotator model provides in many cases a better understanding of the underlying mechanisms.



We propose a different approach to investigate the collective dynamics of globally coupled units which is based on the discrete modeling of a single system introduced in chapter 2. As in the case of the active rotator model, the motivation of our analysis is the simplicity of the discrete state model, which allows for a partly analytical treatment, while at the same time the model has the necessary ingredients to qualitatively reproduce the effects observed in more realistic globally coupled systems.

We start our analysis in section 5.1 with the derivation of a non linear mean field master equation for the Markovian two state system, and show that this model does not exhibit global oscillations. The analysis is then extended to the non Markovian three state model in section 5.2. General necessary conditions for the onset of oscillations are investigated and finally the model is analyzed with sharply peaked waiting times in state 2 and 3 and a Arrhenius type excitation rate, intended to model excitable behavior. The results qualitatively reproduce the behavior of globally coupled excitable FHN systems.

The last section 5.3 generalizes the mean field analysis to units whose dynamics is defined by waiting time distributions which, due to the global coupling, functionally depend on the mean output of the system. The resulting concepts are then applied to a two state model for the FHN system in the bistable regime. Again the global behavior of the coupled FHN system as a function of noise level and coupling strength, namely monostability, oscillations and bistability, is well predicted by the theory.

## 5.1 The two state model for double well potential systems

In order to investigate the behavior of coupled units we start with the simplest model namely the two state Markovian model for a double well potential system [83] as introduced in 2.1.1. The response of such globally coupled bistable units to a periodic signal was studied in [62], showing array enhanced stochastic resonance. This effect can also be found in locally coupled bistable elements [119]. However we consider only the undriven case in the following, which serves as an introductory example to the more complex analysis of the threestate model for excitable system, investigated in the subsection 5.2.

Consider an ensemble of  $N$  double well systems. The global or *mean field* coupling is introduced by making the double well potential a single unit is subjected to, dependent on the global output of the system. On the level of the discrete state description this leads to transition rates  $\gamma_{1\rightarrow 2}$  from left to right and  $\gamma_{2\rightarrow 1}$  from right

to left, which are no longer constant but become dependent on the global output

$$\bar{x}(t) = \frac{1}{N} \sum_{i=1}^N x(\sigma_i(t)),$$

where  $\sigma_i(t) = 1, 2$  denotes the state 1 (left) or 2 (right) of unit  $i$  and  $x^{(1)}$  and  $x^{(2)}$  is the output of a single unit in state 1 or 2 respectively.

Due to the global coupling we do not have to care which unit is in which state, but may describe the micro state of the coupled system by the number of units  $n^{(1)}$  and  $n^{(2)}$  which are in state 1 or 2 respectively. The output of the system is then given by  $\bar{x}(t) = \frac{n^{(1)}(t)}{N}x^{(1)} + \frac{n^{(2)}(t)}{N}x^{(2)}$ . The probability  $p_N(n^{(1)}, n^{(2)}, t)$  that  $n^{(1)}$  units are in state 1 and  $n^{(2)} = N - n^{(1)}$  units are in state 2 at time  $t$  is then governed by the master equation (cf. eq. (2.5))

$$\begin{aligned} \dot{p}_N(n^{(1)}, n^{(2)}, t) = & \quad (5.1) \\ & (n^{(2)} + 1)\gamma_{2 \rightarrow 1} \left( \frac{n^{(1)} - 1}{N}x^{(1)} + \frac{n^{(2)} + 1}{N}x^{(2)} \right) p_N(n^{(1)} - 1, n^{(2)} + 1, t) \\ & + (n^{(1)} + 1)\gamma_{1 \rightarrow 2} \left( \frac{n^{(1)} + 1}{N}x^{(1)} + \frac{n^{(2)} - 1}{N}x^{(2)} \right) p_N(n^{(1)} + 1, n^{(2)} - 1, t) \\ & - (n^{(1)}\gamma_{1 \rightarrow 2} \left( \frac{n^{(1)}}{N}x^{(1)} + \frac{n^{(2)}}{N}x^{(2)} \right) + n^{(2)}\gamma_{2 \rightarrow 1} \left( \frac{n^{(1)}}{N}x^{(1)} + \frac{n^{(2)}}{N}x^{(2)} \right)) p_N(n^{(1)}, n^{(2)}, t). \end{aligned}$$

The first two terms account for the probability influx from a micro state  $(n^{(1)} - 1, n^{(2)} + 1)$  or  $(n^{(1)} + 1, n^{(2)} - 1)$  respectively into state  $(n^{(1)}, n^{(2)})$  while the last two terms account for the probability efflux. As there is a certain number of different units which may perform the corresponding transitions we have to include this number as a prefactor of the rate.

From the linear microscopic master equation (5.1) it is possible to derive in the limit  $N \rightarrow \infty$  of infinitely many globally coupled units a nonlinear equation for the occupation probabilities  $p^{(1)}(t)$  and  $p^{(2)}(t)$  of state 1 or 2 respectively. (For a continuous setting see [24, 25, 116]). To this end we assume that the relative number of units in state  $k$ , which for any finite  $N$  is a *stochastic* process, tends in the limit  $N \rightarrow \infty$  to a *deterministic* function<sup>1</sup>

$$\lim_{N \rightarrow \infty} \frac{n^{(k)}(t)}{N} = p^{(k)}(t), \quad n^{(k)}(t) = \sum_{i=1}^N \delta_{\sigma_i(t), k} \quad (5.2)$$

---

<sup>1</sup>For a stochastic dynamics with continuous state space an analogue convergence has been proven under some assumptions in [24], while in other works [116], the authors claim that such a convergence is a consequence of the law of large numbers, which is obviously misleading, as the law of large numbers does not deal with *dependent* random variables.

such that for an arbitrary continuous function  $f$  we have

$$\lim_{N \rightarrow \infty} \sum_{n^{(1)}+n^{(2)}=N}^{\infty} p_N(n^{(1)}, n^{(2)}, t) f\left(\frac{n^{(1)}}{N}, \frac{n^{(2)}}{N}\right) = f(p^{(1)}(t), p^{(2)}(t)). \quad (5.3)$$

Then obviously

$$p^{(k)}(t) = \lim_{N \rightarrow \infty} \sum_{n^{(1)}+n^{(2)}=N} \frac{n^{(k)}}{N} p_N(n^{(1)}, n^{(2)}, t) \quad (5.4)$$

Taking the time derivative of eqs. (5.4), using the microscopic master equation (5.1) we obtain

$$\begin{aligned} \dot{p}^{(1)}(t) = -\dot{p}^{(2)}(t) = \\ \lim_{N \rightarrow \infty} \sum_{n^{(1)}+n^{(2)}=N} \left[ \gamma_{2 \rightarrow 1} \left( \frac{1}{N} \sum_{i=1}^2 n^{(i)} x^{(i)} \right) \frac{n^{(2)}}{N} p_N(n^{(1)}, n^{(2)}, t) \right. \\ \left. - \gamma_{1 \rightarrow 2} \left( \frac{1}{N} \sum_{i=1}^2 n^{(i)} x^{(i)} \right) \frac{n^{(1)}}{N} p_N(n^{(1)}, n^{(2)}, t) \right] \end{aligned} \quad (5.5)$$

Assumption (5.3) eventually leads to the non linear master equation

$$\dot{p}^{(1)}(t) = -\gamma_{1 \rightarrow 2}(\bar{x}(t)) p^{(1)}(t) + \gamma_{2 \rightarrow 1}(\bar{x}(t)) p^{(2)}(t) \quad (5.6a)$$

$$\dot{p}^{(2)}(t) = \gamma_{1 \rightarrow 2}(\bar{x}(t)) p^{(1)}(t) - \gamma_{2 \rightarrow 1}(\bar{x}(t)) p^{(2)}(t) \quad (5.6b)$$

where the mean output is now given by

$$\bar{x}(t) = \sum_{i=1}^2 p^{(i)}(t) x^{(i)} \quad (5.6c)$$

Note that in the case of uncoupled systems the assumption (5.2) is just the law of large numbers. For an uncoupled system the random variables  $\delta_{\sigma_i(t), k}$  are independent and thus the law of large numbers states

$$\lim_{N \rightarrow \infty} \frac{1}{N} \sum_{i=1}^N \delta_{\sigma_i(t), k} = p^{(k)} \quad \text{almost sure} \quad (5.7)$$

Depending on the type of the coupling, namely on the dependence of the rates  $\gamma_{1 \rightarrow 2}$  and  $\gamma_{2 \rightarrow 1}$  on the mean output  $\bar{x}(t)$ , there might be one or several stationary solutions, which are obtained by setting  $\dot{p}^{(1)}(t) = \dot{p}^{(2)}(t) = 0$  in eqs. (5.6) and solving the resulting nonlinear equations.

Let us investigate the possible types of behavior of this system. Due to the normalization condition  $p^{(1)}(t) + p^{(2)}(t) = 1$  the system is actually one dimensional, which excludes oscillatory solutions of the mean field (5.6c). As the positivity of  $p^{(1)}(t)$  and  $p^{(2)}(t)$  is also preserved, the dynamics is bounded to  $[0, 1]$  and thus there must be at least one stable fixed point  $(p_{\text{st}}^{(1)}, p_{\text{st}}^{(2)} = 1 - p_{\text{st}}^{(1)})$ .

The local stability properties of a given fixed point  $p_{\text{st}}^{(1)}$  and  $p_{\text{st}}^{(2)} = 1 - p_{\text{st}}^{(1)}$  can be derived by linearizing the non linear master equation (5.6) around this fixed point. Setting  $p^{(1)}(t) = p_{\text{st}}^{(1)} + \delta p^{(1)}(t)$  we obtain a linear differential equation for the deviation  $\delta p^{(1)}(t)$  from the stationary solution  $p_{\text{st}}^{(1)}$ ,

$$\frac{d}{dt} \delta p^{(1)}(t) = \left[ -\gamma_{1 \rightarrow 2}(\bar{x}_{\text{st}}) - \gamma_{2 \rightarrow 1}(\bar{x}_{\text{st}}) - \gamma'_{1 \rightarrow 2}(\bar{x}_{\text{st}}) p_{\text{st}}^{(1)} + \gamma'_{2 \rightarrow 1}(\bar{x}_{\text{st}}) (1 - p_{\text{st}}^{(1)}) \right] \delta p^{(1)}(t)$$

with  $\bar{x}_{\text{st}} = x^{(1)} p_{\text{st}}^{(1)} + x^{(2)} (1 - p_{\text{st}}^{(1)})$ . Depending on whether the expression in brackets (which is the eigenvalue of the characteristic equation) is negative or positive the stationary solution is either stable or unstable.

Summing up, the only behavior one can observe in such a globally coupled Markovian two state model for double well potential systems is a stationary state, which due to a change of control parameters may loose stability and thus relaxes into another stationary state. More complex behavior like global oscillations or even chaos can be excluded by the above considerations.

## 5.2 The three state model for excitable dynamics

Having ruled out complex behavior of the globally coupled Markovian two state model we are now interested in the behavior of globally coupled excitable systems. The analysis will be based on the threestate model [88, 103] for excitable systems introduced in section 2.1.2. In this model the excitable dynamics is mapped onto three discrete states. Starting from the rest state 1, the system is excited according to a rate process with rate  $\gamma$  to the firing state 2. In the firing state the system spends a certain time  $\tau$ , which is distributed according to  $w^{(2)}(\tau)$  before passing into the refractory state 3, where it again spends some time  $\tau$  distributed according to  $w^{(3)}(\tau)$ , after which it finally returns to the rest state. To a fair approximation the output of an excitable system assumes a constant high value  $x_1$  in the firing state, while in the rest and refractory state the system has the same low output  $x_0$ . However, to be more general we assume the output to have a value  $x^{(i)}$  if the system is in state  $i$ , i.e. we also allow to distinguish the output in refractory and rest state. The mean output of an ensemble of  $N$  three state units is thus given

by

$$\bar{x}(t) = \frac{1}{N} \sum_{i=1}^N x^{(\sigma_i(t))},$$

where  $\sigma_i(t) = 1, 2, 3$  denotes the state of unit  $i$  at time  $t$ .

As we have already noticed when considering excitable systems driven by external signals, it is to a good approximation only the dynamics of the excitation from the rest state to the firing state, which is affected by the signal. In the globally coupled ensemble this signal is chosen to be the mean output  $\bar{x}(t)$  of the population of excitable systems. Thus we end up with an excitation rate, which depends on the mean ensemble output  $\bar{x}(t)$ .

To derive a mean field equation for this system we start with the microscopic probabilities  $p(\sigma_1, \dots, \sigma_N, t)$  that unit  $i = 1, \dots, N$  is in state  $\sigma_i = 1, 2, 3$  at time  $t$ . In this state the excitation rate for system  $j$  is given by

$$\gamma_j = \gamma \left( \frac{1}{N} \sum_{i \neq j, i=1}^N x^{(\sigma_i)} \right). \quad (5.8)$$

The probability  $p_j^{(k)}(t)$  that unit  $j$  is in state  $k$  can be expressed by summing over the different states of all the other units,

$$p_j^{(k)}(t) := \sum_{\{\sigma_i, i \neq j\}} p(\sigma_1, \dots, \sigma_{j-1}, k, \sigma_{j+1}, \dots, \sigma_N, t). \quad (5.9)$$

In the above equation the sum  $\sum_{\{\sigma_i, i \neq j\}}$  denotes a summation over all possible micro states  $\{\sigma_1, \dots, \sigma_{j-1}, \sigma_{j+1}, \dots, \sigma_N\}$ . The dynamics for the single unit probabilities  $p_j^{(k)}(t)$  can be derived in the same manner as the dynamics for a single unit with an excitation rate which depends on the external signal as done in subsection 3.3.1, eq. (3.35). However we have to take into account the dependence of the excitation rate on the state  $\sigma_i$  of all other units according to eq. (5.8), eventually leading to

$$p_j^{(2)}(t) = \int_0^\infty d\tau \sum_{\{\sigma_i, i \neq j\}} \gamma \left( \frac{1}{N} \sum_{i \neq j, i=1}^N x^{(\sigma_i)} \right) \quad (5.10a)$$

$$p(\sigma_1, \dots, \sigma_{j-1}, 1, \sigma_{j+1}, \dots, \sigma_N, t - \tau) z^{(2)}(\tau)$$

$$p_j^{(3)}(t) = \int_0^\infty d\tau \sum_{\{\sigma_i, i \neq j\}} \gamma \left( \frac{1}{N} \sum_{i \neq j, i=1}^N x^{(\sigma_i)} \right) \quad (5.10b)$$

$$p(\sigma_1, \dots, \sigma_{j-1}, 1, \sigma_{j+1}, \dots, \sigma_N, t - \tau) \int_0^\tau d\tau' w^{(2)}(\tau') z^{(3)}(\tau - \tau').$$

supplemented with the normalization condition  $p_j^{(1)}(t) + p_j^{(2)}(t) - p_j^{(3)}(t) = 1$ . With the help of definition (5.9) we can replace  $p_j^{(i)}(t)$  appearing on the left hand side in eqs. (5.10) by an appropriate sum of the  $p(\sigma_1, \dots, \sigma_N, t)$ , leading to a closed equation in the microscopic probabilities  $p(\sigma_1, \dots, \sigma_N, t)$ . Note however, that these equations are not valid without the summation, i.e. in general (cf. (5.10a))

$$p(\sigma_1, \dots, \sigma_{j-1}, 2, \sigma_{j+1}, \dots, \sigma_N, t) \neq \int_0^\infty d\tau \gamma \left( \frac{1}{N} \sum_{i \neq j, i=1}^N x^{(\sigma_i)} \right) p(\sigma_1, \dots, \sigma_{j-1}, 1, \sigma_{j+1}, \dots, \sigma_N, t - \tau) z^{(2)}(\tau)$$

This is due to the fact that in the finite time interval between the time  $t - \tau$  when we assume unit  $j$  to leave state 1 and the time  $t$  at which we consider the probability of unit  $j$  to be in state 2 the other units may arbitrarily change their state. This is different to the description of the Markovian two state system in section 5.1, which is local in time.

Due to the global coupling all units are equivalent and we may describe the system by the probabilities  $p_N(n^{(1)}, n^{(2)}, n^{(3)}, t)$  that  $n^{(i)}$  units are in state  $i$  at time  $t$ . These probabilities are related to the micro state probabilities  $p(\sigma_1, \dots, \sigma_N, t)$  by

$$\frac{1}{N} \sum_{j=1}^N \sum_{\{\sigma_i, i \neq j\}} p(\sigma_1, \dots, \sigma_{j-1}, k, \sigma_{j+1}, \dots, \sigma_N, t) = \sum_{n^{(1)}+n^{(2)}+n^{(3)}=N} \frac{n^{(k)}}{N} p_N(n^{(1)}, n^{(2)}, n^{(3)}, t)$$

Eqs. (5.10) can thus be rewritten as

$$\sum_{n^{(1)}+n^{(2)}+n^{(3)}=N} \left[ \frac{n^{(2)}}{N} p_N(n^{(1)}, n^{(2)}, n^{(3)}, t) - \right. \quad (5.11a)$$

$$\left. \frac{n^{(1)}}{N} \int_0^\infty d\tau \gamma \left( \sum_{k=1}^3 x^{(k)} \frac{n^{(k)}}{N} \right) p_N(n^{(1)}, n^{(2)}, n^{(3)}, t - \tau) z^{(2)}(\tau) \right] = 0$$

$$\sum_{n^{(1)}+n^{(2)}+n^{(3)}=N} \left[ \frac{n^{(3)}}{N} p_N(n^{(1)}, n^{(2)}, n^{(3)}, t) - \frac{n^{(1)}}{N} \int_0^\infty d\tau \right. \quad (5.11b)$$

$$\left. \gamma \left( \sum_{k=1}^3 x^{(k)} \frac{n^{(k)}}{N} \right) p_N(n^{(1)}, n^{(2)}, n^{(3)}, t - \tau) \int_0^\tau d\tau' w^{(2)}(\tau') z^{(3)}(\tau - \tau') \right] = 0$$

Next we again assume that in the limit of infinitely many coupled units  $N \rightarrow \infty$ , the relative occupation numbers  $\frac{n^{(i)}(t)}{N}$  converge to a deterministic process  $p^{(i)}(t)$ ,

such that for an arbitrary continuous function  $f$

$$\begin{aligned} \lim_{N \rightarrow \infty} \sum_{n^{(1)}+n^{(2)}+n^{(3)}=N} p_N(n^{(1)}, n^{(2)}, n^{(3)}, t) f\left(\frac{n^{(1)}}{N}, \frac{n^{(2)}}{N}, \frac{n^{(3)}}{N}\right) \\ = f(p^{(1)}(t), p^{(2)}(t), p^{(3)}(t)) \end{aligned} \quad (5.12)$$

In this limit we then obtain from eqs. (5.11)

$$p^{(2)}(t) = \int_0^\infty d\tau \gamma \left( \sum_{k=1}^3 x^{(k)} p^{(k)}(t-\tau) \right) z^{(2)}(\tau) \quad (5.13a)$$

$$p^{(3)}(t) = \int_0^\infty d\tau \gamma \left( \sum_{k=1}^3 x^{(k)} p^{(k)}(t-\tau) \right) p^{(1)}(t-\tau) \int_0^\tau d\tau' w^{(2)}(\tau') z^{(3)}(\tau-\tau'). \quad (5.13b)$$

supplemented with the normalization condition

$$p^{(1)}(t) = 1 - p^{(2)}(t) - p^{(3)}(t). \quad (5.13c)$$

In the following, we will analyze the behavior of these nonlinear master equations. Denoting by

$$\langle \tau^{(i)} \rangle := \int_0^\infty d\tau \tau w^{(i)}(\tau) = \int_0^\infty d\tau z^{(i)}(\tau), \quad i = 2, 3$$

the mean waiting time in state 2 and 3, and by

$$\langle \tau^{(1)} \rangle := \frac{1}{\gamma(\bar{x}_{\text{st}})} \quad \text{with} \quad \bar{x}_{\text{st}} = \sum_{k=1}^3 x^{(k)} p_{\text{st}}^{(k)},$$

the mean waiting time in state 1, the stationary solution(s)  $p_{\text{st}}^{(i)}$  of eqs. (5.13) can be implicitly determined by

$$p_{\text{st}}^{(i)} = \frac{\langle \tau^{(i)} \rangle}{\langle \tau^{(1)} \rangle + \langle \tau^{(2)} \rangle + \langle \tau^{(3)} \rangle} \quad (5.14)$$

i.e. the stationary probability to be in a state is given by the mean waiting time in this state, divided by the mean time for one cycle  $1 \rightarrow 2 \rightarrow 3$ .

In contrast to the case of a single unit, where exactly one stable stationary solution exists, the behavior of the globally coupled system may be more complex due to the nonlinearity in eqs. (5.13). Depending on the chosen coupling, i.e. on the dependence of the excitation rate  $\gamma$  on the mean output of the system and thus

on  $p_{\text{st}}^{(2)}$  and  $p_{\text{st}}^{(3)}$ , eqs. (5.14) have one or several solutions, which might be locally stable or unstable. Due to a loss of stability of the stationary solution induced by the coupling the system might undergo a Hopf bifurcation leading to the onset of global oscillations. This behavior will be investigated in the following.

The local stability of a stationary solution can be obtained by inserting the ansatz

$$p^{(i)}(t) = p_{\text{st}}^{(i)} + \delta p^{(i)}(t), \quad \delta p^{(i)}(t) = a^{(i)} \exp(\lambda t) \quad (5.15)$$

into the nonlinear master equation (5.13). Neglecting the nonlinear terms in  $\delta p^{(i)}(t)$ , this results in

$$a^{(2)} = [s^{(2)}a^{(2)} + s^{(3)}a^{(3)} - (a^{(2)} + a^{(3)})r] \hat{z}^{(2)}(\lambda) \quad (5.16a)$$

$$a^{(3)} = [s^{(2)}a^{(2)} + s^{(3)}a^{(3)} - (a^{(2)} + a^{(3)})r] \hat{w}^{(2)}(\lambda) \hat{z}^{(3)}(\lambda) \quad (5.16b)$$

where we introduced the abbreviations

$$s^{(2)} = p_{\text{st}}^{(1)} \frac{\partial \gamma(\bar{x}(p_{\text{st}}^{(2)}, p_{\text{st}}^{(3)}))}{\partial p_{\text{st}}^{(2)}}, \quad s^{(3)} = p_{\text{st}}^{(1)} \frac{\partial \gamma(\bar{x}(p_{\text{st}}^{(2)}, p_{\text{st}}^{(3)}))}{\partial p_{\text{st}}^{(3)}} \quad \text{and} \quad r = \gamma(\bar{x}_{\text{st}}) \quad (5.17)$$

We further introduced the Laplace transforms of the waiting time distributions and survival probabilities

$$\begin{aligned} \hat{w}^{(i)}(\lambda) &:= \int_0^\infty d\tau \exp(-\lambda\tau) w^{(i)}(\tau) \quad \text{and} \\ z^{(i)}(\lambda) &:= \int_0^\infty d\tau \exp(-\lambda\tau) z^{(i)}(\tau) = \frac{1 - \hat{w}^{(i)}(\lambda)}{\lambda}. \end{aligned}$$

In order that the linear equation (5.16) has a solution  $(a^{(2)}, a^{(3)}) \neq (0, 0)$  the determinant has to vanish. This requirement eventually leads to the characteristic equation

$$1 + \frac{1}{\lambda} [s^{(2)}(\hat{w}^{(2)}(\lambda) - 1) + s^{(3)}(\hat{w}^{(2)}(\lambda)w^{(3)}(\lambda) - w^{(2)}(\lambda)) + r(1 - \hat{w}^{(2)}(\lambda)\hat{w}^{(3)}(\lambda))] = 0. \quad (5.18a)$$

Sometimes it is more advantageous to express the characteristic equation in terms of the  $\hat{z}^{(i)}(\lambda)$  as

$$1 + (s^{(3)} - s^{(2)})\hat{z}^{(2)}(\lambda) + (r - s^{(3)})\hat{z}^{(23)}(\lambda) = 0. \quad (5.18b)$$

Here,  $\hat{z}^{(23)}(\lambda) = \hat{z}^{(2)}(\lambda) + \hat{z}^{(3)}(\lambda) - \lambda \hat{z}^{(2)}(\lambda) \hat{z}^{(3)}(\lambda)$  is the Laplace transform of the survival probability  $z^{(23)}(\tau)$  in both state 2 and 3 together,

$$z^{(23)}(\tau) = 1 - \int_0^\tau d\tau' (w^{(2)} \circ w^{(3)})(\tau').$$



The solutions  $\lambda \in \mathbb{C}$  of the characteristic equation (5.18) determine the local stability of the stationary solution. Depending on the chosen waiting time distributions  $w^{(2)}(\tau)$  and  $w^{(3)}(\tau)$  eq. (5.18) possesses several or even countably infinitely many complex solutions  $\lambda$  as the underlying system eqs. (5.13) may be more than two dimensional, due to the integral terms. Starting with an ensemble of uncoupled units, which is known to have exactly one stationary solution which is stable an increasing coupling may cause this unique stationary solution to become unstable, i.e. the real part of some eigenvalues  $\lambda$  passes the imaginary axis. If the imaginary part of  $\lambda$  is non vanishing, this corresponds to a Hopf bifurcation, probably leading to an oscillatory behavior of the occupation probabilities  $p^{(i)}(t)$  and thus of the systems' output  $\bar{x}(t)$ . In general, the concrete solutions of the characteristic equation (5.18) can only be obtained numerically. However in the next subsection we consider some general properties the system has to have in order to observe oscillations. Before we continue we fix some notions. We call a coupling *inhibitory*(*excitatory*) with respect to state  $k$ , if the excitation rate is lower(higher) the more units are in state  $k$ . An inhibitory coupling to state 2 thus implies  $s^{(2)} \leq 0$  while an excitatory coupling to state 3 means  $s^{(3)} \geq 0$ . For the threestate model of excitable systems, where we assume a high output of the single units in the firing state 2 and the same low output in rest state 1 and refractory state 3 the mean output  $\bar{x}(t)$  is completely specified by the number of units in state 2. Therefore, in this case the coupling is with respect to state 2. However there might be other applications of the threestate model, for which the assumption of a coupling to state 3 probably makes sense. Therefore we include this possibility in our considerations.

### 5.2.1 Conditions which do not allow for spontaneous global oscillations

In this subsection we investigate under which restrictions the globally coupled three state system does not exhibit oscillations of the mean field. The strongest statement can be made in the case of exponentially distributed waiting times in state 2 and 3 and a coupling to state 3. For this system we can completely exclude stable limit cycles, i.e. oscillating behavior will not occur whatever initial conditions we choose. If we choose an inhibitory coupling to state 2, allowing for arbitrary waiting time distributions in state 2 and 3, we can exclude a destabilization of the stable stationary solutions, thus the system will not spontaneously start to oscillate. Finally if we omit the refractory state 3, the system will not undergo a Hopf bifurcation. However for an excitatory coupling the stable stationary solution may lose stability, due to a single real eigenvalue becoming positive. If this bifurcation is subcritical, to judge about which is beyond the linear stability

analysis we perform, one cannot exclude that the resulting attractor is a limit cycle.

### Inhibitory coupling to state 2 and no coupling to state 3

We consider the situation that the coupling is inhibitory with respect to state 2 and that there is no coupling to state 3. Thus  $s^{(2)} \leq 0$  and  $s^{(3)} = 0$  and additionally  $r \geq 0$  as, by definition, the excitation rate cannot be negative. Let us assume that the resulting characteristic equation (cf. eq. (5.18b))

$$1 - s^{(2)} \operatorname{Re} \hat{z}^{(2)}(\lambda) + r \operatorname{Re} \hat{z}^{(23)}(\lambda) = 0 \quad (5.19a)$$

$$-s^{(2)} \operatorname{Im} \hat{z}^{(2)}(\lambda) + r \operatorname{Im} \hat{z}^{(23)}(\lambda) = 0. \quad (5.19b)$$

has a solution  $\lambda$  with positive real part. Then the imaginary part eq. (5.19b) has only solutions  $\lambda$  with vanishing imaginary part as the imaginary parts of  $\hat{z}^{(2)}(\lambda)$  and  $\hat{z}^{(23)}(\lambda)$  both have the same inverse sign of  $\operatorname{Im} \lambda$  and are zero if and only if  $\operatorname{Im} \lambda = 0$  (see appendix D.2). However for  $\operatorname{Im} \lambda = 0$  the real part of the characteristic equation has no solution as in this case the real part of both  $\hat{z}^{(2)}(\lambda)$  and  $\hat{z}^{(23)}(\lambda)$  is positive. Thus we can exclude solutions of the characteristic equation with positive real part, i.e. the stationary solution always remains stable.

### Exponentially distributed waiting times and no coupling to state 2

If the waiting times in state 2 and 3 are exponentially distributed,

$$w^{(2)}(\tau) = \gamma^{(2)} \exp(-\gamma^{(2)}\tau) \quad \text{and} \quad w^{(3)}(\tau) = \gamma^{(3)} \exp(-\gamma^{(3)}\tau), \quad (5.20)$$

the transitions between the states become rate processes, rendering the resulting dynamics in terms of  $p^{(1)}(t)$ ,  $p^{(2)}(t)$  and  $p^{(3)}(t)$  Markovian. With the corresponding Laplace transformed quantities

$$\hat{w}^{(2)}(\lambda) = \frac{\gamma^{(2)}}{\gamma^{(2)} + \lambda} \quad \text{and} \quad \hat{w}^{(3)}(\lambda) = \frac{\gamma^{(3)}}{\gamma^{(3)} + \lambda} \quad (5.21)$$

we obtain for the characteristic equation (5.18a)

$$\lambda^2 + \lambda(\gamma^{(2)} + \gamma^{(3)} + r - s^{(2)}) + \gamma^{(2)}(r - s^{(3)}) + \gamma^{(3)}(r - s^{(2)}) + \gamma^{(2)}\gamma^{(3)} = 0. \quad (5.22)$$

This characteristic equation can be as well obtained from the more familiar master equation

$$\begin{aligned} \frac{d}{dt} p^{(2)}(t) &= -\gamma^{(2)} p^{(2)}(t) + \gamma(\bar{x}(t)) p^{(1)}(t) \\ \frac{d}{dt} p^{(3)}(t) &= -\gamma^{(3)} p^{(3)}(t) + \gamma^{(2)} p^{(2)}(t), \quad p^{(1)}(t) = 1 - p^{(2)}(t) - p^{(3)}(t) \end{aligned} \quad (5.23)$$

which can be shown to be equivalent to eqs. (5.13) for the special waiting time distributions eq. (5.20).

Eq.(5.22) is a quadratic equation for the eigenvalue  $\lambda$ , which stems from the fact that due to the rate transitions we are dealing with an ordinary three dimensional system of differential equations for the probabilities  $p^{(1)}(t)$ ,  $p^{(2)}(t)$  and  $p^{(3)}(t)$  subjected to the algebraic normalization condition  $p^{(1)}(t) + p^{(2)}(t) + p^{(3)}(t) = 1$ . If there is no coupling to state 2, i.e.  $s^{(2)} = 0$  or likewise  $\bar{x}(t) = \bar{x}(p^{(3)}(t))$ , we can completely exclude oscillatory behavior, i.e. the existence of stable limit cycles using *Dulac's* criterion (see e.g. [48, 125]). To this end we have to consider the divergence of the flow in the two dimensional phase space spanned by  $p^{(2)}$  and  $p^{(3)}$  as defined by eqs. (5.23). It can be evaluated to

$$-(\gamma^{(2)} + \gamma^{(3)} + \gamma(\bar{x}(p^{(3)})))$$

As the rates are positive the divergence of the flow is everywhere negative, which excludes the existence of a stable limit cycle in a two dimensional phase space by *Dulac's* criterion. Note that in contrast to the previous subsection, where we only showed the local stability of a stationary solution, but could not exclude additional stable limit cycles, in this case we have shown that there are no attractors beside one or several stable fixed points.

If, however we release the restriction of a coupling only to state 3, the above argument fails as the divergence of the flow becomes

$$-(\gamma^{(2)} + \gamma^{(3)} + \gamma(p^{(2)}, p^{(3)}) - (1 - p^{(2)} - p^{(3)})\partial_1\gamma(p^{(2)}, p^{(3)}))$$

This expression cannot in general be assured to be negative in the whole phase space, due to the additional last term, which stems from the dependence of the coupling on the occupation of state 2, which we previously have excluded. However one immediately deduces that if a limit cycle should exist, the coupling to  $p^{(2)}$  has to be necessarily excitatory in some region, i.e.  $\partial_1\gamma(p^{(2)}, p^{(3)}) > 0$  for some  $(p^{(2)}, p^{(3)})$ . And indeed, the onset of global oscillations can be observed in this three state rate system with an excitatory coupling to state 2.

## Two states

Let us assume that there is no refractory state but the system directly changes from the firing state into the rest state and thus can be immediately re-excited. This corresponds to a vanishing waiting time in the refractory state, i.e.  $w^{(3)}(\tau) = \delta(\tau)$  and thus  $\hat{w}^{(3)}(\lambda) = 1$  and  $\hat{z}^{(23)}(\lambda) = \hat{z}^{(2)}(\lambda)$ . The resulting characteristic equation, separated into real and imaginary part is obtained from the general characteristic equation (5.18b) as

$$\begin{aligned} 1 + (r - s^{(2)})\text{Re } \hat{z}^{(2)}(\lambda) &= 0 \\ (r - s^{(2)})\text{Im } \hat{z}^{(2)}(\lambda) &= 0. \end{aligned}$$

Assume that there is a solution  $\lambda$  of these equations with  $\text{Re } \lambda > 0$  and  $\text{Im } \lambda \neq 0$ . Then as shown in appendix D.2  $\text{Im } \hat{z}^{(2)}(\lambda) \neq 0$  and thus from the second equation we deduce  $r-s^{(2)} = 0$ . This however contradicts the first equation, and we conclude  $\text{Re } \lambda \leq 0$  if  $\text{Im } \lambda \neq 0$ . Thus we have show that two states in our setting are not sufficient to generate oscillations via a Hopf bifurcation of the stationary solution, i.e. (at least) three states are a necessary condition for the globally coupled system to start to oscillate. This points out the relevance of a refractory period in globally coupled excitable systems, like for example neurons, in order to exhibit collective oscillations.

## 5.2.2 Application to excitable systems

Having excluded oscillatory behavior for some general settings of the three state model, we now want to analyze its behavior for a more specific case, intended to model excitable behavior. Namely we choose the waiting times in state 2 and 3 to be peaked around some mean waiting times  $\tau^{(2)}$  and  $\tau^{(3)}$ . To model this behavior we consider  $\Gamma$  distributions

$$w^{(2)}(\tau) = \left(\frac{r^{(2)}\tau}{\tau^{(2)}}\right)^{r^{(2)}} \frac{\exp(-\frac{r^{(2)}\tau}{\tau^{(2)}})}{\tau\Gamma(r^{(2)})} \quad \text{and} \quad w^{(3)}(\tau) = \left(\frac{r^{(3)}\tau}{\tau^{(3)}}\right)^{r^{(3)}} \frac{\exp(-\frac{r^{(3)}\tau}{\tau^{(3)}})}{\tau\Gamma(r^{(3)})} \quad (5.25)$$

For  $r^{(i)} = 1$  the waiting time distribution are exponentially decaying, i.e. the transitions are rate processes, rendering the dynamics Markovian. For  $r^{(i)} \rightarrow \infty$  we deal with fixed waiting times. One thus would expect  $r^{(2)}$  and  $r^{(3)}$  to increase with decreasing noise level, however we do not consider the dependence of  $r^{(2)}$  and  $r^{(3)}$  on noise strength, but assume them constant. The mean and variance of the  $\Gamma$  distributions are given by  $\tau^{(k)}$  and  $\frac{(\tau^{(k)})^2}{r^{(k)}}$ , respectively.

The output of a single unit is considered to assume a high value  $x_1$  in state 2 (firing) and a low value  $x_0$  in state 1 (rest) and 3 (refractory). The mean output of the system is therefore given by

$$\bar{x}(t) = x_0(p^{(1)}(t) + p^{(3)}(t)) + x_1p^{(2)}(t) = (x_1 - x_0)p^{(2)}(t) + x_0, \quad (5.26)$$

i.e. it solely depends on the number of units in state 2. The relation between the excitation rate and the system's mean output very much depends on the type of coupling considered. Here we assume that the mean output  $\bar{x}(t)$  modulates the effective potential barrier over which a single unit has to be excited due to noise. This leads to an Arrhenius type rate with a modulated potential barrier,

$$\gamma(\bar{x}(t)) = r_0 \exp\left(-\frac{\Delta U(\bar{x}(t))}{D}\right). \quad (5.27)$$

According to eq. (5.26) the mean output  $\bar{x}(t)$  and thus the excitation rate  $\gamma$  solely depends on  $p^{(2)}(t)$ . Therefore we consider in the following  $\gamma$  as a function of  $p^{(2)}(t)$ , somehow sloppily using the very same symbol  $\gamma$ .

In order to investigate the behavior of our system we have to examine the solutions of the characteristic equation (5.18). The Laplace transforms  $\hat{w}^{(2/3)}(\lambda)$  of the  $\Gamma$ -distributions eqs. (5.25) are given by

$$\hat{w}^{(2)}(\lambda) = \left(1 + \frac{\tau^{(2)}\lambda}{r^{(2)}}\right)^{-r^{(2)}} \quad \text{and} \quad \hat{w}^{(3)}(\lambda) = \left(1 + \frac{\tau^{(3)}\lambda}{r^{(3)}}\right)^{-r^{(3)}}.$$

Multiplying eq. (5.18a) by

$$\left(1 + \frac{\tau^{(2)}\lambda}{r^{(2)}}\right)^{r^{(2)}} \left(1 + \frac{\tau^{(3)}\lambda}{r^{(3)}}\right)^{r^{(3)}}$$

and assuming  $r^{(2)}$  and  $r^{(3)}$  to be integer numbers leads to a polynomial characteristic equation in  $\lambda$  (the terms proportional to  $1/\lambda$  cancel)

$$\left(1 + \frac{\tau^{(2)}\lambda}{r^{(2)}}\right)^{r^{(2)}} \left(1 + \frac{\tau^{(3)}\lambda}{r^{(3)}}\right)^{r^{(3)}} \left(1 - \frac{s^{(2)}}{\lambda} + \frac{r}{\lambda}\right) + \frac{s^{(2)}}{\lambda} \left(1 + \frac{\tau^{(3)}\lambda}{r^{(3)}}\right)^{r^{(3)}} - \frac{r}{\lambda} = 0. \quad (5.28)$$

Again in the Markovian case, i.e. for  $r^{(2)} = r^{(3)} = 1$  the characteristic equation (5.28) reduces to a quadratic equation in  $\lambda$

$$\tau^{(2)}\tau^{(3)}\lambda^2 + (\tau^{(2)} + \tau^{(3)} + (r - s^{(2)})\tau^{(2)}\tau^{(3)})\lambda + 1 - s^{(2)}\tau^{(2)} \quad (5.29)$$

$$+ r(\tau^{(2)} + \tau^{(3)}) = 0 \quad (5.30)$$

Contrary, if we assume fixed waiting times in state 2 and 3, which corresponds to the limit  $r^{(2)}, r^{(3)} \rightarrow \infty$  we obtain the characteristic equation

$$\lambda - s^{(2)}(1 - e^{-\lambda\tau^{(2)}}) + r(1 - e^{-\lambda(\tau^{(2)} + \tau^{(3)})}) = 0 \quad (5.31)$$

Such type of characteristic equation which are not polynomial in the eigenvalue  $\lambda$  but exponential are typical for dynamical systems with a fixed delay [109], which for example might occur in systems controlled via time delayed feedback [59] or in systems which include some time delay in the coupling [57, 132]. In our case the fixed delay is induced by the fixed waiting times in rest and refractory state, though. Such a characteristic equation has infinitely many solutions  $\lambda$  which reflects the fact that although we have only two dynamical variables  $p^{(2)}(t)$  and  $p^{(3)}(t)$  ( $p^{(1)}(t)$  is determined by the algebraic normalization condition) our system is nonetheless infinite dimensional due to the fixed delay introduced by the fixed

waiting times. The complex solutions  $\lambda$  of such exponential equations have been investigated in [8, 51]. Especially the question under which conditions the real part of all solutions is negative and thus the corresponding stationary state of the system is stable, has been considered. However these criteria are not very handy, therefore we resort to the polynomial equation, (5.28), corresponding to waiting time distribution  $w^{(k)}(\tau)$  with some finite  $r^{(k)}$ , i.e. with a non vanishing variance. In order to decide whether a general polynomial equation

$$\sum_{i=0}^n c_i \lambda^{n-i} = 0 \quad (5.32)$$

exhibit solutions with positive real part, there exists the Routh-Hurwitz criterion to evaluate the number of unstable solutions. It is a simple algebraic criterion based on the coefficients  $c_i$  of the polynomial equation, To state this criterion we introduce the quantities  $s_{k,l}$ , which are defined by first assigning the coefficients  $c_n$  of the polynomial eq. (5.32) to  $s_{1,l}$  and  $s_{2,l}$  by

$$s_{1,1}, s_{1,2}, s_{1,3}, \dots = c_0, c_2, c_4, \dots \quad \text{and} \quad s_{2,1}, s_{2,2}, s_{2,3}, \dots = c_1, c_3, c_5, \dots$$

and then iteratively defining the further coefficients  $s_{3,l}, s_{4,l}, \dots$  as

$$s_{k,l} = \frac{s_{k-1,1} s_{k-2,l+1} - s_{k-1,l+1} s_{k-2,1}}{s_{k-1,1}}. \quad (5.33)$$

Coefficients which appear on the right hand side of this equation but are not defined are set to zero. Then equation (5.32) has a solution with positive real part iff all  $s_{k,1}$ ,  $k = 0, \dots, n$  have the same sign. In addition the precise number of solutions  $\lambda$  of eq. (5.32) with positive real part is given by the number of pairs  $(s_{k,1}, s_{k+1,1})$ ,  $k = 0, \dots, n-1$  which have a different sign. This criterion is used in the following to numerically determine the bifurcation diagram. To obtain reasonable results one has to do these calculations with a high precision, which for large  $n$  exceeds machine precision. We have used the arbitrary precision arithmetic of Mathematica, which automatically keeps track of the errors which occur in evaluating eq. (5.33).

Let us first consider the influence of the parameters  $r^{(2)}$  and  $r^{(3)}$ . To this end we have numerically evaluated the number of unstable solutions of the characteristic polynomial eq. (5.28) using the Routh-Hurwitz criterion. In Fig. 5.1 the number of unstable solutions of the characteristic equation is shown as a function of the parameters

$$\gamma(p_{\text{st}}^{(2)}) = r \quad \text{and} \quad \gamma'(p_{\text{st}}^{(2)}) = \frac{s^{(2)}}{p_{\text{st}}^{(1)}} = s^{(2)}(1 + r(\tau^{(2)} + \tau^{(3)}))$$

for three different values of  $n = r^{(2)} = r^{(3)}$ , namely  $n = 1$ ,  $n = 100$  and  $n = 500$ . The mean waiting times in state 2 and 3  $\tau^{(2)} = 65$  and  $\tau^{(3)} = 220$  are chosen to correspond to the waiting times in the FHN system eqs. (3.30) as shown with the corresponding parameters in Fig. 3.2. For large stationary rates  $\gamma(p_{\text{st}}^{(2)})$ , the

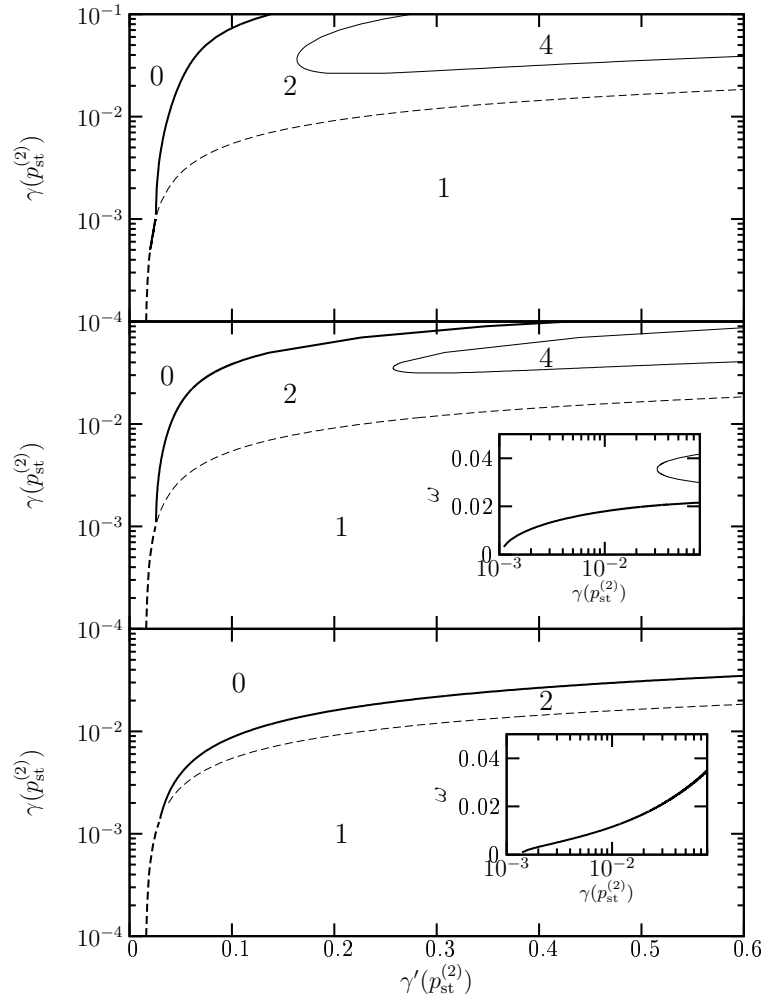


Figure 5.1: Number of unstable solutions of the characteristic equation (5.28) as a function of the stationary rate  $\gamma(p_{\text{st}}^{(2)})$  and its derivative  $\gamma'(p_{\text{st}}^{(2)})$  for different values of  $n = r^{(2)} = r^{(3)}$ . From top to bottom:  $n = 1, 100, 500$ . The solid lines correspond to Hopf bifurcations, i.e. two complex conjugate eigenvalues pass the imaginary axis. The corresponding frequency is shown in the inset. The dashed line indicates the passage through 0 of a single real solution of the characteristic equation.

stationary solution becomes unstable for increasing  $\gamma'(p_{\text{st}}^{(2)})$  via a Hopf bifurcation. This Hopf bifurcation strongly depends on  $n$ . The higher  $n$  the larger is the region

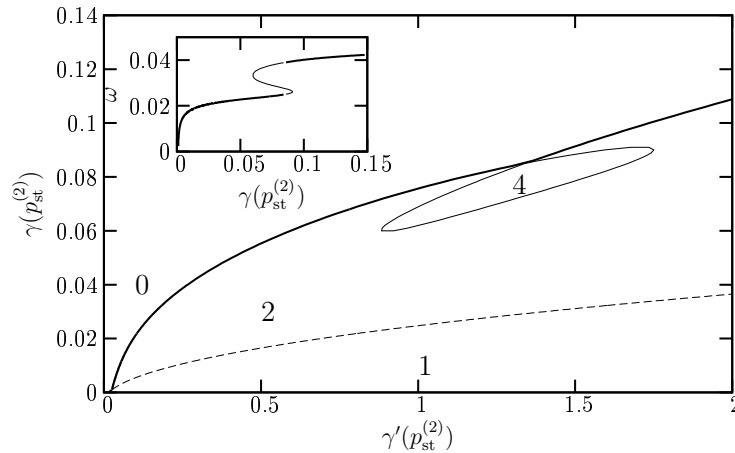


Figure 5.2: Number of unstable solutions of the characteristic equation (5.28) as a function of the stationary rate  $\gamma(p_{st}^{(2)})$  and its derivation  $\gamma'(p_{st}^{(2)})$  for  $n = 20$  as in Fig. 5.1. Due to the loop in the Hopf bifurcation line there is a jump in the frequency of the oscillations.

where the stationary solution is unstable. This implies that a sharply peaked firing and refractory time avails coherent oscillations and thus the synchronization of the units. The frequency at the Hopf bifurcation is shown in the insets of Figs. 5.1 and 5.2. Interestingly, the Hopf bifurcation line makes a loop, which leads to a jump in the frequency along the bifurcation line (see Fig. 5.2).

For small stationary excitation rates  $\gamma(p_{st}^{(2)})$  the stationary solution becomes unstable with increasing coupling  $\gamma'(p_{st}^{(2)})$  due to the passage of a single real eigenvalue through the imaginary axis. This destabilization does not depend on  $n$  and can be understood as follows: A given stationary rate  $\gamma(p_{st}^{(2)})$  uniquely defines the stationary probability stationary probability  $p_{st}^{(2)}$  according to eq. (5.14),

$$p_{st}^{(2)} = \frac{\tau^{(2)}}{\frac{1}{\gamma(p_{st}^{(2)})} + \tau^{(2)} + \tau^{(3)}}. \quad (5.34)$$

Without coupling and thus  $\gamma'(p^{(2)}) \equiv 0$  we have exactly one stable stationary solution (Fig. 5.3 top left). As we are assuming an excitatory coupling, namely an excitation rate, which increases with increasing number of units in state 2, the right hand side of eq. (5.34) increases with increasing  $p_{st}^{(2)}$ . Keeping  $\gamma(p_{st}^{(2)})$  and thus  $p_{st}^{(2)}$  fixed and increasing  $\gamma'(p_{st}^{(2)})$ , which corresponds to moving along a



horizontal line in the plots of Fig. 5.1, we eventually reach the point where

$$\frac{d}{dp_{\text{st}}^{(2)}} \frac{\tau^{(2)}}{\frac{1}{\gamma(p_{\text{st}}^{(2)})} + \tau^{(2)} + \tau^{(3)}} = 1 \quad \text{or} \quad \gamma'(p_{\text{st}}^{(2)}) = \frac{(1 + (\tau^{(2)} + \tau^{(3)})\gamma(p_{\text{st}}^{(2)}))^2}{\tau^{(2)}}. \quad (5.35)$$

At this condition not only the functions on the left and right hand side of eq. (5.34) are identical but also their tangents. This point can be reached in two ways, concerning the stationary solution  $p_{\text{st}}^{(2)}$ . Either there were already two additional solutions generated before (Fig. 5.3 middle left), one of which then merges at condition 5.35 with the considered solution (Fig. 5.3 middle right). The other possibility is shown in Fig. 5.3 top right, for which the additional condition

$$\frac{d^2}{dp_{\text{st}}^{(2)2}} \frac{\tau^{(2)}}{\frac{1}{\gamma(p_{\text{st}}^{(2)})} + \tau^{(2)} + \tau^{(3)}} = 0, \quad (5.36a)$$

has to be fulfilled. This additional condition, which can be transformed to

$$\gamma''(p_{\text{st}}^{(2)}) = \frac{2(\tau^{(2)} + \tau^{(3)})(1 + (\tau^{(2)} + \tau^{(3)})\gamma(p_{\text{st}}^{(2)}))^3}{(\tau^{(2)})^2}, \quad (5.36b)$$

defines a point (or probably some points) on the line in  $\gamma(p_{\text{st}}^{(2)}) - \gamma'(p_{\text{st}}^{(2)})$  space defined by eq. (5.35). Increasing  $\gamma'(p_{\text{st}}^{(2)})$  further we necessarily have (at least) three stationary points (Fig. 5.3 bottom). In terms of  $r$  and  $s^{(2)}$  condition (5.35) reads

$$r = \frac{s^{(2)}\tau^{(2)} - 1}{\tau^{(2)} + \tau^{(3)}}.$$

With this value for  $r$  the characteristic equation (5.28) is solved by  $\lambda = 0$ , i.e. condition (5.35) is represented by the dotted line in the stability diagrams Fig. 5.1 and 5.2 respectively. As argued above the region below this dotted line, where we have just one unstable eigenvalue, corresponds to (at least) three stationary solutions, of which the stability of the unstable middle one is considered (Fig. 5.3 bottom). In the region above this line we cannot explicitly exclude several stationary solutions (compare Fig. 5.3 middle right), we only know for sure that for vanishing coupling,  $\gamma'(p^{(2)}) \equiv 0$  only one stationary solution remains.

In the following we investigate the behavior of the coupled units for the Arrhenius type excitation rate (5.27). Assuming further for simplicity an affine relation between the effective potential barrier and the coupling parameter,

$$\Delta U(p^{(2)}(t)) = \Delta U_0(1 - \sigma p^{(2)}(t))$$

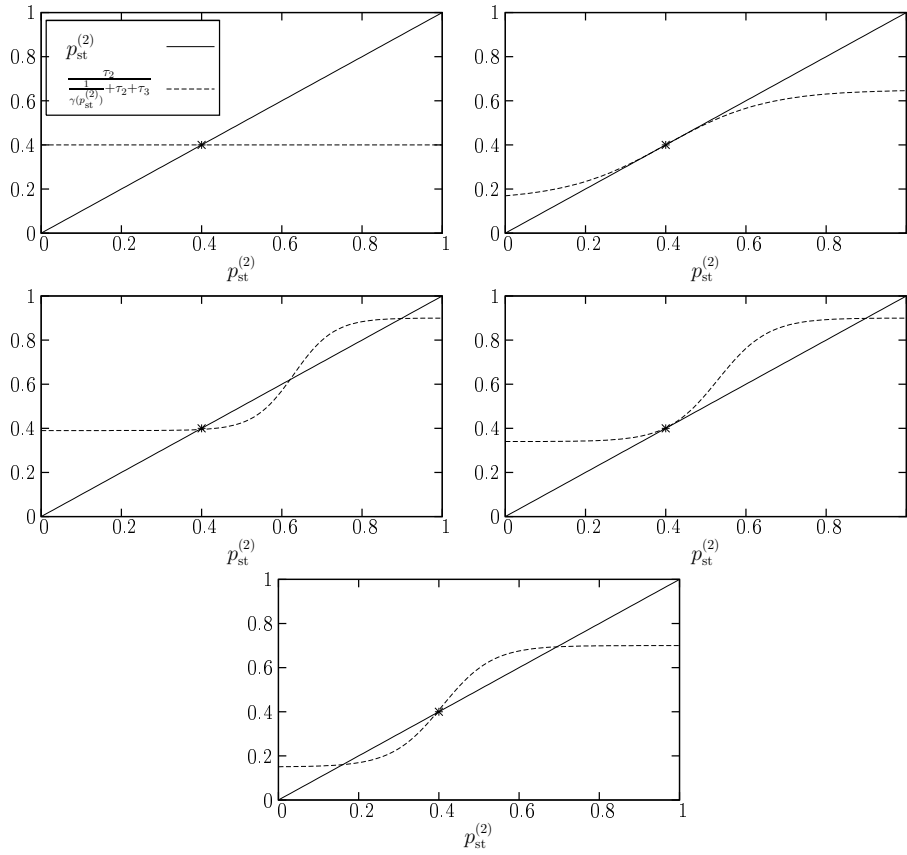


Figure 5.3: Fixing the stationary rate  $\gamma(p_{\text{st}}^{(2)})$  and thus the stationary solutions  $p_{\text{st}}^{(2)}$ , marked by a star, there are different possible scenarios for a given  $\gamma'(p_{\text{st}}^{(2)})$  as explained in the text.

the rate in dependence on  $p^{(2)}(t)$  is given by

$$\gamma(p^{(2)}(t)) = r_0 \exp\left(-\frac{\Delta U_0(1 - \sigma p^{(2)}(t))}{D}\right). \quad (5.37)$$

A given value of  $\gamma(p_{\text{st}}^{(2)})$  and  $\gamma'(p_{\text{st}}^{(2)})$  uniquely determines  $\sigma$  and  $D$  according to

$$\sigma = \frac{\gamma'(p_{\text{st}}^{(2)})T}{\gamma'(p_{\text{st}}^{(2)})\tau^{(2)} + \gamma(p_{\text{st}}^{(2)})T \log\left(\frac{r_0}{\gamma(p_{\text{st}}^{(2)})}\right)}, \quad T = \frac{1}{\gamma(p_{\text{st}}^{(2)})} + \tau^{(2)} + \tau^{(3)}$$

$$D = \frac{\sigma \Delta U_0 \gamma(p_{\text{st}}^{(2)})}{\gamma'(p_{\text{st}}^{(2)})} = \frac{T \Delta U_0 \gamma(p_{\text{st}}^{(2)})}{\gamma'(p_{\text{st}}^{(2)})\tau^{(2)} + \gamma(p_{\text{st}}^{(2)})T \log\left(\frac{r_0}{\gamma(p_{\text{st}}^{(2)})}\right)}$$

However for a given value of  $\sigma$  and  $D$  there might be more than one value of  $\gamma(p_{\text{st}}^{(2)})$ , and thus  $p_{\text{st}}^{(2)}$ , and  $\gamma'(p_{\text{st}}^{(2)})$ .

Choosing  $\Delta U = 0.0002$  and  $r_0 = 0.05$  in eq. (5.37) which is a very rough estimate from the FHN system with the parameters from Fig. 3.2 we can now transform the bifurcation diagrams in  $\gamma(p_{\text{st}}^{(2)}) - \gamma'(p_{\text{st}}^{(2)})$  space Fig. 5.1 to  $\sigma - D$  space. The result is shown for  $n = 100$  in Fig. 5.4. Increasing the coupling  $\sigma$  the system

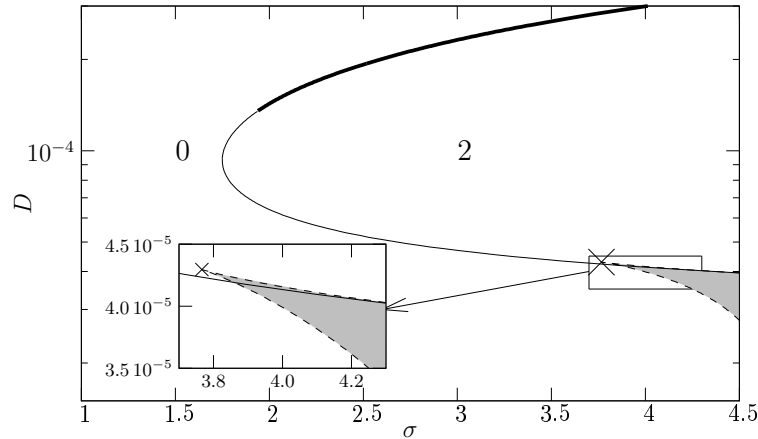


Figure 5.4: Bifurcation diagram in  $\sigma - D$  space for an Arrhenius type rate eq. (5.37) with  $\Delta U_0 = 0.0002$  and  $r_0 = 0.05$  and  $\Gamma$  distributed waiting times in state 2 and 3 with  $r^{(2)} = r^{(3)} = 100$ ,  $\tau^{(2)} = 65$  and  $\tau^{(3)} = 220$ . The thick solid line corresponds to a supercritical Hopf bifurcation, while for the thin solid line, the Hopf bifurcation is subcritical. The dashed lines correspond to the passage of a single real eigenvalue through 0. The cross indicates the point where condition (5.36) is fulfilled. The shaded region corresponds to the existence of three stationary solutions, while for parameters outside this region there is only one stationary solution.

undergoes a Hopf bifurcation if the noise level is appropriately chosen. Depending on the noise level this bifurcation is either sub- or supercritical (see appendix D.1 for a center manifold analysis in an extended phase space which we used to investigate the criticality of the Hopf bifurcation in this system). Increasing the noise strength  $D$  with a sufficiently high coupling  $\sigma$  there is a transition from non oscillating to oscillating and back to non oscillating behavior. This behavior has also been found for the FHN model in [139] using a cumulant expansion method. In Fig. 5.5 this transition from non oscillating to oscillating and back to non oscillating behavior is shown in detail and compared with numerically obtained results for the stationary solutions and oscillation amplitudes of the coupled three state units. This amplitude of the limit cycle shows a maximum at a certain noise level indicating some sort of coherence resonance, i.e. most pronounced oscillations of the mean output at some intermediate noise level. Such an effect was also reported for a globally coupled networks of Hodgkin-Huxley neuron models

in [134]. In Fig. 5.6 we have simulated a system of 100000 coupled units in the

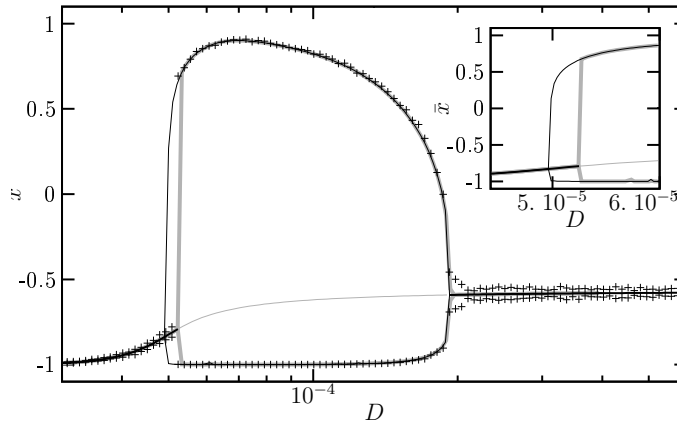


Figure 5.5: Stationary mean output  $\bar{x}$  and minimum and maximum of the mean output  $\bar{x}(t)$  in the case of oscillatory solutions. for an Arrhenius type excitation rate (5.37) with  $\sigma = 2.5$ . Other parameters as in Fig. 5.4. Symbols: simulations of a system of 10000 coupled threestate units. Thick gray line and thin black line: Solution taken from the simulation of the dynamical eqs. (5.13). Thin gray line and thick black line: Stationary solution (stable and unstable) according to eq. (5.34), the stability is obtained from the bifurcation diagram Fig. 5.4. The inset shows in more detail the hysteresis of the subcritical Hopf bifurcation.

oscillatory regime near the super critical Hopf bifurcation at  $\sigma = 3.0$  and  $D = 0.0002$ . Although the oscillation is no longer harmonic and has a high amplitude, as we are not too close to the Hopf bifurcation line, its frequency  $\omega \approx 0.0207$  agrees well with the frequency at the Hopf bifurcation, obtained from the linear stability analysis which for  $\sigma = 3.0$  and  $D = 0.00023$  is  $\omega = 0.02064$ .

### Comparison with globally coupled FHN systems

Finally we want to compare the results from the globally coupled three state system with a globally coupled FHN system. To this end consider an ensemble of  $N$  globally coupled FHN models

$$\dot{x}_i = x_i - x_i^3 - y_i + c\bar{x}(t) + \sqrt{2D}\xi_i(t) \quad (5.38a)$$

$$\dot{y}_i = \epsilon(x_i + a_0 - a_1 y_i) \quad (5.38b)$$

where  $\bar{x}(t) = \frac{1}{N} \sum_{i=1}^N x_i(t)$  is the mean output of the system and  $\xi_i(t)$  is Gaussian white noise,  $\langle \xi_i(t) \rangle = 0$  and  $\langle \xi_i(t)\xi_j(t+\tau) \rangle = \delta_{i,j}\delta(\tau)$ . Again the coupling strength  $c$  together with the noise strength  $D$  will serve as control parameters. The amplitude of the oscillations of the mean value  $\bar{x}(t)$  of the mean field as a function of noise

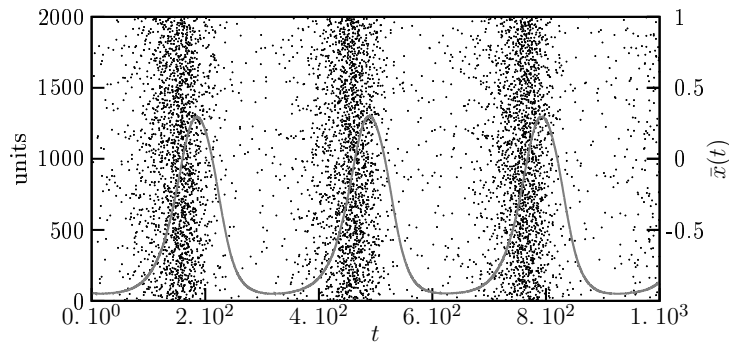


Figure 5.6: Times, at which a unit makes a transition from state 1 to state 2 (black dots) and corresponding mean output  $\bar{x}(t)$  (gray line) of a system of 100000 coupled three state units (only 2000 of which are shown) with  $\sigma = 3.0$  and  $D = 0.0002$ . Other parameters as in Fig. 5.4.

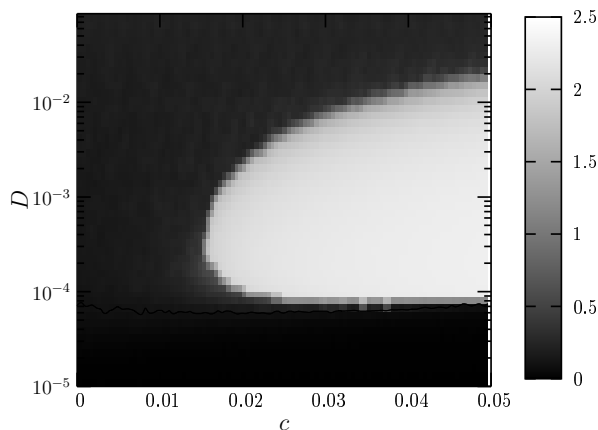


Figure 5.7: Oscillation amplitude of the mean output  $\bar{x}(t)$  of a system of 2000 globally coupled FHN systems eq. (5.38a) as a function of coupling strength  $c$  and noise strength  $D$ . Other parameters as in Fig. 3.2.

strength  $D$  and coupling strength  $c$  is shown in Fig. 5.7. We observe qualitatively the same behavior as for the three state model Fig. 5.4. Also the stationary solutions and oscillation amplitudes as a function of noise strength for a fixed value of the coupling show a good agreement between the excitable FHN system Fig. 5.8 and the three state model Fig. 5.5. Especially the type of the Hopf bifurcation, subcritical when entering the oscillatory regime with increasing noise strength and supercritical when leaving it again is well reproduced.

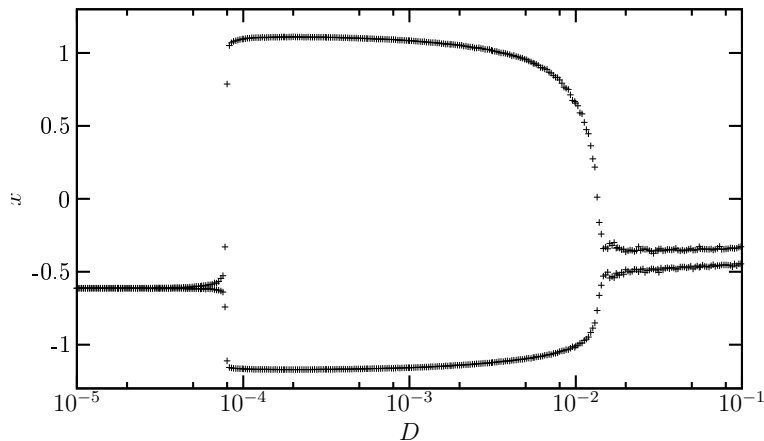


Figure 5.8: Asymptotic maximum and minimum value of the mean output  $\bar{x}(t)$  of a system of 2000 globally coupled FHN systems eq. (5.38a) as a function of noise strength  $D$  for a coupling of  $c = 0.04$ . The non vanishing oscillation amplitude at high noise levels is an effect of the finite number of units, which inevitably has a fluctuating mean output  $\bar{x}(t)$  (compare Fig. 5.5). Other parameters as in Fig. 3.2.

### 5.2.3 Delayed Coupling

If we think of the globally coupled excitable units as for example a population of neurons, connected via synapses, the output of the neurons is delayed, due to the finite propagation speed, before it is fed back into the neuron population. It is well known that a delay incorporated in the coupling may completely change the dynamics of the system, like inducing amplitude death in limit cycle oscillators [108] or oscillations in bistable systems [56]. With an appropriately chosen delay one can induce oscillatory behavior at the same time being able to suppress the oscillations, if the delay is differently adjusted [113]. Such a tuning of a system's behavior is not restricted to globally coupled units, but also single system can be controlled with a time delayed feedback [59, 115].

In our discrete state system a delayed coupling can be easily incorporated by making the excitation rate  $\gamma$  of a single unit dependent on the delayed mean output  $\bar{x}(t - \tau_D)$ , where  $\tau_D$  is the (fixed) delay time. The stationary solutions are not modified by the delay, however their stability might change. The delay leads to an additional prefactor  $\exp(-\lambda\tau_D)$  of  $s^{(2)}$  and  $s^{(3)}$  in the characteristic equation (5.18) which then reads

$$1 + \exp(-\lambda\tau_D)(s^{(3)} - s^{(2)})\hat{z}^{(2)}(\lambda) + (r - \exp(-\lambda\tau_D)s^{(3)})\hat{z}^{(23)}(\lambda) = 0. \quad (5.39)$$

Due to the additional factor  $\exp(-\lambda\tau_D)$  the arguments we used to rule out oscillatory behavior in subsection 5.2.1 fail.

To demonstrate this, let us consider the two state system, which we obtained by neglecting the refractory state 3. Its characteristic equation is given by (cf. eq. (5.24))

$$1 + (r - \exp(-\lambda\tau_D)s^{(2)})\hat{z}^{(2)}(\lambda) = 0. \quad (5.40)$$

Separating this equation into real and imaginary part, setting  $\lambda = \lambda_{\text{re}} + i\lambda_{\text{im}}$  and solving the two resulting equations for  $r$  and  $s^{(2)}$  gives

$$r = \frac{\text{Im } \hat{z}^{(2)}(\lambda) \cot(\lambda_{\text{im}} \tau_D) - \text{Re } \hat{z}^{(2)}(\lambda)}{|\hat{z}^{(2)}(\lambda)|^2} \quad (5.41a)$$

$$s^{(2)} = \frac{e^{\lambda_{\text{re}} \tau_D} \text{Im } \hat{z}^{(2)}(\lambda) \csc(\lambda_{\text{im}} \tau_D)}{|\hat{z}^{(2)}(\lambda)|^2} \quad (5.41b)$$

Let us assume that all parameters except the coupling strength and the time delay  $\tau_D$  are fixed, i.e.  $r$  as well as  $z^{(2)}(\tau)$  are fixed, however  $s^{(2)}$  can assume an arbitrary value by tuning the coupling strength. To show that there are solutions  $\lambda$  with positive real part  $\lambda_{\text{re}}$  and arbitrary imaginary part  $\lambda_{\text{im}} \neq 0$  let us also fix these two values. Then eq. (5.41a) is solved for some  $\tau_D$ , as  $\text{Im } \hat{z}^{(2)}(\lambda) \neq 0$  for  $\lambda_{\text{im}} \neq 0$  (cf. appendix D.2) and the values of  $\cot(\lambda_{\text{im}} \tau_D)$  can be tuned from  $-\infty$  to  $\infty$  by appropriately choosing the delay  $\tau_D$ . Tuning the coupling and thus  $s^{(2)}$  then solves the second equation (5.41b).

For a given  $\tau_D$  which solves eq. (5.41a), there is always a corresponding  $\tilde{\tau}_D = \tau_D + \pi/\lambda_{\text{im}}$  which likewise solves eq. (5.41a) as  $\cot(\lambda_{\text{im}} \tau_D) = \cot(\lambda_{\text{im}} \tilde{\tau}_D)$ , however this corresponding delay leads to an inverse coupling as  $\csc(\lambda_{\text{im}} \tau_D) = -\csc(\lambda_{\text{im}} \tilde{\tau}_D)$  in eq. (5.41a), i.e. if the coupling is excitatory for  $\tau_D$  it must be inhibitory for  $\tilde{\tau}_D$  and vice versa.

This little example shows that a delay is a very powerful mean to generate and control oscillations. An appropriate delay and coupling allow to excite coherent oscillations in the two state system for arbitrary waiting time distributions  $w(\tau)$  and stationary excitation rates  $r$ . Depending on the delay, either an inhibitory or an excitatory coupling generates the oscillating behavior. Even the simple globally coupled Markovian two state model introduced in section 5.1 is known to show oscillatory behavior if the coupling is delayed [56, 57].

### 5.3 An approach based on waiting time distributions

In the previous sections we considered the behavior of globally coupled discrete state models, based on a general master equation description for a single unit,

which in the limit of infinitely many globally coupled units led to a non linear mean field equation. In this section we choose a different starting point, based on waiting time distributions. Again we consider the dynamical behavior of  $N$  globally coupled discrete state units. A single unit  $i$  may be in one out of two states 1 or 2, denoted by  $\sigma_i(t)$ , each having a different output  $x^{(1)}$  or  $x^{(2)}$ . The waiting time of a single unit in state  $i$  is distributed according to  $w^{(k)}(\tau)$  and is assumed to be the same for all units. It is again the global output

$$\bar{x}(t) = \sum_{i=1}^N x^{(\sigma_i(t))} \quad (5.42)$$

which influences the dynamics of a single unit, thereby introducing a global coupling. This is done in the most general way by making the waiting time distributions  $w^{(k)}(\tau)$  functionally dependent on the system's mean output  $\bar{x}(t)$  and thus on the running time  $t$  for which we introduce the notation  $w^{(k)}[\bar{x}](\tau, t)$ . Let us consider one of the  $N$  units. Denoting  $p^{(k)}(t)$  the probability that this unit is in state  $k$  and by  $j^{(1)}(t)$  and  $j^{(2)}(t)$  the probability flux from state 1 to 2 and from state 2 to 1 respectively the resulting dynamics is then given by (cf. eqs. (4.57a) and (4.57b))

$$j^{(1)}(t) = \int_{t_0}^t dt' j^{(2)}(t') w^{(1)}[\bar{x}](t-t', t') + \delta(t-t_0) \quad (5.43a)$$

$$j^{(2)}(t) = \int_{t_0}^t dt' j^{(1)}(t') w^{(2)}[\bar{x}](t-t', t') \quad (5.43b)$$

where we assumed the initial condition that the unit has entered state 1 at time  $t_0$ . Introducing the survival probabilities

$$z^{(k)}[\bar{x}](\tau, t) = 1 - \int_0^\tau d\tau' w^{(k)}[\bar{x}](\tau', t), \quad (5.44)$$

we may relate the probabilities to the probability fluxes by

$$p^{(1)}(t) = \int_{t_0}^t dt' j^{(2)}(t') z^{(1)}[\bar{x}](t-t', t') \quad (5.45a)$$

$$p^{(2)}(t) = \int_{t_0}^t dt' j^{(1)}(t') z^{(2)}[\bar{x}](t-t', t'). \quad (5.45b)$$

The above equations for the evolution of a single unit are not closed, as the mean output  $\bar{x}(t)$  of the coupled units is not yet determined. To close the equations we make the assumption that in the limit of large  $N$  the relative number of units in



state  $k$ , is given by the probability that a single units is in the corresponding state,

$$\lim_{N \rightarrow \infty} \frac{1}{N} \sum_{i=1}^N \delta_{\sigma_i(t), k} = p^{(k)}(t). \quad (5.46)$$

As in section 5.1 and 5.2, this condition will not be proven but we just assume its validity. Then the coupling parameter  $\bar{x}(t)$  (5.42), being the average output of the coupled system can be expressed as,

$$\bar{x}(t) = x^{(1)}p^{(1)}(t) + x^{(2)}p^{(2)}(t).$$

Inserting this expression for the mean output into eqs. (5.43) and (5.45) leads to a closed non linear mean field equation, where now  $p^{(k)}(t)$  can be interpreted as the portion of units which are in state  $k$ . Due to the normalization  $p^{(1)}(t) + p^{(2)}(t) = 1$ , it is sufficient to consider the waiting time distributions and survival probabilities to be only dependent on say  $p^{(2)}(t)$ , which will be done in the following. Although the functional dependence of the waiting time distributions and survival probabilities on  $p^{(2)}$  is different from the dependence on  $\bar{x}(t) = x^{(1)}(1 - p^{(2)}(t)) + x^{(2)}p^{(2)}(t)$  we sloppily use the same notation.

To analyze the asymptotic behavior of this system we have to take the limit  $t_0 \rightarrow -\infty$  in eqs. (5.43) and (5.45) leading to

$$j^{(1)}(t) = \int_0^\infty d\tau j^{(2)}(t - \tau) w^{(1)}[p^{(2)}](\tau, t - \tau) \quad (5.47a)$$

$$j^{(2)}(t) = \int_0^\infty d\tau j^{(1)}(t - \tau) w^{(2)}[p^{(2)}](\tau, t - \tau) \quad (5.47b)$$

and

$$p^{(1)}(t) = \int_0^\infty d\tau j^{(2)}(t - \tau) z^{(1)}[p^{(2)}](\tau, t - \tau) \quad (5.48a)$$

$$p^{(2)}(t) = \int_0^\infty d\tau j^{(1)}(t - \tau) z^{(2)}[p^{(2)}](\tau, t - \tau) \quad (5.48b)$$

These equations have one or several stationary solutions  $p_{\text{st}}^{(1)}$ ,  $p_{\text{st}}^{(2)}$ ,  $j_{\text{st}}^{(1)}$  and  $j_{\text{st}}^{(2)}$ , which are implicitly given by

$$p_{\text{st}}^{(1)} = \frac{\langle \tau^{(1)} \rangle}{\langle \tau^{(1)} \rangle + \langle \tau^{(2)} \rangle} \quad \text{and} \quad p_{\text{st}}^{(2)} = \frac{\langle \tau^{(2)} \rangle}{\langle \tau^{(1)} \rangle + \langle \tau^{(2)} \rangle} \quad (5.49a)$$

and

$$j_{\text{st}}^{(1)} = j_{\text{st}}^{(2)} \equiv j_{\text{st}} = \frac{1}{\langle \tau^{(1)} \rangle + \langle \tau^{(2)} \rangle},$$

where

$$\langle \tau^{(k)} \rangle = \int_0^\infty d\tau \tau w^{(k)}[p_{\text{st}}^{(2)}](\tau)$$

is the mean waiting time in either state. As these mean waiting times depend on the occupation of state 2,  $p_{\text{st}}^{(2)}$ , eqs. (5.49) are in general nonlinear implicit equations for the stationary solutions  $p_{\text{st}}^{(1)}$  and  $p_{\text{st}}^{(2)}$ .

Due to the coupling, these stationary states may lose their stability, thus probably leading to a more complex behavior like oscillations, which will be investigated in the following.

To consider the stability of the stationary solution we introduce small perturbations

$$j^{(k)}(t) = j_{\text{st}}^{(k)} + \delta j^{(k)}(t) \quad \text{and} \quad p^{(k)}(t) = p_{\text{st}}^{(k)} + \delta p^{(k)}(t)$$

Using the Ansatz

$$\delta j^{(k)}(t) = a^{(k)} \exp(\lambda t) \quad \text{and} \quad \delta p^{(k)}(t) = b^{(k)} \exp(\lambda t)$$

the linearized equations (5.47) and (5.48) read

$$a^{(1)} = a^{(2)} \hat{w}_0^{(1)}[p_{\text{st}}^{(2)}](\lambda) + b^{(2)} j_{\text{st}}^{(2)} \hat{w}_1^{(1)}[p_{\text{st}}^{(2)}](\lambda) \quad (5.50)$$

$$a^{(2)} = a^{(1)} \hat{w}_0^{(2)}[p_{\text{st}}^{(2)}](\lambda) + b^{(1)} j_{\text{st}}^{(1)} \hat{w}_1^{(2)}[p_{\text{st}}^{(2)}](\lambda) \quad (5.51)$$

$$b^{(1)} = a^{(2)} \hat{z}_0^{(1)}[p_{\text{st}}^{(2)}](\lambda) + b^{(2)} j_{\text{st}}^{(2)} \hat{z}_1^{(1)}[p_{\text{st}}^{(2)}](\lambda) \quad (5.52)$$

$$b^{(2)} = a^{(1)} \hat{z}_0^{(2)}[p_{\text{st}}^{(2)}](\lambda) + b^{(1)} j_{\text{st}}^{(1)} \hat{z}_1^{(2)}[p_{\text{st}}^{(2)}](\lambda) \quad (5.53)$$

where

$$\hat{w}_0^{(k)}[p_{\text{st}}^{(2)}](\lambda) := \int_0^\infty d\tau e^{-\lambda\tau} w^{(k)}[p_{\text{st}}^{(2)}](\tau, 0) \quad (5.54a)$$

$$\hat{w}_1^{(k)}[p_{\text{st}}^{(2)}](\lambda) := \int_0^\infty d\tau e^{-\lambda\tau} \int dx \frac{\delta w^{(k)}[f](\tau, 0)}{\delta f(x)} \Big|_{f=p_{\text{st}}^{(2)}} e^{\lambda x} \quad (5.54b)$$

$$\hat{z}_0^{(k)}[p_{\text{st}}^{(2)}](\lambda) := \int_0^\infty d\tau e^{-\lambda\tau} z^{(k)}[p_{\text{st}}^{(2)}](\tau, 0) \quad (5.54c)$$

$$\hat{z}_1^{(k)}[p_{\text{st}}^{(2)}](\lambda) := \int_0^\infty d\tau e^{-\lambda\tau} \int dx \frac{\delta z^{(k)}[f](\tau, 0)}{\delta f(x)} \Big|_{f=p_{\text{st}}^{(2)}} e^{\lambda x} \quad (5.54d)$$

Upon using eq. (5.44) we obtain

$$\hat{z}_0^{(k)}[p_{\text{st}}^{(2)}](\lambda) = \frac{1 - \hat{w}_0^{(k)}[p_{\text{st}}^{(2)}](\lambda)}{\lambda} \quad (5.55)$$

$$\hat{z}_1^{(k)}[p_{\text{st}}^{(2)}](\lambda) = -\frac{\hat{w}_1^{(k)}[p_{\text{st}}^{(2)}](\lambda)}{\lambda} \quad (5.56)$$

For eqs. (5.50) to have a solution  $(a^{(1)}, a^{(2)}, b^{(1)}, b^{(2)}) \neq (0, 0, 0, 0)$  the determinant must vanish, which leads to the characteristic equation

$$0 = 1 - \hat{w}_0^{(1)}[p_{\text{st}}^{(2)}](\lambda)\hat{w}_0^{(2)}[p_{\text{st}}^{(2)}](\lambda) + \frac{j_{\text{st}}}{\lambda} \left[ \hat{w}_1^{(2)}[p_{\text{st}}^{(2)}](\lambda)(1 - \hat{w}_0^{(1)}[p_{\text{st}}^{(2)}](\lambda)) + \hat{w}_1^{(1)}[p_{\text{st}}^{(2)}](\lambda)(\hat{w}_0^{(2)}[p_{\text{st}}^{(2)}](\lambda) - 1) \right] \quad (5.57)$$

whose solutions  $\lambda$  determine the stability of the stationary solution(s).

### 5.3.1 Equivalence with the three state model described by a master equation

Let us compare these general results with the three state model investigated in section 5.2. To this end we associate state 2 in the general model presented here with the firing state 2 in the three state model introduced in section 5.2. The waiting time distribution  $w^{(2)}[p^{(2)}]$  is thus given by the original waiting time distribution in the firing state  $w^{(2)}(\tau)$ ,

$$w^{(2)}[p^{(2)}](\tau, t) = w^{(2)}(\tau)$$

and is independent of  $p^{(2)}$  and thus also of the running time  $t$  as the firing time in the three state model was chosen to be not affected by the global coupling. State 1 in the general model considered here corresponds to both the rest state 1 and the refractory state 3 in the three state model. The corresponding waiting time distribution  $w^{(1)}[p^{(2)}]$  is thus a convolution of both waiting time distributions, given by

$$w^{(1)}[p^{(2)}](\tau, t) = \int_0^\tau d\tau' w^{(3)}(\tau') \tilde{w}^{(1)}[p^{(2)}](\tau - \tau', t + \tau')$$

where

$$\tilde{w}^{(1)}[p^{(2)}](\tau, t) = \gamma(p^{(2)}(\tau + t)) \exp\left(-\int_t^{t+\tau} d\tau' \gamma(p^{(2)}(\tau'))\right)$$

is the waiting time distribution in the original state 1 (rest state), which is left by a rate process whose rate depends on  $p^{(2)}(t)$ . According to eqs. (5.54) these waiting time distributions immediately lead to

$$\begin{aligned} \hat{w}_0^{(1)}[p_{\text{st}}^{(2)}](\lambda) &= \frac{\gamma(p_{\text{st}}^{(2)})}{\gamma(p_{\text{st}}^{(2)}) + \lambda} \hat{w}^{(3)}(\lambda), \\ \hat{w}_0^{(2)}[p_{\text{st}}^{(2)}](\lambda) &= \hat{w}^{(2)}(\lambda) \quad \text{and} \quad \hat{w}_1^{(2)}[p_{\text{st}}^{(2)}](\lambda) = 0 \end{aligned} \quad (5.58a)$$

$\hat{w}_1^{(1)}[p_{\text{st}}^{(2)}](\lambda)$  is a little bit more complicated to calculate. One obtains

$$\hat{w}_1^{(1)}[p_{\text{st}}^{(2)}](\lambda) = \frac{\lambda \gamma'(p_{\text{st}}^{(2)})}{\gamma(p_{\text{st}}^{(2)}) (\gamma(p_{\text{st}}^{(2)}) + \lambda)}. \quad (5.58b)$$

eventually leading to the characteristic equation

$$0 = 1 - \frac{\gamma(p_{\text{st}}^{(2)}) \hat{w}^{(2)}(\lambda) \hat{w}^{(3)}(\lambda)}{\gamma(p_{\text{st}}^{(2)}) + \lambda} - \frac{j_{\text{st}} \gamma'(p_{\text{st}}^{(2)}) (1 - \hat{w}^{(2)}(\lambda))}{\gamma(p_{\text{st}}^{(2)}) (\gamma(p_{\text{st}}^{(2)}) + \lambda)}$$

or assuming  $\gamma(p_{\text{st}}^{(2)}) + \lambda \neq 0$ ,  $\gamma(p_{\text{st}}^{(2)}) \neq 0$  and  $\lambda \neq 0$

$$1 + \frac{1}{\lambda} \left[ \gamma(p_{\text{st}}^{(2)}) [1 - \hat{w}^{(2)}(\lambda) \hat{w}^{(3)}(\lambda)] + \frac{j_{\text{st}}}{\gamma(p_{\text{st}}^{(2)})} \gamma'(p_{\text{st}}^{(2)}) [\hat{w}^{(2)}(\lambda) - 1] \right] = 0$$

Noticing that

$$\frac{j_{\text{st}}}{\gamma(p_{\text{st}}^{(2)})} = \frac{1}{\langle \tau^{(1)} \rangle + \langle \tau^{(2)} \rangle}$$

is exactly the stationary probability of the rest state in the threestate model, we recover the characteristic equation (5.18a) obtained for the three state model using a different approach based on a non linear mean field master equation.

### 5.3.2 Application to the FHN system in the bistable regime

Having the general approach at hand, we may apply it to globally coupled FitzHugh-Nagumo systems in the bistable regime. To this end we choose a coupling in the  $y$  variable,

$$\begin{aligned} \dot{x}_i &= x_i - x_i^3 - y_i + \sqrt{2D} \xi_i(t) \\ \dot{y}_i &= \epsilon(x_i + a_0 - c_a \bar{x}(t) - (a_1 + c_p \bar{x}(t)) y_i) \end{aligned} \quad (5.59)$$

where the mean field is again defined as

$$\bar{x}(t) = \frac{1}{N} \sum_{i=1}^N x_i(t).$$

Depending on whether  $c_a$  is different from 0 or  $c_p$  is different from zero, the coupling either shifts the  $y$  nullcline up and down or it rotates the  $y$  nullcline. For the sake of notational convenience, to keep the number of parameters small, we consider the symmetric system  $a_0 = 0$ . In this symmetric setting the waiting time distribution

on either stable branch left or right, is given by the same coupling independent waiting time distribution  $w(\tau)$ , responsible for the motion along the branches followed by a excitation process, which is a rate process with coupling dependent rate (for details see subsection 3.3.2, Fig. 3.6). Denoting by (1) the left state (left stable branch of the cubic nullcline) and by (2) the right state the corresponding Laplace transformed waiting time distributions (5.54) of the two state model are therefore given by (compare eqs. (5.58))

$$\hat{w}_0^{(i)}[p_{\text{st}}^{(2)}](\lambda) = \frac{\gamma^{(i)}(p_{\text{st}}^{(2)})}{\gamma^{(i)}(p_{\text{st}}^{(2)}) + \lambda} \hat{w}(\lambda) \quad \text{and} \quad \hat{w}_1^{(i)}[p_{\text{st}}^{(2)}](\lambda) = \frac{\lambda \gamma^{(i)'}(p_{\text{st}}^{(2)})}{\gamma^{(i)}(p_{\text{st}}^{(2)}) (\gamma^{(i)}(p_{\text{st}}^{(2)}) + \lambda)}.$$

This symmetric system always has a symmetric stationary state  $p_{\text{st}}^{(1)} = p_{\text{st}}^{(2)} = \frac{1}{2}$ , whose stability will be investigated in the following. Due to the symmetry of the system the excitation rate from the left branch and from the right branch are equal if the system is in the symmetric state,  $\gamma^{(1)}(p_{\text{st}}^{(2)}) = \gamma^{(2)}(p_{\text{st}}^{(2)}) =: \gamma$ . However, depending on whether we choose a parametric or an additive coupling, the change of the excitation rates due to a deviation from the symmetric state is different. For the parametric coupling ( $c_a = 0$ ,  $c_p \neq 0$ ) both excitation rates increase and decrease simultaneously,  $\gamma^{(1)'}(p_{\text{st}}^{(2)}) = \gamma^{(2)'}(p_{\text{st}}^{(2)}) =: \gamma'$ , while for the additive coupling ( $c_a \neq 0$ ,  $c_p = 0$ ) one excitation rate increases and the other decreases,  $\gamma^{(1)'}(p_{\text{st}}^{(2)}) = -\gamma^{(2)'}(p_{\text{st}}^{(2)}) =: \gamma'$ , if the units are not balanced between right and left (see subsection 3.3.2, Fig. 3.6).

According to eq. (5.57) the characteristic equation for the symmetric solution of the additively driven system is given by

$$1 - \frac{\gamma^2 \hat{w}(\lambda)^2}{(\gamma + \lambda)^2} + 2j_{\text{st}} \gamma' \left[ \frac{1}{\gamma} - \frac{\hat{w}(\lambda)}{\gamma + \lambda} \right] = 0. \quad (5.60)$$

while for the parametrically driven case it simplifies to

$$1 - \frac{\gamma^2 \hat{w}(\lambda)^2}{(\gamma + \lambda)^2} = 0. \quad (5.61)$$

In this last equation (5.61) the change of the excitation rate with changing output,  $\gamma'$ , canceled. As it is this parameter which describes the coupling and it is the coupling which destabilizes the stationary solution, we can argue that the symmetric solution of the parametrically coupled system remains always stable. Besides, one can also convince oneself that eq. (5.61) really has no solution with  $\text{Re } \lambda > 0$ . To this end assume that  $\text{Re } \lambda > 0$ . Then

$$\left| \frac{\gamma^2 \hat{w}(\lambda)^2}{(\gamma + \lambda)^2} \right| < |w(\lambda)|^2 \leq 1$$

where details of the last step are shown in appendix D.2. Thus eq. (5.61) cannot have any solutions with  $\text{Re } \lambda > 0$ .

Contrary, the symmetric solution of the additively coupled system, may become unstable, leading to global oscillations. To this end we consider its characteristic equation (5.60) and assume that  $\text{Re } \lambda > 0$ . As  $\gamma > 0$  we may multiply this equation with  $\gamma(\lambda + \gamma)^2$ , obtaining that either

$$\hat{w}(\lambda) = \frac{\gamma + \lambda}{\gamma} \quad \text{or} \quad \hat{w}(\lambda) = 2j_{\text{st}} \frac{\gamma'}{\gamma} - \frac{\gamma + \lambda}{\gamma}.$$

The first equation does not have any solutions  $\lambda$  with  $\text{Re } \lambda > 0$ , as one can easily show by considering its modulus. Considering the real part of the second equation, taking in to account that  $|\text{Re } \hat{w}(\lambda)| < 1$  if  $\text{Re } \lambda > 0$  (see appendix D.2), it becomes evident that  $\gamma' > 0$  is a necessary condition for this equation to have a solution  $\lambda$  with  $\text{Re } \lambda > 0$ . Thus the symmetric solution of the additively coupled bistable system may become instable only if  $\gamma' > 0$ . According to the definition of  $\gamma'$  this means that the excitation rate from the left branch to the right branch is larger the more systems are on the right branch and vice versa.

After these principle considerations we finally want to compare the behavior of the two state model with simulations of the globally coupled bistable FHN system. To this end we fix the parameters of the FHN units eqs. (5.59) in the bistable regime with additive coupling as

$$a_0 = 0, \quad a_1 = 1.5, \quad c_p = 0 \quad \text{and} \quad \epsilon = 0.01. \quad (5.62)$$

From the numerically evaluated waiting time distributions of the FHN model we roughly estimate a mean value  $\bar{\tau} = 150$  of the sharply peaked waiting time  $w(\tau)$ . We model this sharply peaked waiting time distribution by a  $\Gamma$  distributed waiting time

$$w(\tau) = \left(\frac{r\bar{\tau}}{\tau}\right)^r \frac{\exp(-\frac{r\bar{\tau}}{\tau})}{\bar{\tau}\Gamma(r)}$$

with  $r = 100$ . We further assume an Arrhenius type excitation rate, whose effective potential barrier is modulated by the coupling,

$$\gamma(\bar{x}(t)) = r_0 \exp\left(-\frac{\Delta U_0(1 - \sigma\bar{x}(t))}{D}\right). \quad (5.63)$$

The output of a single unit is assumed to be  $-1$  in state 1 and  $1$  in state 2, leading to the mean output

$$\bar{x}(t) = -p^{(1)}(t) + p^{(2)}(t) = 2p^{(2)}(t) - 1.$$

We further choose  $r_0 = 0.22$  and  $\Delta U_0 = 0.0002$ . These values are in accordance with the numerically obtained excitation rate  $\gamma = 0.03$  for the uncoupled system at  $D = 0.0001$ . As already the assumption of an Arrhenius rate (5.63) is only an approximation, we did not more precisely determine these values, e.g. by considering different noise values and coupling strength. Additionally the qualitative agreement we obtain does not much depend on these values.

With these ingredients we evaluated the number of unstable zeros of the characteristic equation (5.60), as done for the excitable system in subsection 5.2.2, using again the Routh-Hurwitz criterion. The result is shown in the left plot of Fig. 5.9. For low noise values, i.e. low excitation rates, the stable symmetric solution loses

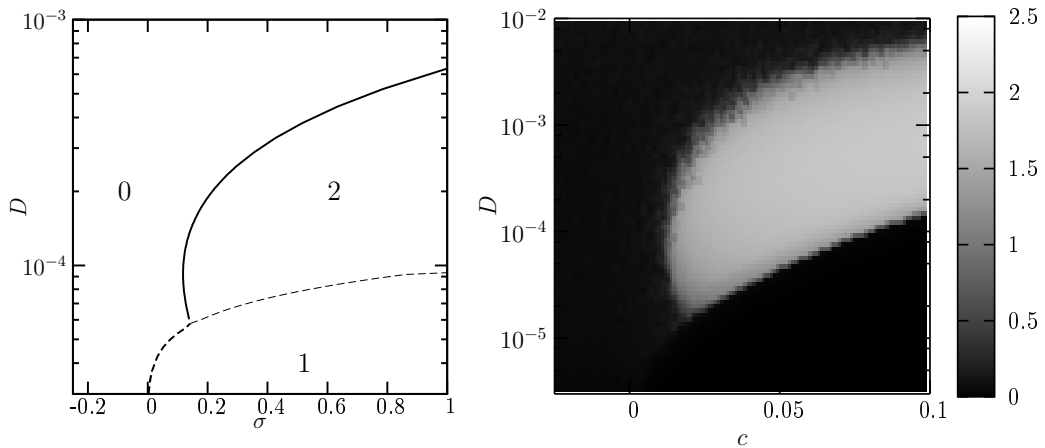


Figure 5.9: Left: Number of unstable eigenvalues of the symmetric solution in  $\sigma-D$  space for an Arrhenius type rate eq. (5.63) with  $\Delta U_0 = 0.0002$  and  $r_0 = 0.22$  and  $\Gamma$  distributed waiting times in state 2 and 3 with  $r^{(2)} = r^{(3)} = 100$ ,  $\tau^{(2)} = 65$  and  $\tau^{(3)} = 220$ . The solid line indicates a Hopf bifurcation while the dashed lines correspond to the passage of a single real eigenvalue through 0. Right: Oscillation amplitude of the mean output  $\bar{x}(t)$  of a system of 2000 globally coupled FHN systems eq. (5.59) and (5.62) with additive coupling ( $c_p = 0$ ) as a function of coupling strength  $c_a = c$  and noise strength  $D$ .

stability due to one real eigenvalue becoming positive. Due to the symmetry of the problem this corresponds to a pitchfork bifurcation, i.e. two additional stable solutions, one with an excess of units on the right branch and thus a positive output and one with an excess of units on the left branch and thus a negative output are generated. For higher noise levels and thus higher excitation rates the stable symmetric solution becomes unstable via a Hopf bifurcation leading to an oscillating mean output.

Finally, we compare these findings to simulations of the FHN system eqs. (5.59). The amplitude of the global oscillations is shown in the right plot of

Fig. 5.9. In Fig. 5.10 we have additionally plotted the minimal and maximal mean output  $\bar{x}(t)$ . Taking into account the random initial condition used in the simulation of the coupled FHN systems, the fluctuating mean values in the lower right corner of the plot reflect the fact that in this regime we have two stable solutions with either positive or negative mean output. This behavior, a single stable symmetric solution without coupling, which for low noise levels bifurcates with increasing coupling into to stable solutions with non vanishing mean, while for higher noise levels starts to oscillate, is well predicted by the discrete model.

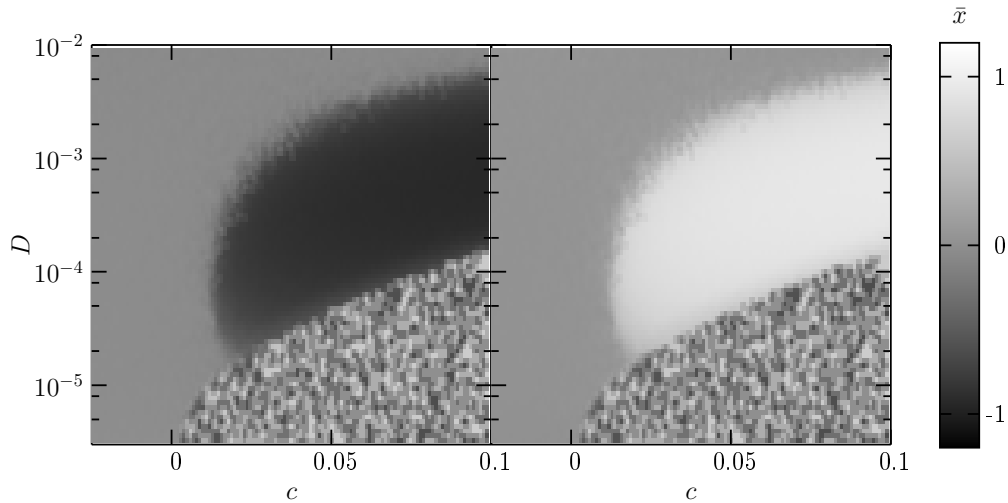


Figure 5.10: Minimum (left) and maximum(right) of the mean output  $\bar{x}(t)$  of a system of 2000 globally coupled FHN systems eq. (5.59) and (5.62) with additive coupling ( $c_p = 0$ ) as a function of coupling strength  $c_a = c$  and noise strength  $D$ .

## 5.4 Summary

We have investigated the behavior of globally coupled excitable and bistable units. The analysis was based on a discrete state model for the single units. Due to its relative simplicity the treatment could be performed analytically to some extent. Our main focus was on synchronization between the coupled units leading to collective oscillation, i.e. oscillations of the mean output. For the Markovian two state model for double well systems we have ruled out the existence of global oscillations. However, the globally coupled non Markovian three state model for excitable systems exhibits the possibility of collective oscillations. We have shown



that three states, in particular the existence of a refractory state, namely a state with low output but without the possibility of reexcitation, is necessary for the global oscillations to be generated by a Hopf bifurcation. Another necessary ingredient to destabilize the stationary solution and thus to probably observe global oscillations is an excitatory coupling, i.e. the more units are firing the higher must be the excitation rate. These prerequisites, however, are dispensable if we allow for an appropriate delay in the coupling.

A comparison with simulations of globally coupled excitable FHN systems showed good qualitative agreement. Especially the transitions with increasing noise strength from non oscillating to oscillating and again back to non oscillating behavior were well reproduced.

Finally we proposed a different concept, based on waiting time distribution. These waiting time distributions were assumed to be functionally dependent on the system's mean output, thus constituting the global coupling. Within this approach we investigated a model for globally coupled FHN systems in the symmetric bistable regime. In contrast to the bistable double well system this bistable system exhibits global oscillation if appropriately coupled. Again theory and simulations qualitatively agree.

# Chapter 6

## Conclusions and Outlook

Simplification and abstraction are common principles in understanding nature. While a good deal of abstraction is done when setting up a mathematical description of the considered system, the resulting models are often still very complicated on a mathematical level. One possibility to simplify them is a reduction to a few discrete states. We investigated the behavior of generic stochastic dynamics, namely bistable and excitable systems, within a discrete state description. While a discrete modeling has become a prevalent approach in the analysis of continuous noisy bistable dynamics, the modeling of excitable dynamics in terms of a few discrete states is less common. This gap has been closed by the introduction of a phenomenological discrete state renewal model for excitable systems consisting of rest, firing and refractory state. To exploit the anticipated advantage of this model, namely a simplified analysis compared to phase space models of stochastic excitable dynamics, we have derived general concepts to treat discrete stochastic systems. Based on these concept we obtained at least partly analytical results. The various results concerning periodically driven or coupled systems show that the behavior of the discrete model qualitatively captures the effects of excitable dynamics as archetypically modeled by the FitzHugh-Nagumo system. Thus the introduced discrete model represents an appropriate simplification of continuous excitable dynamics.

The combined influence of noise and periodic signals plays a crucial role in many fields. We investigated the response of bistable and excitable systems to weak periodic signal by means of the spectral power amplification and signal to noise ratio. To this end a method to calculate these quantities for renewal pulse sequences and delta spike sequences was presented. Applied to the three state model we obtained analytical expressions for an excitable system's SPA and SNR in terms of a few characteristic parameters. In particular optimal signal frequencies, i.e. frequencies which are maximally amplified can be determined. The SNR in the three state model was shown to be constant, i.e. independent of the fre-

quency of the signal. As it is the SNR which quantifies the quality of the signal transmission if the observation is restricted to a finite time interval, this frequency independence renders all signal frequencies equally well distinguishable from the noisy background. This finding may be interesting in all contexts where weak periodic signals are processed by excitable systems, the most prominent of which are neurons.

For larger periodic signals synchronization of the stochastic system to the signal was investigated in terms of the diffusion properties of the spike count for excitable systems and the number of hoppings between the wells for bistable systems. Again we proposed a general theory to calculate these quantities in discrete state renewal systems. The analytical results found for bistable systems show only a one to one synchronization regime. Excitable systems however exhibit different  $m : n$  synchronization regimes.

Besides its application as a model for excitable dynamics, we also considered the three state model as a simple model of a molecular motor. In this context, periodic driving as realized by a periodic modulation of the motors fuel molecule concentration, was shown to lead to a very coherent, regular motion, being probably an appropriate mean to control such motor proteins in technical applications.

Last but not least we investigated coupled excitable and bistable units. While globally coupled Markovian bistable units do not exhibit coherent oscillations, excitable systems may show synchronization. Within the three state model for excitable systems we deduced some necessary ingredient to observe a spontaneous onset of synchronous firing and thus oscillations of the mean output. Besides an excitatory coupling the existence of a refractory period plays a crucial role.

The investigated non Markovian model for excitable system is only a very idealized model. However, even within its limitations, many properties of generic excitable systems, be it synchronization of globally coupled excitable units or synchronization properties of periodically driven excitable systems, are well reproduced and explained. Moreover, the general concepts we have derived, are amenable to an application to more precise but also totally different models. Especially the abstract results on diffusion properties, provide a new tool in the analysis of periodic renewal processes.

# Bibliography

- [1] ANISHENKO, V. S. ; ASTAKHOV, V. V. ; NEIMANN, A. B. ; VADIVASOVA, T. E. ; SCHIMANSKY-GEIER, L.: *Nonlinear Dynamics of Chaotic and Stochastic Systems*. Springer Verlag, 2002
- [2] ANISHENKO, V. S. ; NEIMAN, A. B. ; SAFONOVA, M. A.: Stochastic resonance in chaotic systems. In: *Journal of Statistical Physics* 70 (1993), S. 183–196
- [3] ARIARATNAM, J. T. ; STROGATZ, S. H.: Phase Diagram for the Winfree Model of Coupled Nonlinear Oscillators. In: *Physical Review Letters* 86 (2001), 5, Nr. 19, S. 4278
- [4] ASPECT, A. ; GRANGIER, P. ; ROGER, G.: Experimental Test of Realistic Local Theories via Bell's Theorem. In: *Physical Review Letters* 47 (1981), S. 460
- [5] ASTUMIAN, R.D. ; HÄNGGI, P.: Brownian Motors. In: *Physics Today* 55 (2002), Nr. 11, S. 33
- [6] BARTUSSEK, R. ; HÄNGGI, P. ; LINDNER, B. ; SCHIMANSKY-GEIER, L.: Ratchets Driven by Harmonic and White Noise. In: *Physica D* 109 (1997), S. 17–23
- [7] BELL, J. S.: On the Einstein-Podolsky-Rosen paradox. In: *Physics* 1 (1964), S. 195
- [8] BELLMAN, R. ; COOKE, K. L.: *Mathematics in Science and Engineering*. Bd. 6: *Differential-Difference Equations*. Academic Press, 1963
- [9] BENZI, R. ; PARISI, G. ; SUTERA, A. ; VULPIANI, A.: Stochastic resonance in climatic change. In: *Tellus* 34 (1982), S. 10
- [10] BENZI, R. ; SUTERA, A. ; VULPIANI, A.: The mechanism of stochastic resonance. In: *Journal of Physics A* 14 (1981), S. 453

- 
- [11] BIER, M.: Processive Motor Protein as an Overdamped Brownian Stepper. In: *Physics Review Letters* 91 (2003), 10, S. 148104
- [12] BROECK, C. van d. ; PARRONDO, J. M. R. ; TORAL, R.: Noise-Induced Nonequilibrium Phase Transition. In: *Physical Review Letters* 73 (1994), S. 3395
- [13] BROECK, C. van d. ; PARRONDO, J. M. R. ; TORAL, R. ; KAWAI, R.: Nonequilibrium phase transitions induced by multiplicative noise. In: *Physical Review E* 55 (1997), S. 4084
- [14] CALLENBACH, L. ; HÄNGGI, P. ; LINZ, S. J. ; FREUND, J. A. ; SCHIMANSKY-GEIER, L. S.: Oscillatory systems driven by noise: Frequency and phase synchronization. In: *Physical Review E* 65 (2002), S. 051110
- [15] CASADO-PASCUAL, J. ; GÓMEZ-ORDÓÑEZ, J. ; MORILLO, M. ; HÄNGGI, P.: Two-State Theory of Nonlinear Stochastic Resonance. In: *Physical Review Letters* 91 (2003), 11, Nr. 21, S. 210601
- [16] CASADO-PASCUAL, J. ; GÓMEZ-ORDÓÑEZ, J. ; MORILLO, M. ; I. GOYCHUK, J. L. ; HÄNGGI, P.: Theory of frequency and phase synchronization in a rocked bistable stochastic system. In: *Physical Review E* 71 (2005), 1, S. 011101
- [17] CHOI, M. Y. ; KIM, H. J. ; KIM, D. ; HONG, H.: Synchronization in a system of globally coupled oscillators with time delay. In: *Physical Review E* 61 (2000), S. 371–381
- [18] CHOI, M.H. ; FOX, R.F. ; JUNG, P.: Quantifying stochastic resonance in bistable systems: Response vs. residence-time distribution functions. In: *Physical Review E* 57 (1998), 6, Nr. 6, S. 6335
- [19] C.KURRER ; SCHULTEN, K.: Noise-induced synchronous neural oscillations. In: *Physical Review E* 51 (1995), 6, Nr. 6, S. 6213
- [20] COLLINS, J. J. ; CHOW, C. C. ; CAPELA, A. C. ; IMHOFF, T. T.: Aperiodic stochastic resonance. In: *Physical Review E* 54 (1996), 11, Nr. 5, S. 5575
- [21] COLLINS, J. J. ; CHOW, C. C. ; IMHOFF, T. T.: Aperiodic stochastic resonance in excitable systems. In: *Physical Review E* 52 (1995), 10, Nr. 4, S. R3321
- [22] COX, D. R.: *Renewal Theory*. Chapman and Hall, 1962
- [23] COX, D. R. ; ISHAM, V.: *Point Processes*. Chapman and Hall, 1980

- [24] DAWSON, D. A.: Critical dynamics and fluctuations for a mean-field model of cooperative behavior. In: *Journal of Statistical Physics* 31 (1983), Nr. 1, S. 29
- [25] DESAI, R. C. ; ZWANZIG, R.: Statistical mechanics of a nonlinear stochastic model. In: *Journal of Statistical Physics* 19 (1978), Nr. 1, S. 1
- [26] EBELING, W. ; SOKOLOV, I. M.: *Statistical Thermodynamics and Stochastic Theory of Nonequilibrium Systems*. World Scientific, 2005
- [27] EINSTEIN, A.: Über die von der molekularkinetischen Theorie der Wärme geforderte Bewegung von in ruhenden Flüssigkeiten suspendierten Teilchen. In: *Annalen der Physik* 4 (1905), Nr. 17, S. 549–560
- [28] EINSTEIN, A. ; PODOLSKI, B. ; ROSEN, N.: Can Quantum-Mechanical Description of Physical Reality Be Considered Complete? In: *Physical Review A* 47 (1935), S. 777
- [29] ELPHICK, C. ; HAGBERG, A. ; MERON, E.: Dynamic front transitions and spiral-vortex nucleation. In: *Physical Review E* 51 (1995), Nr. 4, S. 3052
- [30] FARIA, T. ; AES, L. T. M.: Normal Forms for Retarded Functional difference Equations with Parameters and Applications to Hopf Bifurcation. In: *Journal of Differential Equations* 122 (1995), S. 181–200
- [31] FAUVE, S. ; HESLOT, F.: Stochastic resonance in a bistable system. In: *Physics Letters A* 97 (1983), S. 5
- [32] FISCHER, S. ; WINDSHÜGEL, B. ; HORAK, D. ; HOLMES, K.C. ; SMITH, J.C.: Structural mechanism of the recovery stroke in the Myosin molecular motor. In: *Proceedings of the National Academy of Sciences of the USA* 102 (2005), 5, S. 6873
- [33] FITZHUGH, R.: Impulses and physiological states in theoretical models of nerve membrane. In: *Biophysical Journal* 1 (1961), Nr. 6, S. 445–465
- [34] FOKKER, A. D.: Die mittlere Energie rotierender elektrischer Dipole im Strahlungsfeld. In: *Annalen der Physik* 43 (1914), S. 810
- [35] FOX, R. F.: Stochastic resonance in a double well. In: *Physical Review A* 39 (1989), 4, Nr. 8
- [36] FREUND, J. ; NEIMANN, A.B. ; L.SCHIMANSKY-GEIER: Analytic description of noise-induced phase synchronization. In: *Europhysics Letters* 50 (2000), Nr. 1, S. 8–14

- [37] FREUND, J. A. ; KIENERT, J. ; SCHIMANSKY-GEIER, L. ; BEISNER, B. ; NEIMAN, A. ; RUSSEL, D. F. ; YAKUSHEVA, T. ; MOSS, F.: Behavioral stochastic resonance: How a noisy army betrays its outpost. In: *Physical Review E* 39 (2001), S. 4148
- [38] FREUND, J. A. ; SCHIMANSKY-GEIER, L.: Diffusion in discrete ratchets. In: *Physical Review E* 60 (1999), 8, Nr. 2, S. 1304
- [39] FREUND, J. A. ; SCHIMANSKY-GEIER, L. ; BEISNER, B. ; NEIMAN, A. ; RUSSELL, D. ; YAKUSHEVA, T. ; MOSS, F.: Behavioral Stochastic Resonance: How the Noise from a Daphnia Swarm Enhances Individual Prey Capture by Juvenile Paddlefish. In: *Journal of Theoretical Biology* 214 (2002), S. 71–83
- [40] FREUND, J. A. ; SCHIMANSKY-GEIER, L. ; HÄNGGI, P.: Frequency and phase synchronization in stochastic systems. In: *Chaos* 13 (2003), Nr. 1, S. 225
- [41] GAMMAITONI, L. ; HÄNGGI, P. ; JUNG, P. ; MARCHESONI, F.: Stochastic Resonance. In: *Review of Modern Physics* 70 (1998), 1, Nr. 1, S. 223
- [42] GAMMAITONI, L. ; MARCHESONI, F. ; SANTUCCI, S.: Stochastic resonance as a *Bona Fide* resonance. In: *Physical Review Letters* 74 (1995), 2, Nr. 7, S. 1052
- [43] GANG, H. ; DITZINGER, T. ; NING, C. Z. ; HAKEN, H.: Stochastic resonance without external periodic force. In: *Physical Review Letters* 71 (1993), Nr. 6, S. 807
- [44] GARCÍA-OJALVO, J. ; SANCHO, J. M.: *Noise in Spatially Extended Systems*. New York : Springer, 1999 (Institute for Nonlinear Science)
- [45] GERSTNER, W. ; KISTLER, W.: *Spiking Neuron Models*. Cambridge University Press, 2002
- [46] GIBSON, M. A.: Efficient Exact Stochastic Simulation of Chemical Systems with Many Species and Many Channels. In: *Journal of Physical Chemistry A* 104 (2000), S. 1876–1889
- [47] GILLESPIE, D.T.: Master equations for random walks with arbitrary pausing time distributions. In: *Physics Letters* 64A (1977), 11, Nr. 1, S. 22–24
- [48] GLENDINNING, P.: *Stability, instability and chaos: an introduction to the theory of nonlinear differential equations*. Cambridge University Press, 1994 (Cambridge Texts in Applied Mathematics)

- [49] GOYCHUK, I. ; HÄNGGI, P.: Non Markovian stochastic resonance. In: *Physical Review Letters* 91 (2003), 8, Nr. 7, S. 070601
- [50] GOYCHUK, I. ; HÄNGGI, P.: Theory of non Markovian stochastic resonance. In: *Physical Review E* 69 (2004), 2, Nr. 2, S. 021104
- [51] HALE, J. K. ; LUNEL, S. M. V.: *Applied Mathematical Sciences*. Bd. 99: *Introduction to Functional Differential Equations*. Springer Verlag, 1993
- [52] HÄNGGI, P. ; BARTUSSEK, R.: Brownian Rectifiers: How to Convert Brownian Motion into Directed Transport. In: *Nonlinear Physics of Complex Systems – Current Status and Future Trends*. Springer, Berlin, Heidelberg, 1996, S. 294
- [53] HÄNGGI, P. ; TALKNER, P. ; BORKOVEC, M.: Reaction-rate theory: fifty years after Kramers. In: *Review of Modern Physics* 62 (1998), 4, Nr. 2, S. 251
- [54] HODGKIN, A. F. ; HUXLEY, A. L.: A quantitative description of membrane currents and its application to conduction and excitation in nerve. In: *Journal of Physiology* 117 (1952), S. 500–544
- [55] HUA, W. ; YOUNG, E. C. ; FLEMING, M. L. ; GELLES, J.: Coupling of kinesin steps to ATP hydrolysis. In: *Nature* 388 (1997), 7, S. 390
- [56] HUBER, D. ; TSIMRING, L. S.: Dynamics of an Ensemble of Noisy Bistable Elements with Global Time Delayed Coupling. In: *Physical Review Letters* 91 (2003), 12, Nr. 26, S. 260601
- [57] HUBER, D. ; TSIMRING, L. S.: Cooperative dynamics in a network of stochastic elements with delayed feedback. In: *Physical Review E* 71 (2005), 3, S. 036150
- [58] JOHNSON, J.: Thermal Agitation of Electricity in Conductors. In: *Physical Review* 32 (1928), S. 110
- [59] J.POMPLUN ; AMANN, A. ; SCHÖLL, E.: Mean field approximation of time-delayed feedback control of noise-induced oscillations in the Van der Pol system. In: *Europhysics Letters* 71 (2005), S. 366
- [60] JUNG, P.: Periodically driven stochastic systems. In: *Physics Reports* 234 (1993), Nr. 4&5, S. 175–295
- [61] JUNG, P.: Stochastic resonance and optimal design of threshold detectors. In: *Physica A* 207 (1995), S. 93



- [62] JUNG, P. ; BEHN, U. ; PANTAZELOU, E. ; MOSS, F.: Collective Response in globally coupled bistable systems. In: *Physical Review A* 46 (1992), 8, Nr. 4, S. R1709
- [63] KAMPEN, N.G. van: *Stochastic Processes in Physics and Chemistry*. North Holland, 1981
- [64] KENKRE, V.M. ; MONTROLL, E.W. ; SCHLESINGER, M.F.: Generalized master equations for continuous-time random walks. In: *Journal of Statistical Physics* 9 (1973), S. 45
- [65] KISS, I. Z. ; ZHAI, YA. ; HUDSON, J.: Emerging Coherence in a Population of Chemical Oscillators. In: *Science* 296 (2002), Nr. 5573, S. 1676
- [66] KOZYREFF, G. ; VLADIMIROV, A. G. ; MANDEL, Paul: Global Coupling with Time Delay in an Array of Semiconductor Lasers. In: *Physical Review Letters* 85 (2000), 10, Nr. 18, S. 3809
- [67] KRAMERS, H. A.: Brownian motion in a field of force and the diffusion model of chemical reactions. In: *Physica(Utrecht)* 7 (1940), S. 284
- [68] KURAMOTO, Y.: *Chemical Oscillations, Waves, and Turbulence*. Springer, Berlin, 1984
- [69] LANGEVIN, P.: Sur la théorie du mouvement brownien. In: *Comptes Rendu de l'Academie des sciences (Paris)* 146 (1908), S. 530–533
- [70] LAPLACE, Pierre-Simon: *Théorie analytique des probabilités*. 1812
- [71] LASOTA, A. ; MACKEY, M. C.: *Applied Mathematical Sciences*. Bd. 97: *Chaos, Noise and Fractals*. Springer Verlag, 1994
- [72] LINDNER, B.: *Nichtlineare und Stochastische Physik*. Bd. 8: *Coherence and Stochastic Resonance in Nonlinear Dynamical Systems*. Logos Verlag, Berlin, 2002
- [73] LINDNER, B. ; GARCIA-OJALVO, J. ; NEIMAN, A. ; SCHMINASKY-GEIER, L.: Effects of noise in excitable systems. In: *Physics Reports* 392 (2004), S. 321–424
- [74] LINDNER, B. ; SCHIMANSKY-GEIER, L.: Analytical approach to the stochastic FitzHugh Nagumo system and coherence resonance. In: *Physical Review E* 60 (1999), S. 7270–7276

- [75] LINDNER, B. ; SCHIMANSKY-GEIER, L.: Coherence and stochastic resonance in a two-state system. In: *Physical Review E* 61 (2000), S. 6103
- [76] LISTER, I. ; SCHMITZ, S. ; WALKER, M. ; TRINICK, J. ; BUSS, F. ; WEIGEL, C. ; KENDRICK-JONES, J.: A monomeric myosin VI with a large working stroke. In: *European Molecular Biology Organization journal* 23 (2004), S. 1729
- [77] LONGTIN, A.: Stochastic resonance in neuron models. In: *Journal of Statistical Physics* 70 (1993), S. 309
- [78] LONGTIN, A.: Effect of noise on the tuning properties of excitable systems. In: *Chaos, Solitons Fractals* 11 (2000), S. 1835
- [79] MAGNASCO, M. O.: Forced Thermal Ratchets. In: *Physical Review Letters* 71 (1993), 9, Nr. 10, S. 1477
- [80] MARINO, F. ; CATALAN, G. ; SANCHEZ, R. ; BALLE, S. ; PIRO, O.: Thermo-optical "Canard Orbits" and excitable limit cycles. In: *Physical Review Letters* 92 (2004), Nr. 7, S. 073901
- [81] MARTINEZ, K. ; LIN, A. L. ; KHARRAZIAN, R. ; SAILER, X. ; SWINNEY, H. L.: Resonance in Periodically Inhibited Reaction-Diffusion Systems. In: *Physica D* 168 (2002), S. 1–9
- [82] MCNAMARA, B. ; R. ROY, K. W.: Observation of Stochastic Resonance in a Ring Laser. In: *Physical Review Letters* 60 (1988), S. 2626
- [83] MCNAMARA, B. ; WIESENFELD, K.: Theory of stochastic resonance. In: *Physical Review A* 39 (1989), 5, Nr. 9, S. 4854–4869
- [84] MELNIKOV, V. I.: Schmitt trigger: A solvable model of stochastic resonance. In: *Physical Review E* 48 (1993), Nr. 4, S. 2481
- [85] MIKHAILOV, A. S.: *Foundations of Synergetics I*. Springer Verlag, Berlin–Heidelberg–New York, 1990 (Springer Series in Synergetics)
- [86] MIKHAILOV, A. S. ; CALENBUHR, V.: *From Cells to Societies, Models of Complex Coherent Action*. Springer Verlag, Berlin–Heidelberg–New York, 1990 (Springer Series in Synergetics)
- [87] NAGUMO, J. ; ARIMOTO, S. ; YOSHIZAWA, S.: An active pulse transmission line simulating nerve axon. In: *Proc. IRE* 50 (1962), Nr. 6, S. 2061

- [88] NAUNDORF, B. ; PRAGER, T. ; SCHIMANSKY-GEIER, L.: A novel approach to synchronization in coupled excitable systems. In: *arXiv:cond-mat/0211011* (2002)
- [89] NÉDA, Z. ; NIKITIN, A. ; VICSEK, T.: Synchronization of two-mode stochastic oscillators: a new model for rhythmic applause and much more. In: *Physica A* 321 (2003), S. 238–247
- [90] NEIMAN, A. ; SAPARIN, P. I. ; STONE, L.: Coherence resonance at noisy precursors of bifurcations in nonlinear dynamical systems. In: *Physical Review E* 56 (1997), S. 270
- [91] NICOLIS, C.: Stochastic aspects of climatic transitions– Response to a periodic forcing. In: *Tellus* 34 (1982), S. 1
- [92] NISHIYAMA, M. ; HIGUCHI, H. ; YANAGIDA, T.: Chemomechanical coupling of the forward and backward steps of single kinesin molecules. In: *Nature Cell Biology* 4 (2002), S. 790
- [93] NYQUIST, H.: Thermal Agitation of Electric Charge in Conductors. In: *Physical Review* 32 (1928), S. 110
- [94] ÖKTEN, Z. ; CHURCHMAN, L. S. ; ROCK, R. S. ; SPUDICH, J. A.: Myosin VI walks hand-over-hand along actin. In: *Nature Structural and molecular biology* 11 (2004), S. 884
- [95] PANTALEONE, J.: Stability of incoherence in an isotropic gas of oscillating neutrinos. In: *Physical Review D* (1998)
- [96] PARK, K. ; LAI, Y.-C.: Characterization of stochastic resonance. In: *Europhysics Letters* 70 (2005), S. 432–438
- [97] PARK, S. H. ; KIM, S.: Noise-induced phase transitions in globally coupled active rotators. In: *Physical Review E* 53 (1996), 4, Nr. 4, S. 3425
- [98] PARMANANDA, P. ; MENA, C. H. ; BAIER, G.: Resonant forcing of a silent Hodgkin-Huxley neuron. In: *Physical Review E* 66 (2002), 10, S. 047202
- [99] PARRONDO, J.M.R. ; CISNEROS, B.J. de: Energetics of Brownian Motors: A Review. In: *Applied Physics A* 75 (2002), S. 179
- [100] PIKOVSKY, A. ; KURTHS, J.: Coherence resonance in noise-driven excitable systems. In: *Physical Review Letters* 78 (1997), Nr. 3/4, S. 775

- [101] PLANCK, M.: Über einen Satz der Statistischen Dynamik und seine Erweiterung in der Quantentheorie. In: *Sitzungsber. Preuß. Akad. Wiss.* 324 (1917)
- [102] PLESSER, H.E. ; GEISEL, T.: Markov analysis of stochastic resonance in a periodically driven integrate and fire neuron. In: *Physical Review E* 59 (1999), 6, Nr. 6, S. 7008
- [103] PRAGER, T. ; NAUNDORF, B. ; SCHIMANSKY-GEIER, L.: Coupled three-state oscillators. In: *Physica A* 325 (2003), S. 176–185
- [104] PRAGER, T. ; SCHIMANSKY-GEIER, L.: Stochastic resonance in a non Markovian discrete state model for excitable systems. In: *Physical Review Letters* 91 (2003), 12, Nr. 23, S. 230601
- [105] PRAGER, T. ; SCHIMANSKY-GEIER, L.: Phase velocity and phase diffusion in periodically driven discrete-state systems. In: *Physical Review E* 71 (2005), 3, Nr. 3, S. 031112
- [106] PRAGER, T. ; SCHIMANSKY-GEIER, L.: Phase velocity and phase diffusion in periodically driven renewal processes. In: *accepted by Journal of Statistical Physics* (2006)
- [107] PRAGER, T. ; SCHIMANSKY-GEIER, L. ; SOKOLOV, I. M.: Periodic driving controls random motion of Brownian steppers. In: *Journal of Physics Condensed Matter* 17 (2005), S. S3661–S3672
- [108] REDDY, D. V. R. ; SEN, A. ; JOHNSTON, G. L.: Time Delay Induced Death in Coupled Limit Cycle Oscillators. In: *Physical Review Letters* 80 (1998), S. 5109
- [109] REDMOND, B.F. ; LEBLANC, V.G. ; LONGTIN, A.: Bifurcation analysis of a class of first-order nonlinear delay-differential equations with reflectional symmetry. In: *Physica D* 166 (2002), S. 131–146
- [110] REIMANN, P.: Brownian motors: noisy transport far from equilibrium. In: *Physics Reports* 361 (2002), 4, S. 57–265
- [111] RIEKE, F. ; WARLAND, D. ; STEVENICK, R. de R. v. ; BIALEK, W.: *Spikes: Exploring the neural code*. Cambridge University press, 1996
- [112] RISKEN, H.: *The Fokker-Planck Equation*. Springer Verlag, 1984

- [113] ROSENBLUM, M. G. ; PIKOVSKY, A. S.: Controlling Synchronization in an Ensemble of Globally Coupled Oscillators. In: *Physical Review Letters* 92 (2004), S. 114102
- [114] RUSSELL, D. F. ; WILKENS, L. A. ; MOSS, F.: Use of behavioral stochastic resonance by paddlefish for feeding. In: *Nature* 402 (1999), S. 291–294
- [115] SCHÖLL, E. ; BALANOV, A. ; JANSON, N. B. ; NEIMAN, A.: Controlling stochastic oscillations close to a Hopf bifurcation by time-delayed feedback. In: *Stochastic Dynamics* 5 (2005), S. 281
- [116] SHINO, M.: Dynamical behavior of stochastic systems of infinitely many coupled nonlinear oscillators exhibiting phase transitions of mean-field type: H theorem on asymptotic approach to equilibrium and critical slowing down of order parameter fluctuations. In: *Physical Review A* 36 (1987), Nr. 5, S. 2393
- [117] SHIMOKAWA, T. ; PAKDAMAN, K. ; TAKAHATA, T. ; TANABE, S. ; SATO, S.: A first-passage-time analysis of the periodically forced noisy leaky integrate-and-fire model. In: *Biological Cybernetics* 83 (2000), 3, S. 327–340
- [118] SHINOMOTO, S. ; KURAMOTO, Y.: Phase transitions in active rotator systems. In: *Progress in Theoretical Physics* 75 (1986), S. 1105–1110
- [119] SIEWERT, U. ; SCHIMANSKY-GEIER, L.: Analytical study of coupled two-state stochastic resonators. In: *Physical Review E* 58 (1998), Nr. 3, S. 2843
- [120] SOKOLOV, I. M.: A perturbation approach to transport in discrete ratchet systems. In: *Journal of Physics A* 32 (1999), S. 2541–2550
- [121] SOKOLOV, I. M. ; BLUMEN, A.: Thermodynamical and mechanical efficiency of a ratchet pump. In: *Chemical Physics* 235 (1998), S. 39–45
- [122] STEIN, R. B.: Some models of neuronal variability. In: *Biophysical Journal* 7 (1967), S. 37–68
- [123] STOCKS, N. G. ; STEIN, N. D. ; MCCLINTOCK, P.V. E.: Stochastic resonance in monostable systems. In: *Journal of Physics A* 26 (1993), S. L385–L390
- [124] STRATONOVICH, R.L.: *Topics in the Theory of Random Noise*. Gordon and Breach, 1969

- [125] STROGATZ, S. H.: *Nonlinear Dynamics and Chaos*. Perseus Publishing, Cambridge (Massachusetts), 1994 (Studies in Nonlinearity)
- [126] STROGATZ, S. H.: From Kuramoto to Crawford: exploring the onset of synchronization in populations of coupled oscillators. In: *Physica D* 143 (2000), S. 1
- [127] TALKNER, P. ; MACHURA, L. ; SCHINDLER, M. ; HÄNGGI, P.: Statistics of transition times, phase diffusion and synchronization in periodically driven bistable systems. In: *New Journal of Physics* 7 (2005), S. 14
- [128] TANABE, S. ; SHIMOKAWA, T. ; SATO, S. ; PAKDAMAN, K.: Response of coupled noisy excitable systems to weak stimulations. In: *Physical Review E* 60 (1999), 8, Nr. 2, S. 2182
- [129] TASS, P. A.: Desynchronizing double-pulse phase resetting and application to deep brain stimulation. In: *Biological Cybernetics* 85 (2001), S. 343–354
- [130] T.HARMS ; LIPOWSKY, R.: Driven ratchets with disordered tracks. In: *Physical Review Letters* 79 (1997), 10, Nr. 15, S. 2895
- [131] TIMMERMANN, L. ; GROSS, J. ; DIRKS, M. ; VOLKMANN, J. ; FREUND, H.-J. ; SCHNITZLER, A.: The cerebral oscillatory network of Parkinsonian resting tremor. In: *Brain* 126 (2002), Nr. 1, S. 199–212
- [132] TSIMRING, L.S. ; PIKOVSKY, A. S.: Noise-induced dynamics in bistable systems with delay. In: *Physical Review Letters* 87 (2001), 12, Nr. 25, S. 250602
- [133] VISSCHER, K. ; SCHNITZER, M. J. ; BLOCK, A. M.: Single Kinesin molecules studies with a molecular force clamp. In: *Nature* 400 (1999), 7, S. 184
- [134] WANG, Y. ; CHIK, S. T. W. ; WANG, Z. D.: Coherence resonance and noise-induced synchronization in globally coupled Hodgkin-Huxley neurons. In: *Physical Review E* 61 (2000), 1, Nr. 1, S. 740
- [135] WELSH, J. P. ; AHN, E. S. ; PLACANTONAKIS, D. G.: Is autism due to brain desynchronization? In: *International Journal of Developmental Neuroscience* 23 (2005), S. 253–263
- [136] WIESENFELD, K. ; COLET, P. ; STROGATZ, S. H.: Frequency locking in Josephson arrays: Connection with the Kuramoto model. In: *Physical Review E* 57 (1998), 2, Nr. 2, S. 1563

- 
- [137] WIESENFELD, K. ; PIERSON, D. ; PANTAZELOU, E ; DAMES, C. ; MOSS, F.: Stochastic resonance on a circle. In: *Physical Review Letters* 72 (1994), 4, Nr. 14, S. 2125
- [138] WINFREE, A. T.: Biological rhythms and the behavior of populations of coupled oscillators. In: *Journal of Theoretical Biology* 16 (1967), S. 15–42
- [139] ZAKS, M. ; SAILER, X. ; SCHIMANSKY-GEIER, L. ; NEIMAN, A.: Noise induced complexity: From subthreshold oscillations to spiking in coupled excitable systems. In: *Chaos* 15 (2005), S. 026117
- [140] ZAKS, M. A. ; NEIMAN, A. B. ; FEISTEL, S. ; SCHIMANSKY-GEIER, L.: Noise-controlled oscillations and their bifurcations in coupled phase oscillators. In: *Physical Review E* 68 (2003), S. 066206
- [141] ZHOU, T. ; MOSS, F. ; P.JUNG: Escape-time distributions of a periodically modulated bistable system. In: *Physical Review A* 42 (1990), 9, Nr. 6, S. 3161

# Appendix A

## Detailed calculations for chapter 2

### A.1 Equivalence between the semi Markovian master equation and the three state model master equation

Consider a three state system with transitions  $1 \rightarrow 2 \rightarrow 3 \rightarrow 1$ . The waiting time distributions in state  $i$  is denoted by  $w^{(i)}(\tau)$ . The corresponding semi Markovian master equation then reads (compare eqs. (2.14))

$$\frac{d}{dt}p^{(i)}(t) = \int_0^t d\tau \phi^{(j)}(t-\tau)p^{(j)}(\tau) - \int_0^t d\tau \phi^{(i)}(t-\tau)p^{(i)}(\tau), \quad (\text{A.1})$$

$(i, j) = (1, 3), (2, 1), (3, 2)$

where the memory kernels  $\phi^{(i)}(\tau)$  are defined in terms of their Laplace transforms as

$$\hat{\phi}^{(i)}(u) = \frac{u\hat{w}^{(i)}(u)}{1 - \hat{w}^{(i)}(u)}. \quad (\text{A.2})$$

For the three state model of excitable systems the transition from 1 to 2 is a rate process with constant rate  $\gamma$ . The waiting time distribution in state 1 is therefore  $w^{(1)}(\tau) = \gamma e^{-\gamma\tau}$  and its Laplace transform  $\hat{w}^{(1)}(u) = \gamma/(u + \gamma)$ . In this case the convolution kernel  $\phi^{(1)}(\tau)$  can be explicitly calculated as  $\phi^{(1)}(\tau) = \gamma\delta(\tau)$ . Laplace transforming eqs. (A.1), assuming as initial condition  $p^{(1)}(0) = 1$  we arrive at

$$\begin{aligned} u\hat{p}^{(1)}(u) - 1 &= -\gamma\hat{p}^{(1)}(u) + \hat{p}^{(3)}(u)\hat{\phi}^{(3)}(u) \\ u\hat{p}^{(2)}(u) &= \gamma\hat{p}^{(1)}(u) - \hat{p}^{(2)}(u)\hat{\phi}^{(2)}(u) \\ u\hat{p}^{(3)}(u) &= \hat{p}^{(2)}(u)\hat{\phi}^{(2)}(u) - \hat{p}^{(3)}(u)\hat{\phi}^{(3)}(u). \end{aligned}$$



Using the normalization condition which translates into  $\hat{p}^{(1)}(u) + \hat{p}^{(2)}(u) + \hat{p}^{(3)}(u) = 1/u$  and the definition (A.2) of  $\hat{\phi}^{(2/3)}(u)$  we eventually arrive after some algebraic manipulations at

$$\begin{aligned} u\hat{p}^{(1)}(u) - 1 &= -\gamma\hat{p}^{(1)}(u) + \gamma\hat{p}^{(1)}(u)\hat{w}^{(2)}(u)\hat{w}^{(3)}(u) \\ u\hat{p}^{(2)}(u) &= \gamma\hat{p}^{(1)}(u) - \gamma\hat{p}^{(1)}(u)\hat{w}^{(2)}(u) \\ u\hat{p}^{(3)}(u) &= \gamma\hat{p}^{(1)}(u)\hat{w}^{(2)}(u) - \gamma\hat{p}^{(1)}(u)\hat{w}^{(2)}(u)\hat{w}^{(3)}(u) \end{aligned}$$

and finally using the inverse Laplace transform eqs. (2.15) are recovered.

## A.2 Spectral power density of renewal Processes

In this appendix we present a derivation of the spectral power density of a stationary renewal delta spiketrain  $\chi(t)$  eq. (2.20) and a renewal pulse sequence  $\eta(t)$  eq. (2.19). These expressions were first derived by Stratonovich [124].

### A.2.1 The spectral power density of renewal delta spike trains

A renewal delta spike train  $\chi(t)$  consists of delta spikes located at times  $t_i$ ,

$$\chi(t) = \sum_i \delta(t - t_i). \quad (\text{A.3})$$

The interval between two subsequent spikes is distributed according to a waiting time distribution  $w(\tau)$ . Due to the renewal property these intervals are uncorrelated. In order to calculate the spectral power density as defined by eqs. (2.21) we have to insert the renewal delta sequence  $\chi(t)$  into eq. (2.21b) leading to

$$\langle |c_{\omega_n, T}|^2 \rangle = \frac{1}{T^2} \left\langle \sum_{j,k}^{0 < t_j, t_k < T} \exp(-i\omega_n(t_j - t_k)) \right\rangle, \quad \omega_n = \frac{2\pi n}{T}.$$

There are two random components in the above averaging, namely the number  $N_T$  of events in the interval  $(0, T)$ , which determines the number of terms in the summation and the actual spiking times  $t_i$ . Therefore it is not possible to interchange the mean and the summation. However in the limit  $T \rightarrow \infty$  which we are concerned with, the mean and variance of  $N_T$  grow linearly with  $T$  and therefore the variance of  $N_T/T$  will tend to zero while  $N_T/T$  converges to the mean waiting time  $\langle \tau \rangle = \int_0^\infty d\tau \tau w(\tau)$ . Then in this limit  $T \rightarrow \infty$ , which is assumed in the following

$$\langle |c_{\omega_n, T}|^2 \rangle = \frac{1}{T^2} \sum_{j,k=1}^{\langle N_T \rangle} \langle \exp(-i\omega_n(t_j - t_k)) \rangle \quad (\text{A.4})$$

where  $\langle N_T \rangle = T/\langle \tau \rangle$  is the mean number of events in the interval  $(0, T)$ . Introducing the characteristic function of the waiting time distribution

$$\hat{w}(\omega) := \int_0^\infty d\tau e^{-i\omega\tau} w(\tau) = \langle \exp(-i\omega(t_{i+1} - t_i)) \rangle$$

the convolution theorems for Fourier transforms directly lead to

$$(\hat{w}(\omega))^j := \int_0^\infty d\tau e^{-i\omega\tau} w^{\circ j}(\tau) = \langle \exp(-i\omega(t_{i+j} - t_i)) \rangle \quad (\text{A.5})$$

where

$$w^{\circ j}(\tau) = (w^{\circ j-1} \circ w)(\tau) = \int_0^\tau d\tau' w^{\circ j-1}(\tau') w(\tau - \tau')$$

is the  $j$ -fold convolution of the waiting time density  $w(\tau)$ . Inserting eq. (A.5) into (A.4) and splitting the double sum into the three parts  $j = k, j < k$  and  $j > k$  leads to

$$\langle |c_{\omega_n, T}|^2 \rangle = \frac{1}{T^2} \left[ \langle N_T \rangle + \sum_{j=2}^{\langle N_T \rangle} \sum_{k=1}^{j-1} \left( \hat{w}^{j-k}(\omega_n) + (\hat{w}^{j-k}(\omega_n))^* \right) \right] \quad (\text{A.6})$$

In evaluating the double sum we have to distinguish two cases namely  $\omega_n = 0$  and  $\omega_n \neq 0$ . For  $\omega_n = 0$  the normalization condition of  $w(\tau)$  leads to  $\hat{w}(0) = 1$  and thus

$$\langle |c_{0, T}|^2 \rangle = \frac{\langle N_T \rangle^2}{T^2} = \frac{1}{\langle \tau \rangle^2} \quad (\text{A.7})$$

For  $\omega_n \neq 0$  it can be shown that in general  $|\hat{w}(\omega_n)| < 1$ <sup>1</sup>. Thus the geometric sums in eq. (A.6) converge and one ends up with

$$\langle |c_{\omega_n, T}|^2 \rangle = \frac{1}{T^2} \left[ \langle N_T \rangle + \left( \langle N_T \rangle \frac{\hat{w}(\omega_n)}{1 - \hat{w}(\omega_n)} - \frac{\hat{w}(\omega_n)(1 - \hat{w}^{\langle N_T \rangle + 1}(\omega_n))}{(1 - \hat{w}^2(\omega_n))} + c.c. \right) \right] \quad (\text{A.8})$$

In the limit  $T \rightarrow \infty$  and therefore  $\langle N_T \rangle \rightarrow \infty$  the coefficients eq. (A.8) vanish, however the density of the discrete frequencies  $\omega_n$  which have a distance of  $2\pi/T$

<sup>1</sup>For a lattice distribution with period  $\mathcal{T}$ , i.e.  $w(\tau) = \sum_{n=0}^{\infty} w_n \delta(\tau - n\mathcal{T})$  this is not true as  $|\hat{w}(\frac{2\pi}{T})| = 1$ . Such a distribution leads to additional deltaspikes in the spectral power density at  $\omega = \frac{2\pi}{T}$ .

increases at the same time thus leading to a finite value of the spectral power density according to eq. (2.21c),

$$\begin{aligned} S_\chi(\omega) &= \lim_{\epsilon \rightarrow 0} \frac{1}{\epsilon} \int_{\omega - \frac{\epsilon}{2}}^{\omega + \frac{\epsilon}{2}} d\omega' S_\chi(\omega') = 2\pi \lim_{T \rightarrow \infty} \frac{T}{2\pi} \langle |c_{\omega, T}|^2 \rangle \\ &= \lim_{T \rightarrow \infty} \frac{\langle N_T \rangle}{T} \left[ 1 + \frac{\hat{w}(\omega)}{1 - \hat{w}(\omega)} + \frac{\hat{w}^*(\omega)}{1 - \hat{w}^*(\omega)} \right] = \frac{1}{\langle \tau \rangle} \frac{1 - |\hat{w}(\omega)|^2}{|1 - \hat{w}(\omega)|^2}, \quad \omega \neq 0. \end{aligned}$$

In the second step we have used the fact, that in a frequency interval of length  $\epsilon$  there are  $\epsilon T / (2\pi)$  discrete coefficients. We further assumed continuity of the spectral power density at  $\omega$ . This is not the case at  $\omega = 0$ . The non vanishing coefficient for  $\omega_n = 0$  leads to a delta peak in the spectral power density at  $\omega = 0$ . Using again the definition of the spectral power density (2.21c) the weight  $g_0$  of this delta peak can be evaluated to

$$g_0 = \lim_{\epsilon \rightarrow 0} \int_{-\epsilon}^{\epsilon} d\omega' S_\chi(\omega') = 2\pi \lim_{T \rightarrow \infty} \langle |c_{0, T}|^2 \rangle = \frac{2\pi}{\langle \tau \rangle^2} \quad (\text{A.9})$$

Taken together the spectral power density reads

$$S_\chi(\omega) = \frac{2\pi}{\langle \tau \rangle^2} \delta(\omega) + \frac{1}{\langle \tau \rangle} \frac{1 - |\hat{w}(\omega)|^2}{|1 - \hat{w}(\omega)|^2}. \quad (\text{A.10})$$

### A.2.2 The spectral power density of renewal pulse sequence

In the same manner as in the previous section we will derive a formula for the rectangular renewal spike sequence

$$\eta(t) = \begin{cases} a & \text{if } t_i^{(0)} < t \leq t_i^{(1)} \\ b & \text{if } t_i^{(1)} < t \leq t_{i+1}^{(0)} \end{cases} \quad (\text{A.11})$$

where the intervals  $t_i^{(1)} - t_i^{(0)}$  are taken from a waiting time distribution  $w^{(0)}(\tau)$  while the  $t_{i+1}^{(0)} - t_i^{(1)}$  are taken from  $w^{(1)}(\tau)$ . Let us first consider the case  $a = 1$  and  $b = 0$ . Inserting this process into eq. (2.21b) to evaluate  $\langle |c_{\omega_n, T}|^2 \rangle$  we have again to distinguish the two cases  $\omega_n = 0$  and  $\omega_n \neq 0$ . For  $\omega_n \neq 0$  one obtains in the limit  $T \rightarrow \infty$

$$\langle |c_{\omega_n, T}|^2 \rangle = \frac{1}{\omega_n^2 T^2} \sum_{j, k=1}^{\langle N_T \rangle} \langle (e^{-i\omega_n t_j^{(1)}} - e^{-i\omega_n t_j^{(0)}}) (e^{i\omega_n t_k^{(1)}} - e^{i\omega_n t_k^{(0)}}) \rangle \quad (\text{A.12})$$

where

$$\langle N_T \rangle = \frac{T}{\langle \tau^{(0)} \rangle + \langle \tau^{(1)} \rangle}$$

is the mean number of pulses in the interval  $(0, T)$  and  $\langle \tau^{(i)} \rangle$  denotes the mean waiting time in state  $i$ ,

$$\langle \tau^{(i)} \rangle := \int_0^\infty d\tau \tau w^{(i)}(\tau).$$

For  $\omega_n = 0$  one obtains

$$\langle |c_{0,T}|^2 \rangle = \frac{1}{T^2} \sum_{j,k=1}^{\langle N_T \rangle} \langle (t_j^{(1)} - t_j^{(0)})(t_k^{(1)} - t_k^{(0)}) \rangle = \frac{\langle \tau^{(0)} \rangle^2}{(\langle \tau^{(0)} \rangle + \langle \tau^{(1)} \rangle)^2} \quad (\text{A.13})$$

To further evaluate eq. (A.12) we introduce the characteristic functions of the waiting time distributions

$$\begin{aligned} \hat{w}^{(0)}(\omega) &:= \int_0^\infty d\tau e^{-i\omega\tau} w^{(0)}(\tau) = \langle \exp(-i\omega(t_i^{(1)} - t_i^{(0)})) \rangle \\ \hat{w}^{(1)}(\omega) &:= \int_0^\infty d\tau e^{-i\omega\tau} w^{(1)}(\tau) = \langle \exp(-i\omega(t_{i+1}^{(0)} - t_i^{(1)})) \rangle \end{aligned}$$

The independence of the waiting times in state 0 and 1 immediately gives

$$\hat{w}^{(0)}(\omega)\hat{w}^{(1)}(\omega) = \langle \exp(-i\omega(t_{i+1}^{(0)} - t_i^{(0)})) \rangle = \langle \exp(-i\omega(t_{i+1}^{(1)} - t_i^{(1)})) \rangle.$$

Then splitting again the double sum into  $j = k$ ,  $j < k$  and  $j > k$  eq. (A.12) and evaluating the resulting geometric sums leads to

$$\begin{aligned} \langle |c_{\omega_n, T}|^2 \rangle &= \frac{\langle N_T \rangle}{\omega_n^2 T^2} \left[ 2 - \hat{w}^{(0)}(\omega_n) - (\hat{w}^{(0)}(\omega_n))^* + \right. \\ &\quad \left. \left( \frac{\hat{w}^{(0)}(\omega_n)\hat{w}^{(1)}(\omega_n)}{1 - \hat{w}^{(0)}(\omega_n)\hat{w}^{(1)}(\omega_n)} \left( 2 - \hat{w}^{(0)}(\omega_n) - \frac{1}{\hat{w}^{(0)}(\omega_n)} \right) + c.c. \right) \right] + O\left(\frac{1}{T}\right) \\ &= \frac{\langle N_T \rangle}{\omega_n^2 T^2} 2\text{Re} \frac{(1 - \hat{w}^{(0)}(\omega))(1 - \hat{w}^{(1)}(\omega))}{1 - \hat{w}^{(0)}(\omega)\hat{w}^{(1)}(\omega)} + O\left(\frac{1}{T}\right) \end{aligned}$$

where  $O(1/T)$  denotes the terms which decrease faster than  $1/T$  as  $T \rightarrow \infty$ . Performing the same calculations as in the previous section one finally arrives at

$$\begin{aligned} S_\eta(\omega) &= \frac{2\pi \langle \tau^{(0)} \rangle^2}{(\langle \tau^{(0)} \rangle + \langle \tau^{(1)} \rangle)^2} \delta(\omega) \\ &\quad + \frac{2}{\omega^2 (\langle \tau^{(0)} \rangle + \langle \tau^{(1)} \rangle)} \text{Re} \frac{(1 - \hat{w}^{(0)}(\omega))(1 - \hat{w}^{(1)}(\omega))}{1 - \hat{w}^{(0)}(\omega)\hat{w}^{(1)}(\omega)} \end{aligned}$$

To relax the restriction  $a = 1$  and  $b = 0$  we notice that the general process  $\eta_{a,b}(t)$  can be obtained from our special choice  $\eta_{1,0}(t)$  by

$$\eta_{a,b}(t) = (a - b)\eta_{1,0}(t) + b.$$

The factor  $(a - b)$  obviously leads to a factor  $(a - b)^2$  in the spectral power density while the additional constant  $b$  only modifies the weight of the delta peak in the spectral power at  $\omega = 0$ . Thus eventually one obtains the final result

$$S_\eta(\omega) = \frac{2\pi(a\langle\tau^{(0)}\rangle + b\langle\tau^{(1)}\rangle)^2}{(\langle\tau^{(0)}\rangle + \langle\tau^{(1)}\rangle)^2}\delta(\omega) + \frac{2(a-b)^2}{\omega^2(\langle\tau^{(0)}\rangle + \langle\tau^{(1)}\rangle)} \operatorname{Re} \frac{(1 - \hat{w}^{(0)}(\omega))(1 - \hat{w}^{(1)}(\omega))}{1 - \hat{w}^{(0)}(\omega)\hat{w}^{(1)}(\omega)}$$

### A.3 The Wiener-Khinchine theorem

The spectral power density of a stochastic process can be related to its autocorrelation function. This relation is called Wiener-Khinchine theorem and is possible for either stationary (see e.g. [1]) or periodic processes [60, 61]. In the following two subsection we present the Wiener-Khinchine theorem with a short proof for both cases. To this end we split the process  $x(t)$  into the sum of its (in the case of a periodic process time dependent) mean value  $\langle x(t) \rangle$  and the process  $\tilde{x}(t) := x(t) - \langle x(t) \rangle$  which has zero mean value. Then the auto correlation function  $c_{x,x}(t, t') := \langle x(t)x(t') \rangle$  can also be split into two parts, namely

$$c_{x,x}(t, t') := c_{\tilde{x},\tilde{x}}(t, t') + \langle x(t) \rangle \langle x(t') \rangle \quad \text{with} \quad c_{\tilde{x},\tilde{x}}(t, t') := \langle \tilde{x}(t)\tilde{x}(t') \rangle.$$

According to the definition (2.21c), the spectral power density is given by

$$S_x(\omega) = \lim_{\epsilon \rightarrow 0} \frac{1}{\epsilon} \int_{\omega - \frac{\epsilon}{2}}^{\omega + \frac{\epsilon}{2}} d\omega' S_x(\omega') = 2\pi \lim_{T \rightarrow \infty} \frac{T}{2\pi} \langle |c_{\omega,T}|^2 \rangle = S_{\tilde{x}}(\omega) + S_\delta(\omega) \quad (\text{A.14})$$

where in the second step we have used the fact that the frequency of two subsequent Fourier coefficients is separated by  $2\pi/T$  and thus there are  $2\pi\epsilon/T$  Fourier coefficients contributing to the integral. The two parts  $S_{\tilde{x}}(\omega)$  and  $S_\delta(\omega)$  are given by

$$S_{\tilde{x}}(\omega) = \lim_{T \rightarrow \infty} \frac{1}{T} \int_0^T dt \int_0^T dt' e^{-i\omega(t-t')} c_{\tilde{x},\tilde{x}}(t, t') \quad (\text{A.15})$$

$$S_\delta(\omega) = \lim_{T \rightarrow \infty} \frac{1}{T} \int_0^T dt e^{-i\omega t} \langle x(t) \rangle \int_0^T dt' e^{i\omega t'} \langle x(t') \rangle \quad (\text{A.16})$$

To further evaluate  $S_{\tilde{x}}(\omega)$  we apply a variable transformation  $(t, t') \rightarrow (s, \tau) = (t, t' - t)$  (see Fig. A.1) in eq. (A.15) which leads to

$$S_{\tilde{x}}(\omega) = \lim_{T \rightarrow \infty} \frac{1}{T} \left[ \int_{-T}^0 d\tau \int_{-\tau}^T ds e^{i\omega\tau} c_{\tilde{x},\tilde{x}}(t, t + \tau) + \int_0^T d\tau \int_0^{T-\tau} ds e^{i\omega\tau} c_{\tilde{x},\tilde{x}}(t, t + \tau) \right] \quad (\text{A.17})$$

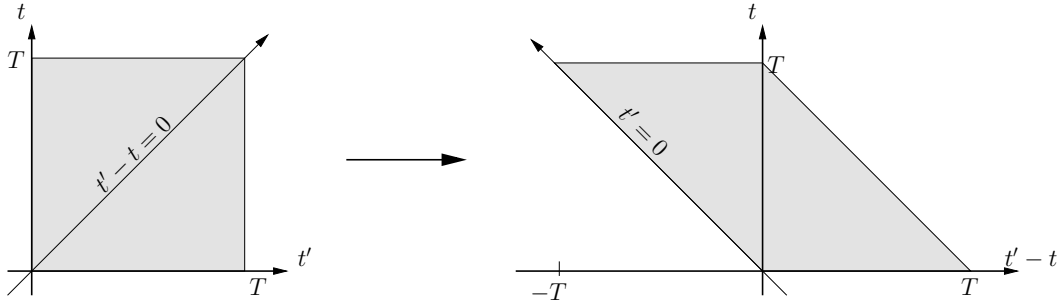


Figure A.1: A schematic view of the variable transformation  $(t, t') \rightarrow (\tau, s) = (t - t', t')$  and its corresponding area of integration

To treat expression (A.16) we need the following result which holds in a distributional sense:

$$\lim_{T \rightarrow \infty} \frac{1}{T} \int_0^T dt e^{-i(\omega - k\Omega)t} \int_0^T dt' e^{i(\omega - l\Omega)t'} = \delta_{k,l} \delta(\omega - k\Omega) = \delta_{k,l} \int_{-\infty}^{\infty} d\tau e^{i(\omega - k\Omega)\tau} \quad (\text{A.18})$$

### A.3.1 Stationary processes

The autocorrelation function  $c_{x,x}(t, t') = \langle x(t)x(t') \rangle$  of a stationary stochastic process  $x(t)$  only depends on the time difference, i.e. in this case  $c_{x,x}(t, t') \equiv c_{x,x}(t - t')$ . Therefore from eq. (A.17) we obtain

$$S_{\tilde{x}}(\omega) = \lim_{T \rightarrow \infty} \left[ \int_{-T}^0 d\tau \left(1 + \frac{\tau}{T}\right) e^{i\omega\tau} c_{\tilde{x},\tilde{x}}(\tau) + \int_0^T d\tau \left(1 - \frac{\tau}{T}\right) e^{i\omega\tau} c_{\tilde{x},\tilde{x}}(\tau) \right]$$

The autocorrelation function  $c_{\tilde{x},\tilde{x}}(\tau)$  of  $\tilde{x}(t)$  can be assumed to decrease sufficiently fast to 0 for large  $\tau$  such that

$$\lim_{T \rightarrow \infty} \frac{1}{T} \int_0^T d\tau \tau e^{-i\omega\tau} c_{\tilde{x},\tilde{x}}(\tau) = 0 \quad \forall \omega.$$

Therefore we obtain

$$S_{\tilde{x}}(\omega) = \int_{-\infty}^{\infty} d\tau e^{i\omega\tau} c_{\tilde{x},\tilde{x}}(\tau).$$

For a stationary process the mean value is constant and thus from eq. (A.16) we obtain according to eq. (A.18)

$$S_\delta(\omega) = \int_{-\infty}^{\infty} d\tau e^{i\omega\tau} \langle x \rangle^2.$$

Summing up both components, we obtain the Wiener-Khinchine theorem for stationary processes,

$$S_x(\omega) = \int_{-\infty}^{\infty} d\tau e^{i\omega\tau} c_{x,x}(\tau) = \int_{-\infty}^{\infty} d\tau e^{-i\omega\tau} c_{x,x}(\tau) \quad (\text{A.19})$$

where in the last step we used the symmetry  $c_{x,x}(\tau) = c_{x,x}(-\tau)$ .

### A.3.2 Periodic processes

For a periodic process  $x(t)$  the autocorrelation function  $c_{x,x}(t, t')$  no longer only depends on  $t - t'$  but periodically on both arguments,

$$c_{x,x}(t, t') = c_{x,x}(t + \mathcal{T}, t' + \mathcal{T}).$$

Due to the periodicity we may expand  $c_{\bar{x},\bar{x}}(t, t + \tau)$  in a Fourier series as

$$c_{\bar{x},\bar{x}}(t, t + \tau) = \sum_{k=-\infty}^{\infty} \hat{c}_{\bar{x},\bar{x},k}(\tau) \exp(ik\Omega t) \quad (\text{A.20})$$

with all  $\hat{c}_{\bar{x},\bar{x},k}(\tau)$  going rapidly to 0 as  $\tau$  goes to  $\infty$ . Also the mean value  $\langle x(t) \rangle$  is periodic in time. We expand it in a Fourier series as

$$\langle x(t) \rangle = \sum_{k=-\infty}^{\infty} \hat{x}_k \exp(ik\Omega t) \quad (\text{A.21})$$

From eq. (A.17) we obtain by inserting the expansion (A.20)

$$\begin{aligned} S_{\bar{x}}(\omega) &= \lim_{T \rightarrow \infty} \left[ \int_{-T}^0 d\tau \left(1 + \frac{\tau}{T}\right) e^{i\omega\tau} \hat{c}_{\bar{x},\bar{x},0}(\tau) + \int_0^T d\tau \left(1 - \frac{\tau}{T}\right) e^{i\omega\tau} \hat{c}_{\bar{x},\bar{x},0}(\tau) \right] + \\ &\quad \lim_{T \rightarrow \infty} \left[ \sum_{k \neq 0} \frac{i}{k\Omega T} \left[ \int_{-T}^0 d\tau (e^{i(\omega-k\Omega)\tau} - e^{ik\Omega T} e^{i\omega\tau}) \hat{c}_{\bar{x},\bar{x},k}(\tau) + \right. \right. \\ &\quad \left. \left. \int_0^T d\tau (e^{i\omega\tau} - e^{ik\Omega T} e^{i(\omega-k\Omega)\tau}) \hat{c}_{\bar{x},\bar{x},k}(\tau) \right] \right] \end{aligned}$$

Due to the assumed rapid decrease of  $\hat{c}_{\tilde{x},\tilde{x},k}(\tau)$  the second term is zero as well as the parts containing  $\frac{\tau}{T}$  in the first term. Writing the zeroth Fourier coefficient  $\hat{c}_{\tilde{x},\tilde{x},0}(\tau)$  as a period averaged,

$$\hat{c}_{x,x,0}(\tau) = \frac{1}{T} \int_0^T dt c_{\tilde{x},\tilde{x}}(\tau, t) =: \bar{c}_{\tilde{x},\tilde{x}}(\tau),$$

we thus eventually obtain

$$S_{\tilde{x}}(\omega) = \int_{-\infty}^{\infty} d\tau e^{-i\omega\tau} \bar{c}_{\tilde{x},\tilde{x}}(\tau).$$

Next we have to calculate the part of the spectral density which stems from  $\langle x(t) \rangle \langle x(t + \tau) \rangle$ . Inserting the expansion (A.21) into eq. (A.16) one immediately obtains

$$\begin{aligned} S_{\delta}(\omega) &= \sum_{k,l} \hat{x}_k \hat{x}_l^* \lim_{T \rightarrow \infty} \frac{1}{T} \int_0^T dt e^{-i(\omega - k\Omega)t} \int_0^T dt' e^{i(\omega - l\Omega)t'} \\ &= \sum_k |x_k|^2 \int_{-\infty}^{\infty} d\tau e^{i(\omega - k\Omega)\tau} \end{aligned}$$

where in the last step we used eq. (A.18). Noticing that according to eq. (A.21)

$$\frac{1}{T} \int_0^T dt \langle x(t) \rangle \langle x(t + \tau) \rangle = \sum_k |x_k|^2 e^{-ik\Omega\tau}$$

we obtain the Wiener-Khinchine theorem for periodic processes,

$$S_x(\omega) = \int_{-\infty}^{\infty} d\tau e^{i\omega\tau} \bar{c}_{xx}(\tau) = \int_{-\infty}^{\infty} d\tau e^{-i\omega\tau} \bar{c}_{xx}(\tau), \quad (\text{A.22})$$

namely the spectral power density is the Fourier transform of the period averaged correlation function. In the last step we used that the period averaged autocorrelation function is symmetric, i.e.  $\bar{c}_{xx}(\tau) = \bar{c}_{xx}(-\tau)$ . Notice however that the full autocorrelation function is not symmetric, i.e.

$$c_{xx}(t, t + \tau) \neq c_{xx}(t, t - \tau).$$





# Appendix B

## Detailed calculations for chapter 3

### B.1 Sum of powers of a Markov operator

Consider the operator  $\mathcal{L}$  acting on the space  $L_1([0, 2\pi])$  of integrable complex valued functions on the interval  $[0, 2\pi]$ . We assume that it has the properties

$$\mathcal{L}f \geq 0 \quad \text{if } f \geq 0 \quad \text{and} \quad \|\mathcal{L}f\| = \|f\|.$$

Such an operator is called a Markov operator. We assume further that  $\mathcal{L}$  has a unique invariant probability density,  $P^{\text{st}} = \mathcal{L}P^{\text{st}}$ . Then (cf. theorem 5.2.2 in [71]) the sequence  $\{A_n P\}_n$  with

$$A_n := \frac{1}{n} \sum_{k=0}^{n-1} \mathcal{L}^k$$

converges strongly for all probability densities  $P$  to the unique stationary probability density  $P^{\text{st}}$ , i.e.

$$\lim_{n \rightarrow \infty} \|A_n P - P^{\text{st}}\| = 0. \tag{B.1}$$

Next we relax the restriction of  $P$  being a probability density but allow for arbitrary functions  $f$ . Such a function can be decomposed into

$$f = c^+ P_r^+ - c^- P_r^- + i(d^+ P_i^+ - d^- P_i^-)$$

where  $P_{r/i}^\pm$  are all probability densities. Then according to eq. (B.1)

$$\begin{aligned} 0 &\leq \lim_{n \rightarrow \infty} \|A_n f - (c^+ - c^- + id^+ - id^-)P^{\text{st}}\| \\ &\leq \lim_{n \rightarrow \infty} \left( |c^+| \|(A_n P_r^+ - P^{\text{st}})\| + |c^-| \|(A_n P_r^- - P^{\text{st}})\| \right. \\ &\quad \left. + |d^+| \|(A_n P_i^+ - P^{\text{st}})\| + |d^-| \|(A_n P_i^- - P^{\text{st}})\| \right) = 0 \end{aligned}$$

and thus using  $(c^+ - c^- + id^+ - id^-) = \langle 1, f \rangle_{\mathbb{C}}$  we obtain the strong convergence

$$\lim_{n \rightarrow \infty} A_n f = \langle 1, f \rangle_{\mathbb{C}} P^{\text{st}} \quad (\text{B.2})$$

Now

$$\frac{1}{n^2} \sum_{k=0}^{n-1} \sum_{j=0}^k \mathcal{L}^j f = \frac{1}{2} A_n f - \sum_{k=0}^{n-1} \frac{k - \frac{n}{2}}{n^2} \mathcal{L}^k f.$$

Because  $\mathcal{L}$  is a Markov operator we have  $\|\mathcal{L}^k f\| = \|f\|$  and thus

$$\left\| \sum_{k=0}^{n-1} \frac{k - \frac{n}{2}}{n^2} \mathcal{L}^k f \right\| \leq \|f\| \left| \sum_{k=0}^{n-1} \frac{k - \frac{n}{2}}{n^2} \right| = \|f\| \frac{1}{2n}.$$

Taken together we have

$$\lim_{n \rightarrow \infty} \frac{1}{n^2} \sum_{k=0}^{n-1} \sum_{j=0}^k \mathcal{L}^j f = \frac{\langle 1, f \rangle_{\mathbb{C}}}{2} P^{\text{st}}$$

and finally we obtain

$$\lim_{T \rightarrow \infty} \frac{1}{T^2} \sum_{k=1}^{\langle N_T \rangle} \sum_{j=1}^k \mathcal{L}^j f = \mathcal{L} \lim_{T \rightarrow \infty} \frac{1}{\bar{\tau}^2 \langle N_T \rangle^2} \sum_{k=0}^{\langle N_T \rangle - 1} \sum_{j=0}^k \mathcal{L}^j f = \frac{\langle 1, f \rangle_{\mathbb{C}}}{2\bar{\tau}^2} P^{\text{st}}. \quad (\text{B.3})$$

## B.2 The Fourier coefficients of the time periodic master operator

Consider the master equation

$$\mathcal{M}_t^{(i)}[p^{(1)}, \dots, p^{(n)}] = 0 \quad (\text{B.4})$$

The master operator is assumed to be periodic with period  $\mathcal{T} = 2\pi/\Omega$ ,  $\mathcal{M}_t^{(i)} = \mathcal{M}_{t+\mathcal{T}}^{(i)}$  and to act linearly on a tuple  $(p^{(1)}, \dots, p^{(n)})$  of functions on  $\mathbb{R}$ . Introducing the operators

$$\mathcal{M}_t^{(i,j)}[f](t) := \mathcal{M}_t^{(i)}[\underbrace{0, \dots, f, 0, \dots}_{f \text{ at position } j}](t),$$

$\mathcal{M}^{(i)}$  can be written, due to its linearity, as

$$\mathcal{M}_t^{(i)}[p^{(1)}, \dots, p^{(n)}](t) = \sum_{j=1}^n \mathcal{M}_t^{(i,j)}[p^{(j)}](t).$$

Next we consider periodic functions  $p^{(j)}$  with the period  $\Omega$  of the driving signal and expand them into a Fourier series as

$$p^{(j)}(t) = \sum_k p_k^{(j)} \exp(ik\Omega t).$$

Again due to the linearity the action of the master operator on these periodic functions may be written as

$$\mathcal{M}_t^{(i,j)}[p^{(j)}](t) = \sum_k p_k^{(j)} \mathcal{M}_t^{(i,j)}[\exp(ik\Omega \cdot)](t)$$

The arising functions  $\mathcal{M}_t^{(i,j)}[\exp(ik\Omega \cdot)](t)$  are also periodic as can be seen exploiting the time translational invariance as follows:

$$\begin{aligned} \mathcal{M}_t^{(i,j)}[\exp(ik\Omega \cdot)](t + \mathcal{T}) &= \mathcal{M}_{t+\mathcal{T}}^{(i,j)}[\exp(ik\Omega \cdot)](t + \mathcal{T}) \\ &= \mathcal{M}_t^{(i,j)}[\exp(ik\Omega(\cdot - \mathcal{T}))](t) = \mathcal{M}_t^{(i,j)}[\exp(ik\Omega(\cdot))](t) \end{aligned}$$

Thus they can likewise be expanded into a Fourier series as

$$\mathcal{M}_t^{(i,j)}[\exp(ik\Omega \cdot)](t) = \sum_l \mathcal{M}_{k,l}^{(i,j)} \exp(il\Omega t)$$

with

$$\mathcal{M}_{k,l}^{(i,j)} = \frac{1}{\mathcal{T}} \int_0^{\mathcal{T}} dt \exp(-il\Omega t) \mathcal{M}_t^{(i,j)}[\exp(ik\Omega \cdot)](t). \quad (\text{B.5})$$

With these Fourier coefficients the master equation (B.4) restricted to periodic probabilities  $p^{(i)}(t)$  can be expressed in Fourier space as

$$\sum_{j=1}^n \sum_{l=-\infty}^{\infty} \mathcal{M}_{k,l}^{(i,j)} p_l^{(j)} = 0.$$

### B.3 The order in the driving signal amplitude

If the periodicity of the renewal process is due to a harmonic periodic signal  $s(t) = A_{\text{in}} \exp(i\Omega t) + c.c.$ , we wonder what is the order in the signal amplitude  $A_{\text{in}}$  of the different quantities occurring in the calculation of the SPA and SNR.

### B.3.1 The order in the signal amplitude of the Fourier coefficients of a general master operator

We assume that the time periodic master operator  $\mathcal{M}_t^{(i,j)}[f](t) \equiv \mathcal{M}_t^{(i,j)}[f, s](t)$  is a smooth functional of the periodic signal  $s(t)$  which generates its periodicity  $\mathcal{M}_t^{(i,j)} = \mathcal{M}_{t+\mathcal{T}}^{(i,j)}$ . Under this assumption we show that for a harmonic signal  $s(t) = A_{\text{in}} \exp(i\Omega t) + c.c.$  the Fourier coefficients (B.5) are of order  $O(|A_{\text{in}}|^{k-l})$ .

Due to the assumed smooth dependence of  $\mathcal{M}_t^{(i,j)}[f, s](t)$  on  $s$  we can perform a functional Taylor expansion around  $s = 0$ ,

$$\mathcal{M}_t^{(i)}[f, s](t) = \sum_{\nu=0}^{\infty} \frac{1}{\nu!} \int dx_1 \dots dx_{\nu} \rho_{\nu}[f](t, x_1, \dots, x_{\nu}) s(x_1) \dots s(x_{\nu}).$$

with

$$\rho_{\nu}[f](t, x_1, \dots, x_{\nu}) := \left. \frac{\delta^{\nu} \mathcal{M}_t^{(i)}[f, h](t)}{\delta h(x_1) \dots \delta h(x_{\nu})} \right|_{h=0} \quad (\text{B.6})$$

Taking into account the time translational invariance

$$\mathcal{M}_t^{(i)}[f, s](t) = \mathcal{M}_0^{(i)}[f(\cdot + t), s(\cdot + t)](0) \quad (\text{B.7})$$

we obtain

$$\begin{aligned} \hat{\mathcal{M}}_{k,l}^{(i,j)} &= \frac{1}{\mathcal{T}} \int_0^{\mathcal{T}} dt \sum_{\nu=0}^{\infty} \frac{1}{\nu!} \int dx_1 \dots dx_{\nu} \rho_{\nu}[\exp(il\Omega(\cdot + t))](0, x_1, \dots, x_{\nu}) \\ &\quad \prod_{n=0}^{\nu} (A_{\text{in}} e^{i\Omega(x_n+t)} + A_{\text{in}}^* e^{-i\Omega(x_n+t)}) \exp(-ik\Omega t) \end{aligned} \quad (\text{B.8})$$

The product  $\prod_{n=0}^{\nu} (A_{\text{in}} e^{i\Omega(x_n+t)} + A_{\text{in}}^* e^{-i\Omega(x_n+t)})$  can be further evaluated leading to

$$\prod_{n=0}^{\nu} (A_{\text{in}} e^{i\Omega(x_n+t)} + A_{\text{in}}^* e^{-i\Omega(x_n+t)}) = \sum_{n=0}^{\nu} A_{\text{in}}^n A_{\text{in}}^{*\nu-n} e^{i\Omega(2n-\nu)t} c_{n,\nu}$$

where  $c_{n,\nu}$  is given by

$$c_{n,\nu} = \sum_{\sigma_{\nu,n}} \exp \left( i\Omega \sum_{i=1}^{\nu} (-1)^{\sigma_i} x_i \right)$$

and the sum over  $\sigma_{\nu,n}$  denotes the sum over all  $\nu$ -tuple consisting of  $n$  times 0 and  $\nu - n$  times 1.

Introducing

$$\tilde{\rho}_{n,\nu}[f] := \frac{1}{\nu!} \int dx_1 \dots dx_\nu c_{n,\nu} \rho_\nu[f](0, x_1, \dots, x_\nu).$$

which, being a linear functional of  $f$ , obviously obeys

$$\tilde{\rho}_{n,\nu}[\exp(il\Omega(\cdot + t))] = \tilde{\rho}_{n,\nu}[\exp(il\Omega\cdot)] \exp(il\Omega t)$$

we obtain from eq. (B.8)

$$\begin{aligned} \hat{\mathcal{M}}_{k,l}^{(i,j)} &= \sum_{\nu=0}^{\infty} \sum_{n=0}^{\nu} \tilde{\rho}_{n,\nu}[\exp(il\Omega\cdot)] A_{\text{in}}^n A_{\text{in}}^{*\nu-n} \\ &\quad \frac{1}{\mathcal{T}} \int_0^{\mathcal{T}} dt \exp(i\Omega(2n-\nu)t) \exp(i\Omega lt) \exp(-ik\Omega t) \end{aligned}$$

Taking into account that  $\frac{1}{\mathcal{T}} \int_0^{\mathcal{T}} dt \exp(i\Omega(2n-\nu)t) \exp(i\Omega lt) \exp(-ik\Omega t) = \delta_{k-l, 2n-\nu}$  and changing the summation variables according to

$$\sum_{\nu=0}^{\infty} \sum_{n=0}^{\nu} \rightarrow \sum_{n=0}^{\infty} \sum_{\nu=n}^{\infty} \rightarrow \sum_{n=0}^{\infty} \sum_{\mu:=\nu-n=0}^{\infty}$$

$$\begin{aligned} \hat{\mathcal{M}}_{k,l}^{(i,j)} &= \sum_{\mu=0}^{\infty} \sum_{n=0}^{\infty} \tilde{\rho}_{n,\mu+n}[\exp(il\Omega\cdot)] A_{\text{in}}^n A_{\text{in}}^{*\mu} \delta_{k-l, n-\mu} \\ &= \begin{cases} \sum_{\mu=0}^{\infty} \tilde{\rho}_{k-l+\mu, k-l}[\exp(il\Omega\cdot)] A_{\text{in}}^{k-l+\mu} A_{\text{in}}^{*\mu} & k-l \geq 0 \\ \sum_{n=0}^{\infty} \tilde{\rho}_{n, l-k}[\exp(il\Omega\cdot)] A_{\text{in}}^n A_{\text{in}}^{*l-k+n} & k-l \leq 0 \end{cases} \end{aligned}$$

Thus  $\hat{\mathcal{M}}_{k,l}^{(i,j)}$  is of order  $O(|A_{\text{in}}^{k-l}|)$ .

### B.3.2 The order in the signal amplitude of the Fourier coefficients of a time dependent waiting time distribution

Consider the Fourier coefficients

$$\hat{w}_k(t) = \int_0^{\infty} d\tau \exp(-ik\Omega\tau) w(\tau, t)$$

of the time dependent waiting time distribution  $w(\tau, t)$  for a fixed entrance time  $t$  as a functional of the driving signal  $s(t)$ ,

$$\hat{w}_k(t) = \hat{w}_k[s](t).$$

We assume that this functional depends sufficiently smooth on  $s$ , such that we can perform a functional Taylor expansion around  $s = 0$ ,

$$\hat{w}_k[s](t) = \hat{w}_k[0](t) + \sum_{\nu=1}^{\infty} \frac{1}{\nu!} \int dx_1 \dots dx_{\nu} \frac{\delta^{\nu} \hat{w}_k[f](t)}{\delta f(x_1) \dots \delta f(x_{\nu})} \Big|_{f=0} s(x_1) \dots s(x_{\nu}).$$

Now  $\hat{w}_k[0](t) = \hat{w}_k[0]$  are the Fourier coefficients of the waiting time distribution without signal and thus time independent. We further exploit the time translation property, that the waiting time density and thus its Fourier coefficients as generated by a signal  $s$  observed at a time  $t + \Delta t$  are the same as the waiting time density generated by a shifted signal  $s(\cdot - \Delta t)$  observed at a time  $t$ ,

$$\hat{w}_k[s](t + \Delta t) = \hat{w}_k[s(\cdot - \Delta t)](t).$$

Thus

$$\begin{aligned} \hat{w}_k[s](t + \Delta t) &= \hat{w}_{k,0} + \\ &\sum_{\nu=0}^{\infty} \frac{1}{\nu!} \int dx_1 \dots dx_{\nu} \frac{\delta^{\nu} \hat{w}_k[f](t)}{\delta f(x_1) \dots \delta f(x_{\nu})} \Big|_{f=0} s(x_1 - \Delta t) \dots s(x_{\nu} - \Delta t) \end{aligned}$$

Now for a harmonic signal  $s(t) = A_{\text{in}} \exp(i\Omega t) + c.c$  we have

$$\begin{aligned} \hat{w}_k[s](t + \Delta t) &= \hat{w}_k[0] + A_{\text{in}} \int dx \frac{\delta \hat{w}_k[f](t)}{\delta f(x)} \Big|_{f=0} e^{i\Omega(x-\Delta t)} + c.c. \\ &\quad + O(A_{\text{in}}^2) \\ &= \hat{w}_k[0] + A_{\text{in}} c_k(t) e^{-i\Omega \Delta t} + A_{\text{in}}^* c_{-k}(t) e^{i\Omega \Delta t} + O(A_{\text{in}}^2) \end{aligned}$$

with

$$c_k(t) = \int dx \frac{\delta \hat{w}_k[f](t)}{\delta f(x)} \Big|_{f=0} \exp(i\Omega x)$$

The Fourier coefficients with respect to  $t$ ,  $\hat{w}_{k,l}$  are defined by

$$\begin{aligned} \hat{w}_{k,l} &= \frac{1}{\mathcal{T}} \int_0^{\mathcal{T}} dt \hat{w}_k(t) \exp(-ik\Omega t) \\ &= \delta_{l,0} \hat{w}_k[0] + \frac{1}{\mathcal{T}} \int_0^{\mathcal{T}} dt (A_{\text{in}} c_k(0) e^{-i(k+1)\Omega t} + A_{\text{in}}^* c_{-k}(0) e^{-i(k-1)\Omega t}) + O(A_{\text{in}}^2) \end{aligned}$$

Therefrom one easily deduces that  $\hat{w}_{k,0}$  is of order  $O(A^0)$ ,  $\hat{w}_{k,\pm 1}$  is of order  $O(A_{\text{in}})$  and all higher Fourier coefficients  $\hat{w}_{k,l}$ ,  $l \geq 2$  are of order  $O(A_{\text{in}}^l)$ ,  $l \geq 2$ . Actually, if one takes into account also higher expansion coefficients in the functional Taylor expansion one can show that  $\hat{w}_{k,l}$  is of order  $O(A_{\text{in}}^{|l|})$ .

# Appendix C

## Detailed calculations for chapter 4

### C.1 Periodically modulated linear growth of the cumulants of a periodic point process

Consider a periodic point process  $\{t_i\}_i$ . This can for example be a periodic renewal process, but also other, stronger correlated periodic point processes can be considered. By  $K_{t_0,t}^{[n]}$  we denote the  $n$ th cumulants of the number of events  $N_{t_0,t}$  in the interval  $(t_0, t]$ . We further define the change in time as

$$\kappa_{t_0,t}^{[n]} := \frac{d}{dt} K_{t_0,t}^{[n]}. \quad (\text{C.1})$$

The first of these coefficients gives the change in time of the mean number of events, which is the instantaneous mean frequency. The second coefficients is the change in time of the variance of the event number, which is twice the instantaneous effective diffusion coefficient. Our aim is to show that asymptotically

$$\kappa^{[n]}(t) := \lim_{t_0 \rightarrow -\infty} \kappa_{t_0,t}^{[n]} \quad (\text{C.2})$$

become periodic functions of time with the period of the external driving. To this end we introduce following [63, 124] the generating functional  $L_{t_0,t}[v]$  of the considered driven renewal process as

$$L_{t_0,t}[v] = \left\langle \prod_{i=1}^{N_{t_0,t}} (1 + v(t_i)) \right\rangle$$

where  $t_i$  are the times of the events in the interval  $(t_0, t]$ . Then the  $n$ th moment  $M_{t_0,t}^{[n]}$  of event number  $N_{t_0,t}$  is given by

$$M_{t_0,t}^{[n]} := \langle N_{t_0,t}^n \rangle = \frac{\partial^n}{\partial u^n} L_{t_0,t}[e^u - 1] \Big|_{u=0}. \quad (\text{C.3})$$



The generating functional  $L_{t_0,t}$  can be expressed in terms of the distribution functions  $f_s(t_1, \dots, t_s)$ , which govern the probability

$$dP = f_s(t_1, \dots, t_s) dt_1 \dots dt_s$$

to find one event in each of the intervals  $(t_i, t_i + dt_i)$ ,  $i = 1, \dots, s$  regardless of how many events are outside these intervals, as [63, 124]

$$L_{t_0,t}[v] = 1 + \sum_{s=1}^{\infty} \int_{t_0}^t d\tau_1 \int_{t_0}^{\tau_1} d\tau_2 \dots \int_{t_0}^{\tau_{s-1}} d\tau_s f_s(\tau_1, \tau_2, \dots, \tau_s) v(\tau_1) \dots v(\tau_s). \quad (\text{C.4})$$

The generating functional can also be expressed in terms of the correlation functions  $g_s(t_1, \dots, t_s)$  as

$$L_{t_0,t}[v] = \exp \left[ \sum_{s=1}^{\infty} \int_{t_0}^t d\tau_1 \int_{t_0}^{\tau_1} d\tau_2 \dots \int_{t_0}^{\tau_{s-1}} d\tau_s g_s(\tau_1, \tau_2, \dots, \tau_s) v(\tau_1) \dots v(\tau_s) \right]. \quad (\text{C.5})$$

Eq. (C.5) together with eq. (C.4) define the correlation functions in terms of the distribution functions.

According to eqs. (C.5) and (C.3) the moments eq. (C.3) can be expressed as

$$M_{t_0,t}^{[n]} = \frac{\partial^n}{\partial u^n} \exp \left[ \sum_{s=1}^{\infty} G_s(t_0, t) (e^u - 1)^s \right] \Big|_{u=0} \quad (\text{C.6})$$

where

$$G_s(t_0, t) := \int_{t_0}^t d\tau_1 \int_{t_0}^{\tau_1} d\tau_2 \dots \int_{t_0}^{\tau_{s-1}} d\tau_s g_s(\tau_1, \tau_2, \dots, \tau_s).$$

From formula (C.6) we can evaluate the corresponding cumulants  $K_{t_1,t_2}^{[n]}$  as (see appendix C.3)

$$K_{t_0,t}^{[n]} = \frac{\partial^n}{\partial u^n} \sum_{s=1}^{\infty} G_s(t_0, t) (e^u - 1)^s \Big|_{u=0}. \quad (\text{C.7})$$

As the considered renewal processes are periodic in time with period  $\mathcal{T}$ , the distribution functions and therefore also the correlation functions are likewise periodic in time,

$$g_s(\tau_1, \dots, \tau_s) = g_s(\tau_1 + \mathcal{T}, \dots, \tau_s + \mathcal{T}). \quad (\text{C.8})$$

Then the time derivative of the function  $G_s(t_0, t)$  yields

$$\begin{aligned} \frac{d}{dt}G_s(t_0, t) &= \int_{t_0}^t d\tau_2 \dots \int_{t_0}^{\tau_{s-1}} d\tau_s g_s(t, \tau_2, \dots, \tau_s) \\ &= \frac{1}{(s-1)!} \int_{t_0}^t d\tau_2 \dots \int_{t_0}^t d\tau_s g_s(t, \tau_2, \dots, \tau_s) \\ &= \frac{1}{(s-1)!} \int_0^{t-t_0} d\tau_2 \dots \int_0^{t-t_0} d\tau_s g_s(t, t - \tau_2, \dots, t - \tau_s) \end{aligned}$$

which can be expressed in the asymptotic limit as

$$\lim_{t_0 \rightarrow -\infty} \frac{d}{dt}G_s(t_0, t) = \frac{1}{(s-1)!} \int_0^\infty d\tau_2 \dots \int_0^\infty d\tau_s g_s(t, t - \tau_2, \dots, t - \tau_s). \quad (\text{C.9})$$

To ensure that this limit exists, we additionally suppose that  $g_s(\tau_1, \dots, \tau_s)$  decreases sufficiently fast to zero for any pair of time difference  $|\tau_i - \tau_j| \rightarrow \infty$ . In [63] this property is called *cluster property*.

According to eq. (C.8) the asymptotic time derivative eq. (C.9) is a periodic function in  $t$  and thus (cf. eq. (C.7)) the coefficients

$$\kappa^{[n]}(t) = \lim_{t_0 \rightarrow -\infty} \frac{d}{dt}K_{t_0, t}^{[n]}. \quad (\text{C.10})$$

are periodic in time, as well.

## C.2 Relation between the Kramers-Moyal coefficient and the growth of the cumulants

Consider the stochastic process  $x(t)$  whose probability distribution is governed by the Kramers-Moyal equation

$$\frac{\partial}{\partial t}\mathcal{P}(x, t) = \sum_{n=1}^{\infty} \frac{(-1)^n}{n!} \kappa^{[n]}(t) \frac{\partial^n}{\partial x^n} \mathcal{P}(x, t) \quad (\text{C.11})$$

We are interested in the growth of the cumulants  $K^{[n]}(t)$  of  $x(t)$ . To this end we first consider the corresponding moments of  $x(t)$ ,

$$M^{[n]}(t) := \langle x^n(t) \rangle = \int_{-\infty}^{\infty} dx x^n \mathcal{P}(x, t)$$

They obey

$$\frac{d}{dt}M^{[n]}(t) = \int_{-\infty}^{\infty} dx x^n \frac{\partial}{\partial t} \mathcal{P}(x, t) = \sum_{j=1}^{\infty} \frac{(-1)^j}{j!} \kappa^{[j]}(t) \int_{-\infty}^{\infty} dx x^n \frac{\partial^j}{\partial x^j} \mathcal{P}(x, t)$$

Assuming further that  $\mathcal{P}(x, t)$  decreases sufficiently fast to 0 for  $x \rightarrow \pm\infty$  such that

$$\lim_{x \rightarrow \pm\infty} x^n \mathcal{P}(x, t) = 0$$

the above expression can be evaluated using integration by parts to give

$$\begin{aligned} \frac{d}{dt} M^{[n]}(t) &= \sum_{j=1}^{\infty} \frac{\kappa^{[j]}(t)}{j!} \int_{-\infty}^{\infty} dx \left[ \frac{\partial^j}{\partial x^j} x^n \right] \mathcal{P}(x, t) \\ &= \sum_{j=1}^n \frac{\kappa^{[j]}(t)}{j!} \int_{-\infty}^{\infty} dx \frac{n!}{(n-j)!} x^{n-j} \mathcal{P}(x, t) \\ &= \sum_{j=1}^n \kappa^{[j]}(t) \binom{n}{j} M^{[n-j]}(t) \end{aligned} \tag{C.12}$$

Generally, the moments and cumulants are related by

$$\sum_{k=0}^{\infty} \frac{z^k}{k!} M^{[k]}(t) = \exp \left[ \sum_{k=1}^{\infty} \frac{z^k}{k!} K^{[k]}(t) \right]. \tag{C.13}$$

and thus by differentiating this equation with respect to  $t$

$$\sum_{k=0}^{\infty} \frac{z^k}{k!} \frac{d}{dt} M^{[k]}(t) = \sum_{k=1}^{\infty} \frac{z^k}{k!} \frac{d}{dt} K^{[k]}(t) \sum_{l=0}^{\infty} \frac{z^l}{l!} M^{[l]}(t).$$

Inserting the moments dynamic eq. (C.12) into the left hand side of this equation we obtain

$$\begin{aligned} \sum_{k=0}^{\infty} \frac{z^k}{k!} \sum_{j=1}^k \kappa^{[j]}(t) \binom{k}{j} M^{[k-j]}(t) &= \sum_{j=1}^{\infty} \sum_{k=j}^{\infty} \frac{z^k}{k!} \kappa^{[j]}(t) \binom{k}{j} M^{[k-j]}(t) \\ &= \sum_{j=1}^{\infty} \frac{z^j}{j!} \kappa^{[j]}(t) \sum_{k=0}^{\infty} \frac{z^k}{k!} M^{[k]}(t) \end{aligned}$$

As the  $M^{[k]}$  and  $z$  are arbitrary we eventually deduce

$$\frac{d}{dt} K^{[n]}(t) = \kappa^{[n]}(t).$$

### C.3 Relation between moments and cumulants

Consider the function the moments  $M^{[n]}$  defined by

$$M^{[n]} = \frac{\partial^n}{\partial z^n} f(z) \Big|_{z=0}. \quad (\text{C.14})$$

for some analytic function  $f(z)$  which is called the moment generating function (see eg. [63]). The relation between moments  $M^{[n]}$  and cumulants  $K^{[n]}$  is defined by

$$\sum_{k=0}^{\infty} \frac{z^k}{k!} M^{[k]} = \exp \left[ \sum_{k=1}^{\infty} \frac{z^k}{k!} K^{[k]} \right]. \quad (\text{C.15})$$

From eq. (C.14) one immediately obtains

$$\sum_{k=0}^{\infty} \frac{z^k}{k!} M^{[k]} = f(z),$$

Then according to eq. (C.15)

$$\sum_{k=1}^{\infty} \frac{z^k}{k!} K^{[k]} = \log f(z)$$

and thus

$$K^{[n]} = \frac{\partial^n}{\partial z^n} \log f(z) \Big|_{z=0}.$$

### C.4 Expansion of the probability density governed by a Kramers-Moyal equation

Consider a probability distribution  $\mathcal{P}(x, t)$  governed by a Kramers-Moyal equation with state independent but time dependent expansion coefficients  $\kappa^{[n]}(t)$ ,

$$\frac{\partial}{\partial t} \mathcal{P}(x, t) = \sum_{n=1}^{\infty} \frac{(-1)^n}{n!} \kappa^{[n]}(t) \frac{\partial^n}{\partial x^n} \mathcal{P}(x, t) \quad (\text{C.16})$$

Our aim is to express the probability distribution  $\mathcal{P}(x - \Delta x, t - \tau)$  in terms of  $\mathcal{P}(x, t)$  and its derivatives with respect to  $x$ ,  $\partial^n / \partial x^n \mathcal{P}(x, t)$ . To this end we start by expanding  $\mathcal{P}(x - \Delta x, t - \tau)$  in a Taylor series around  $x$  and  $t$ ,

$$\mathcal{P}(x - \Delta x, t - \tau) = \sum_{n=0}^{\infty} \sum_{m=0}^{\infty} \frac{(-\Delta x)^n (-\tau)^m}{n! m!} \frac{\partial^{n+m}}{\partial x^n \partial t^m} \mathcal{P}(x, t)$$

To process the time derivatives we use the Kramers-Moyal equation (C.16) taking care of the explicit time dependence of  $\kappa^{[i]}(t)$  which leads to

$$\begin{aligned} \mathcal{P}(x - \Delta x, t - \tau) &= \mathcal{P}(x, t) - \left[ \Delta x + \sum_{m=1}^{\infty} \frac{(-\tau)^m}{m!} \frac{\partial^{m-1} \kappa^{[1]}(t)}{\partial t^{m-1}} \right] \frac{\partial}{\partial x} \mathcal{P}(x, t) \\ &+ \left[ \frac{\Delta x^2}{2} + \Delta x \sum_{m=1}^{\infty} \frac{(-\tau)^m}{m!} \frac{\partial^{m-1} \kappa^{[1]}(t)}{\partial t^{m-1}} + \frac{1}{2} \sum_{m=1}^{\infty} \frac{(-\tau)^m}{m!} \frac{\partial^{m-1} \kappa^{[2]}(t)}{\partial t^{m-1}} \right. \\ &\left. + \sum_{m=2}^{\infty} \frac{(-\tau)^m}{m!} \sum_{l=1}^{m-1} \binom{m-1}{l} \frac{\partial^{m-1-l} \kappa^{[1]}(t)}{\partial t^{m-1-l}} \frac{\partial^{l-1} \kappa^{[1]}(t)}{\partial t^{l-1}} \right] \frac{\partial^2}{\partial x^2} \mathcal{P}(x, t) + O(3). \end{aligned}$$

where  $O(3)$  denotes third or higher derivatives of  $\mathcal{P}(x, t)$  with respect to  $x$ . The sums containing the coefficients  $\kappa^{[n]}(t)$  in a linear way be further evaluated, leading to

$$\begin{aligned} \sum_{m=1}^{\infty} \frac{(-\tau)^m}{m!} \frac{\partial^{m-1} \kappa^{[n]}(t)}{\partial t^{m-1}} &= - \sum_{m=0}^{\infty} \frac{1}{m!} \frac{\partial^m \kappa^{[n]}(t)}{\partial t^m} \int_0^{\tau} d\tau' (-\tau')^m \\ &= - \int_0^{\tau} d\tau' \kappa^{[n]}(t - \tau') \end{aligned}$$

The last term can be simplified to give

$$\begin{aligned} &\sum_{m=2}^{\infty} \frac{(-\tau)^m}{m!} \sum_{l=1}^{m-1} \binom{m-1}{l} \frac{\partial^{m-1-l} \kappa^{[1]}(t)}{\partial t^{m-1-l}} \frac{\partial^{l-1} \kappa^{[1]}(t)}{\partial t^{l-1}} \\ &= \sum_{l=0}^{\infty} \sum_{m=0}^{\infty} \frac{(-\tau)^{m+l+2}}{(m+l+2)!} \binom{m+l+1}{l+1} \frac{\partial^m \kappa^{[1]}(t)}{\partial t^m} \frac{\partial^l \kappa^{[1]}(t)}{\partial t^l} \\ &= \int_0^{\tau} d\tau' \sum_{m=0}^{\infty} \frac{(-\tau')^m}{m!} \frac{\partial^m \kappa^{[1]}(t)}{\partial t^m} \int_0^{\tau'} d\tau'' \sum_{l=0}^{\infty} \frac{(-\tau'')^l}{l!} \frac{\partial^l \kappa^{[1]}(t)}{\partial t^l} \\ &= \int_0^{\tau} d\tau' \kappa^{[1]}(t - \tau') \int_0^{\tau'} d\tau'' \kappa^{[1]}(t - \tau'') \end{aligned}$$

Thus we eventually arrive at

$$\begin{aligned} \mathcal{P}(x - \Delta x, t - \tau) &= \mathcal{P}(x, t) + c_t^{[1]}(\tau, \Delta x) \frac{\partial}{\partial x} \mathcal{P}(x, t) \\ &+ c_t^{[2]}(\tau, \Delta x) \frac{\partial^2}{\partial x^2} \mathcal{P}(x, t) + O(3) \end{aligned} \quad (\text{C.17})$$

where

$$c_t^{[1]}(\tau, \Delta x) = \int_0^{\tau} d\tau' \kappa^{[1]}(t - \tau') - \Delta x \quad (\text{C.18})$$

and

$$\begin{aligned} c_i^{[2]}(\tau, \Delta x) &= \frac{\Delta x^2}{2} - \Delta x \int_0^\tau d\tau' \kappa^{[1]}(t - \tau') \\ &\quad - \frac{1}{2} \int_0^\tau d\tau' \kappa^{[2]}(t - \tau') + \int_0^\tau d\tau' \kappa^{[1]}(t - \tau') \int_0^{\tau'} d\tau'' \kappa^{[1]}(t - \tau'') \end{aligned} \quad (\text{C.19})$$

## C.5 The phase velocity and effective diffusion for the excitable system in Fourier Space

We start by expressing the periodic functions  $\omega(t)$ ,  $\mathcal{D}_{\text{eff}}(t)$ ,  $q^{(0/1)}(t)$  and  $\gamma(t)$  in a Fourier series as

$$\begin{aligned} \omega(t) &= \sum_{k=-\infty}^{\infty} \omega_k \exp(ik\Omega t), & \mathcal{D}_{\text{eff}}(t) &= \sum_{k=-\infty}^{\infty} D_k \exp(ik\Omega t), \\ q^{(0/1)}(t) &= \sum_{k=-\infty}^{\infty} q_k^{(0/1)} \exp(ik\Omega t) & \text{and} & \quad \gamma(t) = \sum_{k=-\infty}^{\infty} \gamma_k \exp(ik\Omega t). \end{aligned}$$

We further introduce

$$\begin{aligned} w_k &:= \int_0^\infty d\tau \exp(-ik\Omega\tau) w(\tau), & v_k &:= \int_0^\infty d\tau \exp(-ik\Omega\tau) \tau w(\tau), \\ z_k &:= \int_0^\infty d\tau \exp(-ik\Omega\tau) z(\tau) & \text{and} & \quad d_k := \int_0^\infty d\tau \exp(-ik\Omega\tau) \tau z(\tau). \end{aligned}$$

From the relation

$$z(\tau) = 1 - \int_0^\tau d\tau' w(\tau')$$

between a waiting time distribution  $w(\tau)$  and the corresponding survival probability  $z(\tau)$  one obtains

$$z_k = \frac{1 - w_k}{ik\Omega} \quad \text{and} \quad d_k = \frac{w_k - 1}{k^2\Omega^2} - \frac{v_k}{ik\Omega} \quad \text{if } k \neq 0$$

and

$$z_0 = v_0 = \langle \tau \rangle \quad \text{and} \quad d_0 = \frac{1}{2} \langle \tau^2 \rangle.$$

where  $\langle \tau^n \rangle := \int_0^\infty d\tau \tau^n w(\tau)$  denotes the moments of the waiting time. We further introduce

$$\begin{aligned} w_{k,l} &:= \int_0^\infty d\tau \exp(-ik\Omega\tau) w(\tau) \int_0^\tau d\tau' \exp(-il\Omega\tau') = \begin{cases} \frac{w_k - w_{k+l}}{il\Omega} & l \neq 0 \\ v_k & l = 0 \end{cases} \\ z_{k,l} &:= \int_0^\infty d\tau \exp(-ik\Omega\tau) z(\tau) \int_0^\tau d\tau' \exp(-il\Omega\tau') = \begin{cases} \frac{z_k - z_{k+l}}{il\Omega} & l \neq 0 \\ d_k & l = 0 \end{cases}. \end{aligned}$$

Then eqs. (4.45) can be written as

$$\sum_{j=-\infty}^{\infty} A_{k,j} q_j^{(0)} = \delta_{k,0} \quad \text{and} \quad \sum_{j=-\infty}^{\infty} A_{k,j} q_j^{(1)} = r_k \quad (\text{C.20a})$$

with

$$A_{k,j} = \delta_{k,j} + z_k \gamma_{k-j} \quad (\text{C.20b})$$

and

$$r_k = \sum_{l=-\infty}^{\infty} q_l^{(0)} \left[ \sum_{j=-\infty}^{\infty} \omega_j \gamma_{k-j-l} z_{k-j,j} - \mathfrak{L} z_k \gamma_{k-l} \right]. \quad (\text{C.20c})$$

The Fourier coefficients  $D_k$  and  $\omega_k$  are then, according to eqs. (4.44a) and (4.44b), given by

$$\omega_k = \mathfrak{L} \sum_{j=-\infty}^{\infty} q_j^{(0)} \gamma_{k-j} \quad (\text{C.20d})$$

$$D_k = \sum_{j=-\infty}^{\infty} \left[ -\mathfrak{L} q_j^{(1)} + \frac{\mathfrak{L}^2}{2} q_j^{(0)} \right] \gamma_{k-j}. \quad (\text{C.20e})$$

For the sake of completeness we present the Fourier coefficients  $\gamma_k$  for a dichotomic and a harmonic rate  $\gamma(t)$  as well as the coefficients  $w_k$ ,  $w_{k,l}$ ,  $z_k$  and  $z_{k,l}$  for a  $\Gamma$ -distributed waiting time. Namely for the dichotomic periodic rate

$$\gamma(t) = \begin{cases} r_1 & \text{if } t \in [n\mathcal{T}, (n + \frac{1}{2})\mathcal{T}) \\ r_2 & \text{if } t \in [(n + \frac{1}{2})\mathcal{T}, (n + 1)\mathcal{T}) \end{cases}, \quad \mathcal{T} = \frac{2\pi}{\Omega}$$

we obtain

$$\gamma_0 = \frac{r_1 + r_2}{2} \quad \text{and} \quad \gamma_k = i(r_1 - r_2) \frac{1 - \cos k\pi}{2k\pi} = \begin{cases} 0 & k \neq 0 \text{ even} \\ \frac{r_1 - r_2}{k\pi} & k \text{ odd} \end{cases}$$

while the harmonic periodic rate

$$\gamma(t) = \frac{r_1 + r_2}{2} + \frac{r_1 - r_2}{2} \cos \Omega t.$$

leads to

$$\gamma_0 = \frac{r_1 + r_2}{2}, \quad \gamma_{\pm 1} = \frac{r_1 - r_2}{4} \quad \text{and} \quad \gamma_k = 0, \quad k \neq 0, \pm 1.$$

A  $\Gamma$ -distributed waiting time

$$w(\tau) = \frac{1}{\Gamma(n)} \left(\frac{\tau n}{T}\right)^n \frac{\exp(-\frac{\tau n}{T})}{\tau}$$

corresponds to

$$w_k = \left(\frac{n}{n + ik\Omega T}\right)^n, \quad v_k = T \left(\frac{n}{n + ik\Omega T}\right)^{n+1} \quad \text{and} \quad \langle \tau^2 \rangle = \left(1 + \frac{1}{n}\right)T^2$$

A fixed, i.e. delta distributed waiting time  $T$  is obtained in the limit  $n \rightarrow \infty$ . Thus for  $w(\tau) = \delta(T - \tau)$  we have

$$w_k = \exp(-ik\Omega T), \quad v_k = T \exp(-ik\Omega T) \quad \text{and} \quad \langle \tau^2 \rangle = T^2$$

With these expressions eqs. (C.20) can be solved numerically after truncation to a finite number of coefficients.

## C.6 The defining equation for $\kappa^{[3]}(t)$ in Fourier space

In this appendix we present the linear infinite dimensional inhomogeneous system of equations for the Fourier coefficients

$$\hat{\kappa}_k^{[3]} = \frac{1}{T} \int_0^T dt \kappa^{[3]}(t) \exp(-ik\Omega t),$$

of the third cumulant growth coefficient

$$\kappa^{[3]}(t) = \sum_{k=-\infty}^{\infty} \hat{\kappa}_k^{[3]} \exp(ik\Omega t)$$

as given by eq. (4.71d). Using the Fourier decomposition of  $\kappa^{[1]}(t)$  and  $\kappa^{[2]}(t)$ , eqs (4.72) as well as

$$\hat{j}_{k,l} = \frac{1}{2} \int_0^\infty d\tau \tau^2 \hat{z}_k(\tau) \exp(-il\Omega\tau).$$



and  $\hat{z}_{k,l}$  and  $\hat{h}_{k,l}$  as defined in eq. (4.73) one eventually obtains from eq. (4.71d)

$$\begin{aligned}
 \sum_{k=-\infty}^{\infty} \hat{\kappa}_k^{[3]} \hat{z}_{m-k,m} = & \tag{C.21} \\
 & 3 \sum_{k=-\infty}^{\infty} \left[ \left[ \sum_{l=-\infty, l \neq 0}^{\infty} \frac{\hat{\kappa}_l^{[2]} \hat{\kappa}_k^{[1]} + \hat{\kappa}_l^{[1]} \hat{\kappa}_k^{[2]}}{il\Omega} (\hat{z}_{m-k-l, m-l} - \hat{z}_{m-k-l, m}) \right] \right. \\
 & \quad \left. + [\hat{\kappa}_0^{[2]} \hat{\kappa}_k^{[1]} + \hat{\kappa}_0^{[1]} \hat{\kappa}_k^{[2]}] \hat{h}_{m-k,m} \right] \\
 & -6 \sum_{k=-\infty}^{\infty} \left[ \left[ \sum_{l=-\infty, l \neq 0}^{\infty} \sum_{j=-\infty, j \neq 0, -l}^{\infty} \right. \right. \\
 & \quad \left. \frac{\hat{\kappa}_k^{[1]} \hat{\kappa}_l^{[1]} \hat{\kappa}_j^{[1]}}{j\Omega^2} \left( \frac{1}{l} (\hat{z}_{m-k-l-j, m-j} - \hat{z}_{m-k-l-j, m-j-l}) \right) \right. \\
 & \quad \left. \left. + \frac{1}{j+l} (\hat{z}_{m-k-l-j, m-j-l} - \hat{z}_{m-k-l-j, m}) \right) \right] \\
 & + \sum_{l=-\infty, l \neq 0}^{\infty} \frac{\hat{\kappa}_k^{[1]} \hat{\kappa}_l^{[1]} \hat{\kappa}_{-l}^{[1]}}{l^2 \Omega^2} (\hat{z}_{m-k, m} - \hat{z}_{m-k, m-l} + il\Omega \hat{h}_{m-k, m}) \\
 & + \sum_{l=-\infty, l \neq 0}^{\infty} \frac{\hat{\kappa}_k^{[1]} \hat{\kappa}_l^{[1]} \hat{\kappa}_0^{[1]}}{il\Omega} (\hat{h}_{m-k-l, m-l} - \hat{h}_{m-k-l, m}) + \hat{\kappa}_k^{[1]} \hat{\kappa}_0^{[1]} \hat{\kappa}_0^{[1]} \hat{j}_{m-k, m} \\
 & + \delta_{m,0}.
 \end{aligned}$$

## C.7 Time derivatives of integrals involving time dependent survival probabilities

For any sufficiently well behaved function  $g(t)$  we have

$$\frac{d}{dt} \int_0^{\infty} d\tau g(t-\tau) z(\tau, t-\tau) = g(t) - \int_0^{\infty} d\tau g(t-\tau) w(\tau, t-\tau). \tag{C.22}$$

This can be seen as follows:

$$\begin{aligned}
 & \frac{d}{dt} \int_0^{\infty} d\tau g(t-\tau) z(\tau, t-\tau) \\
 & = \int_0^{\infty} d\tau \left( -\frac{d}{d\tau} g(t-\tau) z(\tau, t-\tau) + g(t-\tau) \frac{d}{d\tau'} z(\tau', t-\tau) \Big|_{\tau'=\tau} \right) \\
 & = -g(t-\tau) z(\tau, t-\tau) \Big|_{\tau=0}^{\infty} - \int_0^{\infty} d\tau g(t-\tau) w(\tau, t-\tau) \\
 & = g(t) - \int_0^{\infty} d\tau g(t-\tau) w(\tau, t-\tau).
 \end{aligned}$$

where in the last step we assumed that  $g(t - \tau)z(\tau, t - \tau)$  converges to zero as  $\tau \rightarrow \infty$ .

We further have the identity

$$\begin{aligned}
& \frac{d}{dt} \int_0^\infty d\tau g(t - \tau) \int_0^\tau d\tau' g(t - \tau + \tau') z(\tau, t - \tau) \\
&= \int_0^\infty d\tau \left( -\frac{d}{d\tau} \left[ g(t - \tau) \int_0^\tau d\tau' g(t - \tau + \tau') z(\tau, t - \tau) \right] \right. \\
&\quad \left. + g(t - \tau) g(t) z(\tau, t - \tau) - g(t - \tau) \int_0^\tau d\tau' g(t - \tau + \tau') w(\tau, t - \tau) \right) \\
&= g(t) \int_0^\infty d\tau g(t - \tau) z(\tau, t - \tau) \tag{C.23} \\
&\quad - \int_0^\infty d\tau g(t - \tau) \int_0^\tau d\tau' g(t - \tau + \tau') w(\tau, t - \tau).
\end{aligned}$$



# Appendix D

## Detailed calculations for chapter 5

### D.1 Investigation of the criticality of the Hopf bifurcation in the globally coupled threestate model

In this appendix we investigate the criticality of the Hopf bifurcation of the system eq. (5.13) with  $\Gamma$ -distributed waiting times in state 2 and 3, eq. (5.25). Although there exists a center manifold theorem [30, 51] for functional differential equations it is more convenient to enlarge the phase space in order to be able to represent the dynamics as an ordinary differential equation. This possibility relies on the property of the  $\Gamma$ -distribution of order  $r$  with mean  $\tau$  to be a convolution of  $r$  ordinary exponential distributions with rate  $\frac{r}{\tau}$ . The states 2 and 3, whose probabilities  $p^{(2)}$  and  $p^{(3)}$  obey a non Markovian dynamics are represented by a number  $r^{(2)}$  and  $r^{(3)}$  of substates  $(2, i)$  and  $(3, i)$ . The transitions between these substates are rate transitions, finally leading to a set of  $1 + r^{(2)} + r^{(3)}$  ordinary differential equations for the probabilities  $p^{(1)}$ ,  $p_i^{(2)}$  and  $p_i^{(3)}$  replacing the integral equations

(5.13),

$$\begin{aligned}
 \frac{d}{dt}p^{(1)}(t) &= -\gamma\left(\sum_{i=1}^{r^{(2)}}p_i^{(2)}(t)\right)p^{(1)}(t) + \frac{r^{(3)}}{\tau^{(3)}}p_{r^{(3)}}^{(3)}(t) \\
 \frac{d}{dt}p_1^{(2)}(t) &= \gamma\left(\sum_{i=1}^{r^{(2)}}p_i^{(2)}(t)\right)p^{(1)}(t) - \frac{r^{(2)}}{\tau^{(2)}}p_1^{(2)}(t) \\
 \frac{d}{dt}p_i^{(2)}(t) &= \frac{r^{(2)}}{\tau^{(2)}}(p_{i-1}^{(2)}(t) - p_i^{(2)}(t)), \quad i = 2, \dots, r^{(2)} \\
 \frac{d}{dt}p_1^{(3)}(t) &= \frac{r^{(2)}}{\tau^{(2)}}p_{r^{(2)}}^{(2)}(t) - \frac{r^{(3)}}{\tau^{(3)}}p_1^{(3)}(t) \\
 \frac{d}{dt}p_i^{(3)}(t) &= \frac{r^{(3)}}{\tau^{(3)}}(p_{i-1}^{(3)}(t) - p_i^{(3)}(t)), \quad i = 2, \dots, r^{(3)}
 \end{aligned} \tag{D.1}$$

In order to decide whether the Hopf bifurcation occurring in the system eqs. (D.1) is super- or subcritical we rewrite these equations in terms of the new variables  $s_i(t)$ , which describe the deviation from the stationary state  $p_{st}^{(1)}$ ,  $p_{i,st}^{(2)} = \frac{p_{st}^{(2)}}{r^{(2)}}$  and  $p_{i,st}^{(3)} = \frac{p_{st}^{(3)}}{r^{(3)}}$ , i.e.

$$s_1(t) = p^{(1)}(t) - p_{st}^{(1)}, \quad s_{i+1}(t) = p_i^{(2)}(t) - \frac{p_{st}^{(2)}}{r^{(2)}} \quad \text{and} \quad s_{i+1+r^{(2)}}(t) = p_i^{(3)}(t) - \frac{p_{st}^{(3)}}{r^{(3)}}.$$

In terms of these variables eqs. (D.1) can then be rewritten as (we use a sum convention, i.e. the same indices are summed over)

$$\dot{s}_i = A_i^j s_j + B_i^{jk} s_j s_k + C_i^{jkl} s_j s_k s_l + O(s^4),$$

where the tensors  $A_i^j$ ,  $B_i^{jk}$  and  $C_i^{jkl}$  are given by

$$\begin{aligned}
 A_1^1 &= -\gamma_{st}, & A_1^{1+r^{(2)}+r^{(3)}} &= \frac{r^{(3)}}{\tau^{(3)}} \\
 A_1^j &= -\gamma'_{st} p_{st}^{(1)}, & & j = 2 \dots r^{(2)} + 1 \\
 A_2^1 &= \gamma_{st}, & A_2^2 &= -\frac{r^{(2)}}{\tau^{(2)}} \\
 A_2^j &= \gamma'_{st} p_{st}^{(1)}, & & j = 2 \dots r^{(2)} + 1 \\
 A_j^{j-1} &= \frac{r^{(2)}}{\tau^{(2)}}, & A_j^j &= -\frac{r^{(2)}}{\tau^{(2)}}, & j = 2 \dots 1 + r^{(2)} \\
 A_{2+r^{(2)}}^{1+r^{(2)}} &= \frac{r^{(2)}}{\tau^{(2)}}, & A_{2+r^{(2)}}^{2+r^{(2)}} &= -\frac{r^{(3)}}{\tau^{(3)}} \\
 A_j^{j-1} &= \frac{r^{(3)}}{\tau^{(3)}}, & A_j^j &= -\frac{r^{(3)}}{\tau^{(3)}}, & j = 2 + r^{(2)} \dots 1 + r^{(2)} + r^{(3)}.
 \end{aligned}$$

$$\begin{aligned}
 B_1^{1j} &= B_1^{j1} = -\gamma'_{st}, & j &= 2 \dots r^{(2)} + 1 \\
 B_1^{kj} &= -\frac{\gamma''_{st}}{2}, & k, j &= 2 \dots r^{(2)} + 1 \\
 B_2^{1j} &= B_2^{j1} = \gamma'_{st}, & j &= 2 \dots r^{(2)} + 1 \\
 B_2^{kj} &= \frac{\gamma''_{st}}{2}, & k, j &= 2 \dots r^{(2)} + 1
 \end{aligned}$$

$$\begin{aligned}
C_1^{1jk} &= C_1^{j1k} = C_1^{jk1} = -\frac{\gamma_{st}''}{2}, & j, k &= 2 \dots r^{(2)} + 1 \\
C_1^{jkl} &= -\frac{\gamma_{st}'''}{6}, & j, k &= 2 \dots r^{(2)} + 1 \\
C_2^{1jk} &= C_2^{j1k} = C_1^{jk1} = \frac{\gamma_{st}''}{2}, & j, k &= 2 \dots r^{(2)} + 1 \\
C_2^{jkl} &= \frac{\gamma_{st}'''}{6}, & j, k &= 2 \dots r^{(2)} + 1
\end{aligned}$$

At the Hopf bifurcation the matrix  $A$  has two imaginary eigenvalues  $\pm i\omega$ . We choose a real basis  $\{\mathbf{v}_i\}_i$  and corresponding dual basis  $\{\mathbf{u}_j\}_j$ , i.e.  $\langle \mathbf{u}_i, \mathbf{v}_j \rangle = U_i^k V_k^j = \delta_{i,j}$  such that the first two span the center eigenspace. where

$$U_i^k = \mathbf{u}_{ik} \quad \text{and} \quad V_i^k = \mathbf{v}_{ik}$$

In the new coordinates  $q_i = U_i^k s_k$  the dynamical equations then read

$$\frac{d}{dt} q_i = \tilde{A}_i^j q_j + \tilde{B}_i^{jk} q_j q_k + \tilde{C}_i^{jkl} q_j q_k q_l + O(q^4). \quad (\text{D.2})$$

with

$$\begin{aligned}
\tilde{A}_i^j &= U_i^m A_m^n V_n^j, & \tilde{B}_i^{jk} &= U_i^m B_m^{no} V_n^j V_o^k \\
\tilde{C}_i^{jkl} &= U_i^m C_m^{nop} V_n^j V_o^k V_p^l
\end{aligned}$$

Due to the choice of the new basis we have

$$\tilde{A} = \begin{pmatrix} 0 & -\omega & 0 & \cdots & 0 \\ \omega & 0 & 0 & \cdots & 0 \\ 0 & 0 & \tilde{A}_2^2 & \cdots & \tilde{A}_2^{1+r^{(2)}+r^{(3)}} \\ \vdots & \vdots & \vdots & \ddots & \vdots \\ 0 & 0 & \tilde{A}_{1+r^{(2)}+r^{(3)}}^2 & \cdots & \tilde{A}_{1+r^{(2)}+r^{(3)}}^{1+r^{(2)}+r^{(3)}} \end{pmatrix} \quad (\text{D.3})$$

The first two coordinates parameterize the center manifold. In the following, Greek indices run from 1 to 2 while Latin indices run from 3 to  $1+r^{(2)}+r^{(3)}$ . The center manifold can be parameterized in terms of the two coordinates  $q_1$  and  $q_2$  which span the center space,

$$q_i = h_i(q_1, q_2) = h^{[2]i\mu\nu} q_\mu q_\nu + h^{[3]i\mu\nu\rho} q_\mu q_\nu q_\rho + O(q^4) \quad (\text{D.4})$$

where  $O(q^4)$  which are at least of 4th order in  $q_1$  and  $q_2$ . The constant and linear terms in the expansion are zero due to the fact that  $\mathbf{h}(0) = 0$  and  $D\mathbf{h}(0) = 0$  as the center manifold is parallel to the center space at  $\mathbf{q} = 0$ . In order to determine the unknown coefficients  $h^{[2]i\mu\nu}$  and  $h^{[3]i\mu\nu\rho}$  we compare the dynamics of the  $q_i$  as

obtained from eq. (D.4) with the original dynamics (D.2). From eq. (D.4) we obtain on the center manifold

$$\begin{aligned} \frac{d}{dt}q_i &= h^{[2]i\mu\nu} \left( \left[ \frac{d}{dt}q_\mu \right] q_\nu + q_\mu \left[ \frac{d}{dt}q_\nu \right] \right) + h^{[3]i\mu\nu\rho} \left( \left[ \frac{d}{dt}q_\mu \right] q_\nu q_\rho + \right. \\ &\quad \left. q_\mu \left[ \frac{d}{dt}q_\nu \right] q_\rho + q_\mu q_\nu \left[ \frac{d}{dt}q_\rho \right] \right) + O(q^4) \\ &= h^{[2]i\mu\nu} (\tilde{A}_\mu^\rho q_\rho q_\nu + \tilde{A}_\mu^j h^{[2]j\rho\lambda} q_\rho q_\lambda q_\nu + q_\mu \tilde{A}_\nu^\rho q_\rho + q_\mu \tilde{A}_\nu^j h^{[2]j\rho\lambda} q_\rho q_\lambda) + \\ &\quad h^{[3]i\mu\nu\rho} (\tilde{A}_\mu^\lambda q_\lambda q_\nu q_\rho + q_\mu \tilde{A}_\nu^\lambda q_\lambda q_\rho + q_\mu q_\nu \tilde{A}_\rho^\lambda q_\lambda) + O(q^4) \end{aligned} \quad (D.5)$$

$$(D.6)$$

where in the last step we used eqs. (D.2) and (D.4).

On the other hand the dynamics of  $q_i$  is according to eq. (D.2) given by

$$\begin{aligned} \frac{d}{dt}q_i &= \tilde{A}_i^\mu q_\mu + \tilde{A}_i^j h^{[2]j\mu\nu} q_\mu q_\nu + \tilde{A}_i^j h^{[3]j\mu\nu\rho} q_\mu q_\nu q_\rho \\ &\quad + \tilde{B}_i^{\mu\nu} q_\mu q_\nu + \tilde{B}_i^{j\nu} h^{[2]j\mu\rho} q_\mu q_\rho q_\nu + \tilde{B}_i^{\mu j} h^{[2]j\nu\rho} q_\mu q_\nu q_\rho + \tilde{C}_i^{\mu\nu\rho} q_\mu q_\nu q_\rho + O(q^4) \end{aligned} \quad (D.7)$$

The first summand on the right hand side is 0 due to the special coordinate system we have chosen (see eq. (D.3)). From eqs. (D.5) and (D.7) we can obtain the center manifold as defined by  $h^{[2]i\mu\nu}$  and  $h^{[3]i\mu\nu\rho}$  by equating the coefficients of  $q_\mu q_\nu$  and  $q_\mu q_\nu q_\rho$ . We obtain

$$h^{[2]i\rho\nu} \tilde{A}_\rho^\mu + h^{[2]i\mu\rho} \tilde{A}_\rho^\nu - \tilde{A}_i^j h^{[2]j\mu\nu} - \tilde{B}_i^{\mu\nu} + (\mu \leftrightarrow \nu) = 0 \quad (D.8)$$

and

$$\begin{aligned} h^{[2]i\lambda\nu} \tilde{A}_\lambda^j h^{[2]j\rho\mu} + h^{[2]i\nu\lambda} \tilde{A}_\lambda^j h^{[2]j\rho\mu} + h^{[3]i\lambda\nu\rho} \tilde{A}_\lambda^\mu + h^{[3]i\nu\lambda\rho} \tilde{A}_\lambda^\mu + h^{[3]i\rho\nu\lambda} \tilde{A}_\lambda^\mu \\ - \tilde{A}_i^j h^{[3]j\mu\nu\rho} - \tilde{B}_i^{j\nu} h^{[2]j\mu\rho} - \tilde{B}_i^{\mu j} h^{[2]j\nu\rho} - \tilde{C}_i^{\mu\nu\rho} + (\mu \leftrightarrow \nu \leftrightarrow \rho) = 0 \end{aligned} \quad (D.9)$$

Having solved these equations for the  $h^{[2]i\mu\nu}$  and  $h^{[3]i\mu\nu\rho}$  we obtain the dynamics of  $q_1$  and  $q_2$  on the center manifold from equation (D.7) by setting  $i = 1, 2$  as

$$\frac{d}{dt}q_1 = f_1(q_1, q_2) \quad \text{and} \quad \frac{d}{dt}q_2 = f_2(q_1, q_2)$$

Therefrom we can calculate the parameter (see [48])

$$\begin{aligned} a : &= \frac{1}{16} (f_{1,q_1 q_1 q_1} + f_{2,q_1 q_1 q_2} + f_{1,q_1 q_2 q_2} + f_{2,q_2 q_2 q_2}) \\ &\quad + \frac{1}{16\omega} (f_{1,q_1 q_2} (f_{1,q_1 q_1} + f_{1,q_2 q_2}) - f_{2,q_1 q_2} (f_{2,q_1 q_1} + f_{2,q_2 q_2}) \\ &\quad \quad - f_{1,q_1 q_1} f_{2,q_1 q_1} + f_{1,q_2 q_2} f_{2,q_2 q_2}) \end{aligned}$$

with

$$f_{\rho, q_\mu q_\nu} := \left. \frac{df_\rho(q_1, q_2)}{dq_\mu dq_\nu} \right|_{q_1=0, q_2=0}$$

This parameter  $a$  is less than 0 if the Hopf bifurcation is supercritical and greater than 0 if it is subcritical.

The  $f_{\rho, q_\mu q_\nu}$  and  $f_{\lambda, q_\mu q_\nu q_\rho}$  can be further evaluated according to eq. (D.7) as

$$f_{\rho, q_\mu q_\nu} = \tilde{A}_\rho^j h_j^{[2]\mu\nu} + \tilde{B}_\rho^{\mu\nu} + (\mu \leftrightarrow \nu)$$

and

$$f_{\lambda, q_\mu q_\nu q_\rho} = \tilde{A}_\lambda^j h_j^{[3]\mu\nu\rho} + \tilde{B}_\lambda^{j\nu} h_j^{[2]\mu\rho} + \tilde{B}_\lambda^{\mu j} h_j^{[2]\nu\rho} + \tilde{C}_\lambda^{\mu\nu\rho} + (\mu \leftrightarrow \nu \leftrightarrow \rho).$$

## D.2 Some properties of Laplace transforms of waiting time distributions and survival probabilities

Let

$$\hat{w}(\lambda, t) := \int_0^\infty d\tau \exp(-\lambda\tau) w(\tau, t)$$

denote the Laplace transform of the waiting time distribution  $w(\tau, t)$ . Splitting the complex argument  $\lambda$  into real and imaginary part,  $\lambda = \lambda_{\text{re}} + i\lambda_{\text{im}}$  we obtain

$$\begin{aligned} |\hat{w}(\lambda, t)| &= \left| \int_0^\infty d\tau \exp(-\lambda\tau) w(\tau, t) \right| \\ &\leq \int_0^\infty d\tau \exp(-\lambda_{\text{re}}\tau) w(\tau, t). \end{aligned}$$

Therefrom one immediately deduces

$$|\text{Re } \hat{w}(\lambda, t)| < 1 \quad \text{and} \quad |\text{Im } \hat{w}(\lambda, t)| < 1.$$

if  $\lambda_{\text{re}} > 0$ .

The corresponding survival probability  $z(\tau, t)$  is a positive monotonously decreasing function of  $\tau$ . Its Laplace transform is related to  $\hat{w}(\lambda, t)$  by

$$\hat{z}(\lambda, t) = \frac{1 - \hat{w}(\lambda, t)}{\lambda}$$



Assuming again that  $\lambda_{\text{re}} > 0$  we obtain

$$\text{Im } \hat{z}(\lambda, t) = \int_0^\infty d\tau \sin(-\lambda_{\text{im}} \tau) \exp(-\lambda_{\text{re}} \tau) z(\tau, t).$$

As  $z(\tau, t)$  is positive and monotonously decreasing,  $\exp(-\lambda_{\text{re}} \tau) z(\tau, t)$  is also a positive strictly monotonously decreasing function of  $\tau$  and therefore the integral in the above equation is either positive for  $\lambda_{\text{im}} < 0$  or negative for  $\lambda_{\text{im}} > 0$  and assumes the value 0 if and only if  $\lambda_{\text{im}} = 0$ ,

$$\text{sgn Im } \hat{z}(\lambda, t) = \text{sgn } \lambda_{\text{im}} \tag{D.10}$$

# List of Symbols

- $(k, i)$  in the context of alternating renewal processes this notation is used to index that subevent  $i$  happened the  $k$ th time, page 20
- $\wedge$  Laplace transform  $\hat{f}(u) := \int_0^\infty dt \exp(-ut)f(t)$ ; also used to denote the Fourier transform, characteristic function or discrete Fourier coefficients, page 15
- $\langle f, g \rangle_{\mathbb{C}}$  inner product on  $L_2([0, 2\pi])$ ,  $\langle f, g \rangle_{\mathbb{C}} = \int_0^{2\pi} d\phi f^*(\phi)g(\phi)$ , page 50
- $\langle f \rangle$  statistical mean of the quantity  $f$ , page 8
- $\chi(t)$  delta spike sequence assigned to a a renewal process, page 21
- $\eta(t)$  pulse sequence assigned to an alternating renewal process, page 21
- $\kappa^{[i]}(t)$  asymptotic periodic growth (time derivative) of the  $i$ th cumulant of the number of events, page 72
- $\Omega$  angular velocity of a periodic process ( $\equiv$  angular velocity of the periodic external driving), page 32
- $\omega(t)$  instantaneous mean phase velocity,  $\omega(t) = 2\pi v(t)$ , page 81
- $\phi_i$  signal phase of the  $i$ th event in a periodically driven renewal process, page 36
- $\sigma_i$  discrete state of the  $i$ th unit, page 121
- $\tau_D$  delay of the global coupling, page 141
- $\langle \tau \rangle_0$  period averaged mean waiting time of a periodic renewal process, page 52
- $\langle \tau \rangle_{\text{un}}$  mean waiting time of a periodically driven renewal process in the limit of vanishing driving amplitude, page 53

- $\xi(t)$  white noise with mean 0,  $\langle \xi(t) \rangle = 0$  and intensity 1,  $\langle \xi(t)\xi(t + \tau) \rangle = \delta(\tau)$ , page 8
- $\bar{c}_{x,x}(\tau)$  period averaged auto correlation function of a periodic process, page 33
- $c_{\omega_k, T}$  discrete Fourier coefficient corresponding to the frequency  $\omega_k = 2\pi k/T$  of the realization of a stochastic process in the interval  $(0, T)$ , page 23
- $c_{x,x}(\tau)$  autocorrelation function of a stationary process  $x(t)$ ,  $c_{x,x}(\tau) := \langle x(t)x(t + \tau) \rangle$ , page 24
- $c_{x,x}(t, t')$  auto correlation function  $c_{x,x}(t, t') = \langle x(t)x(t') \rangle$  of a time dependent (periodic) process, page 33
- $\bar{D}_{\text{eff}}$  effective diffusion coefficient of the number of events, page 27
- $\mathcal{D}_{\text{eff}}(t)$  instantaneous effective phase diffusion coefficient, page 81
- $D_{\text{eff}}(t)$  instantaneous effective diffusion coefficient of the number of events, page 72
- $j^{(i)}(t)$  probability flux from state  $i$  to state  $i + 1$  at time  $t$ , page 10
- $j_k^{(i)}(t)$  probability that event  $(k, i + 1)$  happens at time  $t$ , page 20
- $j_k(t)$  probability that event  $k + 1$  happens at time  $t$ , page 19
- $\mathcal{M}_t$  periodically time dependent master operator, describing the evolution of the probabilities of a periodically driven alternating renewal process, page 37
- $N_{t_0, t}$  number of events in the time interval  $(t_0, t]$ , page 26
- $\mathcal{P}(x, t)$  continuous probability density extending the discrete probabilities  $p_k(t)$ ,  $\int_{k-\frac{1}{2}}^{k+\frac{1}{2}} dx \mathcal{P}(x, t) = p_k(t)$ , page 77
- $P^{\text{st}}$  stationary distribution of the signal phases at the instants of the events of a periodically driven renewal process, page 50
- $p^{(i)}(t)$  probability to be in the discrete state  $i$  at time  $t$ , page 10
- $p_k^{(i)}(t)$  probability that the last event which happened was  $(k, i)$ , page 20
- $p_k(t)$  probability to have had exactly  $k$  events up to time  $t$ , page 19

- 
- $S_{\text{bg}}(\omega)$  background spectral power density, continuous part of the spectral power density obtained by neglecting the delta peaks at 0 and integer multiples of the driving frequency, page 33
- $S_x(t)$  spectral power density of the stochastic process  $x(t)$ , page 22
- SNR signal to noise ratio, page 34
- SPA spectral power amplification, page 34
- $\mathcal{T}$  period of a periodic process ( $\equiv$  period of the periodic external driving), page 32
- $T$  length of a time interval, page 23
- $t_k^{(i)}$  instant of the event  $(k, i)$  of an alternating renewal process, page 21
- $t_k$  instant of the event  $k$  of a renewal process, page 21
- $\bar{v}$  mean frequency of the events, page 27
- $v(t)$  instantaneous mean frequency of the events, page 72
- $\hat{w}(\omega)$  characteristic function of the waiting time distribution  $w(\tau)$ ,  $\hat{w}(\omega) := \int_0^\infty d\tau e^{-i\omega\tau} w(\tau)$ , the symbol  $\hat{f}$  is also used to denote the Laplace transform of the function  $f$ , page 24
- $w^{(i)}(\tau)$  Distribution of the waiting time  $\tau$  in the discrete state  $i$ , page 10
- $\bar{x}(t)$  mean output of the globally coupled system, page 121
- $\bar{x}_{\text{st}}$  mean output in the stationary state, page 123
- $x(t)$  stochastic process with continuous state space, page 21
- $x^{(i)}$  output of the discrete state system in state  $i$ , page 21
- $x_T(t)$  stochastic process restricted to the time interval  $(0, T)$ , page 23
- $z^{(i)}(\tau)$  probability to survive longer than  $\tau$  in the discrete state  $i$ , page 15



# Acknowledgment

This work would not have been possible without the help of many people. First of all I want to thank my supervisor Prof. Dr. Lutz Schimansky-Geier. His inspiring and valuable support, being never constricting, had a wide influence on this work. The pleasant atmosphere in his research group made the preparation of this thesis an enjoyable task.

I appreciate the nice time I spend with all the present and former members of the research groups “ Theorie Stochastischer Prozesse” and “Statistische Physik und Nichtlineare Dynamik” and the helpful and interesting seminars and discussions we had. Special thanks go to Xaver Sailer, with whom I shared many ups and downs during this work.

I am grateful to the Sonderforschungsbereich 555 “Komplexe Nichtlineare Prozesse”. Beside its financial support I do not want to miss the inspiring impulses of the regularly organized symposia.

Apart from the scientific supporters of this work there are also those that have privately provided continuous encouragement. Among them I want to thank in particular my parents Dr. Magdalene and Dr. Michael Prager.

Last but not least I am deeply indebted to my wife Dr. Arleta Szkoła. Beside her private support, her mathematical insights contributed a lot to this thesis. With her I could always discuss the mathematical problems I faced during the preparation of this work and even in the rare cases where this did not immediately lead to an answer, she always pointed out the right books to me.



# Selbständigkeitserklärung

Hiermit erkläre ich, die Dissertation selbständig und nur unter Verwendung der angegebenen Hilfen und Hilfsmittel angefertigt zu haben.

Berlin, den 10.1.2006